canadian acoustics
acoustique canadienne

2022

Acoustics Week in Canada

Semaine canadienne de l'acoustique

Actes de la conférence
Conference Proceedings

canadian acoustics

acoustique canadienne

EDITOR-IN-CHIEF - RÉDACTEUR EN CHEF

Dr. Umberto Berardi
Ryerson University
editor@caa-aca.ca

DEPUTY EDITOR
RÉDACTEUR EN CHEF ADJOINT

Romain Dumoulin
Soft dB
deputy-editor@caa-aca.ca

JOURNAL MANAGER
DIRECTRICE DE PUBLICATION

Cécile Le Cocq
ÉTS, Université du Québec
journal@caa-aca.ca

EDITORIAL BOARD
RELECTEUR-RÉVISEUR

Pierre Grandjean
Université de Sherbrooke
copyeditor@caa-aca.ca

ADVERTISING EDITOR
RÉDACTEUR PUBLICITÉS

Mr Bernard Feder
HGC Engineering
advertisement@caa-aca.ca

ADVISORY BOARD
COMITÉ AVISEUR

Prof. Jérémie Voix
ÉTS, Université du Québec

Prof. Frank A. Russo
Ryerson University

Prof. Ramani Ramakrishnan
Ryerson University

Prof. Bryan Gick
University of British Columbia

WELCOME TO ST. JOHN'S, NEWFOUNDLAND AND LABRADOR
ACOUSTICS WEEK IN CANADA - SEPTEMBER 28-30, 2022

Website: https://awc.caa-aca.ca/

Organizing Committee

Conference Chairs: Len Zedel, Memorial University of Newfoundland

Ben Zendel, Memorial University of Newfoundland

Technical Chair: Cristina Tollefsen, Defence Research and Development Canada

Sponsorship Chair: Lorenzo Moro, Memorial University of Newfoundland

Website Coordinator: Axel Belgarde, Memorial University of Newfoundland

On-site coordinator: Sarah Sauvé, Memorial University of Newfoundland

W elcome to the first Acoustics Week in Canada in St. John's, Newfoundland and Labrador. We respectfully acknowledge the territory in which we gather as the ancestral homelands of the Beothuk, and the island of Newfoundland as the ancestral homelands of the Mi'kmaq and Beothuk. We would also like to recognize the Inuit of Nunatsiavut and NunatuKavut and the Innu of Nitassinan, and their ancestors, as the original people of Labrador. We strive for respectful relationships with all the peoples of this province as we search for collective healing and true reconciliation and honor this beautiful land together.

In Newfoundland, when you meet someone on the street, it's common to say, "whad'ya'at?" to which you would reply, "Dis's'it!". So, what have we been at? Well, not only is this the first Acoustics Week in Canada's easternmost province, but also the first in-person conference since 2019. We are all really excited to welcome everyone to our city and province, but also back to being together physically. So, when someone asks us, "whad'ya'at?", Acoustics Week 2022 is 'it'. This year's conference will feature over 65 talks in all fields of acoustics. Given our proximity to the ocean, we have 2 plenary sessions related to acoustics in the ocean. Dr. Michael Schutz will present work on how we can improve the effectiveness of safety critical sounds based on knowledge of the acoustics of musical instruments. Representatives from the Department of Fisheries and Oceans will explain how there's more to the Coast Guard than bright red ships and that includes the use of sound as an aid to navigation. In addition to our scientific program, we hope everyone will enjoy a welcome reception on the first day of the conference, an Acoustics Banquet at the main provincial Museum, The Rooms, tours of a ship in St. John's harbour, and a visit to the D.F. Cook Recital Hall in the School of Music at Memorial University.

We would also like to thank the corporate sponsors of our conference. They are listed on the conference website, and in these proceedings. We encourage all attendees to patronize these companies, when possible, as they provide critical support for this conference.

We all hope you have a great time at Acoustics Week in Canada 2022. In addition to our organized scientific and social activities, we hope you can get out an enjoy the warmth and hospitality of St. John's, and the rest of the province.

Len Zedel

Ben Zendel
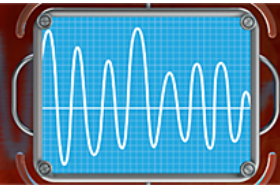
BIENVENUE À ST. JOHN'S, TERRE-NEUVE-ET-LABRADOR
SEMAINE CANADIENNE DE L'ACOUSTIQUE - 28-30 SEPTEMBRE 2022

Site web: https://awc.caa-aca.ca/

Comité organisateur

Présidents de la conférence:	Len Zedel, Memorial University of Newfoundland
	Ben Zendel, Memorial University of Newfoundland
Président technique:	Cristina Tollefsen, Defence Research and Development Canada
Commandites:	Lorenzo Moro, Memorial University of Newfoundland
Site web de la conférence:	Axel Belgarde, Memorial University of Newfoundland
Coordinateur sur place:	Sarah Sauvé, Memorial University of Newfoundland

Bienvenue à la première Semaine canadienne de l'acoustique à St. John's, Terre-Neuve et Labrador. Nous reconnaissons avec respect que le territoire sur lequel nous nous rassemblons est la patrie ancestrale du peuple Beothuk, et que l'île de Terre-Neuve est la patrie ancestrale des peuples Mi'kmaq et Beothuk. Nous souhaitons aussi reconnaître que les peuples Inuit de Nunatsiavut et de NunatuKavut et le peuple Innu de Nitassinan, et leurs ancêtres, sont les premiers peuples du Labrador. Nous nous efforçons d'établir des relations respectueuses avec tous les peuples de cette province pendant que nous cherchons à guérir collectivement et à arriver à une véritable réconciliation pour ensemble honorer ce beau territoire.

À Terre-Neuve, quand on rencontre quelqu'un dans la rue, la phrase "whad'ya'at?" ("kostufa?"*) est souvent entendue, à laquelle on répond, "Dis's'it!" ("c'est ça"*). Donc, effectivement, quel est ce qu'on fait? Cette conférence est non seulement la première Semaine canadienne de l'acoustique dans la province le plus à l'est du pays, mais elle est aussi la première conférence en personne depuis 2019. Nous sommes tous très excités de pouvoir vous inviter à notre ville et notre province, et aussi de pouvoir vous voir en personne. Donc, si quelqu'un nous demande, "kostufa?", la Semaine canadienne de l'acoustique est "ça". Cette année, la conférence comprend plus de 65 présentations dans tous les domaines acoustiques. Étant donné la proximité de l'océan, nous aurons 2 sessions plénières sur l'acoustique dans l'océan. Dr. Michael Schutz nous présentera son travail sur l'amélioration de l'efficacité de sons critiques pour la sécurité, basé sur les connaissances qui existent sur l'acoustique des instruments de musique. Des représentants du Département Pêches et Océans Canada nous expliquerons comment la Garde côtière en comprends beaucoup plus que des navires rouges, et que ceci inclus l'utilisation du son comme aide à la navigation. En plus de notre programme scientifique, nous espérons que tout le monde profitera d'une réception de bienvenue la première journée de la conférence, un Banquet Acoustique au musée provincial The Rooms, des visites sur un navire dans le port de St. John's, et une visite du hall récital D. F. Cook dans l'école de musique de l'Université Memorial.

Nous voulons aussi remercier nos commanditaires corporatifs. Ils sont nommés sur le site web de la conférence, et dans ces actes. Nous encourageons nos participants à fréquenter ces compagnies quand possible, puisqu'ils offrent un support critique à cette conférence.

Nous espérons que vous vous amuserez à la Semaine canadienne de l'acoustique 2022. En plus de nos activités scientifiques et sociales organisées, nous espérons que vous pourrez prendre le temps d'explorer et de profiter de l'hospitalité de St. John's et du reste de la province.

Len Zedel

Ben Zendel

*traduction très approximative d'une expression très locale! "kostufa?" est une contraction de "qu'est-ce que tu fais? "

AWC 2022 SCHEDULE
ST JOHN'S - SEPTEMBER 28 TO 30, 2022

Note: All contributed presentations are scheduled for 15 minutes (12 minutes + 3 for questions)

Day 1	Wednesday, September 28	
	SALON AB	**SALON CD**
8:45-9:00	Welcome	
9:00-10:00	KEYNOTE TALK (1 of 2) - **Michael Schutz**	
10:00- 10:30	Coffee Break	
10:30-12:00	MUSICAL ACOUSTICS 1	ARCHITECTURAL ACOUSTICS 1
12:00-13:30	Lunch	
13:30-15:00	OCCUPATIONAL ACOUSTICS 1	ACOUSTIC MATERIALS & NOISE CONTROL
15:00-15:30	Coffee Break	
15:30-17:00	PERCEPTION	UNDERWATER ACOUSTICS - SHIP NOISE 1
18:00-20:00	**Welcome Reception** - Court Garden - Sheraton Hotel	
20:00-??	**Student social event** - stay tuned for details	

Day 2	Thrusday, September 29	
	SALON AB	**SALON CD**
9:00-10:00	KEYNOTE TALK (2 of 2) - **Canadian Coast Guard**	
10:00- 10:30	Coffee Break	
10:30-12:00	MUSICAL ACOUSTICS 2	UNDERWATER ACOUSTICS - SHIP NOISE 2
12:00-13:30	Lunch	
13:30-15:00	ENVIRONMENTAL ACOUSTICS	ARCHITECTURAL ACOUSTICS 2
15:00-15:30	Coffee Break	
15:30-17:00	OCCUPATIONAL ACOUSTICS 2	UNDERWATER ACOUSTICS - GENERAL
17:00-18:00	**Annual General Meeting (AGM)** - all CAA members welcome to attend	
18:00-22:00	**Banquet** - The Rooms, 9 Bonaventure Ave (A 5 minute walk up Military Road. Taxi chits available at AWC Welcome Desk for anyone who requires transportation.)	

Day 3	Friday, September 30	
	SALON AB	**SALON CD**
9:00-10:30	ACOUSTICAL EDUCATION - presentations	ARCHITECTURAL ACOUSTICS 3
10:00- 10:30	Coffee Break	
11:00	**Bus to harbour** with bagged lunch	
12:00	Ship tour, bagged lunch at harbour	
13:00	**Bus to MUN for School of Music tour** (stop at hotel on the way)	
14:30	Return to hotel, coffee break	
15:00-16:00	ACOUSTICAL EDUCATION - panel discussion	SPEECH PRODUCTION
16:00-17:00	**Awards ceremony** and thanks	

MAIN FLOOR

STAIRS TO COURT GARDEN

OPPIDAN

BIVVER

THE LINK @ SHERATON

GARRISON

SIGNAL

FORT WILLIAM

D

C

B

A

RECEIVING

FRONT DESK

COAT CHECK

RECEPTION BALLROOM

MAIN LOBBY

MAIN ENTRANCE

CLUB LOUNGE

Listening to Music: Improving safety-critical sounds by studying the acoustics of musical instruments

Écouter de la musique:Améliorer les systèmes auditifs critiques pour la sécurité, en étudiant l'acoustique des instruments de musique

Our daily experience is shaped not only by electronic devices, but the ways they convey information. For example, the ubiquity of screens in smart phones and tablets means they now absorb a great deal of our visual attention. In contrast to those visual interfaces, safety-critical devices tasked with conveying time-sensitive information instead use auditory interfaces to avoid reliance on visual attention. These interfaces play a crucial role in high-consequence environments ranging from airplane cock-pits and ship bridges to nuclear power plants and hospital operating rooms. Although the specific tones in each message vary, many rely on highly simplistic "beeps." As they have often been designed with little consideration of human factors, they are widely recognized as suffering from widely recognized problems with masking, learnability, recognition, and annoyance. The well-known complexity of musical sounds raises an intriguing question—is the traditional focus on acoustic simplicity in auditory interface sounds simply misguided?

My team explores how specific properties of musical sounds can improve the efficacy of the auditory interfaces allowing doctors to care for patients, captains to navigate billion-dollar commercial ships, and engineers to monitor nuclear power plans. We have shown numerous ways in which small modifications to individual tones can lower annoyance without harming learning, while actually improving their detection. The potential impact of these changes is enormous given the scale of their use. For example, at any given time tens of thousands of commercial ships navigate the globe generating safety-critical information continuously. Medical devices fill hospitals around the world, providing crucial real time updates on patient status. Therefore, even small changes to the efficacy of their auditory interfaces can have meaningful improvements on both safety and well-being.

Notre expérience quotidienne est façonnée non seulement par les appareils électroniques, mais aussi par la manière dont ils transmettent l'information. Par exemple, l'omniprésence des écrans dans les téléphones intelligents et les tablettes signifie qu'ils absorbent désormais une grande partie de notre attention visuelle. Contrairement à ces interfaces visuelles, les systèmes critiques pour la sécurité chargés de transmettre des informations urgentes utilisent des interfaces auditives pour éviter de dépendre de l'attention visuelle. Ces interfaces jouent un rôle crucial dans les environnements à hautes conséquences; des cockpits d'avions et des ponts de navires aux centrales nucléaires et aux salles d'opération des hôpitaux. Bien que les tonalités spécifiques de chaque message varient, beaucoup s'appuient sur des "bips" très simplistes. Comme ils ont souvent été conçus sans tenir compte des facteurs humains, ils sont largement reconnus comme ayant des problèmes largement reconnus de masquage, d'apprentissage, de reconnaissance et d'irritation. La complexité bien connue des sons musicaux soulève une question intrigante : l'accent traditionnellement mis sur la simplicité acoustique dans les sons de l'interface auditive est-il simplement erroné ?

Notre équipe explore comment les propriétés spécifiques des sons musicaux peuvent améliorer l'efficacité des interfaces auditives permettant aux médecins de soigner les patients, aux capitaines de naviguer des navires commerciaux d'un milliard de dollars et aux ingénieurs de surveiller les plans d'énergie nucléaire. Nous avons montré de nombreuses manières par lesquelles de petites modifications apportées aux tonalités individuelles peuvent réduire l'irritation sans nuire à l'apprentissage, tout en améliorant leur détection. L'impact potentiel de ces changements est énorme compte tenu de l'ampleur de leur utilisation. Par exemple, à tout moment, des dizaines de milliers de navires commerciaux naviguent sur le globe et génèrent en permanence des informations critiques pour la sécurité. Des dispositifs médicaux remplissent les hôpitaux du monde entier, fournissant des mises à jour cruciales en temps réel sur l'état des patients. Par conséquent, même de petits changements dans l'efficacité de leurs interfaces auditives peuvent apporter des améliorations significatives à la fois à la sécurité et au bien-être.

Dr. Michael Schutz

Dr. Michael Schutz

Use of sound signals in aids to navigation

The Canadian Coast Guard presence is generally noticed and recognized by the iconic red and white ships, hovercrafts and helicopters. However, there is much more to the CCG than this, the services provided by the Canadian Coast Guard are vast and include ice breaking, search and rescue, environmental response, Maritime Security, Marine Communications, Marine Navigation, and many others. It is the responsibility of the Canadian Coast Guard to ensure the safety of all mariners on our waters, protect the marine environment and support Canadian economic growth through the safe and efficient movement of maritime trade in and out of Canada's waters, approximately 243,000 km of coastline, the longest of any country in the world.

One of the services, is the provision of Marine Aids to Navigation to facilitate safe navigation. The Aids to Navigation Program uses aids to navigation to help mariners confirm their positions, stay inside navigable channels, and avoid marine hazards. Nationally, there are approximately 17,000 short-range aids to navigation (fixed and floating). In the Atlantic Region, there are approximately 1500 fixed aids to navigation and nearly 6000 floating aids, that consist of day marks, range marks, small and large buoys, towers, lights, and sound.

The intent of this discussion is to focus on the sound component of the aids to navigation network by providing a historical overview on the use of audible aids to navigation, from the early compressor fog horns and lighthouses to the current use of electronic fog detectors that trigger automated fog horns. The Aids to Navigation Program will explain how safe navigation routes are identified and the type of aids identified with a focus on sound. The Maritime and Civil Infrastructure group will identify and discuss some of the equipment used, such as horns, bell and whistle buoys and the installation, maintenance and associated challenges!

DFO Aids to Navigation and Maritime and Civil Infrastructure groups

Utilisation de signaux sonores dans les aides à la navigation

La présence de la Garde côtière canadienne est généralement remarquée et reconnue par les emblématiques navires, aéroglisseurs et hélicoptères rouges et blancs. Cependant, la GCC est bien plus que cela, les services fournis par la Garde côtière canadienne sont vastes et comprennent le déglaçage, la recherche et sauvetage, l'intervention environnementale, la sécurité maritime, les communications maritimes, la navigation maritime et bien d'autres. Il est la responsabilité à la Garde côtière canadienne d'assurer la sécurité de tous les marins sur nos eaux, de protéger l'environnement marin et de soutenir la croissance économique canadienne grâce à la circulation sécuritaire et efficace du commerce maritime à l'intérieur et à l'extérieur des eaux canadiennes, soit environ 243 000 km de côtes, le plus long de tous les pays du monde.

L'un des services est la provision d'aides maritimes à la navigation pour faciliter la sécurité de la navigation. Le Programme d'aides à la navigation utilise des aides à la navigation pour aider les navigateurs à confirmer leurs positions, à rester à l'intérieur des voies navigables et à éviter les dangers maritimes. À l'échelle nationale, il existe environ 17 000 aides à la navigation à courte portée (fixes et flottantes). Dans la région de l'Atlantique, il y a environ 1 500 aides fixes à la navigation et près de 6 000 aides flottantes, qui consistent en balises de jour, balises de distance, petites et grandes bouées, tours, feux et son.

Le propos de cette conférence est de se concentrer sur la composante sonore du réseau d'aides à la navigation en fournissant un aperçu historique de l'utilisation des aides sonores à la navigation, depuis les premiers phares et cornes de brume à compresseur jusqu'à l'utilisation actuelle de détecteurs de brouillard électroniques qui déclenchent des cornes de brume automatisées. Le Programme d'aides à la navigation expliquera comment les itinéraires de navigation sécuritaires sont identifiés et le type d'aides identifié en mettant l'accent sur le son. Le groupe d'Infrastructure maritime et civile identifiera et discutera de certains des équipements utilisés, tels que les avertisseurs sonores, les bouées à cloche et à sifflet, ainsi que l'installation, l'entretien et les enjeux associés à ceux-ci!

Groupes d'Aides à la Navigation et Infrastructure maritime et civile MPO

ACOUSTICAL EDUCATION
PANEL DISCUSSION

Have you ever wanted a better way to present acoustics ideas to your class? Or, maybe you need to explain to a client how your product will improve results? All of us have the challenge of presenting our ideas to an audience. And, in the case of acoustics, there are many ideas that are not immediately obvious to people without background training. Please join us for a panel discussion to share what works for you and maybe what does not work. We'd be pleased to have people share their problems so we can all brainstorm for a solution.

Dr. Len Zedel is Professor and Head of the Department of Physics and Physical Oceanography at Memorial University of Newfoundland.

His research interests focus on how acoustic systems can make measurements of physical ocean processes. He has 30-years-experience in teaching and loves to include demonstrations and real-world examples in lectures at all levels.

Dr. Benjamin Zendel holds the Canada Research Chair in Aging and Auditory Neuroscience and is an Associate Professor in the Faculty of Medicine at Memorial University of Newfoundland.

Dr. Zendel is a hearing and music scientist whose research is focused on the intersection of music, aging, cognitive neuroscience, and auditory perception. In his research he explores the possibility of using music and music training to improve hearing abilities in older adults. In the classroom Dr. Zendel loves to use auditory perceptual illusions to demonstrate how the auditory system works.

AWC 2022 SCHEDULE
ST JOHN'S - SEPTEMBER 28 TO 30, 2022

Note: All contributed presentations are scheduled for 15 minutes (12 minutes + 3 for questions)

Day 1	Wednesday, September 28

	SALON AB	SALON CD
8:45-9:00	Welcome	
9:00-10:00	KEYNOTE TALK (1 of 2) - **Michael Schutz**	
10:00- 10:30	Coffee Break	
10:30-12:00	MUSICAL ACOUSTICS 1	ARCHITECTURAL ACOUSTICS 1
	1. Is melodic expectancy vocally constrained? Evidence from two listening experiments - **Paolo Ammirante**	**1.** Corriger l'acoustique dans un cas d'école existante pour le bien-être des enfants et faciliter le travail du personnel éducatif - **Jean-Philippe Migneron**
	2. Using feedback to manipulate the tonal hierarchy - **Sarah Anne Sauvé**	**2.** The determining impact of architecture on sound in the built environment: Applications in sound masking systems and indoor noise sources - **Viken Koukounian**
	3. Differences between blocked and interleaved music-training on the ability to detect out-of-key notes and the associated brain responses - **Ozgen Demirkaplan**	**3.** Living with upstairs neighbors: recent studies on impact sound in residential buildings - **Markus Mueller-Trapet**
	4. Exploring the neurophysiological interaction between pitch and timing cues for the perception of metre - **Stephen Cooke**	**4.** Acoustic Design Challenges of the Tom Patterson Theatre - **Payam Ashtiani**
		5. Hybrid Assessment Method Web App For Impact Noise Insulation Performance Prediction In Building - **Mathieu Wahiche**
12:00-13:30	Lunch	
13:30-15:00	OCCUPATIONAL ACOUSTICS 1	ACOUSTIC MATERIALS & NOISE CONTROL
	1. Governance and noise exposures on board fishing vessels in Atlantic Canada - **Om Prakash Yadav**	**1.** Finite element design of acoustic metamaterial based on parallel Helmholtz resonators with embedded membranes - **Zacharie Laly**
	2. Using FRAM to support noise exposure management onboard vessels - **Muhammad Sabah Ud Din Ersum**	**2.** Numerical analysis of honeycomb structure with embedded membrane for transmission loss improvement - **Zacharie Laly**
	3. Occupational noise risk perception among fish harvesters in Newfoundland and Labrador - **Om Prakash Yadav**	**3.** Experimental characterization of acoustic materials in the presence of airflow at higher sound pressure excitations using a transfer matrix method - **Zacharie Laly**
	4. Auditory alarms in ship bridges: Understanding current challenges and limitations - **Robert Brown**	**4.** Acoustic Analysis of Electric Ducted Fans - **Joana Rocha**
		5. Vibration Analysis of an Electric UAV Wing Model - **Joana Rocha**
		6. Estimating sound absorption coefficient under various sound pressure fields by combining an automated test bench to sound field reproduction and advanced post-processing techniques - **Magdeleine Sciard**
15:00-15:30	Coffee Break	

15:30-17:00	PERCEPTION	UNDERWATER ACOUSTICS - SHIP NOISE 1

PERCEPTION

1. Identifying Hidden Hearing Loss - **Alicia Follet**

2. A comparison between CROS hearing aids and bone-anchored hearing aids for patients with single-sided deafness: a listening effort-based pilot study - **Olivier Valentin**

3. The effect of vowel lengthening on the intelligibility of occluded Lombard speech - **Xinyi Zhang**

4. A Whispered Christmas: Phonetic Expectations and Type of Masking-Noise Influence Auditory Verbal Hallucinations - **Mark Scott**

5. Study of Auditory Localization with a Wearable Microphone Belt Providing Haptic Feedback - **Ana Tapia Rousiouk**

UNDERWATER ACOUSTICS - SHIP NOISE 1

1. The MARS project: identifying and reducing underwater noise from ships in the St. Lawrence estuary - **Olivier Robin**

2. Identification of sources and their directivity in the global underwater radiated noise from a merchant ship - **Hugo Catineau**

3. Realistic corrections for ship source levels measured at Canadian acoustic ranges - **Cristina Tollefsen**

4. Assessment of the underwater noise levels from a fishing vessel using passive acoustic monitoring and structure hull vibration - **Khaled Mohsen Helal**

| 18:00-20:00 | **Welcome Reception** - Court Garden - Sheraton Hotel |
| 20:00-?? | **Student social event** - stay tuned for details |

Day 2	**Thursday, September 29**

	SALON AB	**SALON CD**
9:00-10:00	KEYNOTE TALK (2 of 2) - **Canadian Coast Guard**	
10:00- 10:30	Coffee Break	

10:30-12:00	MUSICAL ACOUSTICS 2	UNDERWATER ACOUSTICS - SHIP NOISE 2

MUSICAL ACOUSTICS 2

1. BRAMSBioBox: Developing an open research platform for audio and biosignals monitoring - **Jérémie Voix**

2. Measurements of mechanical properties of Adirondack spruce - **Olivier Robin**

3. Classifying the perception of different instruments using single trial EEG - **Praveena Satkunarajah**

4. Some Extensions on C. V. Raman's Study on Drums - **Udayanandan Kandoth Murkoth**

UNDERWATER ACOUSTICS - SHIP NOISE 2

1. Experimental model to predict underwater noise produced by structural radiation - **Jacopo Fragasso**

2. Influence of Background Noise in Propeller Induced Noise Measurement in Atmospheric Towing Tank - **Md Saiful Islam**

3. Interface forces identification using component TPA in-situ method for transfer path analysis (TPA) - **Hamdi Ben Amar**

4. Identification of the dynamic stiffness of vibration isolation interfaces by TPA engineering methods - **Houssine Bakkali**

5. Hybrid Model for Acoustic and Vibration Predictions Based on Vessel Induced Acoustic Vibration: A Review - **Solomon Ochuko Ologe**

| 12:00-13:30 | Lunch | |

13:30-15:00	ENVIRONMENTAL ACOUSTICS	ARCHITECTURAL ACOUSTICS 2

ENVIRONMENTAL ACOUSTICS

1. What is representative in monitoring environmental noise? - **Peter VanDelden**

2. The Impact of Working From Home on Post Pandemic Traffic Distributions and Noise Assessment - **Kathryn Katsiroumpas**

3. Soundscapes from an urban environment bordering on a green space - **Dale D Ellis**

ARCHITECTURAL ACOUSTICS 2

1. Wireless Loudspeaker Technology for More Efficient Sound Transmission Testing - **Jeremy Thorbahn**

2. Comparison of speech privacy metrics for open-plan and closed offices - **Rewan Toubar**

3. 2022 Comparison of the Acoustic Design Requirements of LEED, WELL and Green Globes - **Jessie Roy**

	4. Influence of Locomotive Speed and Throttle Profiles in Noise Modelling **- Gillian Redman**
	5. Analysis of ventilation coefficient and atmosphere stability during the post-monsoon **- Priyanka Singh**

15:00-15:30	Coffee Break
15:30-17:00	OCCUPATIONAL ACOUSTICS 2

4. The Evolution of RR-331 The Guide for Flanking Noise in Buildings **- Jeffrey Mahn**

5. The role of spectrum in subjective interpretation of speech privacy estimates: an analysis of prominent metrics **- Viken Koukounian**

15:30-17:00 — OCCUPATIONAL ACOUSTICS 2

1. Hearing protectors' comfort evaluation in the laboratory **- Said Ezzaf**

2. Impact of Coronavirus Face Masks on the Perceptual Evaluation of Hearing Protectors Comfort **- Olivier Valentin**

3. Effect of the error on the sound speed and microphone position on acoustic image obtained with a spherical microphone array **- Julien St-Jacques**

4. Toward detecting and classifying non-verbal events and biosignals in hearables **- Malahat H. K. Mehrban**

UNDERWATER ACOUSTICS - GENERAL

1. Modelling Split-Beam Sonar **- Axel Belgarde**

2. Remote Detection of Ocean Sound Speed Profile Using Acoustic Profiling Techniques **- seyed Mohammad Reza Mousavi**

3. Investigating Seasonal and Spatial Changes in Acoustic Backscatter Characteristics on the south coast of Newfoundland **- Nurul B. Ibrahim**

4. Measurements and modelling of a one-year under-ice acoustic propagation data set **- Sean Pecknold**

5. Bayesian inversion of ocean acoustic data for seabed geoacoustic profiles **- Stan Dosso**

17:00-18:00	**Annual General Meeting (AGM)** - all CAA members welcome to attend
18:00-22:00	**Banquet** - The Rooms, 9 Bonaventure Ave
	(A 5 minute walk up Military Road. Taxi chits available at AWC Welcome Desk for anyone who requires transportation.)

Day 3	Friday, September 30

	SALON AB	SALON CD
9:00-10:30	ACOUSTICAL EDUCATION - presentations	ARCHITECTURAL ACOUSTICS 3

ACOUSTICAL EDUCATION - presentations

1. Teaching acoustics using smartphones **- Olivier Robin**

2. Demonstrating wave interference using room acoustics **- Len Zedel**

3. Acoustics outreach activities made easy **- Cristina Tollefsen**

4. Teaching Concepts of Acoustical Waves in Air. How They Travel and How they Interact with Room Surfaces to Shape Indoor Acoustical Environments **- William Gastmeier**

5. New and old trends in teaching of building acoustics to future architects **- Jean-Philippe Migneron**

6. Modal propagation through a cylindrical pipe **- Len Zedel**

ARCHITECTURAL ACOUSTICS 3

1. Factors Affecting the ASTC Performance of Double Wood Stud Shear Walls in Mid-rise Residential Construction **- Anil Joshi**

2. Impact Sound Insulation Performance of Floating Floor Assemblies on Mass Timber Slabs under Different Excitation Sources **- Jianhui Zhou**

3. A study of dry linings in mass timber construction **- Wilson Byrick**

4. Comparing Low Frequency Sound Isolation of Different Structures **- Sarah Mackel**

5. Assessing and Controlling Wind Induced Noise from Perforated Aluminum Balcony Railing Panels **- Nathan Gara**

10:00- 10:30	Coffee Break
11:00	**Bus to harbour** with bagged lunch
12:00	Ship tour, bagged lunch at harbour
13:00	**Bus to MUN for School of Music tour** (stop at hotel on the way)

14:30	Return to hotel, coffee break
15:00-16:00	ACOUSTICAL EDUCATION - panel discussion

SPEECH PRODUCTION

1. Initiation and maintenance of lingual bracing posture - **Nicole Ebbutt**

2. Comparing Velum Velocity in Québécois French Nasals - **Annabelle Purnomo**

3. The estimation of tongue stiffness during phonation: An investigation using ultrasound shear wave elastography - **Chenhao Chiu**

16:00-17:00	**Awards ceremony** and thanks

ACOUSTIC MATERIALS - MATÉRIAUX ACOUSTIQUES

EXPERIMENTAL CHARACTERIZATION OF ACOUSTIC MATERIALS IN THE PRESENCE OF AIRFLOW AT HIGHER SOUND PRESSURE EXCITATIONS USING A TRANSFER MATRIX METHOD

Zacharie Laly[*1, 2], Xukun Feng[†2], and Noureddine Atalla [#3]
[1]CRASH, Centre de Recherche Acoustique-Signal-Humain, Université de Sherbrooke, Québec, Canada.

1 Introduction

The measurement with two microphones using transfer function method [1] can provide acoustic properties such as reflection coefficient and the sound absorption coefficient of a tested material. For the transmission performance characterization, more than two microphones are required. Munjal and Doige [2] presented theoretical expressions of two source-location method using four-microphone technique and transfer function approach to evaluate the four pole parameters of an acoustic element in the presence of airflow. The two-load method of ASTM E2611-09 [3] can be used experimentally to obtain the transfer matrix and transmission loss of a sample. However, the effect of the airflow is not included in this standard.

In this study, an experimental methodology based on transfer matrix approach is presented to evaluate the acoustic properties of materials at high sound pressure level (SPL) in the presence of airflow. The equations of ASTM E2611-09 are modified to account for the airflow effect. Two experimental measurements with two different termination loads under flow are required to derive the four-pole parameters of the tested material. The transfer matrix components are given as function of the pressures and velocities at both faces of the material. The proposed method shows good agreement with two-source method for different experimental measurements performed with airflow at high sound pressure levels.

2 Description of the measurement method with airflow

The present method to characterize acoustic materials in the presence of airflow at high SPL with airflow requires two experimental measurements with two different termination loads to retrieve the transfer matrix coefficients of the tested material. The first termination load can be an anechoic termination and the second an opened termination as shown in Fig. 1 that illustrates the sample and the forward and backward traveling waves A, B, C, and D.

In Fig. 1, d is the thickness of the sample, s_1 and s_2 represent the distance between each pair of microphones. The distance between microphone 2 and the front surface of the sample is denoted by L_1 while L_2 is the distance between microphone 3 and the front surface of the sample. The acoustic pressure and particle velocity upstream and downstream the

[*] zacharie.laly@usherbrooke.ca
[†] xukun.feng@usherbrooke.ca
[‡] noureddine.atalla@usherbrooke.ca
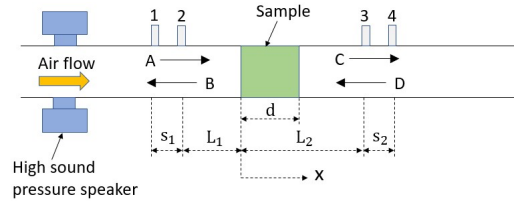
Figure 1: Two-load measurement method with open termination.

sample can be given as

$$p_u(x) = Ae^{-jk_u^+ x} + Be^{jk_u^- x},$$
$$p_d(x) = Ce^{-jk_d^+ x} + De^{jk_d^- x},$$
$$v_u(x) = \frac{1}{Z_u}\left(Ae^{-jk_u^+ x} - Be^{jk_u^- x}\right),$$
$$v_d(x) = \frac{1}{Z_d}\left(Ce^{-jk_d^+ x} - De^{jk_d^- x}\right),$$

(1)

with $j^2 = -1$, Z_u, k_u^+, and k_u^- are respectively the characteristic acoustic impedance and wavenumbers upstream the material, Z_d, k_d^+, and k_d^- the characteristic acoustic impedance and wavenumbers downstream the material. The wave numbers k_u^+ and k_d^+ are calculated using the models proposed by Howe [4] to account for the damping effects of the acoustic wave in the present of airflow. Two measurements with anechoic and opened terminations are performed under flow using the setup described in Fig. 2. These two terminations are denoted by load «a» and load «b». The setup is made of two anechoic terminations and two acoustic sources that can provide a high SPL up to 150 dB. The airflow through the duct is generated by a compressor. A temperature sensor is mounted in the tube to measure the temperature and two static pressure sensors are used to measure the static pressure upstream and downstream the sample. Then, the speed of sound in air c_0 and the density of the fluid ρ_u and ρ_d as well as the airflow Mach numbers upstream and downstream the sample are obtained

$$M_u = \frac{Q_m}{\rho_u c_0 S} \text{ and } M_d = \frac{Q_m}{\rho_d c_0 S}$$

(2)

with Q_m the mass airflow rate in kg/s and S the cross-sectional area of the tube. Four ¼ '' microphones PCB 378A14 are mounted flush with the inner wall of the tube and a NI CompactDAQ system is used for all signals acquisition. The distance between each pair of microphones is 40 mm and the inner diameter of the tube is 54 mm. The distance between microphone 2 and the sample is equal to the one between microphone 3 and the sample, which is 50 mm. A phase and amplitude calibration are done to minimize the error measurement of the microphones.

For the experimental measurements with loads «a» and «b», the complex amplitudes of the acoustic pressure A, B, C, D in Fig. 1 are expressed from Eq. (1) as function of the microphones measurement transfer functions and then the
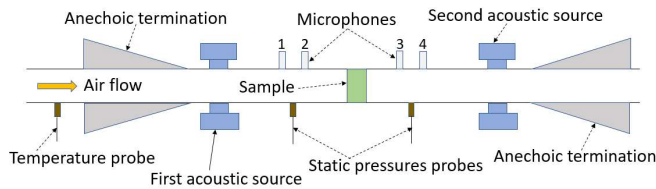
Figure 2: Experimental measurement setup.

pressures and velocities at both face of the material are deduced. From the two measurements with the two different termination loads, the transfer matrix components of the sample in the presence of the airflow are obtained,

$$T_{11} = \frac{p_{0a}u_{db} - p_{0b}u_{da}}{p_{da}u_{db} - p_{db}u_{da}} \text{ and } T_{12} = \frac{p_{0b}p_{da} - p_{0a}p_{db}}{p_{da}u_{db} - p_{db}u_{da}} \quad (3)$$

$$T_{21} = \frac{u_{0a}u_{db} - u_{0b}u_{da}}{p_{da}u_{db} - p_{db}u_{da}} \text{ and } T_{21} = \frac{p_{da}u_{0b} - p_{db}u_{0a}}{p_{da}u_{db} - p_{db}u_{da}} \quad (4)$$

The transmission loss is then calculated using the four components of the transfer matrix in Eqs. (3) and (4).

3 Comparison of the present method with two source method

A perforated silencer containing a single chamber is tested at 145 dB. The inner diameter of the perforated tube and the outer diameter of the silencer are respectively 54 = mm and 149 mm and the length of the perforated tube is 243 mm. The chamber of the silencer is filled with fibrous wool with a mass of 394.2 g. Figure 3 shows the comparison of the transmission loss of the perforated silencer filled with fibrous wool for mass airflow rate of 158 kg/h, which corresponds to airflow Mach number of 0.049. The present method is compared with two-source method that is de-scribed in Ref [2].
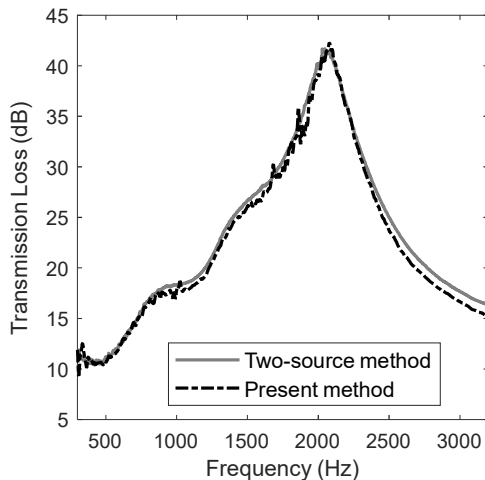
Figure 3: Comparison of the transmission loss of a perforated silencer filled with fibrous wool.

The result of the present method in Fig. 3 agrees well with two-source method. Figure 4 shows the transmission loss of a micro perforated panel absorber made of a panel with slit-shaped holes with a thickness of 0.6 mm backed by a honeycomb structure with thickness of 17.75 mm and a rigid wall. The measurement is performed at grazing incidence for a SPL of 140 dB and airflow Mach number of 0.103.
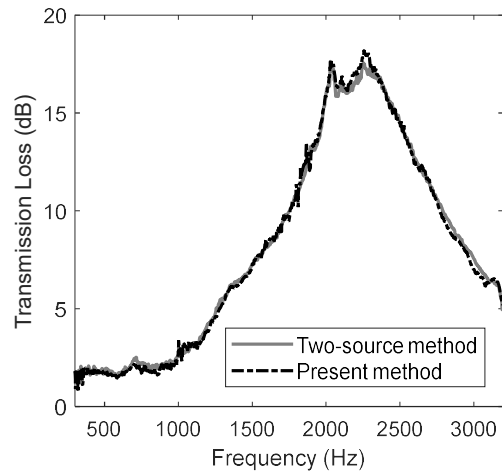
Figure 4: Comparison of the transmission loss of perforated panel absorber with slit-shaped holes at grazing incidence.

In Fig. 4, the present method and two-source method results are in good agreement.

4 Conclusions

An experimental method based on ASTM E2611-09 standard is presented to measure the acoustic properties of material at higher sound pressure excitations in airflow environment. Two experimental measurements with two different termination loads are performed to retrieve the four-pole parameters of the tested material. The proposed method shows good agreement with two-source method. It can be used to characterize experimentally acoustic materials in the presence of airflow at high SPL.

Acknowledgments

References

[1] ISO 10534-2. Acoustics—Determination of Sound Absorption coefficient and Impedance method in Impedance Tubes, Part II: Transfer–Function method, 1998.

[2] M.L. Munjal, and A.G. Doige. Theory of a two source-location method for direct experimental evaluation of the four-pole parameters of an aeroacoustic element. Journal of Sound and Vibration, 141(2): 323-333, 1990.

[3] ASTM E2611-09: Standard Test Method for Normal Incidence Determination of Porous Material Acoustical Properties Based on the Transfer Matrix Method (American Society for Testing and Materials, New York; 2009).

[4] M.S. Howe. The damping of sound by wall turbulent sheer layers. Journal of Acoustical Society of America, 98 (3): 1723–1730, 1995.

FINITE ELEMENT DESIGN OF ACOUSTIC METAMATERIAL BASED ON PARALLEL HELMHOLTZ RESONATORS WITH EMBEDDED MEMBRANES

Zacharie Laly[*1, 2], **Christopher Mechefske**[†2], **Sebastian Ghinet**[‡3], **Behnam Ashrafi**[♦4], and **Charly T. Kone**[#3]

[1]CRASH, Centre de Recherche Acoustique-Signal-Humain, Université de Sherbrooke, Québec, Canada.
[2]Department of Mechanical and Materials Engineering, Queen's University, Kingston, ON, K7L 3N6, Canada.
[3]Aerospace, National Research Council Canada, Ottawa, ON K1A 0R6, Canada.
[4]Aerospace Manufacturing Technology Center, National Research Council Canada, 5145 Decelles Avenue, Montreal, Canada.

1 Introduction

Noise pollution reduction is an environmental necessity. Acoustic metamaterials based on periodic Helmholtz resonators can offer high efficiency in attenuating multi-tonal noise at low frequencies. Laly et al. [1] used the finite element method to develop designs of acoustic metamaterials made of parallel assemblies of Helmholtz resonators, which are periodically embedded within a porous material. The proposed metamaterial designs show multiple transmission loss (TL) peaks. Porous material combined with embedded periodic Helmholtz resonators that contain a membrane in the cavity was investigated numerically by Laly et al [2]. The use of a membrane in the resonator cavity induces multiple TL peaks while only one TL peak is observed with a conventional resonator. They illustrate the influences of the membrane thickness and position on the TL. Guo et al. [3] studied a checkerboard absorber constituted by parallel assemblies of Helmholtz resonators for sound absorption improvement. Mahesh and Mini [4] characterized a parallel assembly of Helmholtz resonators using a parallel transfer matrix method and the analytical results show good agreement with finite element method results. An increase of the sound absorption bandwidth was observed when parallel arrangement of dissimilar Helmholtz resonators was used.

In this study, a design of acoustic metamaterial based on a parallel assembly of four Helmholtz resonators with extended necks is proposed and studied numerically using COMSOL Multiphysics. A damping material in the form of a membrane is inserted into each sub-cavity. The parallel assembly of four Helmholtz resonators is periodically distributed within a porous material. Four TL peaks are observed with the parallel assembly of four resonators without embedded membranes. For membranes with free boundary conditions inside each sub-cavity, eight resonant TL peaks are obtained and for fixed boundary conditions, the TL presents twenty resonant frequencies.

2 Design of acoustic metamaterial based on parallel Helmholtz resonators with embedded membranes

Figure 1(a) shows a parallel assembly of four Helmholtz re-

[*] zacharie.laly@usherbrooke.ca
[†] chris.mechefske@queensu.ca
[‡] sebastian.ghinet@nrc-cnrc.gc.ca
[♦] behnam.ashrafi@nrc-cnrc.gc.ca
[#] tenoncharly.kone@nrc-cnrc.gc.net

sonators with extended necks. The cylindrical cavity is partitioned into four sub-cavities with the same volume that are separated from one another by a wall. A membrane is inserted within the cavity of each resonator. The air inside each neck is characterized using the thermo-viscous acoustic interface to account for the viscous and thermal dissipations effects. The parallel assembly of resonators is embedded periodically within a porous material that is modeled using Johnson-Champoux-Allard model. The geometry of the Periodic Unit Cell (PUC) is illustrated in Fig. 1(b) and the mesh in Fig. 1(c), which consists of 37 580 domain elements and 10 673 boundary elements. Periodic boundary conditions are applied on all parallel plans.
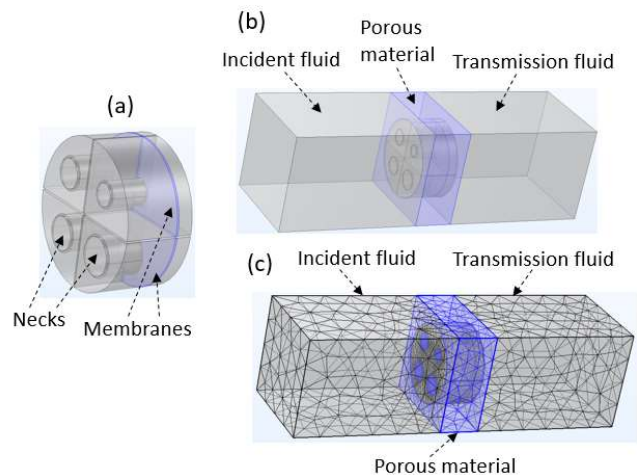
Figure 1: Acoustic metamaterial: (a) parallel assembly of four Helmholtz resonators with embedded membranes (b) geometry of the PUC (c) mesh of the PUC.

The airflow resistivity of the porous material is 26 000 N s m $^{-4}$ with a porosity of 99%. The tortuosity is 1.02, and the characteristic viscous and thermal lengths are respectively 150 μm and 300 μm. The membrane is ethylene-vinyl acetate rubber material with Young's modulus of 5 MPa, a density of 660 kg/m^3 and a Poisson's ratio of 0.45. It is modeled as a linear isotropic material using a solid mechanics interface. The thickness of the membrane is set to 1 mm; the diameter of the global cylindrical cavity is 80 mm with a length of 40 mm that is equal to the thickness of the porous layer. The wall of the resonators is considered rigid. The radii of the necks are respectively 6 mm, 8 mm, 9 mm and 10 mm with the same length of 20 mm. Each membrane inside each sub-cavity is located at 10 mm from the bottom inner wall of the cavity. A normal incidence plane wave with

pressure amplitude of 1 Pa is applied on the inlet plane while plane wave radiation condition is applied on the inlet and outlet planes. The sound transmission loss is given by

$$TL = 10\ log_{10}\left(\frac{W_{in}}{W_{out}}\right) \qquad (1)$$

with W_{in} and W_{out} the incoming power at the inlet plane and the outgoing power at the outlet plane.

3 Finite element results of the proposed metamaterial design

Figure 2 shows the transmission loss of the metamaterial without membranes and the case where the boundaries of each membrane within each sub-cavity are free. In Figure 3, the TL is illustrated for membranes with fixed boundaries conditions.
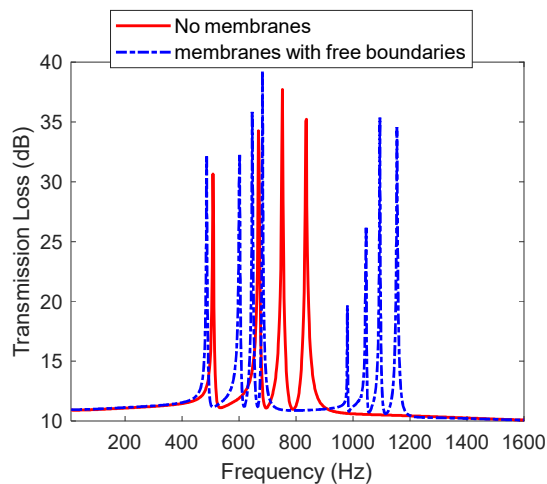
Figure 2: Transmission loss of acoustic metamaterial made of parallel assembly of four Helmholtz resonators.
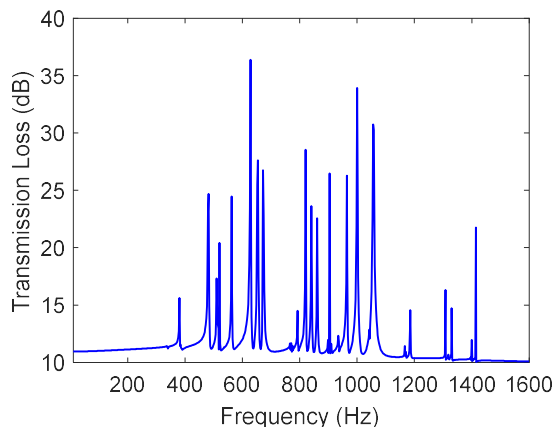
Figure 3: Transmission loss of acoustic metamaterial made of parallel assembly of four Helmholtz resonators containing membranes with fixed boundaries.

In Fig. 2, when there are no membranes within the subcavities of the resonators, there are four transmission loss peaks, which are 30.6 dB, 34.27 dB, 37.72 dB and 35 dB at respective frequencies of 508 Hz, 668 Hz, 752 Hz and 836 Hz. When a membrane is inserted within each sub-cavity with free boundary conditions, the TL presents eight resonant frequencies in Fig. 2, which are 486 Hz, 602 Hz, 646 Hz, 682 Hz, 980 Hz, 1046 Hz, 1094 Hz and 1154 Hz where the values of the TL peaks are respectively 32.24 dB, 32.35 dB, 35.84 dB, 39.26 dB, 19.64 dB, 26.27 dB, 35.37 dB and 34.55 dB. In Fig. 3 where the boundary conditions of each membrane within each sub-cavity are fixed, the TL present 20 resonant peaks. The use of the membrane within each sub-cavity induces multiple TL peaks. This design can be useful for noise mitigation at multiple frequencies simultaneously.

4 Conclusions

A design of acoustic metamaterial made of a parallel assembly of four Helmholtz resonators is proposed and investigated numerically using the finite element method. The cylindrical global cavity is partitioned into four sub-cavities with equal volume, which are separated from one another by rigid walls and an extended neck is connected to each sub-cavity. A damping material in the form of a membrane is inserted into each sub-cavity. The parallel assembly of four Helmholtz resonators is periodically distributed within a porous material. The transmission loss of the parallel assembly of four resonators without embedded membranes presents four resonant peaks. When a membrane is inserted within each sub-cavity with free boundary conditions, eight resonant TL peaks are obtained and for fixed boundary conditions, the transmission loss presents 20 resonant peaks. The proposed acoustic metamaterial design can be used in many industrial applications for multi-total noise reduction.

References

[1] Z. Laly, C. Mechefske, S. Ghinet, and C.T. Kone. Numerical design of acoustic metamaterial based on parallel Helmholtz resonators for multi-tonal noise control. In Proceedings of 2022 Inter-national Congress on Noise Control Engineering, INTER-NOISE 2022, 21-24 August 2022, Glasgow, UK.

[2] Z. Laly, C. Mechefske, S. Ghinet, and C.T. Kone. Numerical modelling of acoustic metamaterial made of periodic Helmholtz resonator containing a damping material in the cavity. In Proceedings of 2022 Inter-national Congress on Noise Control Engineering, INTER-NOISE 2022, 21-24 August 2022, Glasgow, UK.

[3] J. Guo, Y. Fang, Z. Jiang, and X. Zhang. Acoustic characterizations of Helmholtz resonators with extended necks and their checkerboard combination for sound absorption. *Journal of Physics D: Applied Physics, 53,* 505504, 2020.

[4] K. Mahesh, and R.S. Mini. Investigation on the Acoustic Performance of Multiple Helmholtz Resonator Configurations. *Acoustics Australia* 49, 355–369, 2021.

NUMERICAL ANALYSIS OF HONEYCOMB STRUCTURE WITH EMBEDDED MEMBRANE FOR TRANMISSION LOSS IMPROVEMENT

Zacharie Laly[*1, 2]**, Christopher Mechefske**[†2]**, Sebastian Ghinet**[‡3]**, Behnam Ashrafi**[♦4]**, and Charly T. Kone**[#3]
[1]CRASH, Centre de Recherche Acoustique-Signal-Humain, Université de Sherbrooke, Québec, Canada.
[2]Department of Mechanical and Materials Engineering, Queen's University, Kingston, ON, K7L 3N6, Canada.
[3]Aerospace, National Research Council Canada, Ottawa, ON K1A 0R6, Canada.
[4]Aerospace Manufacturing Technology Center, National Research Council Canada, 5145 Decelles Avenue, Montreal, Canada.

1 Introduction

Honeycomb structures find use in many applications because of their high stiffness to weight ratio and excellent mechanical impact energy absorption. However, their acoustic performance is poor. Li et al [1] studied the transmission loss (TL) of lightweight multilayer honeycomb membrane-type acoustic metamaterials experimentally and observed that the sandwich panel acoustic metamaterials exhibit good TL. A lightweight and yet sound-proof honeycomb acoustic metamaterial is investigated by Sui et al. [2] and Lu et al. [3]. The metamaterial structure is made of a lightweight flexible rubber material layer sandwiched between two layers of honeycomb cell plates. They demontrated excellent TL with minimum weight-penalty. Li et al. [4] presented a theoretical model to estimate the TL of acoustic micro-membranes, which demonstrate improved TL at low frequency.

In this study, the transmission loss of a honeycomb structure with embedded membranes is investigated using the finite element method. It is shown that the transmission loss of the honeycomb structure is significantly improved by the embedded membrane while the TL of the honeycomb structure core alone is zero. The influence of the honeycomb structure cell size is illustrated as well as the effect on the membrane material properties. The investigated structure presents good TL especially at low frequencies.

2 Finite element analysis of honeycomb structures with embedded membranes

Figure 1 shows a honeycomb structure with one embedded membrane layer. The thickness of each honeycomb structure layer in Fig. 1(a) is set to 4 mm and the thickness of the membrane is 1 mm. The boundary between the membrane and each honeycomb structure layer is considered fixed. Figure 1(b) illustrates the geometry used in the numerical simulations. An incident fluid and transmission fluid are connected to the structure and all the air domains within the honeycomb structure cells are defined. The cell size with a radius denoted by R_c is illustrated in Fig. 1(c) and the mesh of the geometry is shown in Fig. 1(d), which contains 44 968 domain elements and 14 702 boundary elements. Young's modulus, the den-

sity, and the Poisson's ratio of the honeycomb material structure are respectively 2.7 GPa, 1100 kg/m³ and 0.38 with a cell size of 5 mm. The thickness of the incident and transmission fluid is set to 80 mm and the lateral dimensions of the geometry are 56 mm x 60 mm. A normal incidence plane wave with pressure amplitude of 1 Pa is applied on the inlet plane of the incident fluid domain while a plane wave radiation condition is applied on the inlet and outlet planes to minimize the reflection of the acoustic waves. Acoustic-solid interaction of COMSOL Multiphysics is used for the numerical simulations. The sound transmission loss is determined by the relation

$$TL = 10\, log_{10}\left(\frac{W_{in}}{W_{out}}\right) \qquad (1)$$

where W_{in} and W_{out} are respectively the incoming power at the inlet plane and the outgoing power at the outlet plane.
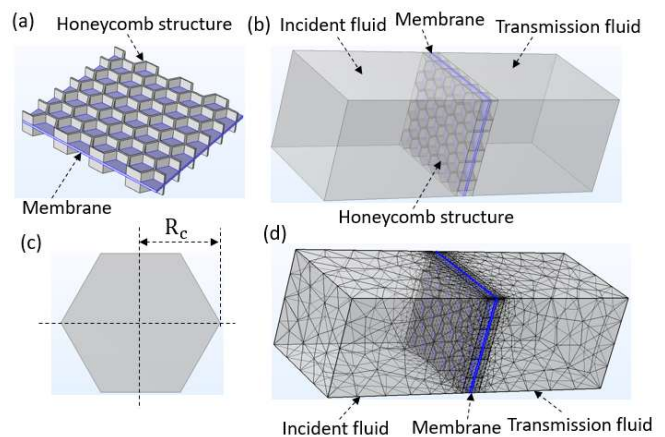
Figure 1: Honeycomb structure: (a) two honeycomb layers with embedded membrane (a) geometry (c) one honeycomb cell (d) mesh.

Different membrane material properties with Young's modulus that are gradually increased from 1.2 MPa to 100 MPa are considered as shown in Table 1. Membrane 1 is butyl rubber while membrane 3 is a silicone elastomer and membranes 2 and 4 are ethylene-vinyl acetate rubbers.

3 Finite element results

The impact of the membrane material properties on the TL is illustrated in Fig. 2 where the damping loss factor of each membrane is set to 0.1.

Table 1: Material properties of the membrane

---
[*] zacharie.laly@usherbrooke.ca

[†] chris.mechefske@queensu.ca

[‡] sebastian.ghinet@nrc-cnrc.gc.ca

[♦] behnam.ashrafi@nrc-cnrc.gc.ca

[#] tenoncharly.kone@nrc-cnrc.gc.net

Membranes	Young's modulus (MPa)	Density (kg/m³)	Poisson's ratio
1	1.2	910	0.4
2	5	660	0.45
3	12	1400	0.48
4	25	850	0.46
5	100	1100	0.49
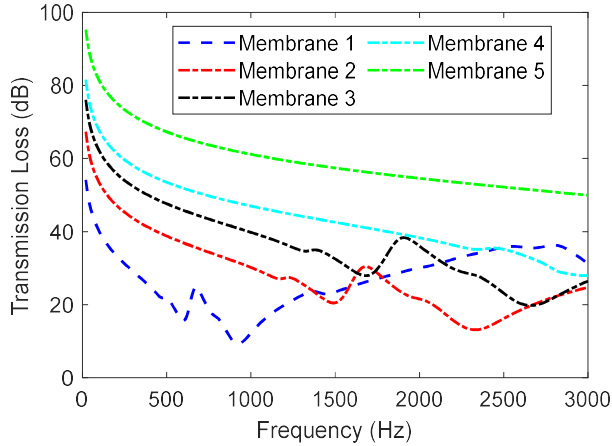
Figure 2: Normal Incidence Transmission Loss of honeycomb structure with embedded membrane.

In Fig. 2, it can be observed that the TL increases over a large frequency band as the membrane Young's modulus increases.

In Fig. 3, the effect of the honeycomb cell size on the TL is illustrated using membrane 2 of Table 1 with a thickness of 0.5 mm. In Fig .4, the influence of the number of membrane layers within the honeycomb structure is presented where membrane 2 of Table 1 is used with a thickness of 1 mm. For the two-membrane layer case, the thickness of the honeycomb cell between each membrane layer is set to 10 mm and for the three-membrane layer case; the thickness of each honeycomb cell is set to 5 mm. The simulations are conducted with one honeycomb cell with membrane fixed boundary conditions, which is connected to incident and transmission fluids.
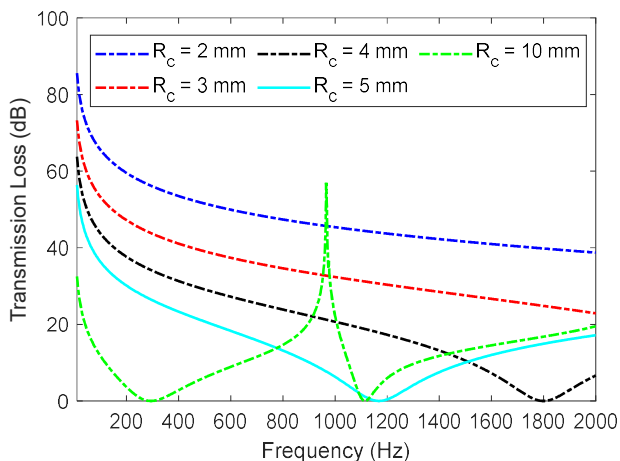
Figure 3: Effect of the honeycomb cell size on the transmission loss.
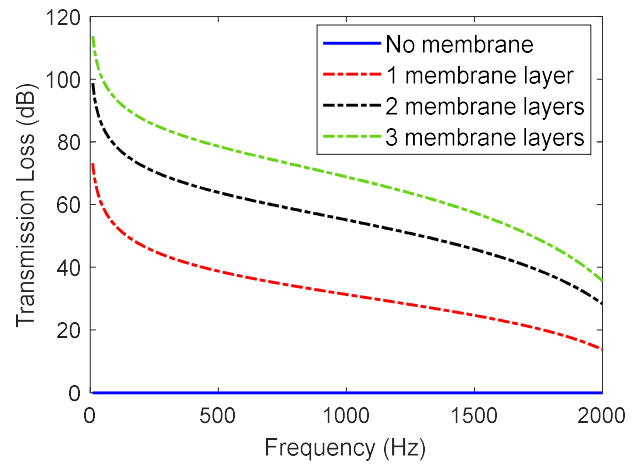
Figure 4: Effect of the number of membrane layers on the transmission loss.

In Fig. 3, the TL for $R_c = 10\ mm$ presents a peak value of 57 dB at 966 Hz. The TL increases over a large frequency band as the honeycomb cell size is reduced. The TL of the honeycomb structure alone without membrane in Fig. 4 is zero and when the number of membrane layers increases, the TL increases over the entire frequency range.

4   Conclusions

The transmission loss of a honeycomb structure with embedded membranes is studied using finite element method. It is shown that the TL increases over a large frequency band when the honeycomb cell size decreases. The influence of the membrane material properties on the TL is presented. The TL of the honeycomb structure alone without membrane is zero and when the number of membrane layers within the structure increases, the TL increases over the entire frequency range. The investigated structure can offer excellent performance in noise control engineering especially at low frequencies.

Acknowledgments

References

[1] Y. Li, Y. Zhang, and S. Xie. A lightweight multilayer honeycomb membrane-type acoustic metamaterial. Applied Acoustics, 168 107427, 2020,

[2] N. Sui, X. Yan, T.-Y. Huang, J. Xu, F.-G. Yuan, and Y. Jing. A lightweight yet sound-proof honeycomb acoustic metamaterial. Appl. Phys. Lett. 106, 171905, 2015.

[3] K. Lu, J.H. Wu, D. Guan, N. Gao, and L. Jing. A lightweight low-frequency sound insulation membrane-type acoustic metamaterial. AIP Advances 6, 025116, 2016.

[4] S. Li, D. Mao, S. Huang, and X. Wang. Enhanced transmission loss in acoustic materials with micro-membranes. Applied Acoustics, 130, 92–98, 2018.

ACOUSTICS EDUCATION - ENSEIGNEMENT DE L'ACOUSTIQUE

TEACHING CONCEPTS OF ACOUSTICAL WAVES IN AIR
HOW THEY TRAVEL AND SHAPE ACOUSTICAL ENVIRONMENTS

William J. Gastmeier, MASc, PEng

HGC Engineering, Mississauga, Ontario, Canada

1 Introduction

This paper has been written to supplement a session in "Teaching Acoustics" at the 2022 CAA conference. It contains materials extracted from 30 years of teaching to Architects at the University of Waterloo and Dalhousie University in Halifax.

The purpose of this session is to provide teachers with practical demonstrations which can be used to enhance learning. It has always been my teaching philosophy that a teacher engages multiple senses to be effective at instilling knowledge, and what is better for architects and acousticians than using sight and sound as well as written materials.

Here are a few demonstrations I have used over the years.

1) The use of a **rope** to demonstrate our collective incorrect assumption that sound travels like waves on water and examine the speed of sound in various media.

2) The use of a **coiled flexible spring** to demonstrate the concepts of transverse and longitudinal waves. Hint: sound in air propagates as a longitudinal spherical wave modified by the directivity of the source.

3) The use of an **electronic oscillator and loudspeaker** to illustrate concepts of frequency and wavelength.

4) The use of **balloons.** Since balloons are 99% air, they are pretty much transparent to sound but they do react to sound in a manner which is instructive to our understanding of the human auditory mechanism and how sound propagates in air and through partitions.

2 Understanding Wave Propagation

There are two types of waves of interest in this regard: transverse and longitudinal.

This is our common intuition of how sound travels. Transverse waves travel on a string or on a surface and particle motion is perpendicular to the direction of propagation. **This is not how sound travels,** but the concept is useful in demonstrating the speed of sound.

2.1 Demonstration 1: The Rope

This demonstration shows the transverse nature of waves on a string as well as the relationship of the speed of sound to the elasticity of the medium. Speed is equal to distance travelled per unit time.

$$c = d\,/t \qquad (1)$$

---

* bill@gastmeier.ca
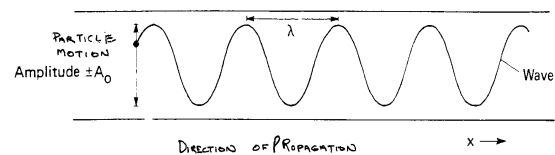
Figure 1: Transverse Waves

The speed of sound depends on elasticity, density and temperature. The relationship of the speed of sound to the elasticity and density is given by the formula $c = k\sqrt{(\varepsilon/\rho)}$

Tie the rope to a solid object, hold it under some tension and puck it like a guitar string. Watch the impulse and the speed at which it propagates. Then pull harder on the rope to increase the tension (elasticity) Note that the wave propagates more quickly. You can also demonstrate reflections in this way

The speed of sound at normal atmospheric pressure and room temperature is **c = 344 m/sec.**

Equate this to a physical situation. How close to you are to the lightning strike? If you hear the thunder one second after seeing the flash it is only 344 m away!

And if you clap your hands in a living room with typical dimensions of 6 meters the sound will be reflected ~50 times in just one second. More often from the ceiling which is less than 3 m high!

Another fun concept to investigate is … does air really have mass and elasticity? We take air so for granted that it is invisible to us in those terms. The mass of air causes an atmospheric pressure of ~ 100 Millibars (weather forecast) or ~ 15 pounds (7 kg) per square inch. Massive!

Concerning elasticity, can you bounce a basketball if it is not inflated with air? The elasticity comes from the air, not the rubber.

So here is another question … Why is the speed of sound faster in water?
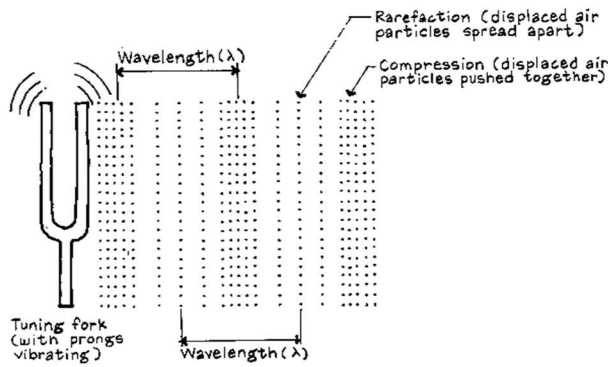
Figure 2: Longitudinal Waves

Because of the relationship of mass and elasticity. Water is more massive than air, but it is also much more elastic. It hurts much more when you belly flop into water than when you are diving through the air.

Longitudinal Waves travel in a bulk (three dimensional) medium. Particle motion is in the same direction as the direction of propagation.

This is how sound travels, although not equally in all directions.

2.2   Demonstration 2: The Coiled Spring

Use a coiled spring (Slinky) to set up longitudinal waves to illustrate the above. Firm up the concept that individual air molecules are pushing against and recoiling from each other as the energy propagates outwards from the source. Make the extension that there are a large number of slinkys connected to any noise source radiating sound in all directions, some more strongly than others (directivity) hence spherical wave propagation.

2.3   Demonstration 3: Oscillator/Speaker

Set up a loudspeaker connected to a variable frequency sinusoidal oscillator. Your laptop or smart phone will not work well for this demonstration. They may be able to produce the tones, but not visually.

Show that the speaker pushes in and out to create longitudinal waves.

Set the oscillator to 100 Hz and let them hear the bass sound. Illustrate with your body (put your arms out and walk around) how a frequency of 100 Hz results in a wavelength of 3.44 meters (~ 10 feet) …. Compression, rarefaction, compression always pushing outwards.

Set the oscillator to 1000 Hz and illustrate with your body how the wavelength has decreased to 1 foot, like the size of their heads (at least the smart ones) and then to 10,000 Hz and the wavelength is ~ 1 inch, roughly the size of their ears.

The important concept here is that our human perception is based on frequency as exhibited by wavelength and that other creatures perceive a different soundscape because of their physical size. Whales tend to communicate with lower frequency signals and bats and birds with higher frequencies.

2.4   Demonstration 4: Balloons

Balloons can be a fun part of all of this.

Have them available and have the students blow them up as they come into the classroom,

Balloons can be used to reinforce all the above concepts in a positive manner. Here are some thoughts for you.

Invite them to hod the balloon lightly with their fingertips and feel the vibration in the balloon from demonstration 3 as the frequency is changed to accommodate the balloons natural frequency of vibration.

What is causing the vibration? Areas of high and low pressure (compression and rarefaction) passing by.

Connect with how our tympanic membrane vibrates from longitudinal waves. OK, that was science speak around the entrance impedance into our middle and inner ear.

Make the extension to sound incident on a wall. Because it is a longitudinal wave, it exerts pressure against the wall which sets it in motion and causes sound to be radiated from the other side.

3   Conclusion

Presenting visual and audible examples and demonstrations can be very important to teachers of acoustics. Providing this kind of baseline knowledge to our communities is important as acoustical fundamentals such as these may not always be taught in our public schools.

References

This material was extracted from course notes prepared for undergraduate students of Architecture at the University of Waterloo and Dalhousie University.

TEACHING ACOUSTICS USING SMARTPHONES

Olivier Robin[*1]

[1]Centre de Recherche Acoustique-Signal-Humain, Université de Sherbrooke, Sherbrooke, Québec, Canada.

1 Introduction

Almost an infinity of smartphone applications exist. Some of them can be related to acoustics and its teaching or be used to encourage experiential learning. This communication presents some possible applications. In particular, three hands-on exercises that are used in an undergraduate course 'Acoustics and noise control' at Université de Sherbrooke (UdeS) are presented.

2 Short overview of acoustics teaching or research approaches using smartphones

Since reviewing all available apps for acoustics and vibration measurement is beyond the scope of this communication, only the three apps used at UdeS are briefly introduced.

Apps for noise measurement.

NoiseCapture [1, 2] is a free and open-source Android application. It allows users to measure sound pressure levels, and to display them as a function of time, frequency, or time/frequency. Each measurement is also combined with its GPS track so that the result can be displayed on an interactive map (Figure 1). A calibration section with different methods is also included in this app (direct, relative). This app has been used in science events for education and awareness purposes for environmental noise assessment (general public/secondary/high school level), for research purposes (crowdsourced noise maps) for indoor noise mapping and finally teacher trainings [1, 2]. *OpeNoise* (Android and iOS) shares the same features as *NoiseCapture*, at the exception of the spatial positioning. Concerning reverberation time measurements, one can cite *APM tool lite* (for Android and iOS). Using hand claps as excitation signals, this app provide reverberation time in octave bands (250 Hz to 4 kHz), and the calculation of additional indicators such as T20, T30 or definition index (D50).

Apps for physics measurements.

Phyphox is an app available for both Android and iOS devices. It provides access to the direct readings from the sensors of your smartphone. Raw data export is straightforward, and remote access to the measuring smartphone from another device is allowed, the measured data can be easily post-processed [3]. Ready-to-play experiments are also available, and any experiment can be built using a web-based design tool on Phyphox website.

3 Smartphones for acoustics teaching.

A series of examples for smartphone-based experiments can be found in the bibliography section of [4] (Refs.[1-8]) and [5] (Refs. [3-11]). These applications include the measure-

---

*olivier.robin@usherbrooke.ca

ment of the speed of sound in air or in water [4], the characterization of Helmholtz resonators or the measurement of the acoustic response of classrooms [5].
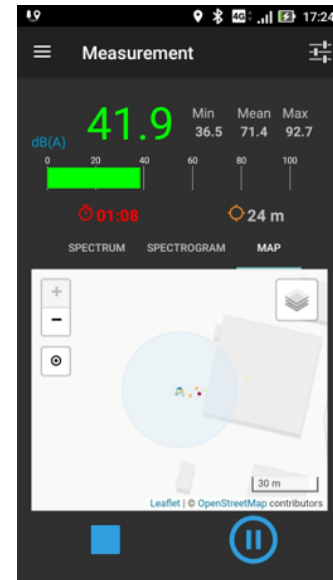
Figure 1: Screen capture of the *NoiseCapture* app with GPS positioning [1].

4 Three examples at UdeS

4.1 Calibrating a smartphone and comparing measured values with other sound level meters.

A first and mandatory example is the calibration of apps to obtain meaningful results. This is also a first step for students to understand the general concept of sensor calibration. Students are asked to calibrate the microphone of their smartphone using a sound source (that can be generated using another smartphone, see Figure 2). The calibration is done by comparison with measurements made using two Class 2 sonometers with digital and needle displays, respectively (Figure 2). Students are asked to make sound pressure level (SPL) measurements for various source types or contexts (they have to chose their own examples) and for at least two different SPL meters. They have then to gather all obtained results in a small report, and these results are discussed during the following course. This laboratory helps students to understand the underlying challenges of sound pressure level measurement (calibration, influence of the measurement position, noise type's influence), and to have a clear idea of the usual SPL encountered in real life applications.

4.2 Mapping sound pressure levels on the university campus.

In this participating laboratory, all the students following the course are asked to contribute to a noise map of the main
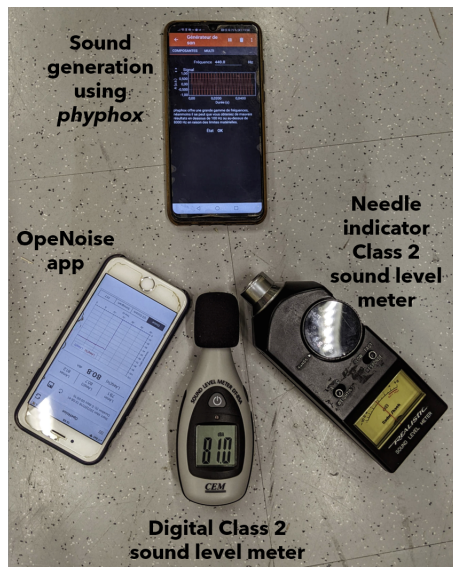
Figure 2: Relative calibration of a smartphone with two Class 2 sonometers - A reference sound source is achieved using another smartphone.

campus at UdeS using the *Noisecapture* app. Between two consecutive courses (one week), the students are asked to use their calibrated smartphones to contribute to a crowd sourced noise map of the campus. This is an occasion for them to be introduced to participating and noise mapping approaches. The results are dicussed during the course.

4.3 Measuring vibration levels and extracting significant features.

This lab is meant to help student making the link between vibration measurements and the extraction of features using simple FFT computations. The goal is to retrieve the idling rpm of a vehicle, as depicted in Figure 3 (note that only idling condition is considered to ensure safety). The students are asked to place the smartphone on a car hood, to launch a vibration measurement using *Phyphox* application, and finally to start the vehicle and stop it after approximately 60 seconds. The raw data (Figure 3-2) is then post-processed using Matlab. A value of 797 rpm is finally estimated by multiplying the identified fundamental frequency (13.31 Hz, see Figure 3-3) by a 60 factor to convert it into rpm (car's tachometer indicates 800 rpm).

5 Discussion and perspectives

This communication briefly introduces the possible uses of smartphones in acoustics teaching, including three examples extracted from a series of ten labs using smartphones developed at UdeS. These labs have several advantages including (1) the fact that laboratories can be handled in actual situations with no specific lab room nor specific tools and (2) the fact that the main lab support, a smartphone, is a common resource to all students making it accessible and flexible. The first results extracted from recent surveys indicate that students engagement and experiential learning are improved.
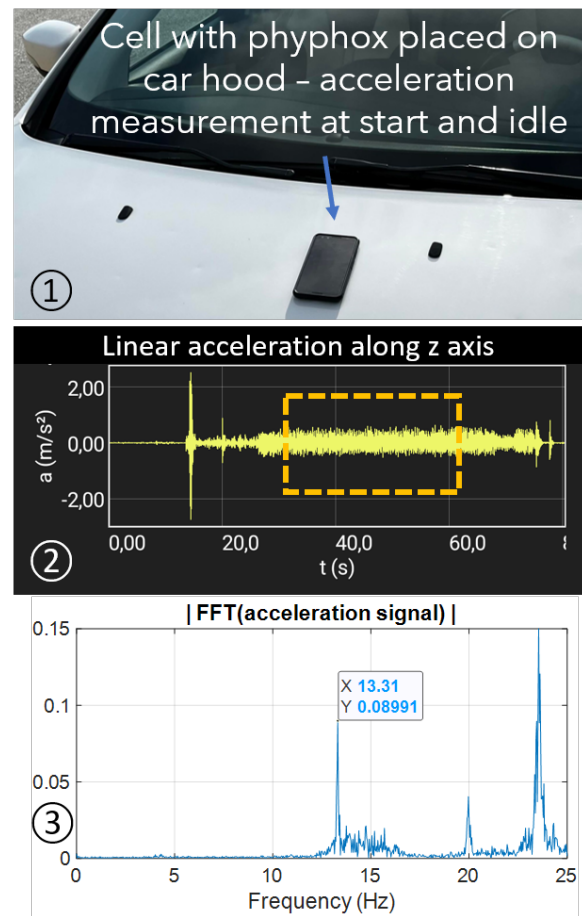
Figure 3: Estimation of the idling rpm of a car - (1) Vibration measurement on the car hood - (2) Raw acceleration time signal (the chosen idling time window is indicated by a dashed orange box) - (3) Computation of the FFT to estimate the engine's fundamental frequency of rotation.

The perspectives include (1) the continuous improvement of acoustics-related labs, and (2) the use of smartphones in a thermal course using infrared smart cameras.

Acknowledgments

References

[1] J. Picaut et al. An open-science crowdsourcing approach for producing community noise maps using smartphones. *Building and Environment*, 148:20–33, 2019.

[2] G. Guillaume et al. Noisecapture smartphone application as pedagogical support for education and public awareness. *J. Acoust. Soc. Am.*, 151(5):3255–3265, 2022.

[3] S. Staacks et al. Advanced tools for smartphone-based experiments: phyphox. *Phys. Educ.*, 53(4):045009, 2018.

[4] M. Monteiro and A. Martí. Using smartphones as hydrophones: two experiments in underwater acoustics. *Phys. Educ.*, 55(3):033013, 2020.

[5] E. Macho-Stadler and M. Elejalde-Garcia. Measuring the acoustics response of classrooms with a smartphone. *Phys. Teach.*, 58:585–588, 2020.

Abstracts for Presentations without Proceedings Paper
Résumés des communications sans article

New And Old Trends In Teaching Of Building Acoustics To Future Architects

Jean-Philippe Migneron, André Potvin, Jean-Gabriel Migneron

Building acoustics is still a challenge for many people working in the construction industry. The teaching of that topic has been offered for many years at the School of Architecture at Université Laval in Quebec City. Based on decades of experience, this discussion aims to review how we are able to introduce noise and reverberation controls to future architects knowing the various changes that have occurred in undergraduate and graduate studies in recent years. Examples between student work presented for jury evaluation, multidisciplinary research, and projects planned by actual practitioners will attempt to highlight how we can adapt building acoustics education today to build a better and sustainable world.

Acoustics Outreach Activities Made Easy

Cristina Tollefsen

Outreach activities by professional acousticians without a formal teaching background can be made easier through exploitation of online resources. For example, in-person activities, computer slide shows, and sound galleries can be used to focus on specific areas of acoustics. With some planning, enthusiasm, patience, and flexibility, presentations can be tailored to a variety of audiences. Following an overview of available and accessible online resources, a sample plan for an acoustics activity session for 7-8 year old children will be discussed.

Demonstrating Wave Interference Using Room Acoustics

Len Zedel

Along with Newton's laws, collisions, and simple harmonic motion, waves and wave interactions are a standard topic covered in introductory physics courses. However, unlike the more mechanical topics that are covered, the possible consequences of wave interactions are not always obvious to students to see. For standing waves, different resonant modes of oscillation can be demonstrated visually using a rope or rubber hose. But a truly engaging example can be made by creating an interference pattern using pure tones played on two widely spaced speakers in a room. In this presentation the simple components that are needed to set-up this demonstration will be presented and if the acoustics are favourable attendees will be able to wander around in the resulting sound field.

Modal Propagation Through A Cylindrical Pipe

Len Zedel

Sound travelling in a wave guide such as a cyllindrical pipe is subject to modeal dispersion where the high order modes travel more slowly than the low order modes. The result is distortion of the sound as it travels through the pipe. Exploring these modes can make for a great class demonstration of modal dispersion. I think it would be a good exercise to develop the associated theory and then develop a lab experiment for student to complete.

ARCHITECTURAL ACOUSTICS - ACOUSTIQUE ARCHITECTURALE

FACTORS AFFECTING THE ASTC PERFORMANCE OF DOUBLE WOOD STUD SHEAR WALLS IN MID-RISE RESIDENTIAL CONSTRUCTION

Anil Joshi, MASc, PEng *1
[1]Valcoustics Canada Ltd., Richmond Hill, Ontario, Canada

1 Introduction

Mid-rise wood-framed multi-unit residential buildings are becoming a common building form. Demising walls between adjacent dwellings are typically constructed of double stud wall assemblies. Structural (shear) requirements often require the addition of structural sheathing on the inner face of the studs. There is limited laboratory test data to establish Sound Transmission Class (STC) ratings for these walls; however, it is well understood that the sheathing layers on the inner face of the studs can reduce the STC ratings of the walls.

This paper presents the results of numerous Apparent Sound Transmission Class (ASTC) field tests done on double stud wall assemblies in mid-rise buildings. The test results provide an indication of the degree to which interior structural sheathing lowers the ASTC ratings of these walls. The test results also suggest that increasing the number of gypsum board layers in these walls can provide adequate ASTC ratings. These findings point to the need for a program of laboratory STC tests to establish STC ratings for these wall types.

2 Background

2.1 Double Wood Stud Demising Walls

A common suite demising wall assembly in wood framed construction is:

- Two rows of 89 mm wood studs spaced 400 mm o.c. on separate 89 mm plates set 25 mm apart
- 89 mm batt insulation on both sides
- 1 layer 16 mm Type X gypsum board on both sides

The National Building Code of Canada (NBC) provides a rating of STC 57 for this wall type based on laboratory testing [1].

In mid-rise construction the above assembly is often modified to use 140 mm rather than 89 mm wood studs. This increased stud depth is expected to increase the STC rating of the assembly; however, there is little laboratory test data for this assembly with 140 mm studs.

Structural sheathing, typically oriented strand board (OSB), is also often added to these walls to provide shear stiffness. Standard practice has the sheathing added on the inner face of the studs to allow insulation, electrical services, etc., to be installed in the stud cavities after the structural elements have been constructed. Figure 1 shows a typical double stud demising wall configuration with and without sheathing added
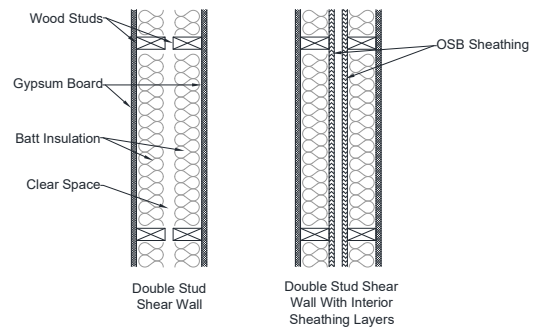
Figure 1: Typical double stud demising wall (left) and double stud demising wall with added OSB sheathing (right)

There is little laboratory test data for these walls with structural sheathing. The NBC does note that a single layer of sheathing, on the inner face of the studs, is expected to reduce the STC rating by 3 points [1]. If sheathing is added to the inner face of both rows of studs, the NBC notes that this may "drastically" reduce the STC rating; however, the NBC does not provide an STC rating [1].

The reduction in the STC rating is due to changes to the wall cavity that result from adding the sheathing. A single layer of sheathing divides the wall cavity into two shallower cavities. Two layers of sheathing divides the wall cavity into three cavities with the middle cavity having a mass-air-mass resonant frequency effect that lowers the STC rating.

2.2 Building Code Requirements

The NBC and provincial building codes that follow the NBC provide several methods to show compliance with the requirements for acoustical separation between residential dwelling units. To demonstrate compliance using a field (ASTC) test, a suite-to-suite demising partition must achieve an ASTC rating of ASTC 47 or higher.

3 Method

Valcoustics Canada Ltd. has done field tests (ASTC) on numerous double stud demising wall assemblies in mid-rise (4 to 6 storey) wood framed multi-residential buildings. ASTC testing was done in accordance with ASTM standard E336 Standard Test Method for Measurement of Airborne Sound Attenuation between Rooms in Buildings.

Test results from four buildings that use similar construction have been selected for presentation here. The tested assemblies all used 16 mm Type X gypsum wall board (GWB), two rows of 140 mm wood studs spaced at 400 mm on centre (o.c.) on separate plates, and batt insulation in both stud cavities. The structural sheathing, where used, was OSB panels applied to the inner face of the studs as shown

Table 1: Tested Assemblies

Material	Assembly			
	A	B	C	D
GWB	1 layer	1 layer	2 layers	2 layers
Wood Studs	140 mm	140 mm	140 mm	140 mm
Batt Insulation	140 mm	140 mm	140 mm	140 mm
OSB Sheathing	None	16 mm	16 mm	19 mm
Clear Space	25 mm	25 mm	25 mm	25 mm
OSB Sheathing	None	16 mm	16 mm	19 mm
Batt Insulation	140 mm	140 mm	140 mm	140 mm
Wood Studs	140 mm	140 mm	140 mm	140 mm
GWB	1 layer	1 layer	2 layers	2 layers

in Fig. 1. Details of the tested assemblies are shown in Table 1.

Assembly A is a typical double stud wall without structural sheathing. Assembly B is the same as A but with the addition of structural sheathing on the inner face of both rows of studs. Assembly C is the same as B but with one additional layer of GWB on the outside of each side of the wall. Assembly D is similar to C but used thicker sheathing.

4 Results

The range of results of the ASTC testing is shown in Table 2 as well as the number of tests completed for each assembly type. Each test was done in a unique pair of adjacent dwelling units.

Figure 2 shows the transmission loss curve for one example of each assembly type.

Table 2: ASTC Test Results

Assembly	Number of Tests	Range of ASTC
A	3	55-57
B	6	43-46
C	1	50
D	2	51-52

5 Discussion

The ASTC test results for Assembly A show compliance with the minimum ASTC 47 requirement of the NBC. The test results for the same assembly with added structural sheathing on the inside of both studs (Assembly B) are below ASTC 47 and significantly lower than Assembly A. Figure 2 shows that Assembly B has lower transmission loss, compared to Assembly A, in low frequency bands (particularly from 125 Hz to 250 Hz). It is expected that the lower performance in these bands is due to the resonance in the cavity between the two layers of structural sheathing.

The ASTC test results for the assemblies with structural sheathing on the inside of both studs and an additional layer of GWB on the outside of the studs (Assemblies C and D) comply with the minimum ASTC 47 requirement of the NBC but are still lower than the results for Assembly A. Figure 2 shows that the low-frequency transmission loss for these assemblies is better than Assembly B, but still lower
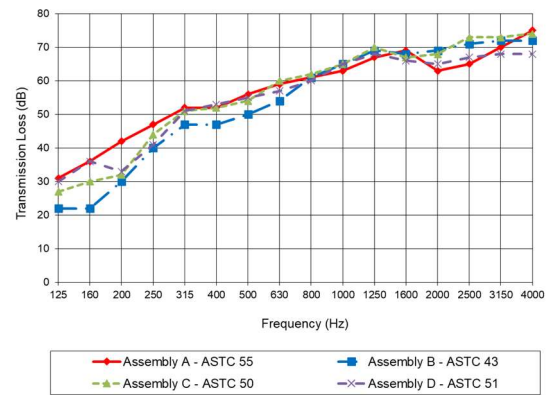
Figure 2: Transmission loss comparison for one example of each assembly type

than Assembly A. It is expected that the somewhat improved low-frequency results are due to the additional mass on the outside of the studs

Field ASTC testing has numerous limitations including the effects of structural flanking, quality of the installation, and differences in adjacent structures between different buildings. Further, the influence of variables such as stud size, stud spacing, insulation depth, air space depth, and sheathing material and thickness could not be examined as testing is limited to as-built assemblies.

Laboratory testing of these wall assemblies has largely been limited to tests sponsored by manufacturers of resilient dry-wall clips to assess the effectiveness of their proprietary products in this application.

The building industry would benefit from a basic laboratory STC study to establish STC ratings for double wood stud demising walls that include structural sheathing on the inside of the studs. The influence of stud size, stud spacing, air space depth, GWB type, number of layers of GWB, insulation depth, and sheathing material and thickness should be examined. It would also be beneficial to examine if the performance of these walls can be improved using typical construction materials such as resilient metal channels or the use of batt insulation in the cavity between the sheathing layers.

6 Conclusion

The ASTC test results presented here indicate that the addition of structural sheathing on the inside of the studs in double wood stud wall assemblies significantly reduces the ASTC rating, due primarily to lower transmission loss in the low frequency bands. The addition of extra layers of GWB appears to compensate, to some degree, for the reduced performance due to the sheathing. Further independent laboratory testing is needed to confirm STC ratings for double wood stud demising walls that include structural sheathing on the inside of the studs.

References

[1] National Research Council of Canada. National Building Code of Canada, 2015.

THE DETERMINING IMPACT OF ARCHITECTURE ON SOUND IN THE BUILT ENVIRONMENT: APPLICATIONS IN SOUND MASKING SYSTEMS AND INDOOR NOISE SOURCES

Viken Koukounian[1]
K.R. Moeller Associates Ltd.

1 Introduction

The field of Architectural Acoustics is predicated on the understanding that the built environment has a determining impact on the behaviour of sound. Yet, the effects of physical features (e.g., room shape, geometry, architectural finishings, furnishings, and fit-outs) on the spectral characteristics of sound are not always differentiated from those of measurement procedures (e.g., location of stationary and moving microphones).

Whereas a previous investigation sought to quantify the variation of sound within a spatial resolution that should be considered more academic than practical, the interest herein is to apply those conclusions and correlations to more context-relevant applications and scenarios, such as electronic masking sound and indoor noise sources [1]. Particular attention is directed to exploring the relation between performance-related parameters of a sound masking system (specifically, control zone size) and the masking sound *actually* delivered in the space.

2 Method

Architectural environment and sound masking system

The test area is a section of open-plan office space of approximately 118.5 m² (1275 ft²) set within a larger facility; see Figure 1. The walls at the boundaries terminate at the ceiling (3 m or 10 ft), except at the top and left. The space incudes nine workstations with 1.67-m (65¾-in) partitions (featuring absorptive panels), as well as office equipment and furniture. The ceiling is acoustical tile (NRC 0.85) and the floor is carpeted. The roof deck is 8.3 m (27 ft). Due to the tall plenum, 18 loudspeakers are installed approximately 0.5 m (1.5 ft) above the ceiling, facing downward. Each is provided an independent signal generator and can be individually adjusted for overall sound level and one-third octave bands between 100 Hz and 10,000 Hz (the full Optimum Masking Spectrum [OMS] published by the National Research Council of Canada) [2]. The full range is important, as it impacts comfort and *acoustical* privacy (i.e., from noise and speech). Loudspeakers can also be adjusted as part of a group, or control zone, of varying sizes.

Unlike other acoustical treatments, the 'product' is not the hardware. Rather, it is the masking sound delivered to the space, which ought to be temporally constant, spectrally balanced and spatially consistent—attributes that depend on the control zone parameters (treatment area and size, number of loudspeakers). Typical design guidelines include loudspeaker center-on-center spacing (e.g., 3 m [10 ft] to 4.6 m [15 ft]) and ensuring zones only cover similar spaces— both architecturally (e.g., geometry, finishings, furnishings)
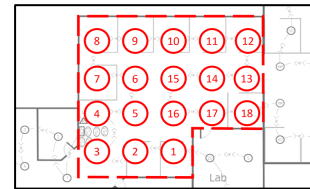
Figure 1: Boundaries of measurement test area. Circles identify 18 loudspeakers, as well as measurement locations. The three-LSCZ are 1-2-3, 4-5-16, 7-8-9, 10-11-12, 6-14-15 and 13-18-17. The six-LSCZ are 1-2-3-4-5-16, 6-7-8-9-10-15 and 11-12-13-14-17-18.

and by function (e.g., meeting or focus room). To the extent possible, these 'best practices' are relied on here, when selecting control zone configurations having more than one loudspeaker. The test area was selected to permit division into one-, three-, six-, and 18-loudspeaker control zones (LSCZ). While groupings were selected with the intent of providing consistent outcomes, other configurations may prove more or less consistent.

Instrumentation and measurements

Two Class 1 sound level meters were used simultaneously, as an assurance against sources of error, including human, instrumentation, methodical, and unknown. A Class 1 sound calibrator was used.

A series of tests were conducted to determine the most appropriate testing method (i.e., stationary, sweep, circular, or spiral). Four 30-second measurements were made at each location to ensure individual points were statistically valid (complying with typical best practices in testing standards). Where measurements at a location were in disagreement, they were repeated. Differences between arithmetic averages of spectra were found to be insignificant (in the order of 0.1 dB).

Thus, the stationary method—four measurements at 1.3 m (4¼ ft), 60° altitude angle and separated by 30 cm ($11\frac{7}{8}$ in) (i.e., a square)—was selected for procedural efficiency. Measurements were conducted at contextually representative locations within the effective area of each loudspeaker.

These testing parameters are not to be confused with those in ASTM E1573-18, *Standard Test Method for Measurement and Reporting of Masking Sound Levels Using A-Weighted and One-Third-Octave-Band Sound Pressure Levels*. Where the Standard offers guidelines to assess 'Test Areas' up to 93 m² (1000 ft²) in open-plan spaces (which may have one or more control zones), the intent here is to describe the spatial consistency at a greater, but still *practical* (i.e., controllable with a single-speaker zone), resolution within those 'Test Areas.'

Adjustment, or 'tuning,' of control zones

To minimize risk of noise interference, measurements were conducted afterhours and in the absence of occupants. Ambient conditions were closely monitored.

---

[1]viken@logison.com
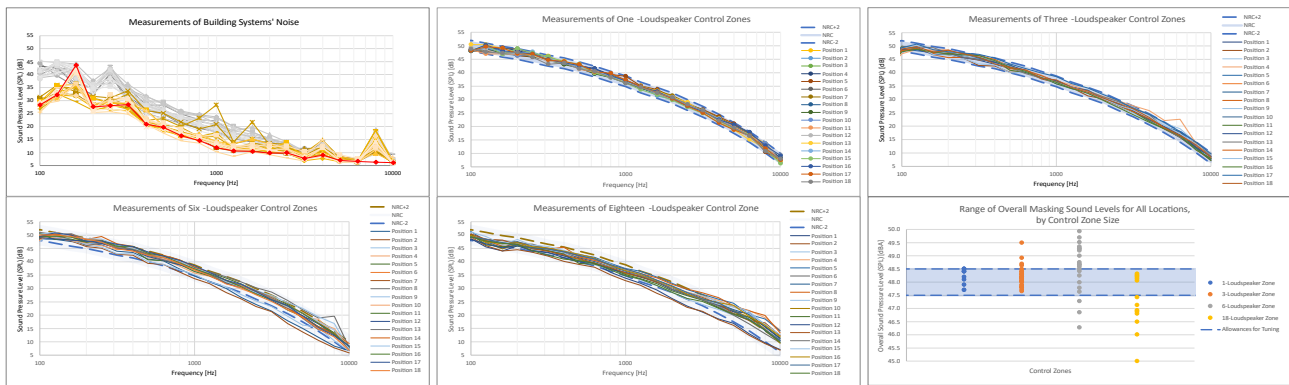
Figure 2: Charts are labeled from left to right, with (a) to (c) in the top row and (d) to (f) in the bottom row. Chart (a) shows noise from building systems. Charts (b) to (e) present the arithmetic average of four measurements at each location, for one-, three-, six and 18-LSCZ, respectively. Chart (f) presents the spread of overall sound levels of all locations for zones having different numbers of loudspeakers.

Testing of locations followed tuning of all control zones—i.e., requiring that each zone be tuned to compliance: an overall masking sound pressure level (SPL) within ±0.5 dBA and ±2 dB for all spectral bands in the OMS.

3 Results

Background noise

Noise from building systems were measured to ensure they did not interfere with the tuning process. Chart (a) in Figure 2 shows ambient measurements at all locations. Measurements were performed with building systems (i.e., HVAC) functioning (Case 1, grey data) and turned off (Case 2, yellow data). The averaged overall sound pressure level for Case 1 and 2 is 36.6 dBA and 30.3 dBA respectively. The 6 dB difference in level (and spectral differences) is significant—perceptually, and, especially, when assessing speech privacy. The light fixtures produced tones at 4,000 Hz and 8,000 Hz, and were turned off for the remainder of testing; the data for one such location is shown in red.

Masking sound

In this investigation, a location is determined to be 'Out of Compliance' (OoC) when the average of its four measurements does not meet the OMS criteria within tuning allowances. Results are in Table 1 and Figure 2 and Figure .

Table 1: Summary of OoC statistics for locations, by LSCZ size.

No. of Speakers per Zone	Percentage of locations OoC	Overall Level Difference μ (min.-max.)	Spectral Level Difference μ (min.-max.)
1	0/18 = 0%	–	–
3	4/18 = 22%	1.0 (0.7–1.5)	2.6 (2.2–3.5)
6	17/18 = 94%	1.1 (0.5–1.9)	2.7 (2.2–4.0)
18	16/18 = 89%	1.4 (0.5–3.0)	3.4 (2.3–5.1)

4 Discussion & Conclusion

The results of this investigation are specific to the tested area. Its architectural details—e.g., high absorption, taller-than-typical workstation partitions, number of loudspeakers, and sound masking system design—could have allowed for more consistent results than what may be possible in other spaces. Such differences in architectural factors will impact the propagation of sound (i.e., spectral and level
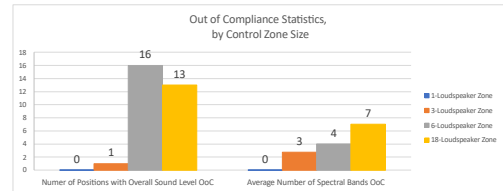
Figure 3: OoC statistics for level and spectrum, by LSCZ size.

variations) and may make it more, or less, challenging to control the consistency of masking sound. In other environments, there have been documented reports of larger variations across areas covered by larger control zones.

At locations within larger LSCZ, architecture caused level differences larger than the tuning allowances; no set of adjustments could bring spectral bands (and/or overall sound level) within limits at each location. This was also true for the three-LSCZ [1-2-3], which was sufficiently variable, architecturally, to push location 3 OoC, reinforcing the need for LSCZ to be limited to similar spaces.

Where the outcome of six- and 18-LSCZ may appear similar, it cannot be interpreted to mean the larger zone offers better or comparable control or performance. Rather, the architectural parameters of this particular space led to those outcomes by chance. It is noteworthy that neither six- nor 18-LSCZ performed better than 89% OoC.

The size of control zones clearly influences the degree of variation in masking sound level and spectrum across an area. The results demonstrate that smaller zones—when tuned individually—enable improved localized control of sound and greater consistency across the facility.

References

[1] V. Koukounian, "A systematic investigation to assess the merits of measurement preconditions critical to speech privacy standards," *The Journal of the Acoustical Society of America,* vol. 151, no. 4, 2022.

[2] J. S. Bradley and B. N. Gover, "RR-262: Development and evaluation of speech privacy measurement software: SPMSoft," National Research Council Canada - Conseil National de Recherches Canada (NRC-CNRC), Ottawa, ON, Canada, 2008.

THE ROLE OF SPECTRUM IN SUBJECTIVE INTERPRETATION OF SPEECH PRIVACY ESTIMATES: AN ANALYSIS OF PROMINENT METRICS

Viken Koukounian[1]
K.R. Moeller Associates Ltd, Burlington, Ontario, Canada.

1 Introduction

Suitable levels of speech privacy should to be recognized as a core objective in all spaces, and part of a larger conversation about our health and wellbeing in the built environment [1]. Reliable psychoacoustic metrics are necessary to determine whether spaces meet occupant needs and expectations, allowing assessment of the impact of factors, such as 'freedom' from distraction, intelligibility and audibility on, for example, comfort, focus and productivity.

2 Methods & Results

Speech privacy theory is derived from that of speech intelligibility. More precisely, losses in speech intelligibility between two positions—whether in open plan or between definably separate spaces—are interpreted as an improvement of privacy. This investigation reaffirms the importance of spectrum and demonstrates the limits of two prominent metrics—the Articulation Index (AI) and Speech Privacy Class (SPC)—by considering the sensitivity of their estimates and their associated subjective interpretations, particularly as some consider applying SPC to open-plan environments.

2.1 Theoretical and literary

Speech privacy metrics

The purpose of AI is to estimate intelligibility; therefore, it assigns greater importance to the one-third octave bands (1/3 OB) between 200 Hz and 5 kHz, which contribute more significantly to intelligibility [2]. The purpose of SPC is to estimate levels of privacy beyond the limits of AI—where speech is not intelligible, but still audible—which is accomplished by averaging 1/3 OB between 160 Hz and 5,000 Hz (L_{avg}). Though there is a correlation between intelligibility and audibility, there is extensive literature demonstrating even a small amount of information in a spectral band in the range of 370 Hz to 6 kHz can result in improved intelligibility [4]. This work reinforces the importance of such differences when assessing privacy between any two positions. Both AI and SPC are, fundamentally, a calculation of the signal-to-noise ratio: the difference in level (herein, DL) between the source and receiver and the ambient sound level at the receiver location. To address the impossibly wide array of environments and acoustic conditions, analytical and numerical strategies are used. Specifically, the contributions of DL are captured in unit steps between 0 and 25 dB. The effects of spectra—which, practically, are a function of both the DL and ambient sound level—are equivalently demonstrated by varying only the ambient conditions.
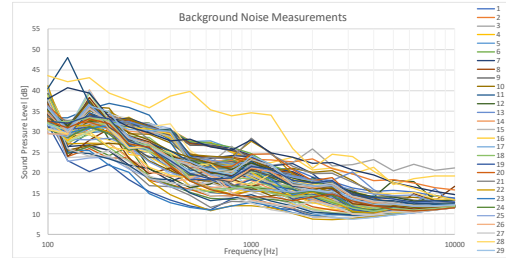
Figure 1: Measurements of ambient conditions—with building systems operational—at 98 locations, prior to occupancy. (μ = 31.6 dBA, σ = 2.9dB, Max. = 43.6 dBA, Min. = 23.8 dBA).

The importance of spectrum

Sound insulating solutions often take primacy over control of background sound, despite the latter's mathematically equivalent impact on speech privacy. However, in spaces that do not control background sound with a sound masking system, it is especially variable and inconsistent. In one investigation, 1,500 unique measurements from different sites were used to produce a distribution of background noise conditions. Their results found a standard deviation of 6 dB (12 dB range) in overall level [5]. While these results are specific to the facilities tested, each architectural environment will have variations; see Figure 1.

While walls are used to offer some degree of acoustical isolation from noise intrusion, sound masking systems are implemented with a view to providing temporal constancy, spectral balance and spatial consistency in ambient conditions. A previous investigation demonstrated the impact of changes in overall masking sound level (holding spectrum constant) on intelligibility. For decibel steps between 42 and 48 dBA in that particular environment, intelligibility estimates (i.e., 'comprehension' of "sentences upon first presentation" [SFP] speech tests) decreased from 76% to 68%, 59%,45%, 35%, 25%, and 14% respectively underlining the importance of having a consistent overall sound level at all locations across a space [6]. Expectedly, the estimates differed between locations for reasons relating to level difference between the source and receiver positions.

A recent investigation explored the impact of architectural details on the behaviour of sound [7]. It looked at the level differences (SLD) (magnitude of nonconformity from

Table 1: Ratios of measurement locations (RML) that are 'Out of Compliance' (OoC). The average overall (AODL) and spectral

Speakers per Zone	RML that are OoC	AODL μ (min.–max.)	SLD μ (min.–max.)
1	0/18 = 0%	–	–
3	4/18 = 22%	1.0 (0.7–1.5)	2.6 (2.2–3.5)
6	17/18 = 94%	1.1 (0.5–1.9)	2.7 (2.2–4.0)
18	16/18 = 89%	1.4 (0.5–3.0)	3.4 (2.3–5.1)

---

[1]viken@logison.com

Table 2: Eight different spectra, equal in A-weighted overall sound level, representing a wide range of real-world spectral conditions

|	160	200	250	315	400	500	630	800	1000	1250	1600	2000	2500	3150	4000	5000	L_{Aeq}	L_{avg}
NRC OMS	48.0	47.2	46.0	44.7	43.7	42.2	40.7	38.7	37.0	34.7	32.7	30.7	28.2	25.7	22.7	19.7	48.0	36.5
Alt. Spectrum	44.7	44.7	44.2	43.7	42.7	41.7	40.7	40.2	38.7	36.7	34.2	31.7	29.7	26.7	24.7	22.7	48.0	36.8
Investigation	48.1	48.1	46.0	45.1	43.6	41.6	39.9	39.2	38.1	35.1	32.8	29.8	26.8	25.6	22.6	19.7	48.0	36.3
Project 1	45.6	47.4	43.6	40.7	38.7	37.2	36.3	38.9	38.9	36.8	36.3	34.6	34.4	34.1	34.5	35.1	48.0	38.3
Project 2	38.7	38.5	38.5	36.3	36.8	40.9	43.7	38.6	36.2	38.7	34.5	36.6	33.4	35.0	31.1	28.9	48.0	36.6
Project 3	48.7	54.9	50.6	46.1	41.1	36.4	31.2	29.1	27.7	25.7	22.3	21.9	21.6	20.7	19.3	17.5	48.0	32.2
Project 4	41.0	41.0	41.5	39.8	37.9	37.3	34.8	35.6	36.4	38.0	38.9	37.0	36.8	36.8	35.2	34.2	48.0	37.6
Project 5	45.1	47.9	45.6	40.4	36.3	36.1	35.7	37.4	39.5	42.4	37.2	32.9	26.0	22.0	20.5	16.1	48.0	35.1
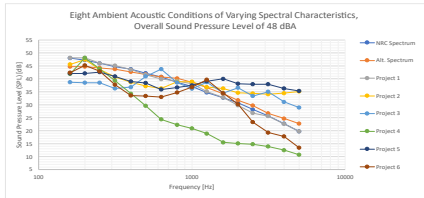
Figure 2: Eight different spectra, equal in A-weighted overall sound level, representing real-world spectral conditions.
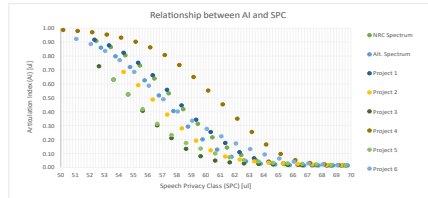

Figure 3: The relationship between AI and SPC, for each spectrum, for a range of DL conditions.

Figure 4: The relationship between SFP comprehension and SPC, for each spectrum, for a range of DL conditions.

the target value) are shown alongside the smallest and largest differences relationship between size (i.e., number of loud-speakers) of control zones within a sound masking system and the variability of masking sound (overall sound level, 1/3 OB). Results for that specific space are in Table 1.

2.2 Analytical, numerical, and empirical tools

The following analyses consider intelligibility scores from SFP tests, which better correlate with 'comprehension' than the alternatives. We reiterate that spectral differences can result from either DL or ambient conditions.

Analytical and numerical methods are used to assess equivalencies between the AI and SPC. The spectra in Table 2 (also Figure 2), which represent a broad range of real-world conditions, are evaluated across a range of DL conditions that correspond with typical values between locations in open-plan spaces. The results are presented in Figure 3. The relationship allows for mathematical substitution; see Figure 4.

3 Discussion and Conclusion

Figure 3 asserts that, for each spectrum, there is a distinct relationship between AI and SPC. Meaning, for small changes in SPC (due to spectral differences affecting L_{avg}), there can be large differences in comprehension; see Table 3. The issue is not that there are wide ranges of acoustic conditions resulting in large differences in comprehension, rather, that a small range of SPC values is resulting in a wide range of compre-

Table 3: Minimum, average, maximum and standard deviation statistics values of comprehension [%] values for 48 dBA ambient conditions with variable spectra for different DL values.

DL	SPC$_{avg}$ (Min.–Max., σ)	SFP$_{avg}$ (Min.–Max., σ)
3 dB	55 (51–57, 2.0)	62% (31%–98%, 23.3%)
5 dB	57 (53–59, 2.0)	45% (17%–95%, 26.6%)
8 dB	60 (56–62, 2.0)	25% (5%–86%, 26.8%)

hension values. Specifically, the overlay of all data from each spectrum shows that, even for a single SPC value, there is a large range of comprehension values.

For the ambient conditions representing real-world spectra (Table 2), divergences between curves are observed between SPC 50 and SPC 70. This range encompasses the majority of acoustic conditions that affect comprehension (i.e., between, rather than beyond, limits).

The results herein are specific to the spectra in Table 2. However, the outcomes clearly demonstrate that SPC is not a sufficiently accurate estimator of comprehension, because frequency composition plays an important role in intelligibility. The significance (i.e., perceptual) of smaller magnitude changes in ambient sound level became apparent with the use of psychoacoustic metrics. SPC remains the appropriate tool for its intended purpose, where speech may no longer be intelligible, but still audible.

References

[1] E. Bourdeau and V. Koukounian, "The role of acoustical privacy in a hierarchical framework for acoustical satisfaction: Past, present and future," in *Inter-noise 2022*, Glasgow, UK, 2022

[2] N. R. French and J. C. Steinberg, "Factors governing the intelligibility of speech sounds," *The Journal of the Acoustical Society of America,* vol. 19, no. 1, pp. 90-119, 1947.

[3] R. M. Warren and K. R. Riener, "Spectral redundancy: Intelligibility of sentences heard through narrow spectral slits," *Perception & Pyschophysics,* vol. 57, no. 2, pp. 175-182, 1995.

[4] J. Loverde and D. W. Dong, "Statistical distribution of ambient noise levels compiled from building acoustics measurements," *The Journal of the Acoustical Society of America,* vol. 145, no. 3, p. 1651, 2019

[5] N. Moeller, "Exploring the impacts of consistency in sound masking," *Proceedings of the Acoustics Week in Canada,* vol. 42, no. 3, 2014.

[6] V. Koukounian, "The determining impact of architecture on sound in the built environment," *Canadian Acoustics,* vol. 50, no. 2, 2022.

CORRIGER L'ACOUSTIQUE DANS UN CAS D'ÉCOLE EXISTANTE POUR LE BIEN-ÊTRE DES ENFANTS ET FACILITER LE TRAVAIL DU PERSONNEL ÉDUCATIF

Jean-Philippe Migneron *[1], **Frank Saavedra** †[1], **Jean-Gabriel Migneron** ‡[1] et **André Potvin** ♦[1]

[1] Groupe de Recherche en Ambiances Physiques, École d'Architecture, Université Laval, Québec

1   Introduction

Dans le contexte actuel, on rencontre plusieurs défis pour la gestion du cadre bâti destiné à l'enseignement et à l'éducation. Des changements dans les besoins sont constatés, en plus de l'augmentation des charges relatives à l'entretien pour permettre de maintenir l'occupation des écoles plus anciennes, ce malgré un nombre grandissant de contraintes. Les acousticiens savent comment rendre l'ambiance sonore plus confortable dans les salles de classe [1], mais il demeure toujours un équilibre à trouver entre les aspects fonctionnels des solutions, leurs coûts et leurs performances, notamment pour le contrôle de la réverbération. La présente étude de cas montre un exemple d'amélioration de la qualité d'un espace de circulation jugé comme critique dans une école spécialisée.

Cette démarche s'inscrit également dans le plus vaste projet Schola mené à l'Université Laval, lequel vise à proposer des outils pour faciliter la conception des projets de rénovation des bâtiments d'enseignement.

2   Objectifs visés par le projet

2.1   Contexte particulier examiné

L'École St-François a pour mission de scolariser des élèves de niveaux primaires et secondaires qui ne trouvent pas leur place dans le reste du système éducatif, ce pour diverses raisons. Il s'agit d'un établissement privé qui accueille autour de 150 enfants ou adolescents en difficulté d'adaptation tant sur les plans personnel, scolaire que social.

L'enseignement s'y distingue par l'individualisation des interventions, en prônant un fort sentiment d'appartenance, notamment par le sport, en plus d'offrir un sentiment de sécurité et de réconfort, ce avec un environnement stable, des classes spécialisées et l'expertise de toute l'équipe-école.

2.2   Problème rencontré dans le corridor des classes primaires

Malgré tous les efforts antérieurs appliqués à l'aménagement de l'école, différentes contraintes limitent toujours les possibilités d'amélioration du confort pour les occupants, notamment en matière de budget ou d'espace disponible. Étant donné les besoins spécifiques aux 4 classes primaires qui sont regroupées dans une même partie du bâtiment, le corridor qui les relie constitue un point tournant qui sert de transition lorsque les élèves ne se trouvent pas dans leur local habituel. Ce corridor d'une superficie de 116 m² devient rapidement bruyant lorsqu'un ou plusieurs enfants crient, ce qui peut nuire à l'ambiance acoustique perceptible dans les classes, même lorsque les portes sont fermées.

Afin de comparer les solutions envisageables et d'ensuite justifier les investissements accordés à des correctifs, la fondation supportant les activités de l'école a fait appel aux membres du Groupe de Recherche en Ambiances Physiques à l'École d'Architecture de l'Université Laval. Un projet d'étude de cas a ainsi été organisé pour caractériser les performances actuelles de l'espace intérieur, puis pour énumérer des pistes de solution.

3   Résultats

3.1   Relevé des temps de réverbération

Une première série de visites a été réalisée afin de bien comprendre les besoins, de compléter l'inventaire des matériaux de finition existants et pour procéder à des mesures des temps de réverbération. Un sonomètre intégrateur muni de la fonction d'enregistrement des décroissances après l'interruption d'une source de bruit rose a été utilisé pour cette tâche.

Comme le confirme la Figure 1, le TR$_{60dB}$ moyen s'élevait initialement à 1,7 s pour les bandes de 500, 1000 et 2000 Hz. Il est à noter que la plupart des matériaux apparents étaient constitués de matériaux réfléchissants, dont un plafond recouvert de stucco.
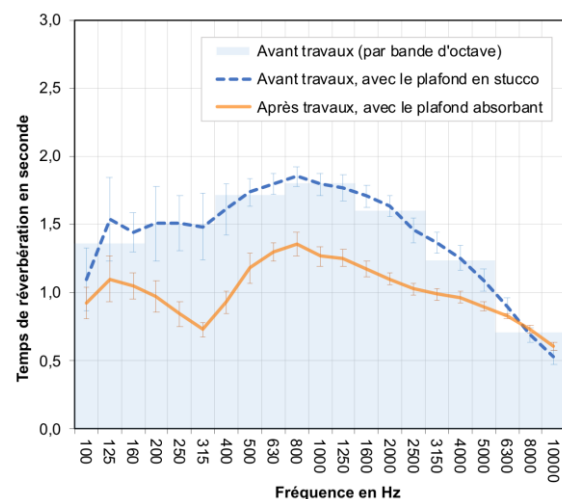

Figure 1: Graphique comparatif des temps de réverbération avant et après la mise en œuvre du traitement du plafond.

* jean-philippe.migneron.1@ulaval.ca
† frank.saavedra.1@ulaval.ca
‡ jean-gabriel.migneron@arc.ulaval.ca
♦ andre.potvin@arc.ulaval.ca

Figure 2: Vue du chantier durant la réalisation du correctif.

Figure 3: Vue du corridor après les travaux d'amélioration.

Durant le processus d'analyse, au moins une quinzaine de scénarios d'intervention ont fait l'objet de projections de manière à trouver un compromis acceptable. L'option retenue consistait à pulvériser le plafond existant avec un nouvel enduit à base de cellulose d'une épaisseur de 25 mm. Selon les données techniques disponibles, la modélisation des performances anticipait une atténuation moyenne des niveaux sonores de l'ordre de 5 dB, réduisant ainsi le TR_{60dB} vers une cible de 0,5 s. Avec la collaboration du fournisseur et de l'installateur, le chantier a pu être réalisé durant un vendredi de congé pédagogique, soit en milieu d'année scolaire. La Figure 2 montre les travaux en cours d'exécution. Il est à remarquer que la mise en place des protections des surfaces non traitées a été une tâche aussi importante que la pulvérisation elle-même.

Relativement à l'évaluation des performances après l'achèvement des travaux, il a été possible de mesurer à nouveau les temps de réverbération dans le corridor traité. Il s'est alors avéré que le TR_{60dB} moyen demeurait de l'ordre de la seconde. Quelques hypothèses ont été formulées afin d'expliquer l'écart ainsi observé, il a été notamment supposé que les coefficients d'absorption présentent une incertitude significative en fonction de la variabilité de la pulvérisation.

3.2 Appréciation des usagers

Bien que la réduction de la réverbération ait été moins importante qu'anticipée, les élèves du secteur primaire de l'École St-François ont eu l'agréable surprise le lundi matin d'entendre une ambiance plus calme dans le corridor ainsi insonorisé. Les usagers ont alors qualifié l'intervention comme une remarquable amélioration, permettant ainsi de meilleures interactions en classe et dans le corridor.

4 Discussion

En contrôle du bruit, la norme ANSI/ASA S12.60 fournit depuis plus d'une dizaine d'années des lignes directrices permettant d'améliorer les qualités des espaces d'enseignement [1]. Néanmoins, il convient de mettre en parallèle les performances suggérées avec l'ensemble des autres aspects à considérer dans l'optimisation des améliorations, car les cadres de vie scolaire doivent ultimement être fonctionnels, confortables, agréables, appropriables et durables.

Aussi, l'exemple de l'École St-François paraît un reflet relativement typique des bâtiments d'enseignement construits avant les années 1990, lesquels présentent souvent des lacunes en ce qui touche aux ambiances intérieures comme l'éclairage, la qualité de l'air ou l'acoustique. En sachant que le parc scolaire québécois majoritairement construit entre 1948 et 1973 devra être rénové afin de prolonger la durée de vie utile des quelque 3300 écoles publiques existantes, le projet Schola a été lancé en 2018. Après avoir rassemblé un inventaire du cadre bâti actuel, l'équipe multidisciplinaire cherche maintenant à proposer une plateforme d'aide décisionnel permettant d'assister les intervenants dans le cadre de futurs travaux d'optimisation du potentiel des différents milieux d'enseignement [2]. La démarche préconisée par Schola comporte 3 volets : comprendre l'école et ses enjeux du point de vue des utilisateurs, particulièrement les étudiants; évaluer l'état des lieux avec des outils diagnostiques qui incluent de surcroît des questions portant sur le mobilier, les équipements intérieurs et extérieurs, en plus de l'ergonomie; puis toutes les facettes de conception des rénovations avec l'élaboration de programmes fonctionnels et techniques plus adaptés aux besoins préalablement identifiés. Il est donc espéré que la plateforme aidera la communauté à partir des prochains mois.

Remerciements

Références

[1] ANSI/ASA S12.60/Part 1-2010, Acoustical Performance Criteria, Design Requirements, and Guidelines for Schools, Part 1: Permanent Schools, Acoustical Society of America, 2014.

[2] C. Després, C. Coté, M. De Blois, C. Demers, M. Doyle, F. Dufaux, C. Gagnon et al. "L'ABC de la rénovation scolaire. Guide de planification immobilière pour les écoles primaires publiques du Québec, Fascicule A", Schola, Université Laval, 2021 (schola.ca).

2022 Comparison of the Acoustic Design Requirements of LEED, WELL and Green Globes

Jessie Roy *[1]

[1]RWDI Consulting Engineers and Scientists, Calgary, Alberta, Canada.

1 Introduction

The LEED, Green Globes, and WELL building rating systems have undergone substantial updates in the last five years, which include revisions to the options associated with acoustics. Some of these updates were made to address continued low occupant satisfaction with acoustic performance, and low interest in the pursuit of the acoustic-related certification options, due to challenges with achieving the requirements. This paper summarizes the changes in the acoustic requirements in the latest versions of these systems, how those changes address some of the common challenges with past versions and highlights key design considerations for achieving the new requirements.

2 Discussion

2.1 LEED (Version 4.1) [1]

In the update to LEED version 4.1, the Building Design and Construction (BD+C) Acoustic Performance credit was modified in an attempt « to encourage more projects to consider acoustic performance during design » [1]. The structure of the credit was changed to allow projects to achieve one point by complying with two of the performance requirement categories: HVAC Background Noise, Sound Transmission or Reverberation Time, and an exemplary performance point if the requirements in all three categories were met. This change addresses a challenging aspect of the previous version which was that every acoustic requirement had to be met in order to earn one point.

The HVAC Background Noise and Reverberation Time requirements of the credit are generally the same as in Version 4. For projects with large spaces, meeting the reverberation time targets may be difficult as the requirements are independent of room volume.

The Sound Transmission requirements have been updated to make the credit relevant to a wider range of projects and addresses an issue with the requirement between offices or conference rooms and corridors in Version 4, as that requirement was frequently a barrier to the pursuit of the acoustic credit. The new requirement is composite sound transmission class rating (STCc) 35 for adjacencies between private spaces and hallways, which is still likely to require acoustic door seals, but is possible to achieve with typical wall, glazing, and door constructions.

In addition, sound reinforcement systems are no longer discussed in the credit and sound masking system requirements have been integrated into the sound transmission requirements, allowing projects with a sound masking system to have sound insulation targets 5 points lower than projects without masking.

2.2 Green Globes (New Construction 2021) [2]

In the 2021 update to the Green Globes rating system the acoustic section was completely redone. It is now broken into three topic areas: Noise Limits and Masking Sound Level, Acoustic Insulation and Vibration Isolation, and Reverberation Time or Ceiling Noise Reduction Coefficient.

In Green Globes, points are earned by answering questions. There are no longer any acoustic questions about prescriptive measures; all questions are now performance requirements. This new format necessitates that an acoustical consultant be involved in the project to answer the questions in the acoustic section. The system still allows for most questions to be evaluated independently (i.e., not achieving a question does not preclude the project from attempting the next question), allowing for a maximum number of points from acoustics to be available.

The acoustics section is structured to encourage the design team to set acoustic targets, complete a theoretical assessment, and then validate performance with measurements post-construction. To achieve the maximum number of points, it is important that an acoustical consultant is involved early in the project, at a time when it is still possible to integrate their recommendations into the mechanical design, and that post-construction measurements are included in the project budget and schedule. For many of the multi-point questions, the number of points achieved by the project are determined from the percentage of spaces that achieve the requirements (both for theoretical assessments, and post-construction measurements).

With the 2021 update, a newer set of standards are referenced, and separate options are provided for education and healthcare projects. Most notably the metric for evaluating background noise has changed from Room Criterion (RC) to Noise Criterion (NC) or A-weighted overall sound level (dBA) and C-weighted overall sound level (dBC), addressing previous difficulties with theoretically assessing RC ratings.

2.3 WELL (Version 2, 2022 Q2) [3]

In the update to WELL Version 2, 'Sound' was elevated to one of the ten concepts that the features of WELL (called preconditions and optimizations) are organized into, recognizing its importance to occupant comfort.

The requirements of the Sound Mapping precondition, which is required for all certified projects, have been considerably relaxed. Identification of loud and quiet zones is still required, but instead of mandatory limits on noise intru-

* jessie.roy@rwdi.com

sion and mechanical background noise levels, a plan or report outlining existing conditions, recommended solutions, and timeline for implementation, is required.

In Version 2, exterior noise intrusion and mechanical noise are assessed together under the Maximum Noise Level optimization. Project performance is evaluated based on measurements of average and maximum sound pressure levels (dBA and dBC) against two levels of performance (tier I and tier II). Although simple to measure, this approach is more complex to model. It is important to note that spaces with operable windows must be measured with windows open, and that tolerances (+4 dB for average and +9 dB for maximum) are permitted for evaluating measured compliance against the thresholds in this feature.

The Sound Barriers and Reverberation Time optimizations have been restructured to allow points for design, as well as verifying performance. The reverberation time requirement for open plan offices have been removed, which resolves a common issue that projects encountered with WELL Version 1. The overlap in the requirements of the Reverberation Time and Sound Reducing Surfaces optimizations, potentially allows a project to earn points under both optimizations for the same sound absorptive materials depending on the location of the materials.

The Minimum Background Sound optimization requires sound masking in a wider range of spaces than in WELL version 1, but the limits are the same. There is also an additional point available for achieving this optimization in combination with the Sound Barriers and Sound Reducing Surfaces optimizations.

Lastly, there are three new beta features in Version 2: Impact Noise Management, Enhanced Audio Devices and Hearing Health Conservation. The Impact Noise feature offers points for designing floor-ceiling assemblies to reduce impact noise and verifying the performance. The Enhanced Audio feature is focused on devices that support speech intelligibility, and organizational policies around their use. The Hearing Health Conservation feature outlines requirements for organizations' hearing conservation programs, including the provision of hearing protection and audiometric testing.

3   Comparison

The background sound, sound insulation and reverberation time (RT60) requirements of the LEED BD+C credit, Green Globes, and WELL systems are compared in Tables 1 to 3.

Table 1: Comparison of Average Background Sound Limits

Building Rating System:	LEED v4.1	Green Globes 2021	WELL v2 (Q2 2022) Tier I	WELL v2 (Q2 2022) Tier II
Space Type	dBA/dBC	dBA/dBC	dBA/dBC	dBA/dBC
Areas for conferencing, learning, or speaking (conference room)	35/60	35/60	40/60	35/55
Enclosed areas for concentration (private offices)	35/60	35/60	45/65	40/60
Open areas for concentration (open plan offices)	45/65	45/65	50/70	45/65
Areas with machinery and appliances used by occupants (e.g., testing/research labs, dining, etc.)	55/75	55/75	55/75	50/70

Table 2: Comparison of Sound Insulation Requirements

Building Rating System:		LEED v4.1	Green Globes 2021	WELL v2 (Q2 2022)
Adjacency Combination		STCc / NIC	STCc	STC / NIC
Private Office	Private Office	45 / 40	45	50 / 45
Private Office	Open Office	45 / 40	45	45 / 40
Private Office	Corridor	35 / 30	40/30*	40 / 35
Conference Room	Private Office	50 / 45	50	55 / 50
Mechanical equipment room	Occupied Area	60 / 55	60	60 / 55

*Green Globes references IgCC2018 which allows for 5-point reduction in target for walls between spaces and corridors, and a 15-point reduction for walls with doors that open to corridors

Table 3: Comparison of Reverberation Time Requirements

Building Rating System:	LEED v4	Green Globes 2021	WELL v2(Q2 2022)
Space Type	RT60 at 500, 1000 & 2000 Hz (s)	RT60 at 500, 1000 & 2000 Hz (s)	RT60 at 500 and 1000 Hz (s)
Executive or private office	< 0.6	≤0.6	N/A*
Conference/ Teleconference room	< 0.6	≤0.6	≤0.6 for V < 10,000ft³ 0.5≤ RT60 ≤0.8 for 10,000ft³≤V≤20,000ft³ 0.6≤ RT60 ≤1.0 for V > 20,000ft³
Open-plan office with sound masking	0.8	≤0.6	N/A**
Areas with machinery and appliances used by occupants	< 1.0	≤1.0	≤1.0

*Offices are not a space type listed in the Reverberation Time feature
**Per WELL FAQ#275 open plan offices are purposefully excluded from the reverberation time feature because they "can fluctuate greatly across the floor plate of open offices, making reverberation time difficult to quantify and design. Furthermore, there is not yet strong evidence that links higher reverberation times in open offices to adverse conditions for occupants."[4]

As can be seen in Tables 1 and 2, the background sound and sound insulation requirements of the systems are similar, mostly within 5 dB or points. Whereas there are fundamental differences in how the systems approach reverberation time for offices and conference rooms.

4   Conclusion

Substantial modifications have been made to all the systems discussed to make it easier for projects to earn points towards certification for considering the acoustic comfort of occupants in their design. All the systems now have a mechanism for projects to earn points when the design partially complies with requirements, recognizing the importance of incorporating any measures that are feasible. The shift to awarding points for both design and post-construction measurements may incentivize projects to conduct post-construction measurements more often, helping to identify deficiencies prior to occupancy.

References

[1] US Green Building Council. LEED v4.1 Building Design and Construction, Getting started guide for beta participants. Jan. 2019.

[2] Green Building Initiative. Green Globes New Construction 2021 Technical Reference Manual. Version 1.0. February 2022.

[3] International WELL Building Institute. The WELL Building Standard v2 with 2022 Q2 Addenda. June 2022.

[4] International WELL Building Institute. WELL v2 Feature S04 FAQ. 2022. https://v2.wellcertified.com/en/wellv2/sound/feature/2

WIRELESS LOUDSPEAKER TECHNOLOGY FOR MORE EFFICIENT SOUND TRANSMISSION TESTING

Jeremy Thorbahn *1

1 Thorbahn Acoustics Inc., Halifax, Nova Scotia, Canada,

1   Introduction/Background

In architectural acoustics consulting, field sound transmission tests in buildings are commonly undertaken to verify the as-built performance of the construction. These tests involve measurements of the sound attenuation provided by the separating assembly between two rooms, the "source" room and the "receiver" room, by playing a calibrated noise spectrum in the source room and measuring the corresponding sound pressure levels in both the source and receiver rooms. To produce a test signal, a loudspeaker (or loudspeakers) placed in the source room and connected to a sound source such as a dedicated signal generator, smartphone or laptop computer is typically used. When the sound source uses a wired connection to the loudspeaker, the user has to physically travel back and forth between rooms to turn on and off the sound source. The logistics of this type of test setup inherently involve a certain amount of extra time to travel between rooms to manipulate the equipment.

The ability to wirelessly control the sound source would overcome the need to travel back and forth between rooms to switch on and off the signal, thereby saving time. For some projects, many partitions are tested in the same day and the time savings would be significant. Aside from time savings, other advantages of wireless control include eliminating the need for using hearing protection to enter the source room to turn off the sound source (since sound pressure levels may exceed 90 dBA), and not having the sound source on when the door is open to minimize the disturbance to building occupants. We reviewed options including power amplifiers with remote control, loudspeakers with Bluetooth audio streaming capability, and loudspeakers with built-in wireless control via smartphone or tablet.

The ASTM Standard E336-20, "Standard Test Method for Measurement of Airborne Sound Attenuation between Rooms in Buildings", which governs the test methodologies for Apparent Sound Transmission Class (ASTC), Noise Isolation Class (NIC) and other common sound transmission tests, states that "Ideally, loudspeaker systems should be omnidirectional. In practice, using multiple driver elements to cover different frequency ranges and placing and aiming sources into trihedral corners of the room will normally be adequate". Both omnidirectional and directional loudspeaker equipment were reviewed since in our experience, both are used in practice by consultants in Canada.

Wireless power amplifiers with remote control are one means of wirelessly controlling a sound source, but typically cost thousands of dollars. Bluetooth is another method of wireless audio transmission. However, until recent years, the Bluetooth protocol was limited in its bandwidth and signal strength to an extent that could limit its ability to maintain audio fidelity, penetrate walls and reach significant distances. Bluetooth 5.0 was released in 2016 and enabled twice the data bandwidth and 4 times the range compared to earlier versions. Some manufacturers of professional audio equipment have begun to include Bluetooth 5.0 in their products. Current smartphones and tablets similarly include Bluetooth 5.0 as a standard feature. Compared to earlier versions of the standard, Bluetooth 5.0 presents a more viable solution for wireless signal transmission in building acoustics testing between rooms due to its higher data bandwidth and increased range.

Some recent Bluetooth-enabled loudspeakers also allow direct control the loudspeaker settings via a smartphone app, so a wired signal generator could be used to avoid any concern about degradation of the wireless audio signal since Bluetooth is only used to turn on and off the loudspeaker.

everal equipment options were reviewed, and tests undertaken to assess the potential benefit of wireless loudspeaker technology in sound transmission testing.

2   Méthode/Method

2.1   Review of Available Technologies

A review of currently available equipment and technologies to enable wireless control of the sound source during field sound transmission tests was undertaken. The criteria for inclusion in this review were that the equipment must be available for shipment to Canada and allow the audio signal from the loudspeaker in the source room to be switched on and off by a user located in the receiver room. The selections included in Section 3.1 are representative and not necessarily an exhaustive list covering all manufacturers.

2.2   Sound Level Measurements of Wired vs. Wireless Audio Signal

Using an NTi Audio XL2 Sound Analyzer, measurements of the equivalent continuous sound pressure level (Leq) were taken for both Bluetooth 5.0 transmitted audio from an iPhone 11 and for a wired signal generator (NTi Audio Minirator MR-PRO) connected to the same loudspeaker (JBL EON710) and playing the same pink noise sound file for 30 seconds using fixed microphone and speaker locations. The output from the Bluetooth sound source was adjusted to produce approximately the same overall A-weighted sound pressure level as the wired source. The measurements were compared to determine whether both

*   jeremy@thorbahn.ca

methods produce approximately the same sound level across the frequency range (125-4000 Hz) used in ASTM E336.

2.3 Time Required to Complete Sound Transmission Measurements using Wired vs. Wireless Loudspeaker Control

Tests were undertaken to assess the time savings associated with wireless loudspeaker control. Two room configurations were tested, one side-by-side (a wall) and one vertically stacked (a floor-ceiling). Tests were carried out according to ASTM E336, and the time to complete the tests was recorded, from the beginning of the first measurement (source level) to the end of the last measurement (background level). Measurements were carried out for 30 seconds each using an NTi Audio XL2 Analyzer, NTi Minirator MR-PRO signal generator and JBL EON710 loudspeaker with its output turned on and off remotely via the JBL ProConnect iOS app for the wireless tests.

3 Results

3.1 Review of Available Technologies

Several powered loudspeakers with Bluetooth audio and/or wireless control were identified, as well as a power amplifier with signal generator and wireless remote intended for use with an omnidirectional sound source as listed in Table 1. The prices for 10" loudspeaker models are listed.

Table 1: Wireless audio equipment available in Canada

Manufacturer	Model	Price ($CAD)
JBL	EON710	$739
Mackie	SRT210	$755
Electro-Voice	ELX200-10P	$899
NTi Audio	PA3 Power Amp.	$3268*

*Approximate based on CAD/USD exchange rate

3.2 Sound Level Measurements of Wired vs. Wireless Audio Signal

Sound pressure level measurements of the same pink noise source file transmitted to the loudspeaker via wired and wireless connections are illustrated in Figure 1.

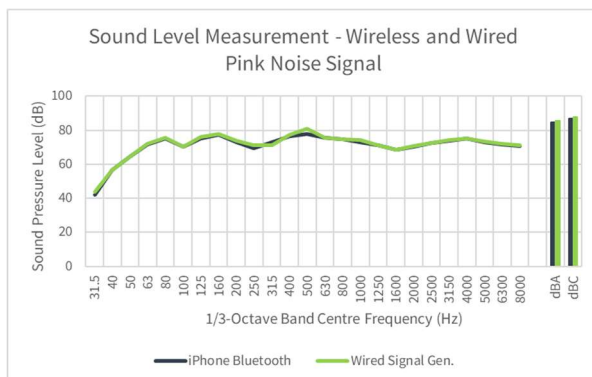The results are within measurement uncertainty of each other across the frequency range measured.

Figure 1: Comparison of wired and wireless audio signal

3.3 Time Required to Complete Sound Transmission Measurements using Wired vs. Wireless Loudspeaker Control

The time required to complete sound level measurements for each test for side-by-side rooms and vertically stacked rooms are listed in Table 2.

Table 2: Time to complete wired and wireless tests

Test Type	Method	Time (s)
Horizontal	Wired	191
Horizontal	Wireless	134 (29.8% faster)
Vertical	Wired	248
Vertical	Wireless	167 (32.7% faster)

As expected, the ability to switch the sound source on and off remotely from the receiver room resulted in significant time savings. The results are based on one user conducting tests in one building, and may vary substantially for different users, equipment and building configurations.

4 Discussion

The cost of recent professional Bluetooth-enabled directional loudspeakers is similar to previous loudspeaker models without wireless capability, and significantly less than a wireless power amplifier which would have previously been perhaps the only method of conducting sound transmission tests with wireless control.

Bluetooth audio transmission can evidently produce nominally the same source room sound level spectrum as a wired signal generator across the frequency range used for sound transmission testing in buildings. Still, our preferred method is to use Bluetooth control via smartphone of the loudspeaker output with a wired signal generator connected, to ensure there is no loss of signal quality or interruption during measurement.

The tests conducted using wireless technology indicate that the time required to complete measurements for sound transmission testing could be up to 30% less than for the wired method.

5 Conclusion

Wireless loudspeaker technology is available in Canada and our tests show that it can be used for sound transmission testing in building acoustics with little potential downside compared to the wired equivalent. Acoustical consultants and engineers should consider these options when purchasing new equipment since in consulting, time savings are cost savings.

References

[1] ASTM E336-20: Standard Test Method for Measurement of Airborne Sound Attenuation between Rooms in Buildings.

Hybrid Assessment Method Web App for Impact Noise Insulation Performance Prediction in Building

Mathieu Wahiche *[1], Raphaël Duée †[1] and Antoine Labrie ‡[1]
[1]Atelier 7hz inc., Acoustic and vibration engineering - Montréal, Québec, Canada

1 Introduction

To carry out a successful acoustic design of a building, noise impacts between rooms need to be controlled. The acoustic performance is now considered as mandatory for new buildings. ASTM E989-21 defined different ratings to assess the impact noise performance between two rooms such as IIC/AIIC. Considering the lack of existing tools to assess these criteria, and some difficulties to use the existing ones, Atelier 7hz induced an innovation project to develop a new Canadian software. The aim of the project is to create a web app to help acoustic and vibration professionals predict impact sound insulation performance between two rooms.

Existing Software Limitations

Different kinds of acoustic software exist to predict impact Insulation Class. Considering the parameters variability, it is difficult to get consistent results for an existing configuration in situ. Software based solely on theoretical calculations needs a lot of different data that are difficult to get. That's why a hybrid calculation method using a mix of measured data and calculation model has been developed to assess existing assemblies' performance. This kind of software exists in Europe using European standards, but the IIC criterion defined in ASTM standards is not implemented.

Hybrid method

The hybrid method used in the software is based on the addition of measurement databases and calculation models:
- AIIC/IIC performance measurements: using the performance data of a similar situation
- Floor covering and ceiling additional performance calculation model,
- ΔAIIC/IIC performance measurements: using the performance data of a similar floor covering and ceiling.
-

2 Web App description

2.1 Web app global principle

The web app is divided into two parts. The first part is the interface to enter a floor-ceiling assembly to assess. The search option will question the database for similar assemblies and their impact noise insulation performances and display several results. The resemblance between assemblies is determined by an algorithm. After choosing one similar assembly, it is possible in the second part of the app to remove,

replace, or add layers from the floor, or the ceiling and the software will compute the new performance based on two methods. The calculation can be done using the Cremer method, which is a numerical method. The other way to get the new performance is using a second database that stores ΔNISPL for different flooring and ceiling materials and computing the new IIC/AIIC value. It is also possible to enter a new measured existing assembly and all its measurement parameters including ANISPL and modify it.

2.2 Division of Floor-Ceiling Assembly

To create the database, a standard typology for floor-ceiling assemblies had to be defined (Figure 1). By looking at an assembly from top to bottom, it can be divided into three sections, the floor, the structural core, and the ceiling. The floor may be composed of up to one soft floor covering such as carpet or vinyl, followed by one or more rigid-elastic complexes each of which is composed of one or more rigid layer followed by one or more resilient membranes. The required structural core is composed of one or more rigid surface as engineered wood or concrete slab, optionally followed by joists and furring channels. The ceiling may include the cavity under the structural core which can be empty or filled, one or more rigid surfaces attached to the structure, a ceiling fixation system such as resilient bars or suspension springs, one or more rigid surface attached to the fixation system.

Floor	Floor covering
	n Rigid-elastic complexes
Structural core (required)	n Rigid surface (required)
	Joists and furrings system
Ceiling	Empty or filled cavity
	n Rigid surfaces
	Ceiling fixation system
	n Rigid surfaces

Figure 1: Division of each layer of the assembly

2.3 Similarity algorithm principle

A complex part of the web tool was to develop the similarity algorithm to determine the resemblance between two floor-ceiling assemblies. The first version of the algorithm uses two different kinds of criteria: exclusive and sorting criteria. Exclusive criteria must be fulfilled to assure a match. The sorting criteria are used to order the assemblies that respected the

---
* mathieu.wahiche@atelier7hz.com
† raphael.duee@atelier7hz.com
‡ antoine.labrie@atelier7hz.com

exclusive criteria to present the best match first. Figure 2 shows the global flow of the algorithm. The different exclusive criteria are listed below:

- Core structure which can be concrete, heavy wood such as CLT and glulam, or light wood such as plywood and joists;
- Floor covering;
- Same number of rigid-elastic complexes;
- Same type of ceiling: no ceiling, a rigid ceiling or resilient system.

Four criteria have been used for ordering, they are currently being used in succession and are the following:

- Area density of the floor and core structure combined;
- Total area density of the ceiling;
- Empty ceiling cavity or cavity filled with absorbing material;
- Type of resilient system in the ceiling if there is one.

The following step is to implement a point-based system which would attribute points for each of these criteria and refine the ordering of the matches to find the best possible one. Other criteria should also be added.
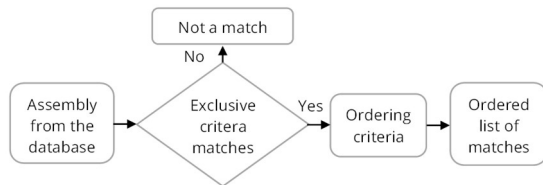

Figure 2: Global flow of the similarity algorithm

3 Method

3.1 Impact Insulation Class IIC/AIIC database

To be able to use measurement results in the software, it is important that the context of the measured situation is precisely described. In addition to numerical results (NISPL), the important data needed for the database is the detailed composition of the floor-ceiling assembly, including the material of each layer, its thickness and area density. Elastic properties are a plus that can be used for calculations. All data comes from tests done following the ASTM method using a standard tapping machine.

A relatively large database has been already built with data coming from multiple different sources. However, more data still needs to be added as the reliability of the tool is very dependent on the amount, the quality, the variety, and the accuracy of data in the database. Finding complete data is difficult as test results often got missing data that are needed for the tool. A large part of data comes from measurements done by the NRC, which are tests done in a laboratory with standardized methods. Other data comes from different sources (Acoustic engineering firms, laboratories, material manufacturers).

3.2 Floor Covering Performance Calculation Model

The Cremer/Ver method has been followed to assess the rigid-elastic complex performance in the app. The attenuation

ΔL at frequency f is then:

$$\Delta L = \mathrm{K} \log\left(\frac{f}{f_1}\right) \, dB$$

With K a constant depending on the kind of reaction. $K=40$ for the locally reacting floating floor more adapted for a heavy structure. $K=30$ for the resonantly reacting floating floor more adapted for small surfaces and a lightweight structure; $f1$ the resonance frequency of the rigid-elastic complex:

$$f_1 = \frac{1}{2\pi} \times \sqrt{\frac{s''}{m_1}} \, hz$$

With: $m1$ the surface mass of the floating coating (in kg/m2); s'' the dynamic stiffness of the resilient layer (in N/m3).

4 Call for participation and further developments

Because the database is an important part of the process, any detailed in situ measurements are welcome. If acoustic and vibration experts reading this paper have this kind of data, they are friendly welcome to contact Atelier 7hz. Access to the web app could be arranged.

Further developments will focus on enlarging the database, separate IIC and AIIC measures and adding the possibility of adding flanking, ceilings noise impact performance calculation model, adding a list of suppliers, side-rooms impact noise assessment and auralization.

5 Conclusion

This new in development Canadian web app to assess impact noise insulation performance is based on a hybrid method combining an extensive measurement database and calculation models for rigid-elastic complexes (Flooring) and ceiling types. With this new software, it is possible to navigate quickly into a large measurement database and partially modify some assemblies to assess different cases performances.

Acknowledgments

References

[1] Warnock, A.C.C. and J.A. Birta, Detailed report for consortium on fire resistance and sound insulation of floors: sound transmission and impact insulation data in 1/3 octave bands, in Internal Report (NRC. IRC), IRC-IR-811, 2000.

[2] Loverde, J. and W. Dong, A dual-rating method for evaluating impact noise isolation of floor-ceiling assemblies. JASA, 2017.

[3] Cremer, L. and M. Heckl, Structure-Borne Sound. 1973.

[4] Vér, I.n., Impact Noise Isolation of Composite Floors. Journal of The Acoustical Society of America - JASA, 1971. 50.

[5] Scholl, W. and W. Maysenholder, Impact Sound Insulation of Timber Floors: Interaction between Source, Floor Coverings and Load Bearing Floor. Building Acoustics, 1999. 6: p. 43-61.

[6] Schiavi, A., Improvement of impact sound insulation: A constitutive model for floating floors. Applied Acoustics, 2018. 129: p. 64-71.

Abstracts for Presentations without Proceedings Paper
Résumés des communications sans article

Acoustic Design Challenges Of The Tom Patterson Theatre

Payam Ashtiani, Sarah Mackel, Doreen Abraham

The original Tom Patterson Theatre was located in a 1906 building that was a former curling rink. The theeatre features an elongated thrust stage that made for very intimate performances and a wrapp-around audience. The theatre has recently re-opened after being demolished and rebuilt. The new hall features a curves and concave surfaces throughout the hall. Acoustically, concave surfaces have the risk of focusing and uneven acoustic balance in a room. This paper will explore the formidable acoustical challenges of designing a theatre space, and the outcomes after opening of the theatre.

A Study Of Dry Linings In Mass Timber Construction.

Wilson Byrick

This paper evaluates various methods to eliminate wet, cementitious toppings as a necessity in mass timber construction. In order for mass timber buildings to meet embodied carbon goals, project timelines and budgets, dry resiliently mounted linings can offer a significant innovation. Airborne and impact ASTM E90 and E492 data is presented on the use of wood based, mixed wood and cement fiber, cementitious and combinations of these various boards. Delta STC is calculated based on laboratory data for some of these dry linings and compared to that of wet toppings. This data is be used in ISO 12354 to calculate ASTC 47 per NBCC. An acoustical analysis of the effect of bonding a wood topping to CLT structure through a resilient layer is presented. Field measurements are compared to laboratory. We hope the conclusions lead to engineering of greener and quieter buildings for future generations.

Assessing And Controlling Wind Induced Noise From Perforated Aluminum Balcony Railing Panels

Nathan Gara, Brian Howe

Modern condo towers are wrapped in balcony railing panels of a countless number of styles, shapes, and materials. Perforated aluminum railings have proven to produce noise and vibration issues during wind conditions commonly found at the upper floors of tall towers. This paper discusses the various mechanisms that can cause unwanted sound and vibration from perforated aluminum balcony panels, including vortex shedding, jet noise, and Helmholtz resonance. Several strategies for assessing the potential for unwanted sound and vibration from balcony railings are investigated. In-situ sound and vibration measurements, modelling techniques, and full-scale mock-up tests inside of a wind tunnel are all discussed.

Comparison Of Speech Privacy Metrics For Open-Plan And Closed Offices

Rewan Toubar, Joonhee Lee, Roderick Mackenzie

Various metrics have been used to quantify the degree of speech privacy in office spaces. Some metrics were developed for measurements within open-plan offices, whilst others are more suitable for measurements between closed offices or meeting rooms. However, there is no single metric that is intended for speech privacy qualification in both open-plan and closed office settings. There is also a limited understanding of the relationships between the various metrics. Thus, this paper aims to compare the most widely-used speech privacy qualification metrics and identify any of the methods that can be used regardless of the office type (open or closed). Speech privacy measurements were carried out in multiple open-plan and closed offices in Quebec, Canada. In each location type, the following speech privacy metrics were evaluated: Speech Privacy Class; Privacy Index; Speech Transmission Index; and Speech Privacy Potential. A statistical analysis reveals relations between the various speech privacy metrics. The effects of the source and receiver locations and their proximity to room boundaries on the privacy metrics are also investigated. Lastly, the strengths and weaknesses of each method are discussed.

Comparing Low Frequency Sound Isolation Of Different Structures

Sarah Mackel, Sean Syman, Ben Phillipson, Logan Miller

In recent years, mass timber construction has become a crucial component in reducing the carbon footprint of the built environment. While the material has many significant positive attributes, mass timber construction

often results in a reduction in low frequency sound transmission loss due to the lighter weight of the structure, particularly when the mass timber structure is left exposed at the ceiling level. Current design standards for residential buildings do not accurately account for the low frequency performance of demising floor assemblies; this can lead to noise intrusion, complaints, and occupant discomfort if not properly addressed. The shift to mass timber construction may require changes to design standards and practices to ensure that future buildings provide a similar living experience and standard of occupant comfort to traditional construction. This paper will compare the measured transmission loss of various mass timber, traditional wood frame, and concrete residential constructions meeting the minimum building code requirements to show how "built to code" floor assemblies in these different structure types can result in noticeably different sound isolation performances.

The Evolution Of Rr-331 The Guide For Flanking Noise In Buildings
Jeffrey Mahn, Iara B Cunha, Markus Müller-Trapet, Bradford N Gover

The state of the art for building acoustics in Canada is constantly improving as more data is collected and analysis is done. The new knowledge with new products on the market and better building acoustics demanded by both the end users and planners using Universal Design can present challenges for designers and consultants. To address these opportunities, the National Research Council is issuing several new editions of the frequently referenced RR series of reports including the 6th edition of the Guide RR-331 both in English and in French. Now with more explanations for the calculations and jam packed with new examples and data, these new editions will be a valuable resource for navigating the uncertainty. This presentation will showcase the new publications and outline the path ahead as other new research reports are due to be issued in the next few years, including guidance on dwellings for Aging in Place and the calculation of flanking from impact sources.

Living With Upstairs Neighbors: Recent Studies On Impact Sound In Residential Buildings
Markus Mueller-Trapet, Iara Batista Da Cunha, Jeffrey Mahn, Sabrina Skoda

This contribution provides a summary of recent studies related to the perceived annoyance due to impact sound and how it relates to impact sound performance metrics derived from standardized measurements. The recordings of different impact sound sources on various floor/ceiling assemblies used for the studies are described along with different listening test setups. The results of these listening tests are discussed in relation to different standardized and non-standardized performance metrics. The goal of these studies is to gain a better understanding of the relevant factors that affect the perceived annoyance, such as the impact source type and the dominant frequency range. The outcome of these studies will support a future change of the National Building Code of Canada to include an impact sound requirement.

Impact Sound Insulation Performance Of Floating Floor Assemblies On Mass Timber Slabs Under Different Excitation Sources
Jianhui Zhou, Zijian Zhao

Mass timber construction is growing its market in North America. The impact sound insulation perforamnce of mass timber slabs is one the key topics for occupancy comfort in mass timber buildings. This research reported the impact sound insulation performance of two types of floating floor assemblies, continous floating concrete floors and discrete raised floating floors. The impact sound tests were conducted using both ISO tapping machine and ISO rubber ball through a mock-up room approach. The test results are compared with sound pressure level measured under normal human walking. It is found that the ISO rubber ball can better represent the impact sound under human walking, however, it is also assembly dependent. More findings will be discussed in the full paper.

ENVIRONMENTAL NOISE - BRUIT ENVIRONNEMENTAL

Soundscapes from an Urban Environment Bordering on a Green Space

Dale D. Ellis[1]

[1]Adjunct Prof., Department of Physics, Mount Allison University, Sackville, NB
[1]Adjunct Prof., Oceanography Department, Dalhousie University, Halifax, NS
[1]Dale Ellis Scientific Inc., Dartmouth, NS

1 Introduction

Acoustic recordings were made over several years in an urban setting bordering on a green space. Recording was 5 minutes every half hour, day and night, except for rainy weather and occasional gaps the order of one month. The recorder was a Wildlife Acoustics SM3 [1], vintage 2015, usually deployed using two microphones, one near ground level and another 10 m away, about 2 m off the ground. Figure 1 shows the dates of the recordings over the past 4 years. Only a cursory look at the data has been done to date. The dominant feature is of course the daily variation due to bird vocalizations, but seasonal and annual variations can be investigated. The latter are the focus of this note.
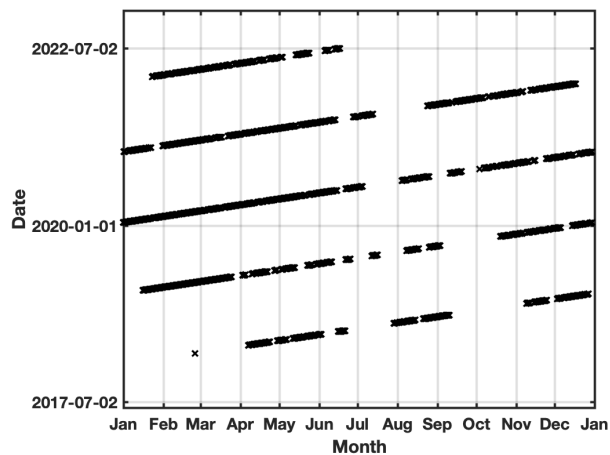
Figure 1: Recordings by month of year from 2018 to 2022.

2 Method

Five-minute recordings centred on the hour and half hour were made at sampling frequency 24 kHz, and the raw data archived as .WAV files. A two pole (12 dB per octave) high-pass filter at 220 Hz was applied to avoid clipping due to the low frequencies. A plot of a five-minute time series and spectrogram using the Audacity software [2] is shown in Fig. 2.

For more analysis, spectra in each 5-minute file were determined using the Matlab [3] command:

```
[S,F,T,P] = spectrogram(data,1024,512,1024,FS,'yaxis');
```

This takes chunks of 1024 points, Hamming window with 50% overlap, and forms the one-sided power spectral density `P` at 513 frequencies `F`. For `FS` = 24 kHz sampling, there are about 1380 time bins `T` of width 0.043 s; `S` is the complex spectrum. The average (P_{avg}) and median (P_{med}) power level of `P` in each bin (about 23.4 Hz wide) were obtained and
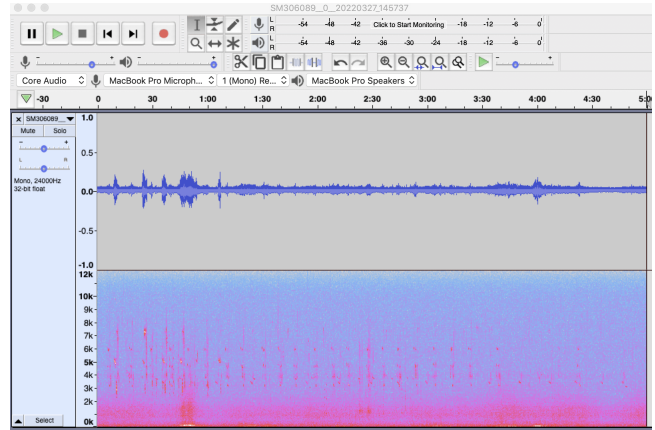
Figure 2: Five minute time series and spectrogram using Audacity [2] software. Note numerous bird calls in 3–8 kHz band.

saved as a compressed summary of the data.
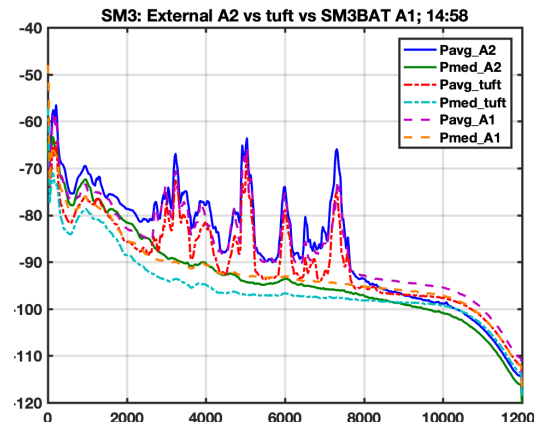
3 Results

Figure 3: Spectrum of average and median power levels of (uncalibrated) on several microphones from 5-minute recording of Fig. 2.

Figure 3 compares the average and median power levels from a number of microphones placed within 30 cm of each other for the time interval shown in Fig. 2. The microphones were the internal ("tuft") microphone in the SM3 recorder, the SMM-A2 external microphone, and the SMM-A1 microphone in a SM3BAT recorder. The internal microphone should be equivalent to the SMM-A1 microphone. Note that these are uncalibrated. Nominal calibration levels are available [1] within 4 dB at 1 kHz, and approximate curves for other frequencies; however, discussion of calibration is beyond the scope of this note. Here we work with the uncalibrated spectral levels.

Figure 4 shows the average levels over 10-day intervals during January and June. On the display there are occasional gaps due to bad weather; during the gaps the last previous recording is repeated until recording was restarted.
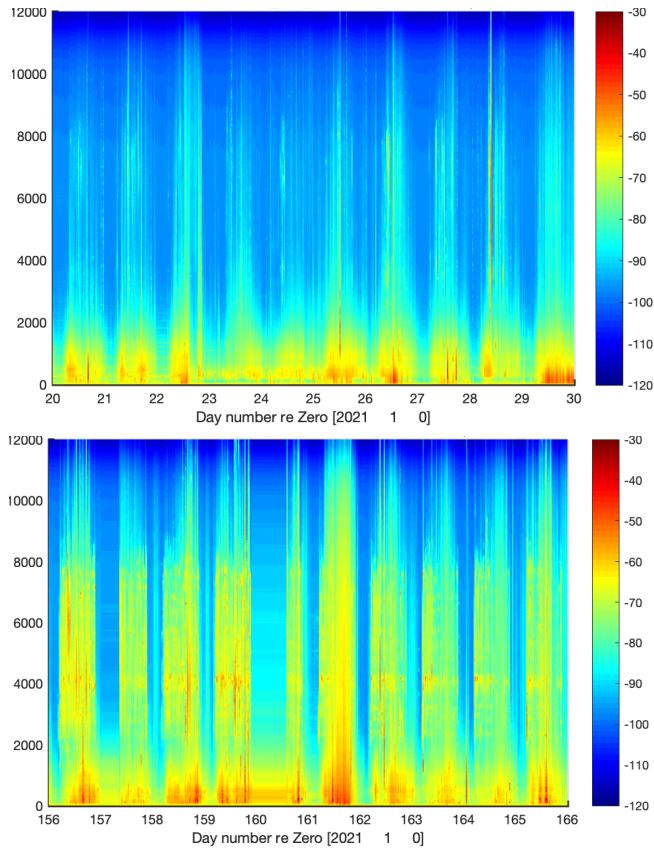

Figure 4: Spectrogram of average 5-minute levels over a 10-day interval in January (upper) and June (lower).

Figure 5 shows median levels for January to March 2019, 2020, and 2021 at four frequencies. The levels are smoothed with a Hann window over 100 recordings (about two days). One can see the day-to-day fluctuations on each plot, and year-to-year differences by comparing the upper, middle and lower plots. There is no obvious "Covid" effect in late March 2020.

4   Summary

This has just been a quick overview of the available data, and a look at the temporal dependence of median levels. More work needs to be done; e.g., calibrated spectra should be compared, and there are interesting features like spectra of individual bird calls that can be investigated.

Acknowledgments

References

[1] Wildlife Acoustics. Song Meter SM3 BIOACOUSTICS RECORDER User Guide, 2020. SM3-USER-GUIDE-20200805.pdf. `https://www.wildlifeacoustics.`
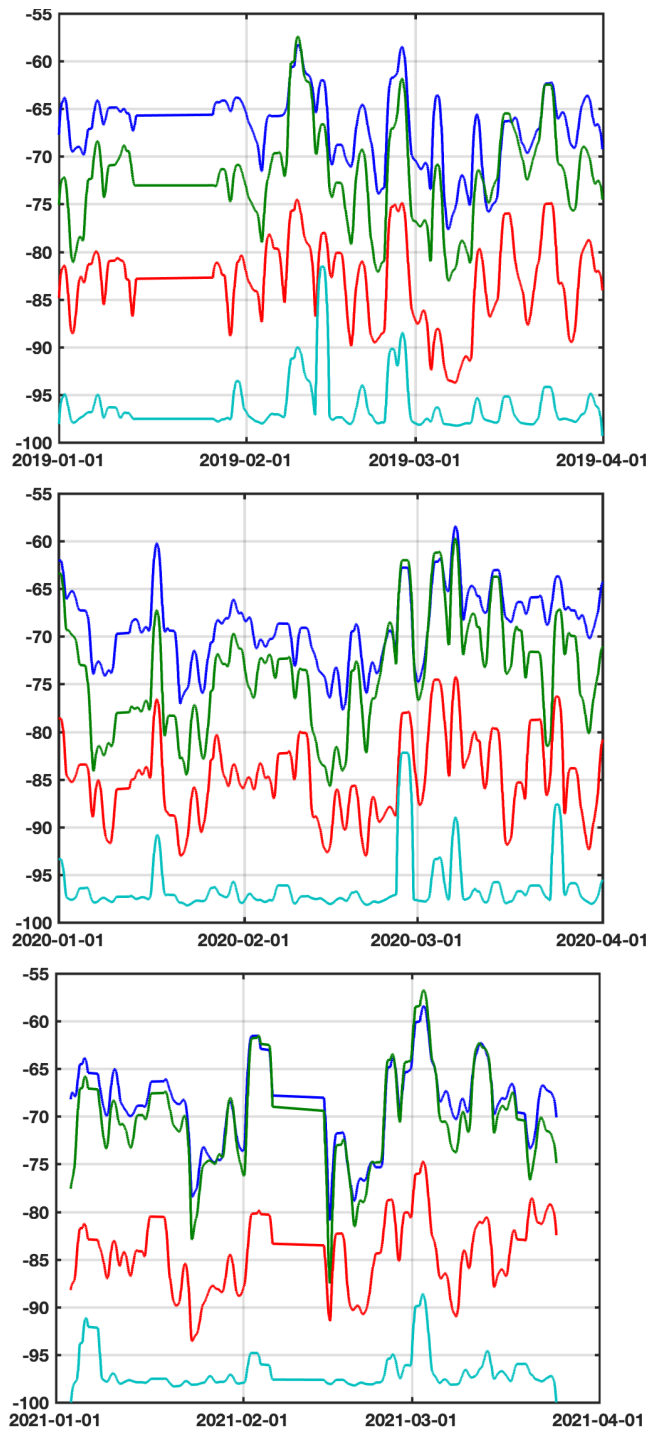

Figure 5: Median spectral levels for January-March in 2019, 2000, and 2001 at 4 frequencies: 117 (blue), 398 (green), 1500 (red), and 6000 (cyan) Hz.

`com/resources/user-guides`; last accessed 2022 Apr 09.

[2] Audacity. *Audacity 2.4.1 Manual*, 2018. `https://manual.audacityteam.org`; last accessed 2022 Jul 29.

[3] The Mathworks, Natick, MA. *MATLAB*, 2017. Version R2017a.

INFLUENCE OF LOCOMOTIVE SPEED AND THROTTLE PROFILES IN NOISE MODELLING

Gillian Redman *[1] **and Ben Coulson** †[1]
[1] RWDI, Guelph, Ontario Canada

1 Introduction

Locomotive speed and throttle settings are key parameters when modelling sound levels from diesel trains. Typically, for large stretches of rail corridors, average speeds and throttle settings are used to model noise emissions. In many cases, this is an appropriate approach to approximate the emission of sound from railways, however, there are scenarios where this approach can significantly affect the accuracy of predicted results. In the context of this study, the requirement for noise mitigation was based on an increase in sound level from an existing scenario to a future scenario. Further complicating the assessment was a change in train technology from diesel to electric locomotives. As seen in Figure 1, the predicted sound levels from diesel trains (at throttle < 6) and electric trains differ significantly at lower speeds.
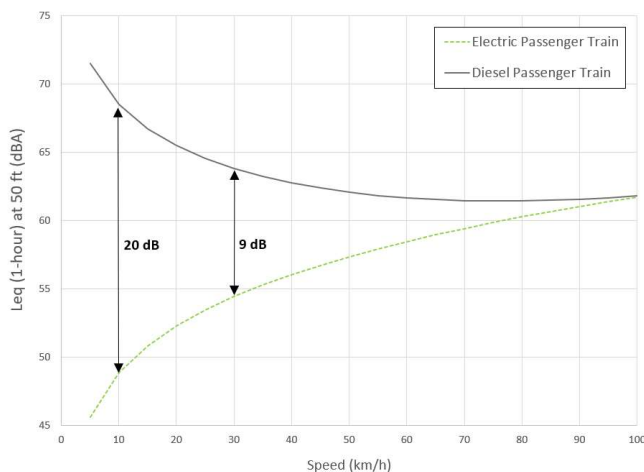

Figure 1: Comparison of Predicted Sound Levels from Diesel and Electric Passenger Trains

Consequently, a new approach to incorporate detailed speed and throttle setting variability along railway corridors was necessary to accurately model rail sound. The detailed modelling would accurately represent the change in sound levels that would occur at lower speeds, particularly around commuter rail stations.

2 Method

To determine the variability of the speed and throttle settings on a train within the study area, speed and throttle setting were obtained from data loggers on the locomotive. As seen in Figure 2, speed and throttle settings vary significantly along the rail corridor.
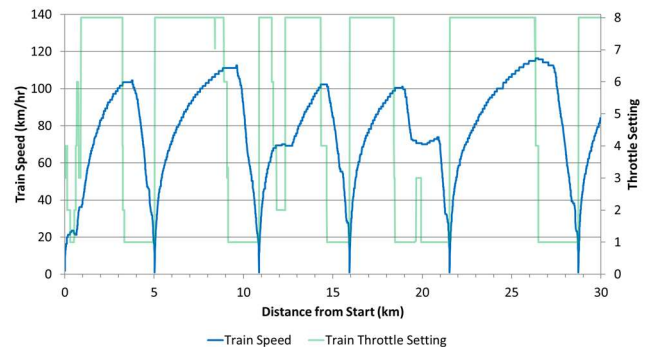

Figure 2: Typical Speed and Throttle Settings for a Locomotive on a Passenger Train

The data obtained was post-processed to generate the average speed and throttle setting for each 10 m segment of railway. This post-processing was done for each type of speed and throttle profile that would occur on the rail corridor, including such things as: local and express trains, non-revenue train movements (i.e. no station stops), direction of travel (i.e. eastbound or westbound), and the inclusion of the effect of new stations in the future.

Modelling of train emission levels was done with the Federal Transportation Authority's railway model (FTA, 2018) implemented with Cadna/A, a commercially available 3-D noise propagation software package. Within Cadna/A the rail corridor was modelled in 10 m segments with unique speed and throttle settings for each segment, reflecting the typical operations of each train. A sample of resulting predicted sound levels for diesel and electric trains are presented in Figures 3a and 3b, respectively.
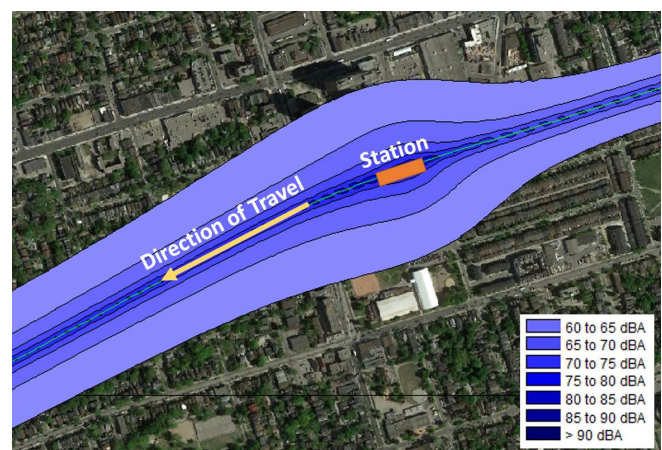

Figure 3a: Sample of Predicted Sound Level Contours Incorporating Speed and Throttle Profiles – Diesel Locomotive

---
* Gillian.Redman@rwdi.com
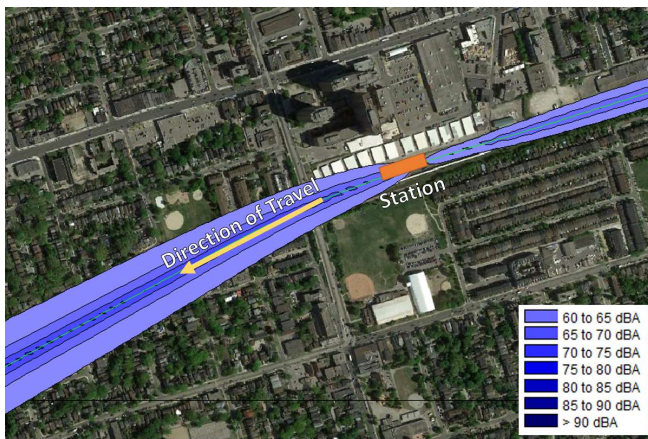† Ben.Coulson@rwdi.com

Figure 3b: Sample of Predicted Sound Level Contours Incorporating Speed and Throttle Profiles – Electric Locomotive

These figures demonstrate the change in predicted sound level that occurs from incorporating detailed speed throttle settings into the modelling. The variation in the sound level contours in Figures 3a and 3b are a result of speed and throttle settings only. In Figure 3a it can be seen that as a train pulls into a station, its speed decreases and the throttle is set to 1; resulting in lower sound levels. As the train pulls out of the station, although the speed is slow, the throttle setting is at 8 resulting in higher predicted sound levels. In Figure 3b, where only speed influences the predicted sound levels of electric locomotives, sound levels decrease significantly around the station where speeds are low.

3 Results

In general, we see the largest differences from using the average in lieu of detailed data around stations, with localized differences in prediction over 10 dB in some cases. With FTA predictions, the use of average speed and throttle settings are likely to over-predict sound for electric trains and under-predict sound for diesel trains. Figures 4a and 4b demonstrate the difference in predicted sound levels when using detailed data in lieu of average data. In these figures, the average speed was 65 km/h and the average throttle was 5.
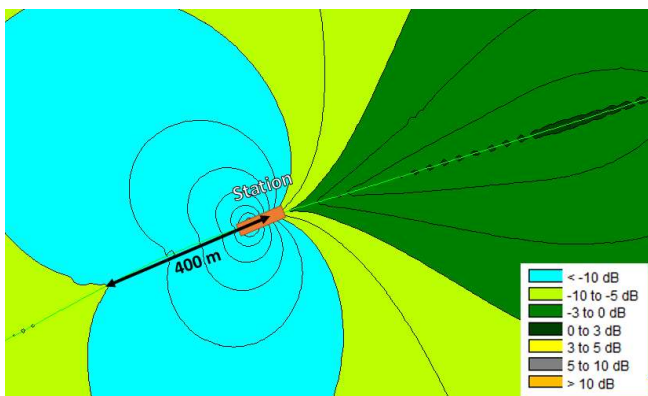

Figure 4a: Difference in Predicted Sound Level Contours Between Average and Detailed Speed and Throttle Profiles – Diesel Locomotive
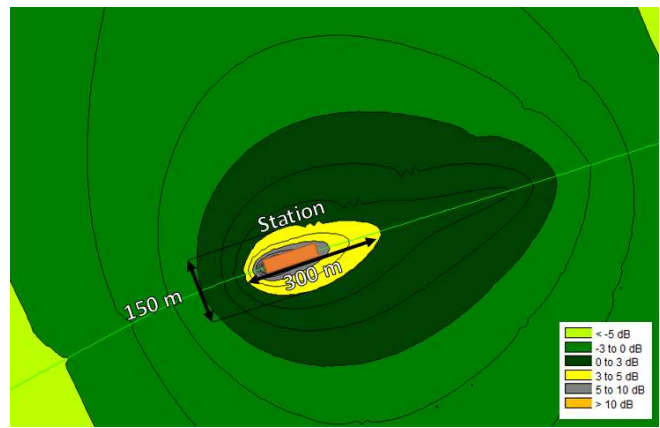

Figure 4b: Difference in Predicted Sound Level Contours Between Average and Detailed Speed and Throttle Profiles – Electric Locomotive

When considering changes in sound level, as is typically done for rail assessments in Ontario, the inaccuracy of using average speed and throttle settings can be compounded when accompanied by changes in locomotive technology.

4 Discussion

Based on the results of this study, the use of detailed speed and throttle profiles is critical in areas surrounding stations, where trains will be slowing to a stop and accelerating out of the station. Given the significant influence the throttle setting of the train has on the predicted sound level (+6 dB between throttle 5 and throttle 8) this is critical for diesel locomotives. In scenarios where a change in locomotive technology is incorporated into the analysis, these detailed profiles are again critical at lower speeds due to the large difference between predicted emissions from electric and diesel locomotives at these speeds (20 dB at 10 km/h and 9 dB at 30 km/h). For scenarios where trains are travelling at continuous speeds, or speeds are generally high, the detailed speed and throttle profiles will not significantly improve the accuracy of the modelling. In these scenarios, the use of average speed and throttle data would be appropriate.

5 Conclusion

The incorporation of detailed speed and throttle profiles improves the accuracy of predicted sound levels using the FTA algorithms. This is particularly critical when considering train movements around stations, at low speeds, or when changes in locomotive technology are being considered.

References

[1] U.S. Department of Transportation, Federal Transit Administration. Transit Noise and Vibration Impact Assessment Manual, 2018.

The Impact Of Working From Home On Post Pandemic Traffic Distributions And Noise Assessment

Kathryn Katsiroumpas, Morgan Austin

The COVID-19 pandemic influenced many factors of everyday life. Some of these changes were transient while others have had longer lasting effects. Working from home has remained an acceptable alternative for many workplaces, while a number have transitioned to a hybrid model with employees travelling to the office part of the week. Hybrid employees are beginning to exhibit strong preferences to work from home on certain days of the week. In addition, workplaces are more accommodating to office hours that don't conform to the standard "9 to 5". These are some of the factors that are expected to have prolonged impact on commuter traffic in urban areas. Acousticians typically use universally accepted standards of hourly traffic distribution, from sources such as the ITE, when analysing road traffic noise. Post pandemic traffic distributions and "real-time" traffic congestion in urban Toronto have been examined and compared to these historical distributions to determine the implications on sound exposure analysis. This includes assessing predictive future road traffic noise impacts as well as establishing current sound level limits for stationary noise sources using hourly ambient generated by road traffic.

Noise Mapping: Current Trends And Areas For Improvement

Jean-Philippe Migneron, Frédéric Hubert, Jean-Gabriel Migneron

After several months dedicated to the study of noise mapping techniques, this presentation shares insights on the final remarks made during the research project answering some of the questions asked by the environmental noise expert group at the Quebec government. In addition to the findings of the previous literature review, some experiments have shown that the implementation of noise maps in the province is not an easy process, especially with larger scales. For example, data collection can be complicated between all the departments or agencies holding the information. This work has allowed us to draw a certain portrait of current practices and to suggest ways to improve them in order to facilitate the work of multiple stakeholders likely to prepare, use or interpret noise maps in the Canadian context. A few steps must be taken forward between what is available today and what could be expected from real-time noise assessment tools imagined around the concept of smart cities while caring for public health purposes.

Analysis Of Ventilation Coefficient And Atmosphere Stability During The Post-Monsoon

Priyanka Singh

In this study comparative analysis of atmospheric boundary layer height and ventilation coefficient over four regions of north India namely Delhi, Hisar, Alwar, and Aligarh have been made using real time SODAR (Sound Detection and Ranging) data. It's important to note that the Indo-Gangetic plain, particularly the western portion, has the highest anthropogenic aerosol emissions during the post-monsoon season. For this reason, data from the post-monsoon months of October, November, and December have been included in the current article. Different stability classes have also been investigated throughout all of these locations utilising the various SODAR ecogram structures. According to a diurnal study on ABL height, Alwar has the greatest average hourly ABL height, followed by Delhi, Aligarh, and Hisar. To determine the dispersion of air pollution in the atmosphere at these locations, additional ventilation coefficient analysis was also conducted. It is observed that during the post-monsoon season, Alwar had the highest ventilation coefficient, followed by Delhi, Hisar, and Aligarh, with Aligarh having the lowest VC, indicating poor air quality. Ventilation and unstable atmospheric conditions are more correlated. Wind speed, temperature, and variations in the atmospheric circulation during the day and night all have an impact on ventilation.

MUSICAL ACOUSTICS - ACOUSTIQUE MUSICALE

MEASUREMENTS OF MECHANICAL PROPERTIES OF ADIRONDACK SPRUCE

Olivier Robin[*1]**, Élie Garot**[†1,2]**, and Kerem Ege**[‡2]

[1]Centre de Recherche Acoustique-Signal-Humain, Université de Sherbrooke, Sherbrooke (QC) J1K2R1, Canada
[2]LVA- INSA Lyon, 25 bis av. Jean Capelle 69621 Villeurbanne, France

1 Introduction

Adirondack spruce (*Picea rubens*), also known as Eastern red spruce or Appalachian spruce, is a conifer found primarily in New England, the Appalachians and eastern Canada. This wood has been historically used in the production of fancy foods such as spruce beer and spruce gum (from the needles especially), but also as construction lumber, pulpwood and even as Christmas trees. Adirondack spruce wood began to be used in the 19th century for piano, guitar and mandolin soundboards. Prior to World War II, it was indeed the preferred soundboard tone wood for several guitar makers and is still widely in use for this purpose. Despite its large use in various fields, Adirondack spruce's mechanical properties (like Young's moduli in longitudinal and radial directions, and damping loss factor) are not well documented. In this work, several methods are used to evaluate such properties of twelve quarter-cut orthotropic plates selected for guitar soundboards (2nd grade). The identified values for the elastic and damping constants of this orthotropic material are summarized and compared as a function of frequency.

2 Tested structures and test conditions

The tested structures are twelve quarter-cut plates intended to be used as left and right parts of six guitar soundboards (see Fig. 1). The measured mean dimensions of the plates are 560 mm x 227 mm x 5 mm (Length L_x x Width L_y x Thickness h, with a variation of $\pm$ 1 mm for length and width, and $\pm$ 0.2 mm for thickness). The mean mass density, ρ, is obtained from geometrical measurements and a balance of 0.1 kg precision, and equals 443 kg/m³. Two series of measurements are conducted. The first consists in impact testing using a miniature impact hammer (PCB 086E80) and an single-axis accelerometer (PCB 353B18). Excitation and measurement point are identical and positioned on each side of the soundboard. Acceleration over force frequency response functions (FRF) are calculated using five averages and the H1 estimator (sampling frequency is 20280 Hz, frequency resolution equals 1.25 Hz). The raw time domain signal from the accelerometer is used to calculate the loss factor using the decay rate method. The second series of measurements uses a piezo exciter (see Fig. 1) with a white noise input. Using a scanning laser Doppler vibrometer (LDV Polytec PSV400), the spatial vibration measurement is measured over two grids corresponding to two frequency ranges : 19×9 points (for modal identification between 50 and 400 Hz), and 77×37 points (for IWC method between 400 and 5000 Hz). For all tests, the boards are supported by two bungees at two attach-

[*]olivier.robin@usherbrooke.ca
[†]elie.garot@usherbrooke.ca
[‡]kerem.ege@insa-lyon.fr

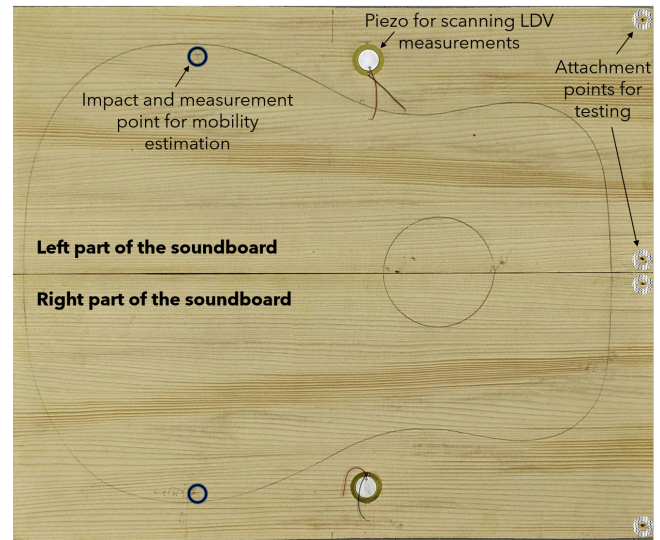ment points, as shown in Fig. 1.

Figure 1: Left and right parts of soundboards 6L and 6R, including position for mobility measurement, position of the piezo exciter and attachments points.

3 Methods

Modal identification. In [1], a simple yet reasonably accurate method is detailed for the determination of 'elastic and damping constants of orthotropic sheet materials'. These constants are deduced from the identification of the lowest 'bending beam' vibration modes using their corresponding shapes in free-free boundary conditions. From the resonance frequencies of these modes ($f_{r,l}$, subscripts r and l standing for radial and longitudinal directions), the rigidity constants $D_{1,3}$ for orthotropic materials in x and y directions can be estimated following the approximated relation $D_{1,3} \simeq 0.0789 f_{r,l}^2 \rho L_{x,y}{}^4 h$. By linking rigidity to corresponding Young's modulus $E_{x,y}$ in x and y directions, $D_{1,3} = \frac{E_{x,y} h^3}{12(1-\nu_{xy}\nu_{yx})}$ and finally $E_{x,y} = \frac{D_{1,3} 12(1-\nu_{xy}\nu_{yx})}{h^3}$.

Inhomogeneous wave correlation (IWC). The IWC method uses the 2D wave field of a vibrating plane structure, in order to identify the angle-dependent dispersion curve by comparing it with an inhomogeneous wave (i.e. a damped plane wave). It results into the identification of a complex wave number [2]. In this work, the real part of the identified wave number in the longitudinal and radial directions is used to estimate the corresponding Young's moduli. Spatial vibration measurements (LDV) are post-processed at frequencies of 500, 1000, 2000, 3000, 4000 and 5000 Hz.

Decay rate method. In this case, the measured impulse reponse is filtered in the time-domain using third order band-

pass Butterworth filters (with lower and upper frequencies bounds defined following those of third octave bands between 125 Hz and 1250 Hz). The Schroeder's backward integration method is then applied to each time-filtered signal, and the slope is identified over a 10 dB decay using a first order polynomial curve fitting. The loss factor η equals $Dec/27.3f$, where Dec is the identified decay in dB per second and f is the central frequency of the considered third octave band [3].

Half-power bandwidth method (-3 dB method). In this method, the resonant frequency f_p for each well-separated vibration mode is identified, as well as the upper and lower frequencies ($f_{2,1}$) around this peak for which the amplitude equals the amplitude at resonance divided by the square root of two (-3 dB for $20 \log_{10}$ of the FRF). The loss factor η is now calculated following $(f_2 - f_1)/f_p$.

4 Results

In table 1, the results obtained using the identification of specific vibrations modes are summarized (Left and Right parts of soundboards are indicated by letter L or R, respectively). The mean values (and standard deviation) for E_x and E_y are 9.66 GPa (0.38 GPa) and 0.89 GPa (0.14 GPa), respectively.

Table 1: Results obtained following the approximation from [1]

Soundboard	1L	1R	2L	2R	3L	3R
ρ (kg.m^{-3})	422	408	442	429	427	424
E_x (GPa)	10,17	9,07	9,39	9,10	10,04	9,49
E_y (GPa)	0,61	0,69	1,00	0,98	1,00	0,99
-	4L	4R	5L	5R	6L	6R
ρ (kg.m^{-3})	461	460	456	461	459	464
E_x (GPa)	9,99	9,45	9,72	9,68	10,18	9,60
E_y (GPa)	0,72	0,84	0,96	0,94	0,92	0,97

Theses results are compared with those obtained using IWC methods in the upper part of Figure 2. The estimated value of E_y is fairly constant with increasing frequency, and the methods based on [1] and [2] provide similar results, with a mean value of 0.63 GPa. The estimation of E_x shows larger variations. The IWC method is indeed sensitive to measurement noise and provides more biased estimations in the high frequency domain when the energy is more localised near the source. Based on these first results, the implementation of the method will be applied with a finer frequency step and will include other directions than only longitudinal and radial ones, as well as loss factor estimation. Concerning this parameter, the mean estimated values using the Decay Rate Method and the Half Bandwidth Method are 1.95% and 2.19%, respectively (see lower part of Figure2).

The values presented in this section for Adirondack spruce are in the range of those reported in the literature for spruce. Identified orthotropic ratio ($E_x/E_y \approx 10$) and loss factor ($\approx 2\%$) are also consistent with published studies on other resonant woods [4,5]. One can note that the experimental systematic estimation of structural loss factor of wood for musical instruments up to 1 kHz is not common in the literature.
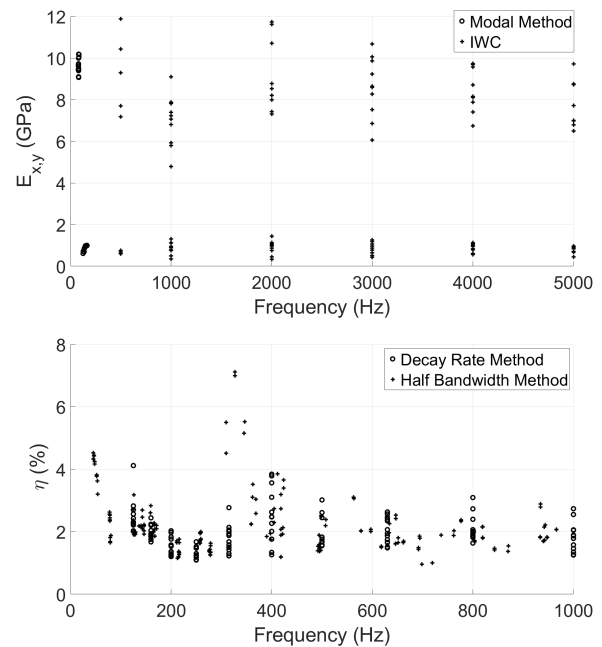

Figure 2: (Upper part) Summary of the results obtained concerning Young's modulus in principal (E_x) and longitudinal (E_y) directions - (Lower part) Summary of the results obtained concerning loss factor estimation.

5 Conclusions

This paper reports identified values for the elastic and damping constants of Adirondack spruce soundboards. The next steps of this work are (1) to link those parameters to grading criteria used in tone wood selection for guitar crafting, and (2) to develop classification indicators that will be evaluated along the whole crafting process (i.e. from the initial soundboard selection to the final instrument).

Acknowledgments

References

[1] M.E. McIntyre and J. Woodhouse. On measuring the elastic and damping constants of orthotropic sheet materials. *Acta Metall*, 36(6):1397–1416, 1988.

[2] J. Berthaut et al. K-space identification of apparent structural behaviour. *J Sound Vib*, 280(3):1125–1131, 2005.

[3] B.C. Bloss and M.D. Rao. Estimation of frequency-averaged loss factors by the power injection and the impulse response decay methods. *J Acoust Soc Am*, 117(1):240–249, 2005.

[4] D.W. Haines. On musical instrument wood. *Catgut Acoust. Soc. Newsletters*, 31:23–32, 1979.

[5] R. Viala et al. Simultaneous non-destructive identification of multiple elastic and damping properties of spruce tonewood to improve grading. *J Cult Herit*, 42:108–116, 2020.

USING FEEDBACK TO MANIPULATE THE TONAL HIERARCHY

Sarah Sauvé *[1], Dominique Vuvan †[2] and Benjamin Rich Zendel ‡[1]

[1]Faculty of Medicine, Memorial University of Newfoundland, St. John's, NL A1C 5S7

[2]Psychology Department, Skidmore College, 815 North Broadway, Saratoga Springs, NY 12866

1 Introduction

Tonality is the complex hierarchical structure that governs the organization of pitch in Western music and is learned implicitly [1–4]. This implicit knowledge allows non-musicians to rate the belongingness of probe tones within a tonal context in a manner consistent with music theoretical descriptions of tonality [5]. Recent work has shown that the tonal hierarchy can be manipulated using random performance feedback when participants listened for tonal incongruities in melodies [6]. Random feedback reduced accuracy and confidence in identifying "out-of-key" notes in melodies and suppressed the late positive electrical brain responses usually elicited by the conscious detection of such a note [7]. This leads to the possibility of using reversed performance feedback to alter the perception of a single note.

2 Méthode/Method

2.1 Participants

Twelve volunteers took part in this study. They provided written informed consent in accordance with the Interdisciplinary Committee on Ethics in Human Research at Memorial University of Newfoundland. All participants were healthy, free of any cognitive deficit, hearing or visual impairments and had less than five years of formal musical training with no music theory training. Participants received a small cash honorarium for their participation.

2.2 Stimuli and Procedure

Tonal judgement task

A set of 160 melodies of between 7 and 15 successive tones were composed by two trained musicians for this study. Stimulus files are available at https://osf.io/pyrt7/. Melodies were synthesized in two versions, one "good" (in-key) and one "bad" (out-of-key), resulting in 320 melodies in total. The changed pitch always affected the same tone, which was 500 ms in duration and fell on the first downbeat in the third bar. For in-key melodies, target tones were either the II or IV scale degrees, and for out-of-key melodies, the target tones were bII or #IV (tritone).

For each trial, the participant heard two versions of the same melody and was asked which melody contained a bad note, and if they were sure or unsure of their choice. The type of performance feedback was manipulated across 3 Blocks (40 trials each): No feedback (*Baseline*), bad feedback (F*eedback*) and correct feedback (*Recovery*). During the *Feedback*

block, bad feedback was only given for melodies containing the II and bII scale degrees. That is, when the participant reported that the bII was 'bad', they were told they were wrong, and when they reported that the II was 'good', they were told they were wrong, and vice versa. During the *Recovery* block the feedback provided was correct

Probe tone paradigm

To determine how each participants' ratings for each of the chromatic notes changed as a function of reversed feedback, a standard probe-tone paradigm was used. Each trial consisted of a 100 ms burst of white noise, followed by the *context*, an arpeggio of 7 tones, and finished with a *probe tone*, which was one of the twelve notes of the chromatic scale. The arpeggio in the key of C was: C (I) E (III), G (V), C (+1 octave), G, E, C. Each tone was 500ms long, with a 200 ms silent period between each tone. The probe tone was 1200ms after the final tone of the context. All stimuli can be found on the project's OSF page (https://osf.io/pyrt7/). For each trial, participants rated how well the probe tone "fit" into the context on a scale of 1-7. Each tonal hierarchy block covered 4 keys and consisted of 48 trials. This was repeated 4 times throughout the study (*PT1, PT2, PT3, PT4*)

Overall Procedure

The study took place over two days and involved deception. Participants were told as part of the informed consent process that the feedback provided was designed to improve their performance. On day 1, participants completed the *PT1*, the *Baseline* block, two *Feedback* blocks and the *PT2*. On the second day, participants completed the *PT3*, two *Feedback* blocks, the *PT4*, a debriefing and the *Recovery* block (optional). Before being debriefed, participants were asked if they had noticed anything strange about the feedback. No participant identified the reversed feedback pattern. Seven of the twelve participants completed the recovery block.

3 Résultats/Results

We use frequentist statistics, alpha = .05. All analysis ran in R 3.6.2 with RStudio using the tidyverse package [8].

3.1 Tonal judgement task

In all blocks, correctly identifying the 'bad' note (i.e., bII or #IV) as 'bad' was considered correct, regardless of the feedback provided. Confidence was scored as *sure* or *not sure*, regardless of accuracy. Figure 1 plots mean accuracy and confidence in each Block for each Scale Degree. In a linear model predicting Accuracy with Block, Scale Degree and their interaction as predictors (Figure 1A), the main effect of

---
* sarah.a.sauve@gmail.com
† d.vuvan@gmail.com
‡ bzendel@mun.ca

scale degree was significant. While coefficients decreased for each successive block, it was not a significant predictor. Accuracy for scale degree 2 was always better than scale degree 4, and sometimes that difference was significant in follow-up t-tests with Bonferroni correction.

In a linear model predicting confidence with block, scale degree and their interaction as predictors (Figure 1B), all predictors were significant. Confidence was lower during *Feedback* blocks compared to *Baseline* and *Recovery* blocks, and was lower for the IV/#IV judgment compared to the II/bII judgement.
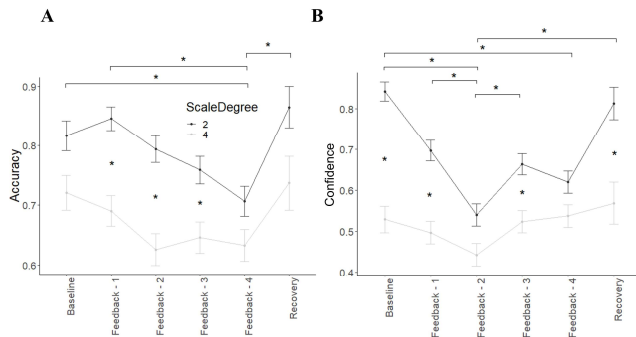
Figure 1: Mean accuracy (A) and confidence (B) in each block for each scale degree. Error bars show standard error of the mean. Significant differences are marked by brackets and asterisks, p < .0005.

3.2 Probe tone paradigm

Figure 2 shows mean ratings (A) mean ratings for each manipulated scale degree bII, II, IV and #IV for *PT1, PT2, PT3 and PT4*. We expected ratings for the bII to increase from *PT1-4*, and for ratings of the II to decrease from *PT1-4* due to the *Feedback* blocks.

In a linear model predicting rating with scale degree, block and their interaction, scale degree was a significant predictor. A linear model predicting standard deviations (proxy for confidence) with scale degree, block and their interaction, scale degree was a significant predictor.
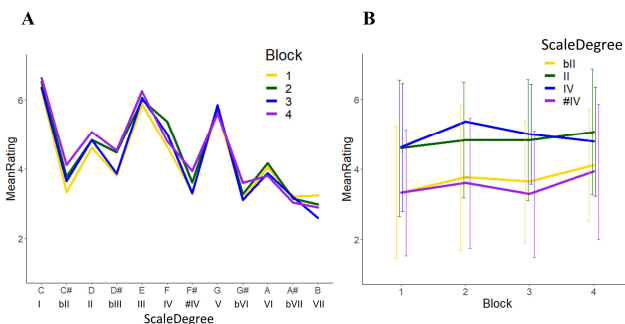

Figure 2: Mean ratings for all scale degree and blocks (A) and for manipulated scale degrees for each block (B).

4 Discussion

Participants were not convinced that a "bad" note was "good", nor did manipulation systematically alter their overall tonal hierarchy schema. Though accuracy decreased over time, assuming a continued linear trend, it would take longer

exposure to bad feedback to cause the intended switch. Accuracy decreased slowly even as certainty decreased quickly.

It is noteworthy that accuracy and certainty were higher for II than for IV. Typically perceived as an especially dissonant note, the tritone (#IV) should be the easiest to identify as "bad". However, most notes can be manipulated to be perceived as well-fitting with context alone. It is possible that the #IV was consistently approached and resolved in a way that promoted more "fit" than the bII.

5 Conclusion

Within the feedback blocks, our work replicates previous studies that found decreases in confidence and accuracy when inaccurate feedback is provided, although our accuracy results failed to reach significance [6]. More importantly, by using a probe tone paradigm our results suggest that perception of a single note in the tonal hierarchy is resistant to targeted manipulation using bad feedback, suggesting that representation of the tonal hierarchy is stable.

Remerciements/Acknowledgments

References

[1] T. Collins, B. Tillmann, F. S. Barrett, C. Delbé, and P. Janata, "A combined model of sensory and cognitive representations underlying tonal expectations in music: From audio signals to behavior.," *Psychol. Rev.*, vol. 121, no. 1, p. 33, 2014.

[2] C. L. Krumhansl, *Oxford psychology series*. Cognitive foundations of musical pitch. New York, NY, US: Oxford University, 1990.

[3] J. R. Saffran, E. K. Johnson, R. N. Aslin, and E. L. Newport, "Statistical learning of tone sequences by human infants and adults," *Cognition*, vol. 70, no. 1, pp. 27–52, Feb. 1999, doi: 10.1016/S0010-0277(98)00075-4.

[4] B. Tillmann, J. J. Bharucha, and E. Bigand, "Implicit learning of tonality: a self-organizing approach.," *Psychol. Rev.*, vol. 107, no. 4, p. 885, 2000.

[5] L. L. Cuddy and B. Badertscher, "Recovery of the tonal hierarchy: Some comparisons across age and levels of musical experience," *Percept. Psychophys.*, vol. 41, no. 6, pp. 609–620, 1987.

[6] D. T. Vuvan, B. R. Zendel, and I. Peretz, "Random feedback makes listeners tone-deaf," *Sci. Rep.*, vol. 8, no. 1, pp. 1–11, 2018.

[7] J. Polich, "Updating P300: an integrative theory of P3a and P3b," *Clin. Neurophysiol.*, vol. 118, no. 10, pp. 2128–2148, 2007.

[8] H. Wickham, "Welcome to the tidyverse.," *J. Open Source Softw.*, vol. 4, no. 43, p. 1686, 2019, doi: https://doi.org/10.21105/joss.01686.

BRAMSBioBox: Developing an Open Research Platform for Audio and Biosignals Monitoring

Floris van Vugt [*1,3,4], **Valentin Pintat** [†2], **Dawn Merrett** [‡1,3,4], **Simone Dalla Bella** [§1,3,4], **and Jérémie Voix** [¶1,2,4]

[1]International Laboratory for Brain, Music and Sound Research (BRAMS), Montréal, Canada
[2]École de technologie supérieure, Montréal, Canada
[3]Département de Psychologie, Université de Montréal, Montréal, Canada
[4]Center for Research on the Brain, Language and Music (CRBLM), Montréal, Canada

1 Introduction

1.1 Context

Music is an inherently social phenomena. Virtually all cultures use music in the context of group rituals, parent-to-infant connection or to reinforce social identity. A key feature of music is thus the social context in which it is embedded. Research on music, as well as neuroscience at large, is progressively moving from studying individual humans in sterile audio booths, to investigating multiple humans simultaneously engaging interactively in real-world musical behaviors, for example dancing to music or creating a joint beat in social drumming. A unique window into social dynamics that unfold under these conditions is our physiology: cardiac rhythms, respiration, perspiration. These physiological signals are linked not only to emotions [1], which are a crucial element of music experience, but also to elusive social constructs such as rapport [2, 3] affiliation [4] and group dynamics [5, 6]. Since these measures tap into the autonomous nervous system, they allow us to tap into implicit processes underpinning our reaction to music. Physiological measures are less prone to subjective or social desirability biases and thus more reliable than self-reported measures typically used. What is more, physiological measures can be collected continuously. This possibility offers an unparalleled opportunity to capture the interaction process as it is unfolding, without having to interrupt participants at various points in time to ask them to complete a questionnaire. These measures can then be compared between participants in an activity, for example by probing how musical activities synchronize respiration and cardiac rhythms. Such physiological linkage has been shown to predict the amount of social affiliation [4]. Thus, studying physiology of multiple participants interacting in musical contexts is a key avenue to understand the social nature of music [7].

1.2 Challenge

In order to record physiology of multiple participants simultaneously in real-life settings, we need to solve a number of methodological challenges. (1) Data of different modalities needs to be collected simultaneously: cardiac signals, respiration, motion, and audio, to name but a few; (2) Recordings from multiple participants need to be aligned in time,

that is, we need to know which moment in one participant's time series corresponds to the same moment in another participant's; (3) Data needs to be collected wirelessly, so that participants can move unimpeded as they would in natural musical settings (nothing as annoying as tripping over a wire while showing off your summit dance move); (4) The setup needs to be scalable, so that in principle more devices can be added allowing measurement of dozens or more participants. Existing frameworks: Commercial frameworks exist that do some combinations of the above. These solutions typically do not provide tangible guarantees about synchronization, such as upper limits on time delays, which, especially when it comes to audio, is critical for music research. Indeed, when put to the test these solutions often perform only moderately well [8]. Moreover, their price tags are several thousand dollars per unit and upwards. Such prices make these units impractical for studying real-life musical behaviors, because we cannot buy as many of them as are needed for studying group behaviors, let alone carry them out of the lab as we need to do if we want to study real-life musical behaviors in concert halls, dance venues or parks. What is needed is a device that is fully synchronized across modalities and between people, low-cost, portable, non-invasive and scalable.

2 Method

2.1 Proposed solution

In this project, we will develop an elegant solution that delivers on all these requirements. The design (see figure 1) is based on a recently published framework for measuring physiology of a single person [9]. We will produce a custom 3D-printed box, roughly the size of a cell phone, which contains a Teensy microcontroller - essentially a small computer. This microcontroller reads a handful of sensors (more can be added) that tap into respiration, cardiac signals, whole-body movement, as well as audio, for a single participant. The data is stored locally on an SD card, from which we can, after the experiment, download the data for offline analysis. The data is also transmitted in real-time through a WiFi signal. The device is powered by a battery and attached to a belt worn by the participant. Electrocardiogram (ECG) sensors are attached to participants' body and respiration is measured using a belt over their thorax which contains a force sensor, measuring contraction and expansion of the chest to assess respiration. Multiple participants each wear one such device, which can operate simultaneously in parallel, streaming their data to a central PC. This computer records the incoming data in a synchronized manner, using the Laboratory Streaming Layer

---

[*]floris.van.vugt@umontreal.ca
[†]vpintat@critias.ca
[‡]dawnmerrett@gmail.com
[§]simone.dalla.bella@umontreal.ca
[¶]jeremie.voix@etsmtl.ca

(LSL) [10], which cleverly estimates the delays in each of the data streams coming from the various devices, in order to realign them in time. Data will be available for online visualization routines but also saved in the standardized HDF5 data format. Further preprocessing pipelines will be developed.
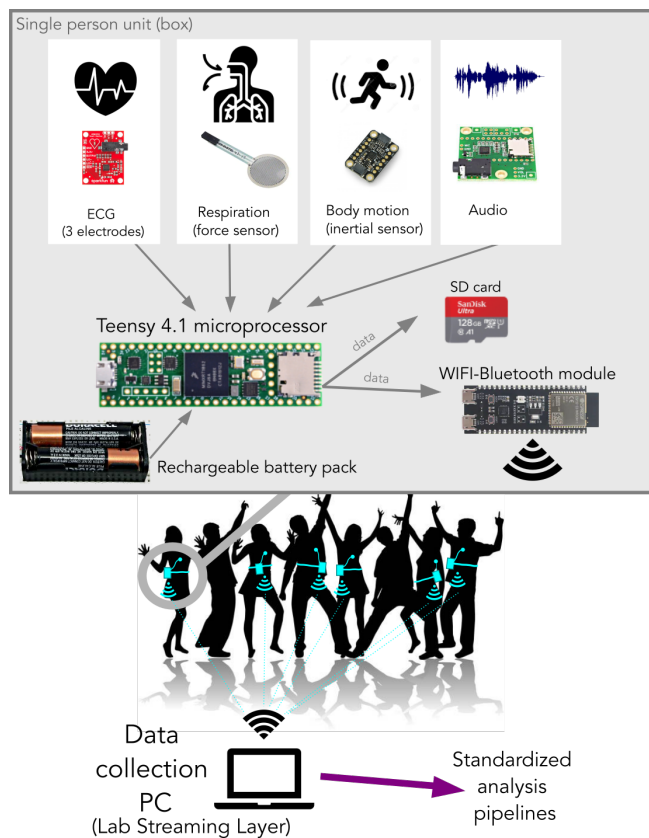

Figure 1: Overview of the BRAMS-BioBox input sensors, architecture and communication stack.

2.2 Validation experiment

To test whether this proposed solution delivers on all promises, and to assess its precision and reliability, we will test this on five groups of four participants who engage in a joint clapping task. This experiment will be performed in the BRAMS laboratories so that we can compare the to-be-developed device with an existing commercial solution, representing our ground truth. We will compare the data collected by the two frameworks using correlation (to test agreement) and absolute differences (to test discrepancies), following validation experiments for other devices [11, 12].

3 Perspectives

The potential research applications for this device are many. For example, in its current form it can be used, as we are planning to, to measure the dynamics of social cohesion in choirs. We can study the intensity of emotional experience of a group dancing to music at a party. We can map out whether emotions are shared between performers in a concert hall and their audience. Other sensors can be added straightforwardly, such as galvanic skin response to measure stress

and psychological safety. Future work can also expand on this design where data captured by these devices are streamed live and in synchrony to a central computer for biofeedback purposes. Other sensors are also currently being integrated, such as thermoresistor for respiration sensing and a photoplethysmography (PPG) sensor on earlobe. The BRAMS-BioBox device design blueprint as well as all code that will be developed will be made available freely on Github, and all relevant documentation will be made available at website `https://bioarp.org` that is also a gateway hub for any future commercial offer of such open hardware & software platform for the research community.

Acknowledgments

References

[1] M.M. Bradley and P.J. Lang. *Measuring emotion: Behavior, feeling, and physiology. in Cognitive neuroscience of emotion 242–276*. Oxford University Press, 2000.

[2] W. Tschacher and D. Meier. Physiological synchrony in psychotherapy sessions. *Psychother. Res*, 30:558–573, 2020.

[3] C.D. Marci, J. Ham, E. Moran, and S.P. Orr. Physiologic correlates of perceived therapist empathy and social-emotional process during psychotherapy. *J. Nerv. Ment. Dis*, 195:103–111, 2007.

[4] C. Danyluck and E. Page-Gould. Social and physiological context can affect the meaning of physiological synchrony. *Sci. Rep*, 9:8222, 2019.

[5] D. Mønster, D.D. Håkonsson, J.K. Eskildsen, and S. Wallot. Physiological evidence of interpersonal dynamics in a cooperative production task. *Physiol. Behav*, 156:24–34, 2016.

[6] A. Tomashin, I. Gordon, and S. Wallot. Interpersonal physiological synchrony predicts group cohesion. *Frontiers in Human Neuroscience*, page 439, 2022.

[7] S.E. Wright, V. Bégel, and C. Palmer. Physiological influences of music in perception and action. *Elem. Percept*, 2022.

[8] L. Menghini. Stressing the accuracy: Wrist-worn wearable sensor validation over different conditions. *Psychophysiology*, 56:13441, 2019.

[9] C. Maitha. An open-source, wireless vest for measuring autonomic function in infants. *Behav. Res. Methods*, 52:2324–2337, 2020.

[10] S. Blum, D. Hölle, M.G. Bleichner, and S. Debener. Pocketable labs for everyone: Synchronized multi-sensor data streaming and recording on smartphones with the lab streaming layer. *Sensors*, 21:8135, 2021.

[11] B.G. Schultz and F.T. Vugt. Tap arduino: An arduino microcontroller for low-latency auditory feedback in sensorimotor synchronization experiments. *Behav. Res. Methods*, 48:1591–1607, 2016.

[12] F.T. Vugt. The teensytap framework for sensorimotor synchronization experiments. *Adv. Cogn. Psychol*, 16:302–308, 2020.

ABSTRACTS FOR PRESENTATIONS WITHOUT PROCEEDINGS PAPER
RÉSUMÉS DES COMMUNICATIONS SANS ARTICLE

Is Melodic Expectancy Vocally Constrained? Evidence From Two Listening Experiments

Paolo Ammirante

Listeners show strong agreement about what note should come next in an unfamiliar melody. Where do these expectancies come from? One prominent view is that expectancies reflect innate Gestalt-like grouping rules; another is that expectancies reflect statistical learning through previous musical exposure. Listening experiments support both views but in limited contexts, e.g., using only instrumental renditions of melodies. A less-explored third view is that expectancies are vocally constrained (Russo & Cuddy, 1999). In other words, listeners expect that the next tone will be a "singable" one, operationalized here as having an absolute pitch height that falls within the modal voice register. Drawing on evidence from the singing literature, I predicted that vocal constraints on melodic expectancy should emerge for sung rather than instrumental renditions of melodies. To test this, I replicated two previous experiments - one from the grouping rules perspective (Schellenberg et al., 2001), and one from the statistical learning perspective (Hansen & Pearce, 2014) - but with an additional manipulations of timbre (instrumental vs. sung renditions matched for pitch, timing and loudness) and pitch height (modal vs. falsetto registers). Listeners heard melodic fragments and gave goodness-of-fit ratings on the final tone (Experiment 1) or rated how certain they were about what the next note would be (Experiment 2). Findings for the instrumental conditions were highly consistent with the original findings. But, as expected, findings for the sung conditions were consistent with the vocal constraints model. I discuss how the model may be extended to include predictions about note duration and higher-order melodic features such as pitch interval and contour.

Exploring The Neurophysiological Interaction Between Pitch And Timing Cues For The Perception Of Metre.

Stephen Cooke, Jon Prince, Dominique T Vuvan, Benjamin R Zendel

Exploring the neurophysiological interaction between pitch and timing cues for the perception of metre. Stephen Cooke (1) Jon B. Prince (2) Dominique T. Vuvan (3) Benjamin Rich Zendel (1) 1. Faculty of Medicine, Memorial University of Newfoundland 2. Discipline of Psychology, Murdoch University 3. Psychology Department, Skidmore College Meter is the subjective and hierarchical organization of beats in music. For example, a march meter follows a strong-weak pattern of beats, while a waltz follows a strong-weak-weak pattern of beats. Although the perception of meter is subjective, acoustic features can impact that perception. For example, a large change in pitch or a longer duration note can both be used to emphasize a strong beat. In the brain, it has been shown that both acoustic cues and listeners subjective interpretation of the meter are represented in oscillatory brain activity recorded using EEG. Behaviourally, it has been shown that when conflicting cues for meter are presented simultaneously that pitch-based cues dominate over time-based cues. The impact of how conflicting acoustic cues impact the neural oscillatory activity associated with meter has not been explored. Accordingly, we presented participants with a series of 9 melodies, that had a note every 500 ms (i.e., 2 Hz). Each melody could contain a pitch cue for a waltz, a march or no metre and a time cue for a waltz, a march or no metre. Consistent with previous findings, when metric cues conflicted, participants were more likely to report the metre defined by the pitch cue. Oscillatory brain activity was consistent with these findings. When the pitch cue was a march (i.e., 1Hz), a 1 Hz neural oscillation was observed, with almost no activity at 0.67 Hz. When the pitch cue was a waltz (i.e., 0.67 Hz), a 0.67 Hz neural oscillation was observed. These findings support the idea that the perception of meter is subjective but dominated by pitch-based acoustic cues.

Differences Between Blocked And Interleaved Music-Training On The Ability To Detect Out-Of-Key Notes And The Associated Brain Responses.

Ozgen Demirkaplan, Benjamin R Zendel

Short-term musical training, over the course of a few weeks or months, has been shown to enhance both auditory and cognitive abilities, which suggests that music training may be useful as a form of rehabilitation. Music education programs are designed for making musicians, and curricula can last for many years. Accordingly, if music training is to be used as a form of rehabilitation, it is critical to optimize the training so that it is effective for rehabilitative purposes in the shortest time possible. Here, we compared two formats of music training on their capacity to improve auditory processing abilities. Twenty-eight, nonmusicians were recruited and randomly assigned to one

of two groups: Blocked or Interleaved. Both groups learned to play 5 novel melodies on a digital piano over the course of 8 training sessions. During each training session, the Blocked Group practiced each melody 9 times before moving on to the next melody. The Interleaved Group practiced the same melodies the same number of times in each session, but the order of the melodies was randomized. Before and after training, EEG was recorded while each participant was presented with a different series of short novel melodies that sometimes contained an Out-of-Key (OoK) note. Event-related brain potentials were time locked to a target note in each melody that could be In-Key or OoK. The OoK note evoked an Early Right Anterior Negativity (ERAN) in all participants. The ERAN is a well-known ERP that is related to the automatic registration of the OoK note in the auditory system. After training, the ERAN was enhanced in the Interleaved group compared to the Blocked group. Results from this study highlight that interleaving practice sessions likely leads to stronger transfer to auditory processing abilities. More importantly, it highlights that delivery of music-based forms of auditory rehabilitation can be optimized.

Some Extensions On C. V. R Aman ' S Study On Drums

Udayanandan Kandoth Murkoth

Sir C. V. Raman's studies on drums were focused on the har-monics of the Indian drum Mridangam. In this paper, westudy the harmonics of some more drums like Maddalam,Tabla and Edakka and show that Edakka is the best musicaldrum with perfect harmonics. The shape of the drum head,the vibration of the drum head membrane have high impacton the properties of the sound produced by drums. On con-tinuing Raman's studies on Mridangam that paved pathwayto a systematic analysis of musical drums, we arrived at someinteresting findings. The alteration in mass density on thedrum head affects the ratios of harmonics and this resultedin the formation of two varients of Mridangam -male and fe-male. There are some other drums that produce distinct pitchdue to symmetric loading on the drum head such as Tabla andMaddalam and among them, Tabla creates excellent harmon-ics analogous to the Mridangam. Comparably, Maddalam isless harmonic. Distinct from all these drums, Edakka pro-duces fine harmonics by varying tension on the drum head.Apart from drums with definite pitch, rhythmic drums are ca-pable to generate great enjoyment and among them Chenda(a drum from Kerala) is the most popular due to its ability togenerate seamless rhythmic patterns and highly varying am-plitudes that generates high fractal dimension. Interestingly,the circular symmetry of the drums makes them capable toproduce harmonics by providing sufficient degenerate modesthat are splitted and shifted to produce integer ratios for theirfrequencies.

Classifying The Perception Of Different Instruments Using Single Trial Eeg

Praveena Satkunarajah, Benjamin Zendel

Many users of hearing aids report challenges when listening to music. In the future, it may be possible to develop hearing aids that have an electrode which monitors brain activity in real-time and adapts the filters on the hearing aid to match the volitions of the user. In music, this could mean amplifying the sound of the instrument the listener wants to hear. One of the first steps in this research is to determine if a machine learning algorithm can identify to which instrument an individual is listening, based only on the EEG signal. To test this possibility, participants were presented with a series of brief tones that varied in timbre (trombone, clarinet, cello, piano and pure tone) while their ongoing EEG was recorded from 73 electrodes. A Gradient Boosting classifier was used within each individual participant using spectral entropy as a feature. The classifier performed 10-20

NOISE CONTROL - CONTRÔLE DU BRUIT

ACOUSTIC ANALYSIS OF ELECTRIC DUCTED FANS

Nick Cunnington-Bourbonniere [*1] **and Joana Rocha** [†1]

[1]Department of Mechanical and Aerospace Engineering, Carleton University, Ottawa, Ontario

1 Introduction

The scope of this paper is to study the initial conceptual design and acoustic analysis of a ducted fan. The fan design was reverse engineered from a reference geometry as used in an UAV (Unmaned Aerial Vehicle) for VTOL (Vertical Take-Off and Landing) applications [1], here called Manta UAV. Ansys CFX was used to analyze the performance [2]. The objective of the analysis was to obtain fan noise, while predicting thrust and torque, with focus in hover flight rather than cruise flight. Electric ducted fans operate with increased efficiency in cruise and reduced operating noise relative to open-rotor configurations. Additionally, the duct can add up to 30% extra thrust in cruise due to the reduction in area allowing for lower power requirement in cruise flight [1]. The smaller fan diameter, however, is less efficient in hover flight.

2 Method

The fan noise was investigated using Ansys CFX. While some of the methods are limited, as they do not consider the duct effects or the rotor-stator interaction, they can be useful to compare different configurations to reduce fan noise in future design iterations. Ansys considers three ways of deriving acoustic energy from kinetic energy [3]. The monopole source is the most efficient technique, the method calculates acoustic energy by forcing gas within the fixed region of space to fluctuate with no reflections at boundaries. Dipole source is predominant in fans during low-speed operation., the method uses two sources that create pulsating spheres that interfere with one another. Lastly, the quadrupole source is least efficient and is best applied when sound is generated aerodynamically without motion of solid boundaries. The current analysis considered that the fluid is compressible, inviscid, without a mean flow, and mean pressure and density are uniform throughout the fluid. The most common way to quantify the acoustic intensity in ANSYS is by using sound pressure level or sound power level. Sound power level was found to be dependant on local reference density as determined by Boussinesq model for buoyant flows [2]. Since this value cannot be calculated analytically, the focus of this analysis was shifted to the sound pressure level (SPL), which is defined by :

$$SPL = 10 log_{10}\left(\frac{P_{ac}}{P_{ref}}\right)^2 \qquad (1)$$

with the acoustic pressure defined as following :

$$P_{ac} = \frac{Hn \ Nb^2 \ \omega}{2\pi\sqrt{2}d_{obs}cos(\theta_{obs})F_{blade,x}(Hn \ Nb)^{Lc}besselJ(0, Df)} \qquad (2)$$

∗. NickCunningtonBourbo@cmail.carleton.ca

†. Joana.Rocha@carleton.ca

in which Hn is harmonic number, Nb is the number of rotor blades, ω is the absolute angular velocity, Df is the Doppler factor, Lc is the blade loading coefficient, $F_{blade,x}$ is the axial blade loading, and the acoustic reference pressure is $P_{ref} = 2\times10^{-5}$ Pa. A standard sea level speed of sound of $340 ms^{-1}$ and a loading coefficient of 2.2 were used. The blade loading coefficient for axial compressors is defined as the ratio of the work done by the blade to the blade velocity squared. The acoustic pressure is derived from the dipole source model as the noise is primarily generated by blade forces. Comparisons were completed for the 1st harmonic frequency.

3 Results and discussion

3.1 Noise versus number of blades per fan

Figure 1 displays the SPL determined at different numbers of rotor blades (Nb) per fan for propulsion configurations of 4, 8, 16, 24 and 36 fans, N_{fans}. While both Nb and $F_{blade,x}$ are variables in Eq. 2, Nb was calculated based on the total thrust, $T = 9.81W$ (in which the total weight is $W = 3000$ kg), divided by the total number of blades of the aircraft, i.e :

$$F_{blade,x} = \frac{9.81 \ W}{Nb \ N_{fans}} \qquad (3)$$

The results show a noise reduction for configurations with more fans and an increased number of rotor blades per fan; hence, the selection converged to the 24 fans configuration. While increasing the configuration to 36 fans would decrease hover efficiency, fan noise could be reduced by increasing the number of rotor blades to better distribute the blade loading. A further increase of number of rotors from 31 to 40 would result on a noise reduction of 3 dB.
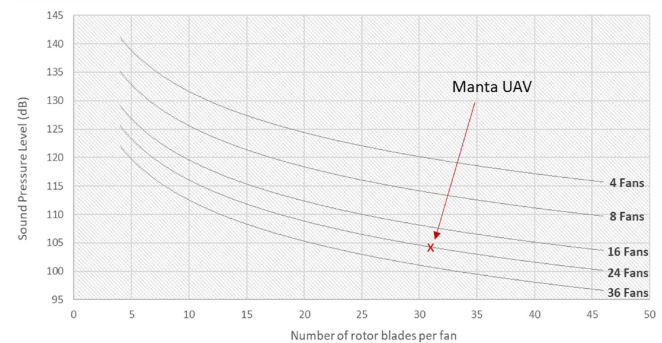

FIGURE 1 – Propulsion configuration vs. noise sensitivity study at varying numbers of rotor blades per fan for different number of ducted fans on aircraft (observer distance of 10 m).

3.2 CFD analysis of the ducted fan

A CFD simulation of the fluid flow within the ducted fan was performed to determine thrust and noise of the Manta UAV

configuration in hover. The rotor was set to rotate at 10000 rpm, a rotational speed towards the higher end of the chosen motor's capability. The rotor shroud was set as a nonslip counter rotating wall with no tip clearance, and an upwind differencing scheme was used. The mixing plane method was chosen to model the interface between the rotor and stator. The inlet-outlet boundary conditions were set as 102 kPa total pressure at the inlet and 101.35 kPa static pressure at the outlet. The turbulence model selected was the shear stress transport model, which combines the k-epsilon model (better away from wall) and the k-omega model (better at wall) to provide turbulence modelling over the entire domain. Two approaches were used to validate the CFD results. First, the analytical prediction (Eq. 1) was compared to the CFD results. Second, a rotor with well documented performance parameters [4] was run with the same conditions applied. The analytical model resulted in a SPL of 108.1 dB for the 1st harmonic, while CFD predicted a SPL of 107.7 dB for the same harmonic. The difference can likely be attributed to the different blade loading, since the ducted fan design is not guaranteed to provide the full/ideal thrust as the one analytical determined (originally considered to be 2452.5 N per fan in hover flight, with a safety factor of 1.5). The same CFD approach and methods used on Manta UAV were applied to the NASA rotor 67 [4]. Table 1 displays the CFD results along with the true values, showing that numerical results agree with the performance data, validating the methods used in the simulation. Figure 2 displays the velocity streamlines for the

TABLE 1 – Comparison of ANSYS CFX results with NASA performance data for the rotor 67 geometry [4].

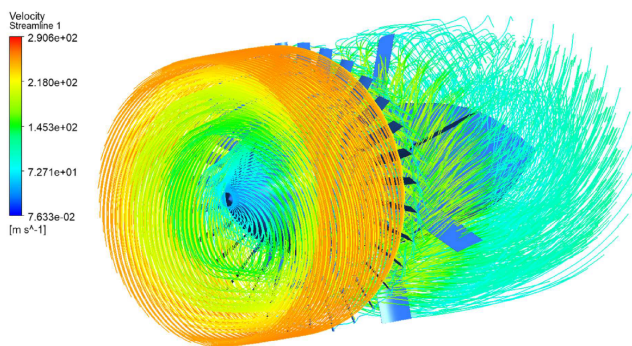| Parameter	CFD results	NASA data
Mass Flow	33.63 kg s^{-1}	33.25 kg s^{-1}
Total Pressure Ratio	1.65	1.63
Inlet tip Mach number	1.44	1.38

FIGURE 2 – Velocity streamlines for Manta ducted fan geometry.

Manta ducted fan CFD simulation. The flow characteristics resembles what is expected and observed in the rotor 67 (i.e., highest velocity at blade tip), even though the geometries are different. The thrust was determined from the mean-line results, derived from a simple mass balance as following :

$$T = \dot{m}_{in}(V_{exit} - V_{in}) + A_{exit}(P_{exit} - P_{in}) \quad (4)$$

Thrust was determined to be 1990 N per fan from velocity, pressure, and mass flow values obtained from the Manta UAV ducted fan CFD results. The simulation predicted a torque on the rotor of 282.4 Nm. The CFD results show that the used geometry produces less thrust than the one originally considered. This difference could likely be attributed to the degree of flow separation occurring at the rotor (as shown in Figure 3), which could be improved or corrected by increasing the stagger angle of the rotor.
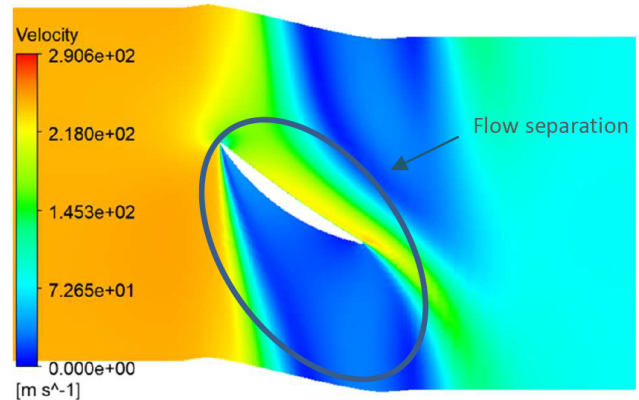

FIGURE 3 – Velocity contour at 0.8 span for the Manta ducted fan.

4   Conclusions

A reversed engineered fan was investigated in order to predict noise, thrust and torque during hover. A sensitivity study was conducted to determine fan noise at different fan configurations. The analysis resulted in the selection of a 24-fan configuration for the Manta UAV, with 31 rotor blades per fan. Analytical predictions estimated a SPL of 108.1 dB for the 1st harmonic, while CFD predicted a SPL of 107.7 dB, validating the CFD model. In addition, the same CFD approach and methods used on Manta were applied to NASA rotor 67, showing that numerical results agree with the performance data. CFD results showed that the rotor-stator geometry produced less thrust compared to initially values used for the design process. This difference could be a result of the degree of separation occurring on the rotor, which could potentially be corrected by increasing the stagger angle of the rotor.

Acknowledgments

References

[1] B. Raeisi. Aerodynamic study of tilting asymmetrical ducted fans mounted at the wing tips of a vtol uav. *Thesis, Ryerson University*, 2016.

[2] Ansys cfx-solver theory guide. *ANSYS, Inc.*, 2009.

[3] A. Naseri, M. Boroomand, and S. Sammak. Numerical investigation of effect of inlet swirl and total-pressure distortion on performance and stability of an axial transonic compressor. *Journal of Thermal Science*, 25(6) :501–510, 2016.

[4] A. Strazisar, J. Wood, M. Hathaway, and K. Suder. Laser anemometer measurements in a transonic axial-flow fan rotor. *NASA TP-2879*, 1989.

ESTIMATING SOUND ABSORPTION COEFFICIENT UNDER VARIOUS SOUND PRESSURE FIELDS BY COMBINING AN AUTOMATED TEST BENCH TO SOUND FIELD REPRODUCTION AND ADVANCED POST-PROCESSING TECHNIQUES

Magdeleine Sciard[*1], Alain Berry[†2], Franck Sgard[‡3], Olivier Robin[♦2] and Thomas Dupont[♯1]
[1] Mechanical engineering dept, École de Technologie Supérieure, Montréal, QC, Canada
[2] Mechanical engineering dept, Université de Sherbrooke, Sherbrooke, QC, Canada
[3] IRRST, Montréal, QC, Canada

1 Introduction

Two normalized methods are currently used to characterize sound absorbing materials. The first one, namely the impedance tube method, allows the measurement of the sound absorption coefficient under plane waves and normal incidence only. The samples used are small and possibly not representative of the whole material. The second method is the reverberant room method and provides diffuse field sound absorption coefficient on large samples. A large surface of materials and specific mounting conditions are required as well as a room with minimum volume (over 150 m^3). The results are often overestimated (larger than unity) and show poor reproducibility.

Researchers seek to develop more reliable methods, that can also address *in situ* like conditions. In particular, a sound field reproduction approach was proposed by Robin et al., 2019 and estimates the absorption coefficient of materials under a synthetized acoustic field, using a virtual sound source array. Results show good agreement with Transfer Matrix Method simulations and need no specific mounting of the samples. Results are not overestimated and *in situ* measurements are possible. However, results are biased under 400 Hz, due to two reasons: the use of a simplified spherical wave propagation model, and measurements uncertainties, mainly concerning microphone or source positions [1].

This article suggests improvements of this method by using an automated test bench to reduce the measurement uncertainties, a more general propagation model, namely Allard's model and an advanced post-processing technique.

2 Measurements and post-processing method

2.1 Experimental measurements

An automated test bench allowing a point source to be moved along a plane above the surface material has been developed and measurement uncertainties minimized. Measurements were done on five different materials in a semi-anechoic room, with a virtual array of 49 sources separated by 15 cm in each (x-y) direction, a source height z_s of 30 cm above the material and two microphones placed at $z_{r1} = 5$ cm and $z_{r2} = 10$ cm above the sample, respectively.

[*] magdeleine.sciard.1@ens.etsmtl.ca
[†] alain.berry@usherbrooke.ca
[‡] franck.sgard@irsst.qc.c
[♦] olivier.robin@usherbrooke.ca
[♯] Thomas.Dupont@etsmtl.ca

Transfer functions between the two microphones $H_{12} = p_2/p_1$ (H_1 estimator) are then calculated for each source position.
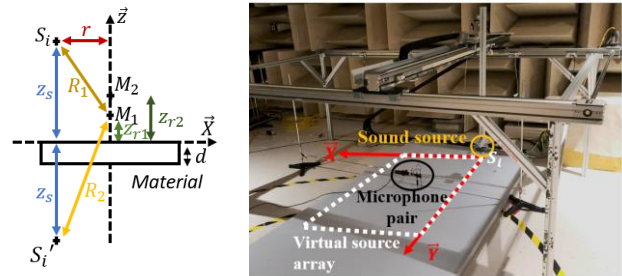

Figure 1: Automated test bench, virtual source array and geometrical parameters of the method.

2.2 Post-processing technique

2.2.1 Identification of materials parameters

An advanced post-processing technique is suggested using the automated test bench measurements and the Allard theoretical model of sound propagation above a material [2]. From this model, the total sound pressure at a given microphone and at angular frequency ω follows equation 1.

$$p_{tot}(r, z_r; \omega) = j\omega\rho_0 \left[\frac{e^{-jk_0R_1}}{R_1} - \frac{e^{-jk_0R_2}}{R_2} + \int_{k=0}^{\infty} \frac{2\rho_m}{\rho_m v_0 + \rho_0 v_m \tanh(v_m d)} e^{-v_0(z_s+z_r)} J_0(kr) k \, dk \right] \quad (1)$$

with, ρ_0, the air density, R_1, the distance between the real source and microphone, R_2, the distance between the image source and microphone, $v_0 = \sqrt{k^2 - k_0^2}$, $v_m = \sqrt{k^2 - k_m^2}$, k_0, the acoustic medium wavenumber, d, the material's thickness, r, the distance between the real source and microphone along the material's surface and $J_0(kr)$, the zero order Bessel function.

The idea followed here is to recover the frequency-dependent, complex density ρ_m and complex wavenumber k_m of the material by inverting Allard's model. The `fmincon` Matlab function is used to minimize a cost function, which is the sum of squared differences between the measured transfer functions H_{12} on the test bench and those predicted by Allard's model over all point source positions of the virtual array, as in equation (2).

$$(\rho_m, k_m) = \min \left(\sum_i \left| H_{12\,TestBench,i} - H_{12\,Allard,i} \right|^2 \right) \quad (2)$$

2.2.2 Plane wave sound absorption coefficients

Using estimated ρ_m and k_m values and under a plane wave assumption, the sound absorption coefficient for a given incidence angle θ is calculated with the usual equation. The sound absorption coefficient under a diffuse acoustic field is obtained by averaging the oblique sound absorption coefficient over angles θ between 0 and $\pi/2$.

3 Results and discussion

In this paper, results are only provided for a single material (2-inches thick melamine sample with $1.8\,\text{m} \times 2.5\,\text{m}$ surface).

3.1 Test bench uncertainties

The measurement uncertainties on the geometrical parameters, in particular on microphones and sources positions, are limited and show small impact on the results. The automation allows more reproducible and faster tests compared with previous works in which the source was manually translated [1].

3.2 Allard's model inversion to obtain complex density and complex wavenumber

Figure 2 shows the optimized acoustic quantities ρ_m and k_m obtained with the Allard's model inversion based on 10 measured transfer functions H_{12}, those obtained with the impedance tube method and those predicted by the Johnson-Champoux-Allard (JCA) model. The results derived from the test bench shows good agreement with the impedance tube data and JCA model, but below 700 Hz, a few peaks are observed certainly caused by the presence of the test bench.
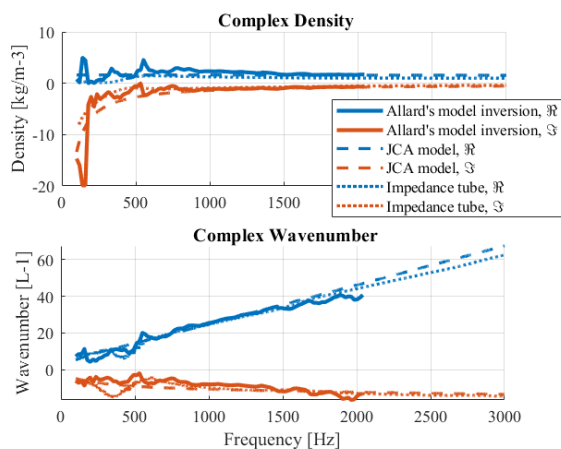

Figure 2: Complex density and complex wavenumber, methods comparison.

3.3 Absorption coefficient

Figure 3 shows the estimated absorption coefficients obtained under normal plane wave, oblique plane wave and diffuse field incidence. Impedance tube tests are used as a comparison for the normal incidence [1]. The results obtained from the Allard's model inversion agree with the impedance

tube results, as well as with the JCA model. Diffuse field absorption coefficients obtained with the proposed approach are in good agreement on the whole considered frequency range [1]. Abnormal absorption peaks are observed (same as for the complex density and wavenumber).
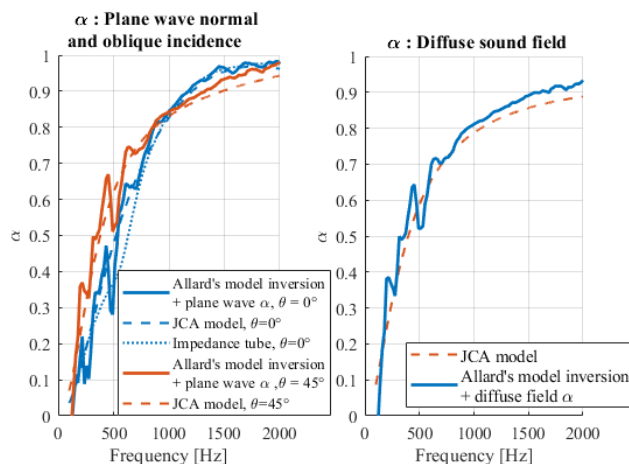

Figure 3: Absorption coefficient, methods comparison.

4 Conclusion

A method for estimating the absorption coefficient of absorbing materials for normal, oblique, or diffuse field incidence has been presented. The method is closer to real conditions, more reliable and provides improved results in the low frequency domain. This article proposed the automation of a test bench and reduced measurement uncertainties.

An improved post-processing technique using the Allard's model inversion shows encouraging results for the melamine sample, especially in the low frequencies. Tests on other materials (glass wool, rock wool, recycled cotton and PU foam, not shown here) show consistent results too. However, spurious peaks were observed below 700 Hz, certainly caused by diffraction or reflection effects on the test bench's sides or of the semi-anechoic room.

Another method using sound field reproduction and a power definition for the absorption coefficient is currently being tested.

References

[1] O. Robin, A. Berry, C. Kafui Amédin, O. Doutres et F. Sgard, "Laboratory and in situ sound absorption measurement under a synthetized diffuse acoustic field", *Building Acoustics*. 26(4), 223-242 (2019).

[2] J.-F. Allard, W. Lauriks, C. Verhaegen, "The acoustic sound field above a porous layer and the estimation of the acoustic surface impedance from free-field measurements". *The Journal of the Acoustical Society of America*. 91(5),3057-3060 (1992).

Vibration Analysis of an Electric UAV Wing Model

Noah Veenstra [†1] and Joana Rocha [†1]

[1]Department of Mechanical and Aerospace Engineering, Carleton University, Ottawa, Ontario.

1 Introduction

This paper outlines the random vibration analysis of a structural wing model designed for an electric Vertical Takeoff and Landing (VTOL) Unmanned Aerial Vehicle (UAV) called the Manta. The Manta is designed for agricultural cargo operations as part of the Carleton University Bio-inspired Environmentally Friendly Aerial Vehicle (BEFAV) capstone project. This analysis expands on and updates the original structural analysis of the Manta to determine the vibrational response of the wings caused by the engine and aerodynamic vibration using ANSYS modal and random vibration tools.

2 Wing Design

The base model of the Manta wing is designed in Catia V5. Catia allows for comprehensive design of bodies, surfaces, and part connections. The model is imported into ANSYS Spaceclaim 3D software to finalize the wing topology for use in ANSYS Mechanical. Figure 1 below shows the model setup.
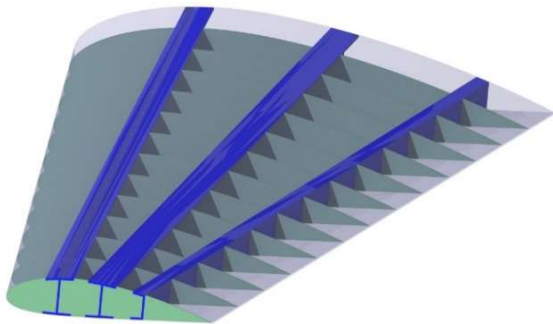

Figure 1: Catia model of the Manta UAV wing – fans omitted for clarity.

The structure is comprised of three aluminum 2024-T3 spars. The two forward I-spars are designed to take the bulk of the load around the leading edge and mid-chord of the airfoil. The aft spar serves primarily as a mounting point for the rotating ducted fan propulsion system mechanism. The wings also feature 6061-T6 aluminum ribs and a composite wing skin. Material data is shown in Table 1.

3 Analysis Setup

The method selected for this analysis is the ANSYS random vibration solver. This platform is used to reduce the complexity of the model. In lieu of providing advance loads from turbulent flow models or aeroelastic responses, the solution uses

---
[*] NoahVeenstra@cmail.carleton.ca
[†] Joana.Rocha@carleton.ca

the statistical Power Spectral Density (PSD) data [2]. Consequentially, the results produced by this simulation are statistical. By utilizing the material data above, the likeliness of wing failure over a certain spectrum of vibration is determined.

Table 1: Material data for Manta UAV wing

Component	Material	Ultimate Strength (MPa)
Skin	Composite Metal Foam	175*
Ribs	Al 6061-T6	296 [1]
Spars	Al 2024-T3	427 [1]

[*] Material data comes from Manta materials engineer.

Prior to running the random vibration analysis, the natural modes of vibration of the wing must be determined. ANSYS has a modal solver that does exactly this by solving the following homogeneous differential equation [2]:

$$[M]\{\ddot{u}\} + [K]\{u\} = 0 \qquad (1)$$

The modal analysis is setup by treating the wing like a cantilevered beam as is done in [3]. Through this approach, the boundary condition considered for the analysis is a fixed support at the wing root. The spars and wing skin at the root are fixed accordingly. Due to the complex curvature of the wing and its components, linear mesh elements are selected for the analysis. The mesh convergence analysis is done over a size range of 160 mm to 61 mm to ensure the solutions are independent of the mesh size. Figure 2 below shows the first three modes of vibration of the Manta wing determined through the modal analysis.

The modal data is then used to form a random vibration solution. The PSD spectrum data used in this case comes from methods as deinned in MIL-STD-810H for environmental testing of mechanical and aerospace systems [4]. Figure 3 shows the chart of the PSD acceleration spectrum used for the random vibration analysis. In this instance, the bulk of the noise comes from the ducted fans on the Manta wings and canards [4]. Since Manta UAV uses electric ducted fans for propulsion that run at higher RPMs, and thus higher frequencies. These frequencies are outside of the spectrum ranges typically used for propeller aircraft PSD data [4]. For this reason, the Manta can be considered a jet aircraft. Using the PSD data input in ANSYS, the statistical stress level results are computed, as shown in the next section

4 Analysis Results and Discussion

The primary results computed for the current analysis are the total stresses in each type of component, including the skin,
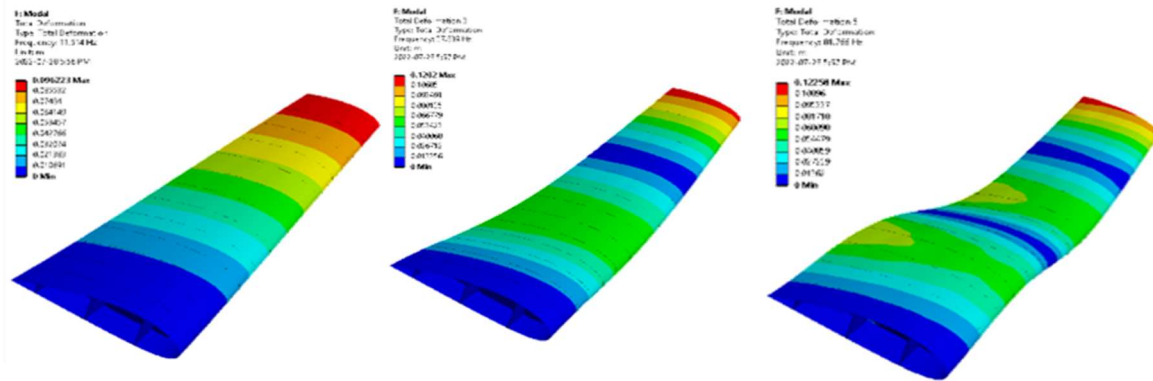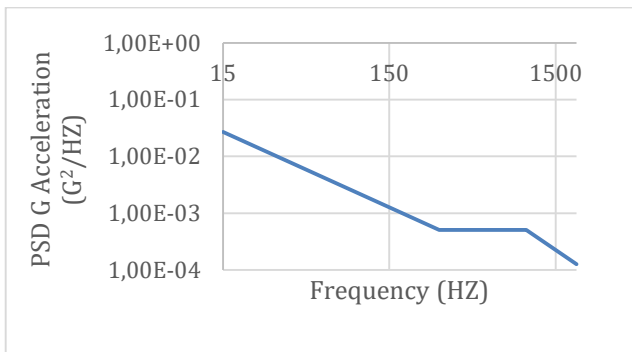
Figure 2: Manta wing vibration modes.

Figure 3: PSD G vibration spectrum from ducted fans.

ribs, and spars. The values presented correspond to the 1-sigma and 3-sigma standard deviations for the stress. The stress calculation in ANSYS is performed using the Von Mises criteria. The ultimate strength values earlier shown in Table 1 are compared with the stress level results.

Table 2 shows the stress levels in each wing component. It is expected that the maximum stress for each component would be low due to the ducted fan vibration – this is due to the fact that ducted fans produce less noise and vibrations than larger propeller and jet engines as seen in [4]. It is also important to note that the Manta UAV flies at much lower Mach numbers and is subject to less aerodynamic vibration as a result [4].

The vibrations are ultimately less intense and cause less disturbance in the structure. As is evident in Table 2, the vibrations caused by the engine and aerodynamic vibrations do not cause any component failures.

Table 2: Statistical stress levels in Manta wing components.

Component	1σ Stress Level (MPa)	2σ Stress Level (MPa)
Skin	0.9	2.7
Ribs	12.2	36.5
Spars	10.9	32.6

The scope of the current analysis is limited by the nature of the vibrations caused by the ducted fans. To expand these results, one can also consider the superposition of effects such as aeroelasticity as well as the effects of more severe aerodynamics like gusts and turbulence.
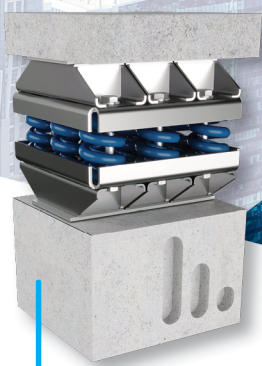
5 Conclusion and Future Work

Through random vibration analysis of the Manta wings for the engine and aerodynamic vibrational PSD load it was determined that the structure will not fail. Future expansion on this analysis will focus on looking at other vibrational loads and performing the analysis with additional meshes.

References

[1] Federal Aviation Administration, *Metallic Materials Properties Development and Standardization (MMPDS)*, Vol. 4. Battelle Memorial Institute, 2009.

[2] *Theory Reference for the Mechanical APDL and Mechanical Applications*, 12th ed., ANSYS Inc., Canonsburg, PA, USA, 2009, pp 977-1038.

[3] J. E. Ballesteros, "Failure Prediction of Structures Subjected to Random Vibrations," M.S. Thesis, Dept. of Mech. and Aero. Eng., University of Arizona, USA, 2018.

[4] *Environmental Engineering Considerations and Laboratory Tests*, MIL-STD-810H, United States Department of Defense, Jan. 2019.

OCCUPATIONAL ACOUSTICS - BRUIT AU TRAVAIL

Hearing Protection's Comfort Evaluation in the Laboratory

Said Ezzaf *[*1]**, Olivier Valentin** [†1,2]**, Alain Berry** [‡1,2]**, Philippe-Aubert Gauthier** [⁑2,3]**,
Alessia Negrini** [⸾4]**, Djamal Berbiche** [⸙5]

[1]Groupe d'Acoustique de l'Université de Sherbrooke, Université de Sherbrooke, Sherbrooke, Québec, Canada.
[2]Centre for interdisciplinary research in music media and technology (CIRMMT), Montreal, Quebec, Canada
[3]École des arts visuels et médiatiques, Université du Québec à Montréal, Montréal, Québec, Canada
[4]Institut de recherche Robert-Sauvé en santé et en sécurité du travail, Montréal, Québec, Canada
[5]Département des sciences de la santé communautaire, Université de Sherbrooke, Sherbrooke, Québec, Canada

1 Introduction

Hearing Protection Devices (HPDs), such as earmuffs and earplugs, are used to protect workers exposed to high noise levels in their work environment. Since HPDs tend to not be comfortable, they are not worn at all or not worn consistently or correctly [1]. In a recent literature review dedicated to HPDs, the global perception of HPD comfort is defined as a balanced measure of four dimensions (physical, acoustical, functional, and psychological) that characterize the relationship between the user and the HPD in the work environment [1]. Most laboratory studies related to the perception of HPDs comfort did not study the effect of the noise of the environment because the associated tests were carried out in a quiet environment [2]. Only one special and constant noise was used for two laboratory studies on HPDs comfort [2] that were carried out in a noisy environment and the results cannot be generalized because the characteristics of this noise remained the same for all the tests of these studies.

This laboratory study focuses on the evaluation of earplugs comfort because: (1) they are the most used protectors in the field, (2) they provide less reliable protection than earmuffs, as it is more difficult to position them correctly in the ear canal, and (3) earmuff's comfort has already been studied in the literature using both subjective and objective approaches [1, 2]. The main objectives of this work are to (1) evaluate the global perception of the comfort of earplugs, and (2) study the effect of the sound environment on the four dimensions of comfort (physical, acoustical, functional, and psychological).

2 Method

2.1 Reproduced sound environments

Two virtual industrial environments that served as background noise during this study, were generated using multi-channel Acoustic Background Spectrum (ABS) synthesis [3], and *in-situ* recordings collected at two different workstations in two industrial organizations using a stacker (environment 1) and a granulator (environment 2). A square array of 96 loudspeakers was used to recreate the virtual sound environments in a 4m × 4m space. The first sound environment was calibrated at 90.9 dB (SPL) and the second one at 93.0 dB (SPL) [3].

2.2 Participants and hearing protectors

A sample of 24 naive (inexperienced regarding hearing protectors), normal-hearing participants, having hearing thresholds below 25 dB HL, tested three different earplugs in the two different reproduced sound environments. The earplugs used by the participants were either roll-down foam earplugs (3M™ E-A-R Classic), premolded earplugs (3M™ E-A-R UltraFit), or push-to-fit foam earplugs (3M™ E-A-R Push-ins), which are an alternative between the roll-down foam and the premolded earplugs.

2.3 Laboratory tests

The laboratory tests were performed in three measurement sessions. In each session, the participant tested one earplug chosen randomly from the three earplugs in the two sound environments also chosen randomly. During the tests, the participant had to complete a simulated work task (moving boxes in the region surrounded by the reproduction loudspeakers). For each sound environment, the participant was asked to complete alarm detection tests, speech in noise detection tests, and answered questionnaires to assess HPDs comfort. Those tests were carried out while the participant wore the earplug.

2.3.1 Alarm detection tests

Alarm signals were presented at five different signal-to-noise ratios (SNRs) relative to the reproduced background noise, from -10 dB (most difficult) to +10 dB (easiest) with a 5 dB step.

2.3.2 Speech in noise detection tests

A total of 60 stimuli (4 stimulation levels × 15 repetitions) consisted of sentences pronounced in French were presented to the participants in random order. The stimulation levels were calibrated to 62.4, 68.3, 74.9, and 82.3 dB (SPL), which correspond respectively to the level of normal, raised, loud, and shouted voice [4].

2.3.3 Subjective questionnaires

Participants answered a set of questionnaires, which is an adapted version of the COPROD questionnaire (COnfort

---

[*] Said.Ezzaf@USherbrooke.ca
[†] m.olivier.valentin@gmail.com
[‡] Alain.Berry@USherbrooke.ca
[⁑] gauthier.philippe-aubert@uqam.ca
[⸾] Alessia.Negrini@irsst.qc.ca
[⸙] Djamal.Berbiche@USherbrooke.ca

des PROtections auDitives/COmfort of hearing PROtection Devices) [5].

The purpose of these questionnaires was to evaluate the attributes of the four mentioned dimensions of earplug comfort as well as the overall comfort.

2.4 Statistical analyses

Statistical analyses were carried out on the data collected during the tests below using the SPSS software (Statistical Package for the Social Sciences) and R 3.6.1 with MASS 7.3–51.4. The objective of these analyses was to determine the influence of the earplug model and sound environment on the perception of comfort.

3 Results

3.1 Alarm detection tests

Alarms presented with the highest stimulation levels were always heard by the participants, while the participants were not able to hear clearly alarms presented with the lowest stimulation level. Moreover, sound environment 1 had the lowest detection scores at a low stimulation level (SNR = -15 dB) compared to sound environment 2 for the three earplugs. Therefore, the sound environment has an effect on alarm detection when the task is difficult (SNR = -15 dB).

3.2 Speech in noise detection tests

For the normal and raised voice (difficult conditions), it was impossible for the participants to discriminate the speech from the noise. Thus, when the task was difficult, the speech was never understood. Speech detection is thus affected by the sound environment when the task is difficult.

For the loud and shouted voice (easy conditions), participants were able to discriminate speech from noise with more or less success depending on the sound environment. Mostly, and despite the fact that the SPL was larger for sound environment 2, it had higher speech detection scores compared to sound environment 1.

3.3 Questionnaires on comfort perception

Comparative analyses were performed to evaluate, according to the earplug family and the sound environment, the perception of physical, functional, acoustical, and psychological comfort in relation to the general items (for each dimension of comfort from the COPROD - NAQ).

Results showed no differences in comfort for the three tested earplugs, except for functional comfort. More specifically, push-to-fit foam earplugs were considered more functional while roll-down foam earplugs were less functional.

Results showed a significant effect of the sound environment on participants' perception of hearing useful sounds (alarm signals). More specifically, sound environment 2 allowed to better hear the alarm signals compared to sound environment 1.

4 Discussion and conclusion

Sound environment 2 has less energy than sound environment 1 in the frequency ranges from 562 Hz to 6300 Hz. On the other hand, both speech and alarm signals have their maximum energy in this frequency range. Such differences contributed to an increase in the masking effect induced by sound environment 1 on the alarms and the speech signals. Moreover, the earplugs' contribution to the masking effect remained the same and cannot explain the difference observed in the results obtained in the two sound environments, because the participants were instructed to never remove their hearing protectors during the whole experience, which means that the attenuation provided by the earplugs remained the same throughout the experience.

When the speech comprehension task is difficult ("raised voice" and "normal voice" conditions), the masking effect created by the background noise is large enough that it prevents participants from understanding the speech, regardless of the sound environment. Since sound environment 2 has less energy than sound environment 1 in the same frequency range, the masking effect induced by environment 2 on the speech stimuli is less problematic than the one induced by environment 1.

To conclude, earplugs' perceived comfort is affected by the type of earplugs and the frequency content of the sound environment.

Acknowledgments

References

[1] Doutres, O., Sgard, F., Terroir, T., Perrin, N., Jolly, C., Gauvin, C., & Negrini, A. (2019), "A critical review of the literature on comfort of hearing protection devices: definition of comfort and identification of its main attributes for earplug types", *International Journal of Audiology*, 58:12, 824-833, DOI: 10.1080/14992027.2019.1646930.

[2] Doutres, O., Sgard, F., Terroir, T., Perrin, N., Jolly, C., Gauvin, C., & Negrini, A. (2020), "A critical review of the literature on comfort of hearing protection devices: analysis of the comfort measurement variability", *International Journal of Occupational Safety and Ergonomics*, DOI: 10.1080/10803548.2020.1772546.

[3] Valentin, O., Gauthier, P.-A., Berry, A., and Proulx, F. (2020), "Objective evaluation of sound environment reproduction for comfort of hearing protector devices: Acoustic background spectrum synthesis versus multichannel cross-synthesis". *In Proceedings of Forum Acusticum 2020*, Lyon, France, pages 1–6.

[4] Pavlovic, C. 1997, "Sii—Speech intelligibility index standard: ANSI S3.5 1997", *The Journal of the Acoustical Society of America*, vol. 143(3), pp. 1906–1906.

[5] Terroir, J., Perrin, N., Wild, P., Doutres, O., Sgard, F., Gauvin, C., & Negrini, A. (2021) "Assessing the comfort of earplugs: development and validation of the French version of the COPROD questionnaire", *Ergonomics*, 64:7, 912 925.

Towards Detection and Classification Non-Verbal Events and Biosignals in Hearables

Malahat H.K. Mehrban [*1], **Jérémie Voix**[†2,3], **and Rachel E. Bouserhal**[‡1,3]

[1]Electrical Engineering Department, Université du Québec (ÉTS), Montréal, Canada
[2]Mechanical Engineering Department, Université du Québec (ÉTS), Montréal, Canada
[3]ÉTS-EERS Industrial Research Chair in In-Ear Technologies (CRITIAS)

1 Introduction

The miniaturization of sensors coupled with advancements in Machine Learning (ML) have facilitated the achievement of portable health monitoring. In particular, in-ear wearable devices, or hearables, have gained popularity in recent years. This is because within the stable position of the occluded earcanal, hearables can capture various events using only an in-ear microphone [1]. The detection and classification of in-ear biosignals such as heartbeats and respiration have already been achieved with conventional signal processing techniques [2]. However, these conventional techniques rely on peak detection and are affected by movement artifacts. ML methods that are popular for their rapid computation and comprehensive learning capacity may be more robust to such challenging conditions. The goal of this work is to collect an open-access database of various in-ear microphone signals and to develop advanced techniques to detect and classify breathing and heart rate in various acoustically challenging conditions.

2 Background

2.1 Previous Work

Health monitoring methods that use acoustic data to measure physiological signals using traditional digital signal processing (DSP) have already been proposed in the literature. For instance, peak extraction and envelope detection to measure respiration and heart rate from in-ear recordings were proposed in [2]. Authors in [3], used heart sounds recorded from the neck to measure respiration and heart rate using Continuous Wavelet Transform (CWT). In general, DSP methods work well with data captured in controlled environments but are often not robust to real-world disturbances such as noise and movement.

Recently, ML algorithms have been used for various tasks in detection and classification of audio events. Authors in [4], extracted Mel Frequency Cepstral Coefficients (MFCCs) and Spectrogram Image Features (SIF) as features and employed ML algorithms such as Support Vector Machine (SVM), Hidden Markov Models (HMM) and Deep Learning (DL) models like Convolutional Neural Networks (CNNs) to detect sound events in noise-corrupted real-world data. Similarly, in [5], an approach was proposed to detect non-speech audio events using SVM, HMM and Multi Layer Perceptron (MLP). The features which were extracted

---

by the authors to train the aforementioned algorithms consisted of MFCCs, Zero Crossing Rate (ZCR), fundamental frequency, as well as brightness and bandwidth from the extracted spectrogram. Bag-of-Audio-Words (BoAW) or Bag-of-Feature techniques which are inspired by Bag-of-Words to be used for audio event detection were utilized by researchers in [6,7] and [1]. Also, as an efficient ML algorithm to classify non-verbal events in audio data, Gaussian Mixture Models (GMMs) were used in [8], [9], and [10].

Currently, there exists no algorithm capable of detecting and classifying various physiological and non-verbal events captured with an in-ear microphone. In addition, there is a need for a large database of the relevant in-ear microphone signals captured in the various realistic use cases of a hearable. This work will result in a ML algorithm to detect and classify heartbeats and respiration as well as an open-access database of various non-verbal and physiological signals captured with different sensors, including an in-ear microphone.
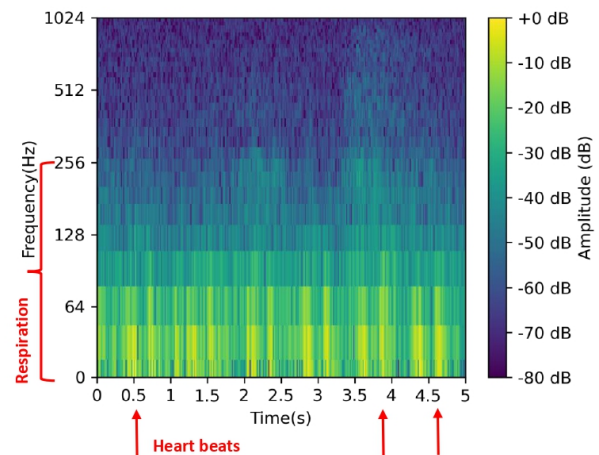
Figure 1: An illustration of the spectrogram of normal nose breathing for one subject is provided, demonstrating that both respiration and heart beat can be captured with the in-ear microphone.

3 Methodology

3.1 Database Creation

To explore the potential of ML for the detection and classification of physiological signals captured from inside the earcanal, more data in various acoustical conditions is required. Data will be collected using an occluding intra-aural earpiece featuring in-ear microphones, outer-ear microphones and miniature loudspeakers in each ear. Recordings

---
[*]mmehraban@critias.ca

[†]jeremie.voix@etsmtl.ca

[‡]rachel.bouserhal@etsmtl.ca

will be made in protected mode (attenuating outside sounds) and transparent mode (environmental sounds are played back in the earcanal) in quiet as well as in noise. Various human-produced sounds will be also included, ranging from a cough to the blink of an eye.

3.2 Classification of Biosignals

In this section, the steps to achieve the detection algorithm for non-verbal events and physiological signals are described. The primary challenge will be the detection and classification of breathing sounds and heartbeats which are relatively faint and occur simultaneously as other signals. Furthermore, the physiological signal detector and classifier must be compatible with that proposed in [10] which detects and classifies various non-verbal audio events captured from inside the occluded earcanal. Since in-ear recordings have a limited bandwidth, of about 2 kHz, raw audio samples are downsampled fronm 44.1 kHz to 8 kHz. Signals are then framed into 5-second frames. Features are then extracted from each 5-second frame. Various features are of interest including the spectrogram (an example can be seen in Figure 1), MFCCs, ZCR, and Per Channel Energy Normalization (PCEN). Feature reduction are used to reduce the computational complexity of the algorithm. Various classifiers will be explored including CNN and SVM models. Figure 2 illustrated the main structure of this approach.

4 Conclusions

With the fast development of in-ear health monitoring technologies there is a need for accurate, efficient and quick algorithms to detect and classify real-time information. The proposed open-access database will serve to improve existing ML algorithms and speed up research in this field. In addition, the achievement of the proposed approach will open up the door to various health monitoring applications with hearables, including vital sign tracking as well as emotion classification.

Acknowledgments

References

[1] Rachel E. Bouserhal, Philippe Chabot, Milton Sarria-Paja, Patrick Cardinal, and Jérémie Voix. Classification of nonverbal human produced audio events: A pilot study. In *Interspeech 2018*, pages 1512–1516. ISCA, 2018-09-02.

[2] A. Martin and J. Voix. In-ear audio wearable: Measurement of heart and breathing rates for health and safety monitoring. 65(6):1256–1263, 2018-06. PRJ: 209.

[3] Guangwei Chen, Syed Anas Imtiaz, Eduardo Aguilar–Pelaez, and Esther Rodriguez–Villegas. Algorithm for heart rate extraction in a novel wearable acoustic sensor. 2(1):28–33, 2015. _eprint: https://onlinelibrary.wiley.com/doi/pdf/10.1049/htl.2014.0095.
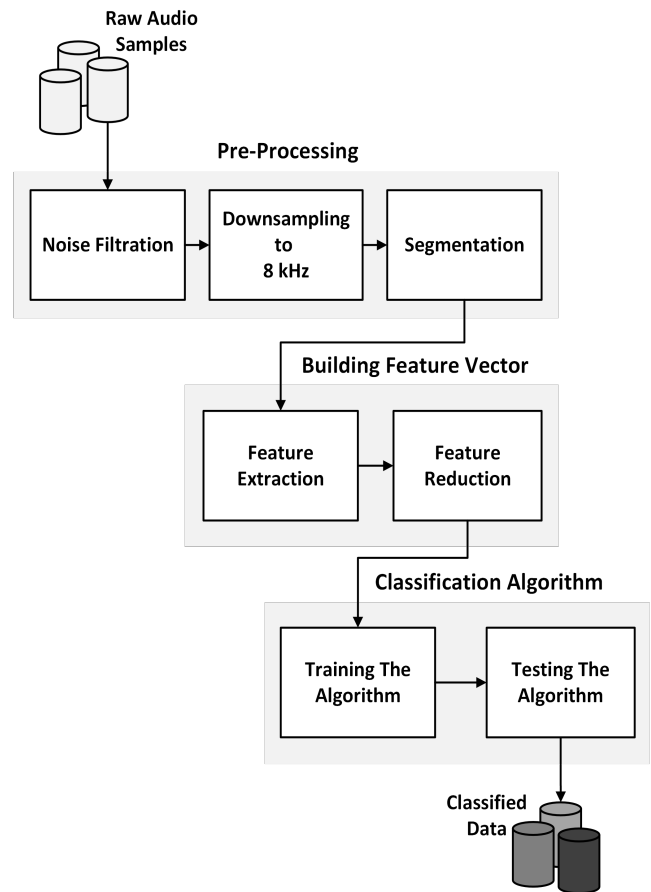
Figure 2: Block diagram of the proposed approach.

[4] I. McLoughlin, H. Zhang, Z. Xie, Y. Song, W. Xiao, and H. Phan. Continuous robust sound event classification using time-frequency features and deep learning. 12(9), 2017.

[5] J. Portêlo, M. Bugalho, I. Trancoso, J. Neto, A. Abad, and A. Serralheiro. Non-speech audio event detection. pages 1973–1976, 2009. ISSN: 1520-6149.

[6] Stephanie Pancoast and Murat Akbacak. Bag-of-audio-words approach for multimedia event classification. Technical report, SRI International Menlo Park United States, 2012.

[7] Maximilian Schmitt, Christoph Janott, Vedhas Pandit, Kun Qian, Clemens Heiser, Werner Hemmert, and Björn Schuller. A bag-of-audio-words approach for snore sounds' excitation localisation. page 5.

[8] Jurgen T. Geiger and Karim Helwani. Improving event detection for audio surveillance using gabor filterbank features. In *2015 23rd European Signal Processing Conference (EU-SIPCO)*, pages 714–718. IEEE, 2015-08.

[9] Jens Schröder, Jorn Anemuller, and Stefan Goetze. Classification of human cough signals using spectro-temporal gabor filterbank features. In *2016 IEEE International Conference on Acoustics, Speech and Signal Processing (ICASSP)*, pages 6455–6459, 2016.

[10] Philippe Chabot, Rachel E. Bouserhal, Patrick Cardinal, and Jérémie Voix. Detection and classification of human-produced nonverbal audio events. 171:107643, 2021-01.

EFFECT OF THE ERROR ON THE SOUND SPEED AND MICROPHONE POSITION ON ACOUSTIC IMAGE OBTAINED WITH A SPHERICAL MICROPHONE ARRAY

Julien St-Jacques [*1], **Kevin Rouard** [1], **Franck Sgard** [2], **Hugues Nélisse** [2], **Alain Berry** [3], **Nicolas Quaegebeur** [3], **François Grondin** [3], **Loic Boileau** [3], **Olivier Doutres** [1] **and Thomas Padois** [1].

[1]École de technologie supérieure, Montréal, Québec, Canada.
[2]Institut de recherche Robert-Sauvé en santé et en sécurité du travail, Montréal, Québec, Canada.
[3]Université de Sherbrooke, Sherbrooke, Québec, Canada.

1 Introduction

To reduce the noise level in a workplace, the main sources have to be localized. This task can be done with a spherical microphone array (SMA). When the microphones are flush mounted to a rigid sphere surface, the SMA is referred to as rigid. In this case, the Spherical Harmonic Beamforming (SHB) algorithm is preferred since it allows to account for the scattering effect of the acoustic waves on the rigid sphere [1,2]. When the microphones are fixed on an open wire frame, i.e., transparent with respect to the acoustic waves, the SMA is referred to as open and the Generalized Cross-Correlation (GCC) algorithm in the time domain can be used [2]. Both algorithms require the knowledge of the sound speed and the microphones position. In this study, the effect on the acoustic image of an error committed on these parameters is investigated numerically. The error is introduced by using a reference value for both parameters which is different from the one used to generate the microphones signals. More specifically, the microphones signals captured by a rigid or an open SMA placed in a room are obtained numerically using a sampled range of sound speed values and degrees of precision of microphone position. Then these signals are used as input to the SHB and GCC algorithms to calculate the acoustic image but with the reference value for the sound speed and the microphone position instead of those used to generate the input signals. The main lobe area is the criterion used to evaluate the parameters influence on the acoustic image.

2 Algorithms

2.1 Spherical Harmonic Beamforming

The SHB algorithm principle is the decomposition of the acoustic wave field measured on the surface of a sphere into spherical harmonics. Modal matrix of weights is given by

$$w_{nm}^*(kr_a, \theta_l, \varphi_l) = Y_n^m(\theta_l, \varphi_l) \frac{d_n}{b_n(kr_a)} \qquad (1)$$

with k the wavenumber, r_a the SMA radius and (θ_l, φ_l) respectively the elevation and azimuthal coordinates of the scan grid points. In Eq. (1), Y_n^m is the spherical harmonic matrix, b_n is the contribution of plane waves amplitude on the sphere and d_n is a weight parameter used to optimize the directivity. The modal pressure is given by

$$p_{nm}(kr_a, \theta_q, \varphi_q) = \alpha_q Y_n^{m^*}(\theta_q, \varphi_q) p(kr_a, \theta_q, \varphi_q) \qquad (2)$$

with α_q a weight parameter and p the acoustic pressure measured at the microphone located at (θ_q, φ_q). The spherical harmonic function is then given by

$$Y_n^m(\theta, \varphi) = \sqrt{\frac{2n+1}{4\pi} \frac{(n-m)!}{(n+m)!}} P_n^m(cos\theta) e^{im\varphi} \qquad (3)$$

2.2 Generalized Cross-Correlation

The GCC algorithm employs the inverse Fast Fourier Transform of the cross spectrum C_{uv} to estimate the cross-correlation $R_{uv}(\tau)$ between two microphones signals (u, v)

$$R_{uv}(\tau) = \sum_{j=0}^{N_f-1} C_{uv}(\omega_j) e^{i\omega_j \tau/N_f}, \qquad (4)$$

with the time lag τ, discrete frequency j and number of elements of the frequency vector N_f [2]. The acoustic image $A(\theta_l, \varphi_l)$ is then obtained with the arithmetic mean of the projected cross-correlations

$$A(\theta_l, \varphi_l) = \frac{1}{Q_p} \sum_{p=1}^{Q_p} R_{uv}(\tau_{uvl}) \qquad (5)$$

where Q_p is the number of microphone pairs included in an array composed of Q microphones and τ_{uvl} is the time difference of the time delays of two microphones (u, v).

3 Methodology

3.1 Simulation parameters

The simulated environment is a room of 18 m in length, 12 m in width and 5 m in height. The room reflection coefficient β is 1%. The SMA is in the center of the room. The source is a monopole located at 4 m, $\varphi = 0°$ and $\theta = 90°$, relative to the SMA. The source signal is a sine wave with frequencies ranging from 250 to 2000 Hz. The microphones signals are provided by the convolution of a source signal with the room impulse response. One rigid and one open SMA are considered. Both SMA have a radius of 20 cm and include 48 microphones following a t-design geometry.

3.2 Sound speed parameter

Speed of sound at atmospheric pressure depends on the temperature and humidity. The range used for the sound speed is based on the value of the sound speed between -40°C to 50°C. Different sound speed values are considered for the calcul-

* julien.st-jacques.1@ens.etsmtl.ca

ation of the microphone's signals (as described in sec. 3.1) ranging from 306 to 360 m/s. To simulate the error on the sound speed, the reference value of 343 m/s (20 °C) is used to obtain the acoustic image using the SHB and GCC algorithms for each set of microphones signals instead of the actual sound speed used to generate the microphones signals.

3.3 Microphone position parameter

This study considers multiple degrees of precision of microphone position on the SMA. First, the microphones signals are computed by each SMA with microphones coordinates rounded to 0.001°, 0.01°, 0.1°, 1°, 2°, the nearest factor of 5° and finally the nearest factor of 10°. To simulate the error on the microphones position, the computation of the acoustic image using the SHB and GCC is done using the coordinates rounded to 0.001° for each set of microphones signals instead of the actual positions used to generate the micro-phones signals.

3.4 Ellipse area at -3 dB

The quality of an acoustic image can be defined by the width of its main lobe. On a 2D map, an ellipse can be drawn at -3 dB from the maximum of the main lobe. The area of this ellipse is then used as a criterion for the acoustic image. A smaller ellipse area translates to a more precise acoustic image. The ellipse area for the sound speed assessment is normalized by the value measured at 343 m/s. For the microphone position, the ellipse area is normalized by the value measured with positions rounded to 0.001°. The normalized ellipse area is denoted NEA in the following.

4 Results

4.1 Sound speed

Figure 1 compares the NEA for both the SHB algorithm with a rigid SMA and the GCC with an open SMA for frequencies ranging from 200 to 2000 Hz and sound speed values ranging from 306 to 360 m/s. The sound speed has a low impact on the NEA for both the SHB and the GCC. The NEA is either increased or decreased by less than 15% which is not visible on the acoustic image. For the SHB, the NEA increases as the sound speed value grows for the frequencies lower than 1000 Hz and close to 2000 Hz. For the GCC, the NEA increases as the sound speed value grows for the full frequency range.

4.2 Microphone position

Figure 2 compares the NEA for both SMA's. The frequencies range from 200 to 2000 Hz and the precision of the microphone positions range from 0.001° to 10°. For the GCC, the microphone position has close to no impact on the NEA for the full frequency range. When the microphone position is rounded to 1° and higher, the SHB is not able to localize the acoustic source at the lower frequencies. In this case, the NEA values are meaningless.

5 Conclusion

This paper investigated separately the effect of an error on the sound speed and microphones position on the acoustic image obtained using the SHB algorithm (rigid SMA) and the GCC algorithm (open SMA). The microphones signals captured by a rigid and an open SMA were numerically generated beforehand using a sampled range of sound speed values and degrees of precision of microphones position. Then, the computation of the acoustic image was done using the reference values (343 m/s, 0.001°) instead of the actual value for each set of microphones signals. The ellipse area at -3 dB is the criterion used to evaluate the influence of both parameters. Results have shown that an error on the sound speed has a low impact on the SHB and GCC. It has been observed that the SHB is sensitive to an error committed on the microphones position, while the GCC is more robust. This can be explained by the dependency of the SHB on the orthogonality property which depends on the microphone position on the spherical array.
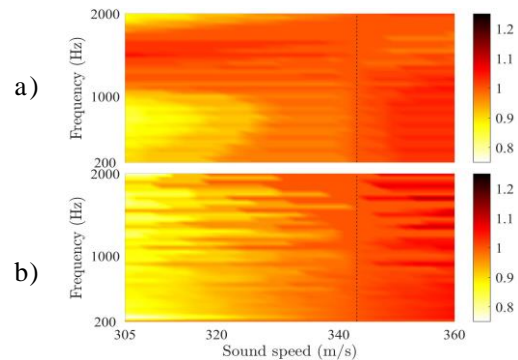

Figure 1: Normalized ellipse area per value of sound speed, a) rigid SMA, SHB, b) open SMA, GCC. Dashed line at sound speed reference value (343 m/s).
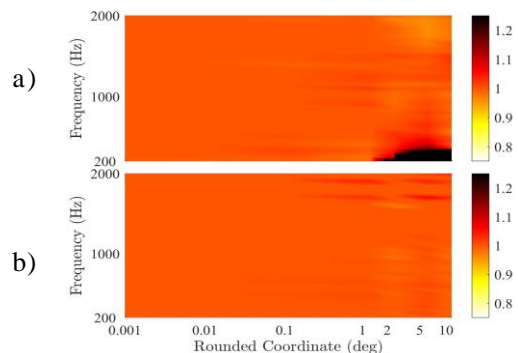
Figure 2: Normalized ellipse area per rounded coordinates of microphone position, a) rigid SMA, SHB, b) open SMA, GCC.

References

[1] S. O. Petersen. *Localization of Sound Sources using 3D Microphone Array*. M.Sc. Thesis, University of Southern Denmark, 2004.

[2] K. Rouard, J. St-Jacques, F. Sgard, H. Nélisse, A. Berry, N. Quaegebeur, F. Grondin, O. Doutres and T. Padois. *Numerical comparison of acoustic imaging algorithms for a spherical microphone array*. 9th Berlin Beamforming Conference – 9th BeBeC, 2022.

IMPACT OF CORONAVIRUS FACE MASKS ON THE PERCEPTUAL EVALUATION OF HEARING PROTECTORS COMFORT

Olivier Valentin [*1,2,3], **Philippe-Aubert Gauthier** [†2,3], and **Alain Berry** [‡1,2]

[1]Groupe d'Acoustique de l'Université de Sherbrooke, Université de Sherbrooke, Sherbrooke, Quebec, Canada
[2]Centre for interdisciplinary research in music media and technology (CIRMMT), Montreal, Quebec, Canada
[3]École des arts visuels et médiatiques, Université du Québec à Montréal, Montreal, Quebec, Canada

1 Introduction

Conducting research activities involving human participants during the COVID-19 pandemic raised new ethical and practical challenges. When most research activities requiring presence in labs resumed, human research requiring close contact had to comply with COVID-19 health and safety requirements, given the risks associated with potential direct and/or airborne transmission between and among researchers and participants. Therefore, wearing a procedure mask or a N95 mask and adhering to mitigation measures quickly became the new standards to observe. Embracing this new ways of conducting research raised questions among the research community, especially in social and behavioral sciences where scientists start to wonder if wearing a face mask could influence the research being conducted.

Prior to the COVID-19 outbreak, laboratory evaluations of earplugs comfort were conducted at the *Groupe d'Acoustique de l'Université de Sherbrooke*, as part of a multidisciplinary and multi-centric research project on the perceived comfort of hearing protectors. The new mitigation measures shed a new light on this project when it resumed : could the discomfort, annoyance or pain induced by the ear-loop elastics around the auricle interact with the multi-dimensional comfort of earplugs ?

In the absence of sufficient conclusive evidence in the literature, we decided to compare the earplugs' comfort evaluations obtained before (i.e., without mask) and after (i.e., with mask) the implementation of mitigation measures to control the spread of the severe acute respiratory syndrome coronavirus 2 (SARS-CoV-2), in an attempt to conclude to the question "Does wearing a face mask influence the earplugs' comfort evaluation ?". Responses to subjective questionnaires on earplugs' comfort were used to assess the influence of wearing a face mask on the physical, functional, acoustical, and psychological dimension of the earplugs' comfort. Additionally, Personal Attenuation Ratings (PAR) and results from speech in noise tests and alarm detection tests were used to complement the subjective comfort assessments.

2 Material and Method

2.1 Participants

Twenty-three individuals (seventeen males, six females) aged between 22 and 32 and having hearing thresholds below 25 dB HL (pure tone audiometry between 125 to 8000 Hz) participated in this research work. All participants were inexperienced regarding hearing protectors. 3M Classic earplugs were tested by 23 participants (13 without mask, 10 with mask), 3M UltraFit by 23 participants (12 without mask and 11 with mask), and the 3M Push-ins by 20 participants (9 without mask and 11 with mask). The experimental protocol was reviewed and approved by the *Comité d'éthique pour la recherche Lettres et Sciences Humaines*, one of the Internal review Boards at *Université de Sherbrooke* in Sherbrooke, Canada (approval no. 2019-1929). Informed consent was obtained from all participants before they were enrolled in the project.

2.2 Hearing Protectors and Face Masks

The earplugs used by the participants were either roll-down foam earplugs (3M™ E-A-R Classic), premolded earplugs (3M™ E-A-R UltraFit), or push-to-fit earplugs, which are an alternative between the roll-down foam and the premolded earplugs (3M™ E-A-R Push-ins). They were worn in an order randomly chosen prior to the measurement sessions.

The face mask worn by the participants was a single-use procedure mask from AMD-Ritmed®. These pleated style mask with ear-loops meet the current ASTM F2100 standard for "Level 2 Barrier" medical face mask [1] and were provided by *Université de Sherbrooke* for all in-person activities, including research projects involving human participants.

2.3 Sound Environments

Spatial sound synthesis was used to generate the two virtual industrial sound environments that served as background noise during all laboratory measurement sessions. These virtual industrial environments were generated using multichannel Acoustic Background Spectrum (ABS) Synthesis [2] inspired from Tarzia's work [3] on acoustic fingerprints, multichannel uncorrelated noises, and *in-situ* recordings collected at two industrial sites (a granulator and a stacker).

2.4 Subjective Questionnaires

A questionnaire was completed before and after each series of speech in noise and alarm detection tests performed by the participant, using a touchscreen computer monitor. These "Comfort Assessment" questionnaires aimed to evaluate the attributes of the main components of comfort (physical, acoustical, functional, and psychological) as well as comfort as a whole. They are derived from the French version of the COPROD questionnaire [4] which was designed to evaluate the multidimensional aspects of comfort [5, 6].

∗. m.olivier.valentin@gmail.com
†. gauthier.philippe-aubert@uqam.ca
‡. Alain.Berry@usherbrooke.ca

2.5 Speech in Noise Tests

The Speech Perception in Noise Tests were conducted using the *Test de Phrases dans le Bruit* described in [7]. Stimuli consisted of sentences pronounced in French, randomly picked-up from a database of 324 sentences. Each sentence contained a subject, a verb and a color to be identified by the participants from a list displayed on the touchscreen monitor placed in front of them. For example, if the stimulus was *Les amis cherchent des ballons jaunes* ("Friends are looking for yellow balloons") the correct answers to pick using the touchscreen monitor were *Les amis* ("Friends") for the subject, *cherchent* ("are looking") for the verb and *jaune* ("yellow") for the color. The presentation order of the sentences was randomized across participants. The stimulation levels were calibrated at the position of the participants to 62.4, 68.3, 74.9, and 82.3 dB(SPL), which correspond respectively to the level of normal, raised, loud and shouted voice as defined in ANSI S3.5 1997 [8]. A total of sixty (4 stimulation levels $\times$ 15 repetitions) stimuli were presented to the participants using a supplementary M-Audio speaker Studiophile DX4 placed in frontal incidence for the purpose of this task. The two virtual industrial sound environments used as background noise were calibrated at 90.9 dB(SPL) and 93.0 dB(SPL).

2.6 Alarm Detection Tests

The signal used for the alarm detection tests was a tonal gateway alarm captured at an industrial workstation using an Edirol R09 portable recorder with a FG-23652 condenser microphone (Knowles Electronics). Background noise was removed from the recording using Reaper v6.02 and the plugin "ReaFir." Each alarm detection test included a total of fifty alarms (5 signal-to-noise ratios $\times$ 10 repetitions) with a duration of 10 seconds each. The alarms were presented at five different signal-to-noise ratios (SNRs) (-10, -5, 0, +5, +10 dB) using a Motorola piezo supertweeter CTS KSN-1188. Each SNR was computed relatively to the background noise SPL measured at the center of the test room. The interval between consecutive alarm signals was randomly set between five and ten seconds.

3 Results and Discussion

Prior to being able to move forward on our research question about the perceived comfort of earplugs, it was mandatory to determine whether the earplugs' comfort evaluations performed with a face mask can be aggregated with those obtained without a face mask to avoid introducing a bias due to a potential effect induced by wearing a face mask. Wilcoxon unpaired tests revealed no significant difference between the mask condition and the no mask conditions, with the PAR values and the alarm detection results. No significant difference was found using the speech in noise results, except with the condition "3M™ Classic with shouted voice and the environment #1". Additionally, Fisher exact tests showed no significant difference for 990 of the 993 items of the questionnaires-based evaluations and the observed differences for the three

remaining questionnaires' items remain marginal (*p*-values very close to 0.05). Therefore, as we failed to find significant statistical differences between the condition with mask and without mask, data can be regrouped in a larger data-set.

4 Conclusion

Wearing a face mask does not influence the perceptual evaluation of hearing protectors comfort. Therefore, we think that the most common face masks should not influence the way people use and wear earplugs.

References

[1] American Society for Testing and Materials. Standard specification for performance of materials used in medical face masks, 2021. ASTM F2100-21.

[2] O. Valentin, P.-A. Gauthier, A. Berry, and F. Proulx. Objective evaluation of sound environment reproduction for comfort of hearing protector devices : Acoustic background spectrum synthesis versus multichannel cross-synthesis. In *Proceedings of Forum Acusticum 2020, Lyon, France*, pages 1–6, 2020.

[3] Stephen P. Tarzia, Peter A. Dinda, Robert P. Dick, and Gokhan Memik. Indoor localization without infrastructure using the acoustic background spectrum. In *Proceedings of the 9th International Conference on Mobile Systems, Applications, and Services, Bethesda, MD, USA*, pages 155–168, 2011.

[4] J. Terroir, N. Perrin, P. Wild, O. Doutres, F. Sgarf, C. Gauvin, and A. Negrini. Assessing the comfort of earplugs : development and validation of the french version of the coprod questionnaire, 2021. Ergonomics, available at : https ://doi.org/10.1080/00140139.2021.1880027.

[5] J. Terroir, O. Doutres, and F. Sgard. Towards a "global" definition of the comfort of earplugs. In *INTER-NOISE and NOISE-CON Congress and Conference Proceedings*, pages 108–114, 2017.

[6] O. Doutres, F. Sgard, J. Terroir, N. Perrin, C. Jolly, C. Gauvin, and A. Negrini. A critical review of the literature on comfort of hearing protection devices : definition of comfort and identification of its main attributes for earplug types. *International Journal of Audiology*, 58(12) :824–833, 2019.

[7] Josée Lagacé, Benoît Jutras, Christian Giguère, and Jean-Pierre Gagné. Development of the "test de phrases dans le bruit" (TPB). *Revue canadienne d'orthophonie et d'audiologie*, 34(4) :261–270, 2010.

[8] Caslav Pavlovic. SII—Speech intelligibility index standard : ANSI S3.5 1997. *The Journal of the Acoustical Society of America*, 143(3) :1906–1906, 1997.

Using Fram To Support Noise Exposure Management Onboard Vessels

Muhammad Sabah Ud Din Ersum, Lorenzo Moro, Doug Smith

Occupational noise exposure is a major health hazard on ships and can cause noise-induced hearing loss in crew members. Prolonged noise exposure also causes fatigue in the crew members, which may lead to human errors, and thus increase the possibility of maritime accidents. Previous studies have suggested different solutions to mitigate noise exposure, such as the use of hearing protection in accordance with relevant standards, the increase of insulation of onboard spaces, and the insulation and structural decoupling of acoustic sources. Differently from previous studies, this research activity will focus on finding systemic ways to mitigate noise exposures during jobs of the crew onboard the ship, with the aim of minimizing the risk of noise-induced hearing loss and noise-induced fatigue. This study will help identify the tasks associated with hazardous noise levels and to suggest possible measures to reduce noise exposure through work process management. This study involves interviewing the crew onboard the vessel to acquire information on their activities, working shifts, and the locations where they work. Based on work patterns of crew, appropriate measurement strategy i.e. task-based, job-based and full-day measurement approach is selected to assess their noise exposures using personal dosimetry. The Functional Resonance Analysis Method (FRAM) is used to model the crew's tasks during the voyage. The FRAM is a technique to model complex socio-technical systems. FRAM focuses on the system's functionality where the potential functional variability is accessed. Connecting the FRAM model to the noise contribution of each task will help to understand the work processes within the operation which could lead to high noise exposure. The FRAM helps manage the tasks of the work so that desired safe exposure level can be achieved by adjusting the work patterns of the crew to decrease their exposure times in high noise locations of the vessel.

Auditory Alarms In Ship Bridges: Understanding Current Challenges And Limitations

Robert Brown, Michael Schutz

Auditory alarms hold great potential as useful tools for quickly conveying critical information, and have particular utility when safety is of paramount importance. Consequently they play an important role in domains such as healthcare, where doctors receive real-time updates while caring for patients during surgery. They also play a crucial role in a wide variety of domains such as monitoring safety in nuclear power plants, updating pilots navigating airplanes, and conveying information in ship bridges crucial for navigation. Unfortunately, the particular sounds used as part of these auditory alerting systems have often been designed without consideration of human factors. Consequently, problems with noise, alarm confusion, annoyance, and alarm fatigue are endemic. Having applied principles of music perception to improve safety critical alarms in healthcare, Michael Schutz is now exploring potential applications of these insights to alarm systems in ship bridges with colleague Robert Brown. The first step of this research involved recording a variety of different ship bridge alarm sounds signalling a need for officers of the watch to react. This was followed by a series of interviews with experienced maritime professionals to help us outline some shortcomings of current auditory designs. Analysis of these recordings and interviews offers useful insight into a principled redesign of problematic alerting systems, which we will discuss. With almost 55,000 commercial ships at sea as of January 1, 2021 (excluding fishing vessels), this holds significant implications for safety in high consequence environments such as the navigation of ships, which are crucial for the modern economy.

Governance And Noise Exposures On Board Fishing Vessels In Atlantic Canada

Om Prakash Yadav, Desai Shan, Lorenzo Moro

Introduction: Fishing is considered to be one of the most hazardous occupations globally, and fish harvesters are exposed to many work-related risks at sea, including physical and psychological hazards. Noise is a significant physical health hazard for fish harvesters. Long or repeated exposure to sound levels of 85 dB (A) or more can have adverse health effects, including both auditory and non-auditory health problems such as noise-induced hearing loss (NIHL), stress, annoyance, hypertension, sleeping disorders, and impaired cognitive performance. Methods: A qualitative research and regulatory review was conducted to evaluate how fish harvesters in Newfoundland and Labrador (NL) manage occupational noise exposure and perceive noise-induced health problems, as well as the barriers and challenges associated with controlling occupational noise exposure. Results: Fish harvesters reported that their workplace is noisy. Over time, fish harvesters adapt to their environment and learn to tolerate loud

noises, displaying a fatalistic behaviour. Fish harvesters reported avoiding using hearing protection onboard due to safety concerns such as accidents caused by a lack of communication. Fish harvesters reported hearing loss as well as other non-auditory health problems. Based on the research findings, some gaps have been identified, including inadequate noise control measures by employers onboard, a shortage of a sufficient supply of hearing protection and hearing testing, and lack of training and education. Discussion and Conclusions: The above-mentioned gaps can be filled by implementing NL occupational health and safety regulations, and developing hearing conservation initiatives by employers. NL fishing organizations, provincial and federal governments should initiate training and education campaigns to help fish harvesters understand noise risk and adopt preventive measures. Adoption of new technology in vessel design should be encouraged by fishing organizations and governments to reduce noise levels onboard.

Occupational Noise Risk Perception Among Fish Harvesters In Newfoundland And Labrador

Om Prakash Yadav, Desai Shan, Atanu Sarkar, Veeresh Gadag

Introduction: Noise exposure is a significant hazard for fish harvesters and causes serious health problems (auditory and non-auditory) and impairs the quality of life and well-being. Therefore, a study was proposed to investigate noise risk perception and assess the self-reported hearing loss among fish harvesters in Newfoundland and Labrador (NL). Methods: A survey was conducted using a pre-validated noise risk perception questionnaire in NL fish harvesters. The questions were based on the Health Belief Model, which is used to drive initiatives for health promotion and disease prevention and consist of five dimensions to predict health behaviour: perceived benefits, barriers, self-efficacy, attitude, and susceptibility. Additional questions were asked to assess self-reported hearing loss. Results: The survey data of 76 fish harvesters analyzed. Approximately 44

PERCEPTION - PERCEPTION

THE EFFECT OF VOWEL LENGTHENING ON THE INTELLIGIBILITY OF OCCLUDED LOMBARD SPEECH

Xinyi Zhang[*1], **Meghan Clayards**[†2,3]**, and Rachel E. Bouserhal**[‡1]
[1]Department of Electrical Engineering, École de technologie supérieure, Montréal, Québec, Canada
[2]School of Communication Sciences and Disorders, McGill University, Montréal, Québec, Canada
[3]Department of Linguistics, McGill University, Montréal, Québec, Canada

1 Introduction

When speaking in noise, people's vocal effort is automatically adjusted in order to improve the intelligibility of their speech; this phenomenon is called the Lombard effect [1]. However, when the ear canals are blocked by, for example, hearing protection devices or hearables, the occlusion of the ears causes significant changes in speech production, particularly in noise [2]. The result is a Lombard speech that is less intelligible than its typical form; we refer to this as occluded Lombard speech (*OLS*). The change in speech production is due to the lowered noise levels at the ear canals caused by the passive attenuation of the in-ear devices, as well as a change in the talkers' perception of their own voice. One main characteristic of the open-ear Lombard speech is elongated vowels. However, by analyzing the SpEAR database [3], an open-access bilingual in-ear speech database that includes OLS, this elongation has been found to be much shorter in OLS. This discrepancy leads to our research question: Can elongating the vowels in the OLS improve its intelligibility?

2 Method

Thirteen people from the Great Montreal Area volunteered to participate in this research. All participants self-reported to be native speakers of French with no history of speech or hearing disorders.

The sentence recordings (stimuli) that the participants listened to were derived from the French portion of SpEAR. Hearing In Noise Test sentences were used as the speech materials in this database. Seventy-eight OLS sentences with relatively similar speech levels were selected.

These sentences were further modified to have different signal-to-noise ratios (SNRs) and different vowel lengthening conditions. Four SNRs were chosen: -3, 0, 5, and 10 dB. The SNR manipulation was achieved by modifying the sound level of the sentence recordings relative to a noise (same for all conditions). Additionally, in each SNR condition, half of the sentences had their vowels elongated to 1.5 times of the original length (an addition of 48 ms on average).

The experiment was conducted in a sound-attenuated booth. On each trial, participants heard one of the stimuli, repeated and recorded what they heard, then rated how easy it was to understand using a rating scale. Participants completed each task at their own pace. The accuracy was calculated using the number of words repeated correctly out of the

---
[*]xinyi.zhang.1@ens.etsmtl.ca
[†]meghan.clayards@mcgill.ca
[‡]rachel.bouserhal@etsmtl.ca

total number of words in a given sentence. The reaction time for each stimulus was measured by the difference between the time that a stimulus finished playing and the time that the participant clicked to start the repetition recording. After each sentence repetition, the participants were instructed to rate the ease of understanding of the stimulus on a 1000-pixel long slider with the leftmost being the most difficult and the rightmost being the easiest.

3 Results

Three measurements of the intelligibility of the stimuli are presented: the accuracy of the sentence repetition task, the participant-rated stimuli ease of understanding (EoU), and the reaction time (RT) for the sentence repetition task in milliseconds, where a shorter RT indicates a higher intelligibility.

Sentence repetition task word accuracy

Table 1: Descriptive statistics for sentence repetition accuracy.

	Unlengthened		Lengthened	
SNR	*Mean*	*SD*	*Mean*	*SD*
-3	0.61	0.38	0.50	0.37
0	0.82	0.30	0.81	0.27
5	0.96	0.12	0.90	0.20
10	0.98	0.08	0.89	0.20

Table 1 shows that with the increase of SNR, the sentence repetition accuracy increases and a ceiling effect can be observed. The group mean accuracy of the unlengthened conditions are always higher than in the lengthened condition except at SNR = 0, where they coincide. At SNR = 5 and SNR = 10, the group means of unlengthened condition are almost perfect with a small SD of approximately 0.1. However, group means plateaued at around 0.9 with a larger SD of 0.2 for the lengthened condition.

Participant-rated ease of understanding

As can be seen from Figure 1, on average, as the SNR goes up, so does the EoU. However, a large SD is observed at all SNRs for both of the vowel-lengthening conditions. In addition, the average EoU in the vowel-lengthened conditions is consistently lower than in the unlengthened conditions with the exception of SNR = 0.

Reaction time for sentence repetition task

As can be seen from Figure 2, for SNR from -3 to 5, RT negatively correlates with the SNR level as expected. However,
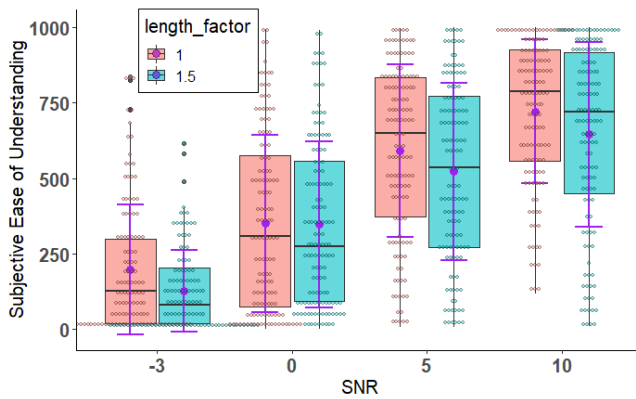
Figure 1: A box-plot overlaid with a dot-plot that compares the EoU of the stimuli, grouped by vowel lengthening condition and SNR levels. Group means and standard deviations are indicated by purple.
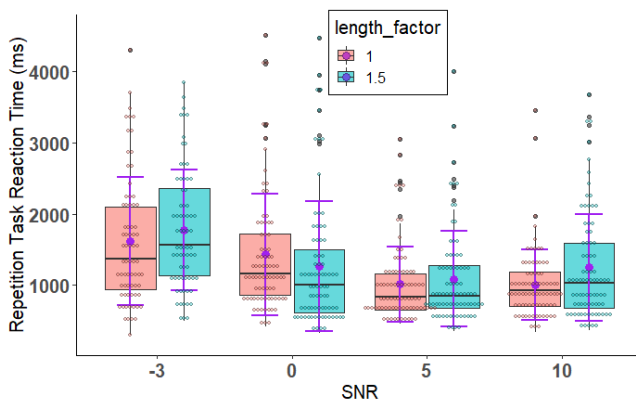

Figure 2: A box-plot overlaid with a dot-plot that compares the reaction time for the sentence repetition task, grouped by vowel lengthening condition and SNR levels. Group means and standard deviations are indicated by purple.

at SNR = 10, RT seems to have stagnated or even increased. The average RT of the unlengthened conditions are lower than of the lengthened ones at all SNRs but SNR = 0, where the lengthened condition has a lower RT.

4 Discussion and Conclusions

As shown in the results section, increasing SNR correlates with an increase in intelligibility. Comparing the two vowel-lengthening conditions, in general, vowel-lengthening seemed to correlate with a worsened intelligibility instead of an improvement. This may have happened because of the unnaturalness from the elongation manipulation (and/or its artefacts), even though the current degree of lengthening was chosen to have natural-sounding stimuli.

Another limitation related to the quality of naturalness of the stimuli was their non-communicative nature. Since Lombard speech is an instinctual adaptation for improving *communication* in noise, the elongation without the context of communication may have made the sentences sound less natural.

Interestingly, the participants seem to have behaved dif-

ferently at SNR = 0 than at the other SNRs. To elaborate, the intelligibility of the stimuli at SNR = 0 did not seem to be worsened by vowel lengthening; in fact, looking at the reaction time results, it even seemed to have improved intelligibility. However, a large SD is seen for the unlengthened SNR = 0 condition compared to the other SNRs. Thus, it is possible that the unlengthened SNR = 0 stimuli were perceived to be less intelligible than they should have been, instead of the lengthening here being a (hypothetical) anomaly. Further inferential statistics with mixed-effects modelling needs to be performed for this apparent finding. Multivariate models that take into account all three measurements simultaneously may be preferred to have a higher power of analysis. In the mixed-effects modelling, in addition to treating participants and sentences as random effects, the speakers of the stimuli, eight in total, should be considered, too. It has been noticed that the speaker composition is not the same for every condition, and the intelligibility of the stimuli may vary due to the speakers' accents (given that all participants spoke Quebec French), especially in noise.

In case this finding should be statistically significant, why SNR = 0 is a special case here may be investigated with follow-up studies. Could it be that the effect of lengthening depends both on SNR and the *degree* of elongation, and the currently selected degree (i.e., 1.5 times) happened to be closer to the (hypothetical) optimal elongation at SNR = 0, compared to the other SNR - elongation combinations? Or could it be that SNR = 0 is in some way perceptually *categorically* different from the other SNR levels?

To conclude, the effects of vowel-lengthening on the intelligibility of occluded Lombard speech are still unclear, but it is unlikely that the current manipulation should improve intelligibility, especially independent of the SNRs. What cannot be ruled out, though, is the possibility that if the stimuli were perceived to be more natural-sounding, vowel-lengthening could still be a valid approach for intelligibility improvement.

Acknowledgments

References

[1] Henrik Brumm and Sue Anne Zollinger. The evolution of the lombard effect: 100 years of psychoacoustic research. *Behaviour*, 148(11-13):1173–1198, 2011.

[2] Jennifer B Tufts and Tom Frank. Speech production in noise with and without hearing protection. *The Journal of the Acoustical Society of America*, 114(2):1069–1080, 2003.

[3] Rachel E. Bouserhal, Antoine Bernier, and Jérémie Voix. An in-ear speech database in varying conditions of the audio-phonation loop. *The Journal of the Acoustical Society of America*, 145(2):1069–1077, February 2019.

A Whispered Christmas: Phonetic Expectations and Type of Masking-Noise Influence Auditory Verbal Hallucinations

Mark Scott[*1]

[1]Memorial University of Newfoundland – Department of Psychology, Qatar University

1 Introduction

Auditory Verbal Hallucinations (AVH) are most commonly associated with schizophrenia, being one of the key diagnostic symptoms [1]. However, c. 9.6% of people with no known psychological issues also report this experience [2]. A common technique for inducing hallucinations in healthy volunteers is to present them with masking noise and suggest the presence of sound under the noise. The most famous demonstration of this is the 'White Christmas' effect in which participants are played stochastic 'white' noise and told to indicate when they hear the song 'White Christmas' underneath the noise. Participants often report hearing the song, despite there being nothing in the audio signal but noise [3]. Many replications have demonstrated this effect with speech [4–6].

The 'White Christmas' effect induces hallucinations through sensory expectation and masking. However, there has been little research conducted on how the phonetic details of the sensory expectation or how the type of masking noise modulate the effect. The current experiment addresses this gap by examining two types of phonetic expectation (expecting normal modal speech vs expecting whispered speech) and two types of masking noise (multitalker babble vs spectrally-matched speech-shaped stochastic noise). Masking relations likely play a key role as the 'White Christmas' effect is similar to *phoneme restoration*, in which expectation causes people to hear speech-sounds that are absent, but only if there is masking that *would* have obscured the missing sound [7]. It is predicted that there will be more AVH for multitalker babble than for speech-shaped noise masking, as multitalker babble is a more effective masker. Similarly, there should be more AVH for expecting whispered than for expecting spoken voice, as whisper is quieter and easier to mask. An interaction is also predicted by which AVH should be disproportionately more common when expecting a normal voice under babble noise, as the periodicity of normal voice should be particularly masked by babble.

2 Method

The experiment was conducted at Qatar University. Participants sat in front of a computer screen wearing sound-isolating headphones. On each trial, participants were presented with a target word in Arabic and were told to listen for this word during the noise that followed. Whenever they heard the full word (not just part of it), they were to hit the spacebar. They were told that the word could appear multiple times during a trial, so they could hit the spacebar more than once per trial. They were also told that the word may not occur at all, so it was fine not to hit the spacebar. When ready to start a

trial, the participant hit the 'enter' key at which point either multitalker babble or spectrally-matched speech-shaped noise played for thirty-five seconds. The noise factor (**Babble** vs **Speech-shaped** noise) was run *within-subjects*. There were 14 trials in the experiment (7 each of **Babble** and **Speech-shaped** noise). The voice conditions (**Spoken** vs **Whisper**) were run *between-subjects*. Participants in the **Spoken** condition were told they would hear a spoken voice under the noise, participants in the **Whisper** condition were told they would hear a whispered voice. The experiment, including instructions and practice, lasted about twenty minutes.

Two lists of seven Arabic words were created as the 'to-be-listened-for' sounds, one for each noise condition. The assignment of word-list to noise condition was reversed for half of the participants, so the assignment was counterbalanced over the full run of the experiment. The words were all chosen to be concrete, easily imageable nouns. The words in these lists were selected to use phonetically similar sounds (roughly equal numbers, between the lists, of e.g., nasals, sibilants, stops). This phonetic balancing was an extra precaution to minimize possible variability (within each run of the experiment) in how easy these words might be to hallucinate. The lists of words are provided in table 1 :

Table 1: Word lists for the two conditions.

List One		List Two	
Arabic	**English gloss**	**Arabic**	**English gloss**
tuffah	'apple'	*katef*	'shoulder'
maktab	'desk'	*minshaar*	'saw'
shooka	'fork'	*furshaah*	'brush'
korsi	'chair'	*kitab*	'book"
mismaar	'nail'	*sikkin*	'knife'
shafra	'razor'	*sariir*	'bed'
bedla	'suit'	*dulab*	'cupboard'

The multitalker babble was created using audio from the Qatari Arabic Corpus. Twenty-one files were selected without music or other non-speech sounds. They were normalized to the same intensity and transitions were cut at crossing points in the waveform to avoid pops at the joins. These sounds were then overlapped to create a multitalker babble of c. 30 voices. While individual words could not be distinguished in this babble, as an extra precaution the transcripts of the recordings were searched for the fourteen target words and none of them occurred in the sections used.

The speech-shaped noise was created by Praat script [8]. This measured the long-term average spectrum and intensity profile of the multitalker babble and applied these to stochastic noise of equal duration. The two noise sounds thus had

---

∗. mark.a.j.scott@gmail.com

equal intensity profiles and average spectra.

There were 28 Arabic-speaking female participants (14 each for **Spoken** and **Whisper** conditions). Participants were paid or given course credit for their participation.

3 Results

A mixed ANOVA found a main effect of **Noise Type** (F[1,26] = 10.9, p = 0.003) and a marginal main effect of **Voice Type** (F[1,26] = 3.42, p = 0.075]). There was no significant interaction of **Noise Type** by **Voice Type**. These results are shown in figure 1.
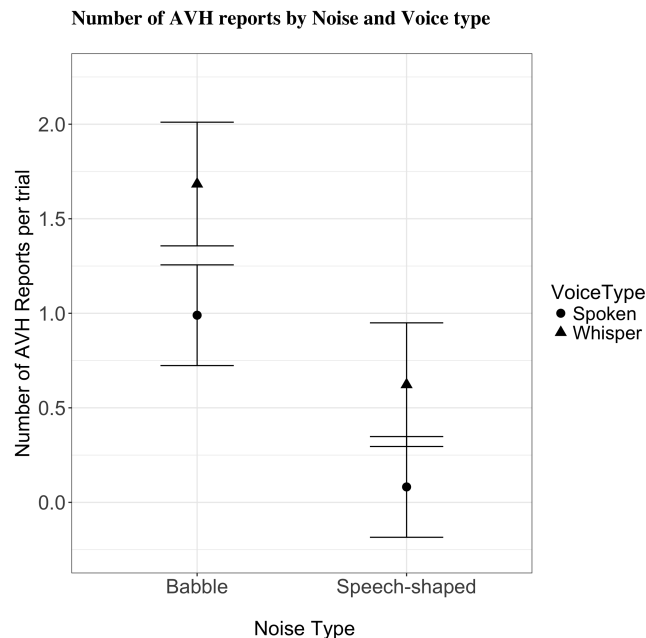

Figure 1: Results.

4 Discussion

These results show that speech hallucinations are influenced by both phonetic expectation and type of masking noise. With multitalker babble masking-noise, the rates of AVH are, as predicted, higher. Similarly, when the participant is told to expect whisper, hallucination rates are (marginally) higher. These results fit with findings on phoneme restoration, in which people can be induced to hear a missing speech-sound based on the surrounding context as long as there is sufficient masking that the absent sound *would* have been obscured had it been present. Multitalker babble is a more effective masker than stochastic noise, and whisper is more easily masked than modal voice. Contrary to prediction, there was no interaction between phonetic expectation (voice-type) and masking (noise-type). Attention may play a role in this, given that attentional demands for detecting a sound in noise are greater when the sound is similar to the noise – as occurs for detecting normal speech in babble. However, perhaps the data set is simply too small to reveal an interaction.

These findings are consistent with a proposed mechanism of hallucination in which a perceptual *schema* of a sound

is compared against auditory input looking for a match. When there is sufficient similarity, the person reports hearing the sound [9]. Multitalker babble contains bits of speech with phonemes that will occasionally match part of the word being listened for, and so this should increase the likelihood of a listener reporting a 'match' with the expected target word.

Given the links between hallucination and imagery, these results are likely related to research showing that ambiguous speech sounds can be shaped by expectations provided by speech imagery [10, 11].

5 Conclusions

This experiment shows that both phonetic expectation and type of masking noise influence speech hallucinations in the 'White Christmas' effect. In line with predictions based on the phoneme-restoration effect, greater masking (multitalker babble) and a more easily masked expected-sound (whisper) induce more AVH. No interaction was found between these factors. These are preliminary data – a larger and more detailed data set has been collected and is being analyzed.

Acknowledgments

References

[1] Chris D. Frith. *The cognitive neuropsychology of Schizophrenia*. Lawrence Erlbaum Associates, Hove, 1992.

[2] Kim van Slobbe-Maijer. *Auditory hallucinations in youth : occurrence, clinical significance and intervention strategies*. PhD thesis, University of Groningen, 2019.

[3] Theodore Xenophon Barber and David Smith Calverley. Empirical evidence for a theory of "hypnotic" behavior : Effects of pretest instructions on response to primary suggestions. *The Psychological Record*, 14(4) :457–467, 1964.

[4] Steven R. Feelgood and Andrew J. Rantzen. Auditory and visual hallucinations in university students. *Personality and Individual Differences*, 17(2) :293–296, August 1994.

[5] Charles Fernyhough, Kirsten Bland, Elizabeth Meins, and Max Coltheart. Imaginary companions and young children's responses to ambiguous auditory stimuli : implications for typical and atypical development. *Journal of Child Psychology and Psychiatry*, 48(11) :1094–1101, 2007.

[6] Samantha Hartley, Sandra Bucci, and Anthony P. Morrison. Rumination and psychosis : an experimental, analogue study of the role of perseverative thought processes in voice-hearing. *Psychosis*, 9(2) :184–186, 2017.

[7] Makio Kashino. Phonemic restoration : The brain creates missing speech sounds. *Acoustical Science and Technology*, 27(6) :318–321, 2006.

[8] Paul Boersma and David Weenink. Praat, a system for doing phonetics by computer. *Glot International*, 5(9/10) :341–345, 2001.

[9] Ulric Neisser. *Cognition and reality : Principles and implications of cognitive psychology*. Henry Holt & Co., New York, 1976.

[10] Mark Scott, H. Henny Yeung, Bryan Gick, and Janet F. Werker. Inner speech captures the perception of external speech. *Journal of the Acoustical Society of America Express Letters*, 133(4) :286–293, 2013.

[11] Mark Scott. Speech imagery recalibrates speech-perception boundaries. *Attention, Perception & Psychophysics*, 78(5) :1496–1511, 2016.

Study of Auditory Localization with a Wearable Microphone Belt Providing Haptic Feedback

Ana Tapia Rousiouk [*1 2], **François Grondin**[†3], **and Victoria Duda**[‡1 2]

[1]Université de Montréal

[2]Institut universitaire de réadaptation en déficience physique de Montréal

[3]IntRoLab, Université de Sherbrooke

1 Introduction

Spatial orientation and navigation in our acoustic surroundings are known to rely on auditory localization abilities. The aim of our study is to examine the precision and accuracy of human auditory localization with the contribution of a haptic-coupled hearing assistive device called the SmartBelt [1]. We wish to determine whether this multi-microphone belt providing haptic feedback around the waist results in better sound source localization in normal-hearing participants with simulated visual and hearing losses. The results of the study will serve as a milestone for the fine-tuning and design of assistive hearing devices for guiding people with sensory deficits such as single-sided deafness, as well as dual visual and hearing impairments.

2 Method

Twenty normal-hearing adults (11 females, 19-46 years of age) participated in the study. They were blindfolded and wore an earplug in the right ear to simulate a dual sensory loss. All participants completed an auditory screening which included a visualization of the ear canal, tympanometry and a measure of audiometric hearing thresholds. Participants were retained if their ear canals were unoccluded with normal middle ear function, and audiometric thresholds were at or below 15 dBHL between 250 to 8000 Hz. The SmartBelt (as shown in figure 1) was then calibrated to the participants' waist size according to the previously described methodology [1].
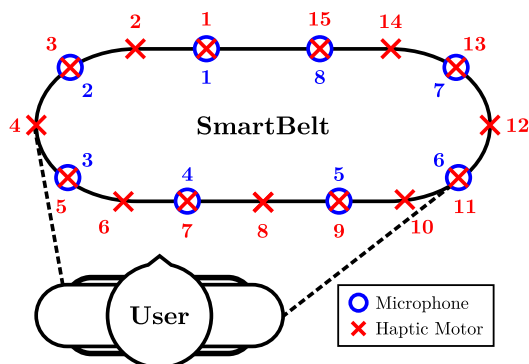

Figure 1 – Schema of the SmartBelt [1]

Participants underwent a training session prior to the localization task. The localization task took place in a sound booth with 20 loudspeakers surrounding the participants in a 360-degree circular array, named the Auditory Localization Evaluation System (SELA) [2] (see Figure 2). Participants wore a laser-helmet, aligned to their nose, to point to the angle of the loudspeaker, which was hidden behind a mesh curtain in the SELA. They were instructed to localize the sound source by turning their head and body to face the perceived location of the sound and pressing a button. An assistant inside of the booth read aloud the angle indicated by the participant. The stimulus was a 65 dBA, 3 second wide-band sound which simulated traffic noise on dry pavement. There were three test conditions corresponding to sections of the SELA array : frontal, right-side and left-side. Each condition contained 22 sound stimuli emitted by different loudspeakers in a randomized order. Participants wore the SmartBelt and each condition was tested twice with the device being either activated or deactivated. The six conditions were in randomized order and blind to the participants and assistant. Following the testing, participants completed the Quebec User Evaluation of Satisfaction with Assistive Technology (QUEST) questionnaire [3] to rate their experience with the SmartBelt.
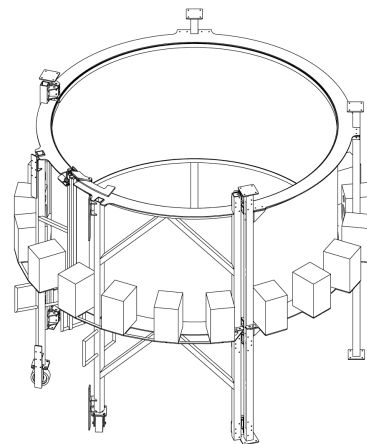
Figure 2 – The SELA sphere : a 20 loud-speaker system arranged 360° around the participant who is placed in the center of the sphere (image taken from the original manufacturing drawings, the 2006-2019 version was equipped with 11 loudspeakers).

3 Results

3.1 SELA

Localization performance within the SELA was defined as correctly identifying the source within 9 degrees of its actual location. Figure 3 shows there was a performance improvement when activating the SmartBelt in one out of the three conditions. Performance increased in the frontal condi-

---

∗. ana.tapia.rousiouk@umontreal.ca

†. francois.grondin2@usherbrooke.ca

‡. victoria.duda@umontreal.ca

tion, however it worsened in the left-side condition. The right-side condition did not show significant changes when the belt was activated. A two-way analysis of variance (ANOVA) was conducted by condition (frontal, right-side, left-side), and activation (ON, OFF). It showed a significant effect of condition, $F(2, 36) = 3.81, p = 0.03$, and a significant condition x activation interaction, $F(2, 36) = 5.23, p = 0.01$. Paired t-tests revealed a significant difference between the activation and deactivation of the belt in the frontal ($p = 0.07$) and the left-side ($p = 0.05$) but not the right-side ($p = 0.70$) conditions.
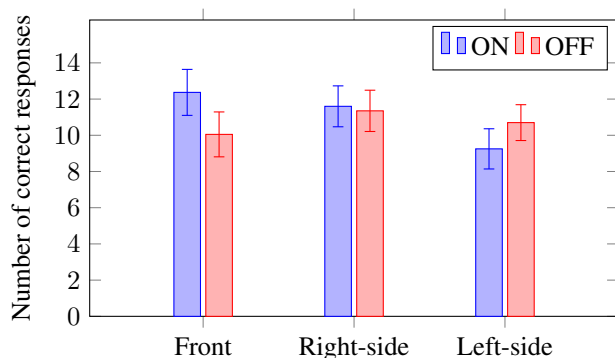
FIGURE 3 – Average score ($n = 20$) for participants using the SELA sphere. Brackets indicate standard error. There was a significant increase in correct responses for the frontal condition only when activating the belt. Right- and left-side conditions showed unchanged, and reduced performance, respectively.

3.2 QUEST Questionnaire

The QUEST questionnaire identified multiple advantages to wearing the belt : the training was simple and the effort was minimal to use the device efficiently. Functional performance of the device, which increases autonomy of the participant, also received high ratings. In contrast, appearance, practicality, and weight received lower ratings. Finally, the temporal characteristics of the haptic feedback (i.e. the timing occurring between the vibrotactile stimuli) as well as the positioning of the motors around the waist were determined as areas of improvement by most participants.

4 Discussion

This study demonstrates the effectiveness of using the Smart-Belt, a vibrotactile technology that is activated in the direction of a sound source. The SmartBelt appears to increase the localization performance of individuals with a simulated dual sensory auditory and visual impairment when sounds occur in front of the user. The belt was not effective when the source of the sounds were located on either the left or right side.

The redundancy of the hearing and visual systems help provide complementary information about the sensory environment. When a person has a dual auditory/visual impairment, this redundancy is lost and localization performance will diminish [4]. Based on these results, compensating for this redundancy using a device-driven vibrotactile stimulation can compensate for the reduced audio-visual informa-

tion. However it is still unknown whether this technology could be effective in the presence of competing noise, which is more likely what a user would encounter in a real-world environment. Future studies on the efficacy of the belt in the presence of non-target background noise, would be necessary for better external validation of this technology.

The reduced efficacy of the localization performance on the left or right sides may be due to the sub-optimal positioning of the haptic motors around the the user's waist. One example of a new distribution of the motors would be to remove the belt buckle and to place a motor at all four cardinal points (ex. $0°$, $90°$, $180°$ and $270°$) specifically fit to each user. This may better aid the participant to map the sound source to the body. Another modification could be to reduce the size of the backpack so that the system is more aesthetically pleasing and comfortable.

Vibrotactile technology such as the SmartBelt may be an additional assistive technology for the improvement of auditory localization. Those who present poor auditory localization such as in those with dual sensory loss, are typically treated with amplification technology and auditory rehabilitation. This technology offers a new approach if current practices are insufficient to return auditory localization to normal limits.

5 Conclusions

The SmartBelt combines the use of auditory and haptic feedback to improve frontal localization. These findings suggest this vibrotactile device may benefit the localization abilities of those with dual sensory loss. Haptic-coupled hearing devices are a promising yet challenging domain of investigation today. Research in auditory localization with haptic feedback must be pursued to find appropriate and effective technical hybridizations and configurations (especially in terms of body placement and sensitivity) that take the perceptual experience of people with sensory impairments into account.

Acknowledgments

References

[1] S. Michaud, B. Moffett, A. T. Rousiouk, V. Duda, and F. Grondin. SmartBelt : A wearable microphone array for sound source localization with haptic feedback. *arXiv preprint arXiv :2202.13974*, 2022.

[2] J. Dufour, A. Ratelle, T. Leroux, and M. Gendron. Auditory localization training model : Teamwork between audiologist and O&M specialist—pre-test with a visually impaired person using bilateral cochlear implants. *International Congress Series*, 1282 :109–112, 2005.

[3] L. Demers, R. Weiss-Lambrou, and B. Ska. Development of the quebec user evaluation of satisfaction with assistive technology (QUEST). *Assistive Technology*, 8 :3–13, 1996.

[4] H. J. Simon and H. Levitt. Effect of dual sensory loss on auditory localization : Implications for intervention. *Trends in Amplification*, 11(4) :259–272, 2007.

A COMPARISON BETWEEN CROS HEARING AIDS AND BONE-ANCHORED HEARING AIDS FOR PATIENTS WITH SINGLE-SIDED DEAFNESS: A LISTENING EFFORT-BASED PILOT STUDY

Olivier Valentin [*1,2,3,4,5], François Prévost [†1,6], Don Luong Nguyen [‡1,2,5,7], and Alexandre Lehmann [§1,2,3,4,5]

[1]Laboratory for Brain, Music and Sound Research (BRAMS), Montreal, Quebec, Canada
[2]Centre for Research on Brain, Language or Music (CRBLM), Montreal, Quebec, Canada
[3]Centre for interdisciplinary research in music media and technology (CIRMMT), Montreal, Quebec, Canada
[4]McGill University, Faculty of Medicine, Department of Otolaryngology–Head and Neck Surgery, Montreal, Quebec, Canada
[5]Research Institute of the McGill University Health Centre (RI-MUHC), Montreal, Quebec, Canada
[6]McGill University Health Centre (MUHC), Department of Speech Pathology and Audiology, Montreal, Quebec, Canada
[7]Jewish General Hospital, Department of Audiology and Speech Pathology, Montreal, Quebec, Canada

1 Introduction

Single-sided deafness (SSD) is characterized by the near or total loss of hearing in one ear with normal hearing in the contralateral ear. SSD gives rise to a functional listening handicap : it impairs speech recognition in noise, sound localization, and decreases awareness of sounds due to the head acoustic shadowing in the auditory hemifield ipsilateral to the impaired ear [1–3]. The dominant therapeutic approach consists in rerouting incoming acoustic signals from the impaired ear to the non-impaired ear. This is done using either air conduction (e.g., contralateral-routing-of-signal – CROS – hearing aids) or bone conduction (e.g., bone-anchored – BA – hearing aids).

However, the relative benefits of using BA or CROS hearing aids are difficult to assess clinically. The inability to assess which device produces the best results for a given patient makes the clinical management of SSD patients challenging. In practice, device choice often relies on subjective patients reports of reduced listening effort and funding modalities that tend to differ for each device.

This research aims to address this long-standing issue, by using a combination of tests assessing how hearing aids impact SSD patients hearing outcomes. To do so, we used subjective (NASA Task Load Index) and objective (pupillometry) measurements of listening effort, together with behavioral performance assessment, to compare those two types of hearing aids during a speech-in-noise task.

2 Material and Method

2.1 Participants

Six adult men with single-sided sensorineural deafness, defined as having no residual bone conduction hearing with no residual speech recognition in one ear, and air conduction audiometric thresholds better than or equal to 25 dB HL at 0.25, 0.5, 1, 2, 3 and 4 kHz in the other ear, were assessed. Participants were native English speakers with no history of neurological disorders, no excessive caffeine intake prior to the measurement session, and no otologic co-morbidity in the good ear. During the measurements, participants remained seated in a comfortable chair inside a double-walled audiometric booth of the MUHC Department of Speech Pathology and Audiology. The study was reviewed and approved by the Research Ethics Board (REB) of the McGill University Health Centre (MUHC). Informed consent was obtained from all participants before they were enrolled in the study.

2.2 Experimental Procedure

Behavioral performance was assessed using Hearing-In-Noise Test (HINT) [4] conducted via the Oticon Medical Experiment Platform (OMEXP) in three conditions : while wearing a CROS hearing aid (Oticon CROS with OpenSoundNavigator™ 2), while wearing a BA hearing aid (Oticon Medical Ponto™ 4), and with no hearing aid. A total of 60 sentences was presented in the BA-fitted (20 sentences), CROS-fitted (20 sentences) and unaided (20 sentences) conditions. Speech signals were presented using a loudspeaker in frontal incidence and a white noise was presented using a second loudspeaker in the auditory hemifield ipsilateral to the good ear. The stimulation levels were determined via an adaptive HINT conducted prior to starting the experiment, by which the signal-to-noise ratio (SNR) yielding a 70% speech reception threshold (SRT) with no hearing aid was identified. Participants were instructed to listen and repeat aloud the sentences heard or understood. No feedback was provided.

While the participants were performing the behavioral task, pupil size and location in both eyes were measured using the Pupil Core eye-tracking platform (Pupil Labs, Berlin, Germany). Peak pupil dilation (PPD) was extracted during a time window corresponding to the pause between the sentence offset and the prompt to repeat the sentence [5]. This metric was then averaged across sentences for a given condition.

At the end of each condition, subjective assessment of listening effort was performed using the NASA Task Load Index (NASA-TLX) via a tablet computer. This subjective and multidimensional assessment tool is used to evaluate the mental workload level (MWL) of tasks performed by a participant, which in the present context was to repeat sentences heard in noise.

∗. m.olivier.valentin@gmail.com
†. francois.prevost@muhc.mcgill.ca
‡. don.nguyen@mail.mcgill.ca
§. alexandre.lehmann@muhc.mcgill.ca

3 Results

Preliminary results indicate no effect of the device on behavioral performance (HINT scores, Fig. 1A), in line with previous reports [6, 7]. We observed a trend in peak pupil dilation indicating that both CROS and BA hearing aids conditions require less cognitive effort compared to the unaided (UNAI) condition (Fig. 1B). Subjective effort result trends suggest that participants perceive requiring less cognitive effort during a speech-in-noise task when using BA hearing aids (Fig. 1C).

4 Conclusion and Future Work

The presented paradigm provides a combination of objective and subjective approaches to inform device choice and assessment in patients with SSD. Preliminary results suggest a reduced effort in SSD patients when aided, in absence of behavioral improvement. Future work will recruit more patients. Results might lead to the development of an objective biomarker that could be used in a clinical setting to provide personalized recommendations. Additionally, this would allow clinicians to longitudinally track patients' progress during their follow-up visits.

Acknowledgments

References

[1] N.Y. Dwyer, J.B. Firszt, and R.M. Reeder. Effects of unilateral input and mode of hearing in the better ear : Self-reported performance using the speech, spatial and qualities of hearing scale. *Ear and hearing*, 35(1) :126–136, 2014.

[2] H.Y. Andersen, S.A. Schroder, and P. Bonding. Unilateral deafness after acoustic neuroma surgery : subjective hearing handicap and the effect of the bone-anchored hearing aid. *Otology & Neurotology*, 27(6) :809–814, 2006.

[3] B. McLeod, L. Upfold, and A. Taylor. Self reported hearing difficulties following excision of vestibular schwannoma. *International journal of audiology*, 47(7) :420–430, 2008.

[4] M. Nilsson, S.D. Soli, and J.A. Sullivan. Development of the hearing in noise test for the measurement of speech reception thresholds in quiet and in noise. *The Journal of the Acoustical Society of America*, 95(2) :1085–1099, 1994.

[5] A.A. Zekveld, S.E. Kramer, and J.M. Festen. Cognitive load during speech perception in noise : the influence of age, hearing loss, and cognition on the pupil response. *Ear and Hearing*, 32 :498–510, 2011.

[6] J.P. Peters, A.L. Smit, I. Stegeman, and W. Grolman. Review : Bone conduction devices and contralateral routing of sound systems in single-sided deafness. *The Laryngoscope*, 125(1) :218–226, 2015.

[7] J. Fogels, R. Jönsson, A. Sadeghi, M. Flynn, and T. Flynn. Single-sided deafness-outcomes of three interventions for profound unilateral sensorineural hearing loss : A randomized clinical trial. *Otology & Neurotology*, 41(6) :736–744, 2020.
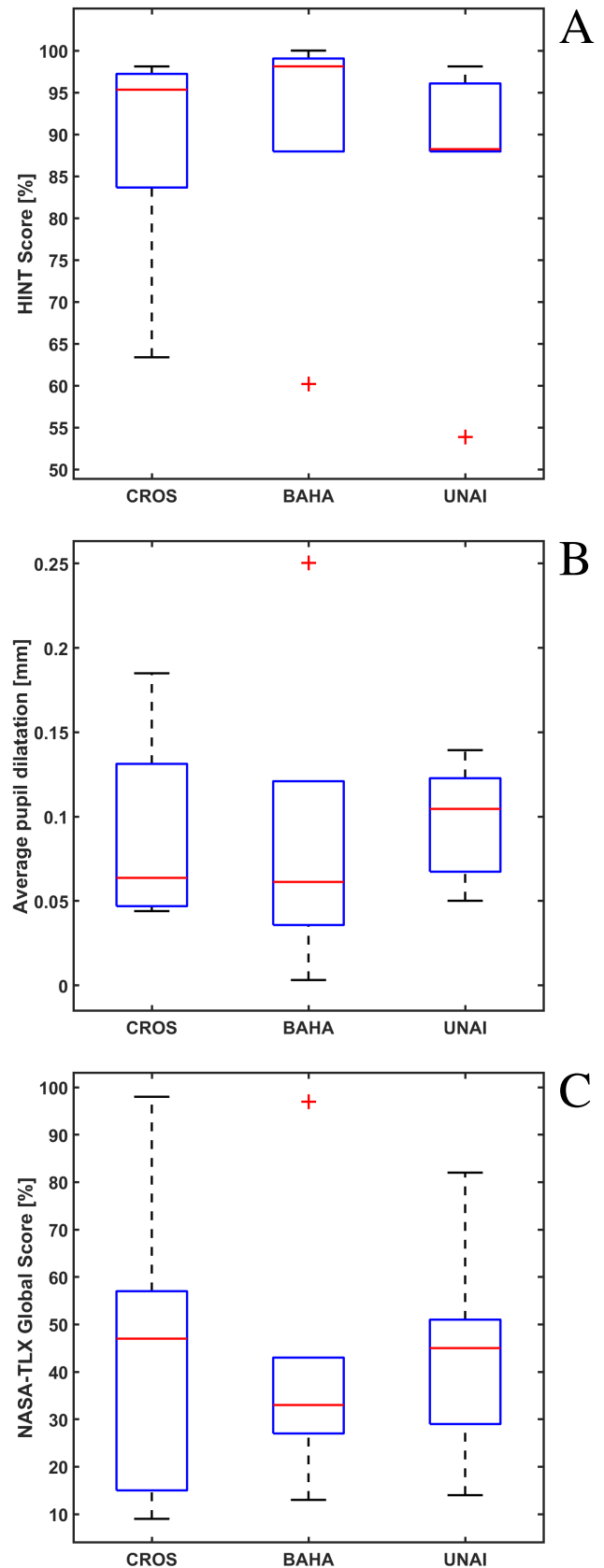
FIGURE 1 – Behavioral (A), objective (B), and subjective (C) results obtained with six SSD patients, with hearing aids (BAHA and CROSS conditions) and without hearing aid (UNAI condition). Medians are indicated by red central marks and outliers are plotted using "+" red markers.

Abstracts for Presentations without Proceedings Paper
Résumés des communications sans article

Identifying Hidden Hearing Loss
Alicia Follet, Benjamin Zendel

Age-related hearing loss is one of the most commonly reported health issues for older adults. Clinically, hearing deficits are normally identified by using pure-tone thresholds (PTT), a test of the ability to detect a near-threshold tone. Interestingly, there are some individuals who report difficulties with hearing, despite having normal PTT. One of the main hearing difficulties reported by this group is a difficulty understanding speech when there is loud background noise. Understanding speech in noise is a supra-threshold auditory task, and in the cochlear nerve, there are neurons specialized for near-threshold stimuli and others specialized for supra-threshold stimuli. It is thought that synaptopathy of the neurons specialized for supra-threshold stimuli leads to a 'hidden' hearing loss (HHL), because this hearing loss is not observed in pure-tone thresholds. Very little is known about the neurophysiology and genetics of HHL in humans. Accordingly, the purpose of this study was to identify a subset of participants who have HHL, in order to conduct follow-up research on them. To identify a sample of people with HHL, PTT were compared with performance on two speech in noise assessments: the Hearing in Noise Test (HINT) and the Quick Speech in Noise test (QuickSIN). In most participants, we found PTT to be predictive of both the HINT and the QuickSIN; however, a small sample of participants performed significantly worse on the HINT and QuickSIN than would be predicted given their PTT. It is very likely that this sample of participants has HHL. Future research will use this sample of participants to study the genetics and neurophysiology of HHL.

SPEECH PRODUCTION - PRODUCTION DE LA PAROLE

INITIATION AND MAINTENANCE OF LINGUAL BRACING POSTURE

Nicole Ebbutt[*1]**, Yadong Liu**[†1]**, Annabelle Purnomo**[‡1]**, Charissa Purnomo**[♦1]**, Kyra Hung**[#1] **& Bryan Gick**[+1,2]

[1]Department of Linguistics, University of British Columbia
[2]Haskins Laboratory, New Haven

1 Introduction

Lateral bracing, in which the sides of the tongue are held in contact with the palate and upper molars [1], has been found to be maintained throughout running speech, across all languages observed to date [2]. This braced posture is released only for select sounds, including laterals (such as [l] in English) and low vowels (such as [ɔ]) [3], and is even maintained through non-lingual and lingually neutral sounds such as labial and glottal consonants which require no lingual movement, and schwa [3], which has a neutral tongue position [4].

The present study aims to examine these non-lingual and neutral contexts to determine whether lateral tongue bracing is a transient activation or a tonic activation that spreads onto unspecified, neutral sounds. We hypothesize that the raised (braced) and lowered (unbraced) tongue postures function as distinct postural settings that are maintained through sequences of lingually neutral sounds, suggesting that such postures may be initiated by a preceding postural "trigger."

2 Methods

2.1 Participants

Twenty-two participants took part in this study and were recruited through the SONA linguistics portal at the University of British Columbia (UBC) or by word of mouth. 5 participants were excluded from analysis because they were not native speakers of North American English (NAE) according to a language background questionnaire; participants were considered to be native speakers if they acquired English before eight years of age and continued to use it as a primary language at work, school, or home. The data from another 9 participants were excluded due to poor ultrasound image quality. The remaining 8 participants were native speakers of NAE and were students at UBC between the ages of 18 and 22. In order to adhere to COVID-19 safety protocols, masks were worn by the participants throughout the experiment.

2.2 Experiment

Participants were seated in an experiment chair with a headrest stabilization mechanism. An ultrasound probe was posi-

[*] nicoleebbutt@gmail.com
[†] yadong.liu@ubc.ca
[‡] a3purnomo@gmail.com
[♦] cpurnomo26@gmail.com
[#] kyrahung@gmail.com
[+] gick@mail.ubc.ca

tioned to view a coronal image of the posterior portion of the participant's tongue. The recording of audio and ultrasound video was then started.

Participants were presented with a series of stimuli consisting of four blocks of sentences, each of which consisted of seven sentences. The target word present in each sentence was "hubba-bubba" [həbəbəbə] (HB), which was selected because it contains a sequence of four syllables made up entirely of non-lingual and lingually neutral sounds. Flanking this target sequence were words containing either lingual consonants, sounds that require tongue bracing (e.g., chews, wants, has, eats, chewing gum) or /l/, a sound known to interfere with tongue bracing (e.g., love, lump, plum, lots). The blocks were randomized so that participants read one of twenty-four possible block orders in their stimuli. Participants were asked to read the entire set of stimuli three times, the first acting as a practice round.

Figure 1: Thresholded VKG of data from the left side of the tongue for one participant. Tracing of the tongue surface is shown in white pixels.

2.3 Analysis

Analysis A: The spreading of lingual bracing (ultrasound):
The timestamps of HB within the second and third stimuli reading in each video file were extracted from manual TextGrid annotations using Praat [5]. All frames of the ultrasound imaging video were extracted, and only the frames within each utterance of the manually labeled target word were selected for further analysis. ImageJ software [6] was used to open each set of image sequences, adjust their brightness and contrast in order to more clearly see the tongue's surface and then threshold the images to black and white. Finally, the image sequences were converted into videokymographs (VKG) in ImageJ, creating an image of the tongue's tracing over time (shown in white pixels) for each utterance of HB. Separate VKGs were produced for the left and right sides of the tongue.

The side of the tongue with the clearest and most consistent imaging was selected for further analysis. From the chosen VKGs, the tongue position at the beginning of each HB sequence was examined. We then normalized the original tongue position in pixel values for comparison across participants with z-scores. The normalized initial tongue positions of HB produced in different conditions (braced vs unbraced) were fitted into a linear mixed effect (LME) model with preceding condition as a fixed effect and speaker as a random effect with both random slope and intercept. In order to determine whether the preceding target could

cause a triggering effect of bracing, the LME model was compared to a null model without a preceding condition as a fixed effect using a likelihood ratio test.

Analysis B: Acoustics of the spreading of lingual bracing: An acoustic analysis was conducted on participants' production of each of the two central [bə] syllables in the HB sequence (i.e., [həbəbəbə]). We chose the central [bəbə] syllables in order to minimize possible effects of local coarticulation with the preceding and following segments. The first two vowel formants (F1 and F2) were extracted at the midpoint of each [bə] syllable and the average of F1 and F2 across the two syllables was calculated. In order to determine the effect of preceding condition on the vowel formants of schwa in HB, we fitted mean F1 and F2 values of the central [bəbə] syllables in a similar LME model as in Analysis A and compared the model with a null model using a likelihood ratio test.

3 Results

3.1 Lorem ipsum dolor sit amet

Analysis A: The spreading of lingual bracing (ultrasound): After comparing the tongue height of 56 HB productions from 8 participants, results (see figure 2) show that the sides of the tongue remain in a significantly higher position when preceded by a braced target compared (mean height in z-score 0.43) to an unbraced target (mean height in z-score -0.45) (p<0.001).
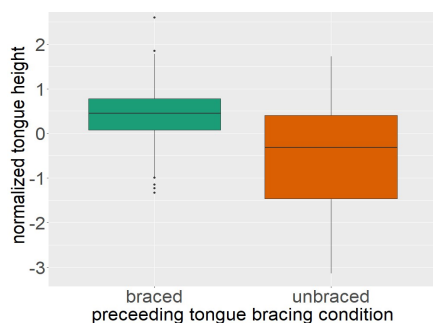
Figure 2: Boxplot depicting the normalized mean tongue height during the production of HB for the 8 speakers analyzed in braced vs. unbraced preceding conditions.

Analysis B: Acoustics of the spreading of lingual bracing: Mean F1 and F2 values of the central [bəbə] syllables of HB are shown in Figure 3. Neither F1, F2 values were significantly different between the preceding target conditions.

4 Discussion

Our results suggest that the maintenance and suppression of the lateral tongue bracing posture spreads to the following non-lingual productions. Given that the preceding context appears to act as a trigger for the following segments, this may indicate that the tongue toggles or switches between these two postures, braced and unbraced.
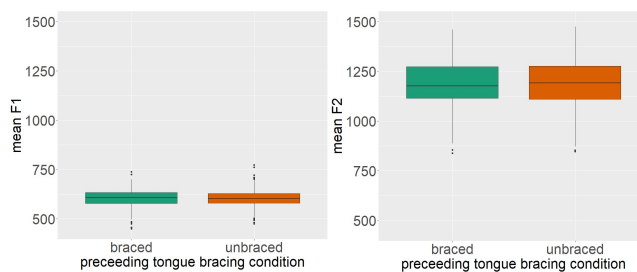
Figure 3: Boxplot depicting normalized mean F1 and F2 during the production of the two central ([bəbə]) syllables of HB for the 8 speakers analyzed in braced vs. unbraced preceding conditions.

As no significant effects of braced or unbraced condition were found on F1 and F2 values, this suggests that not all changes in tongue behaviour/position lead to significant changes in acoustic output.

Some notable limitations to our study which future research should attempt to overcome include the limited sample size and the fact that using ultrasound only shows tongue height and cannot definitely show tongue-palate contact. Also, since tongue contour was not always visible in the regions of interest, some position data was lost throughout collection with the ultrasound [2]. Future work will involve running the present experiment with a larger sample size and investigating the carryover and anticipatory influence of lateral tongue bracing posture.

References

[1] Gick, B., Wilson, I., & Derrick, D. (2013). Articulatory phonetics. John Wiley & Sons.

[2] Liu, Y., Tong, F., de Boer, G., & Gick, B. (2022). Lateral tongue bracing as a universal postural basis for speech. Journal of the International Phonetic Association, 1-16.

[3] Gick, B., Allen, B, Roewer-Després, F., & Stavness, I. (2017). Speaking tongues are actively braced. Journal of Speech, Language, and Hearing Research, 60(3), 494-506.

[4] Giegerich, H. J. (1992). English phonology: An introduction. Cambridge University Press.

[5] Boersma, P. & Weenink, D. (2022). Praat: doing phonetics by computer [Computer program]. Version 6.2.12, retrieved 17 April 2022 from http://www.praat.org/

[6] Abramoff, M. D., Magalhaes, P. J., & Ram, S. J. (2004). Image Processing with ImageJ. Biophotonics International, 11(7), 36-42.

Comparing Velum Velocity in Québécois French Nasals

Annabelle Purnomo [*1], Nicole Ebbutt [1], Charissa Purnomo [1], Jahurul Islam [1], Gillian de Boer [1] and Bryan Gick [1,2]
[1] Department of Linguistics, University of British Columbia, Vancouver, Canada
[2] Haskins Laboratory, New Haven, Connecticut, United States of America

1 Introduction

The velum is a speech articulator which separates the oral and nasal cavities. During the production of oral sounds, the velum is raised, keeping the velopharyngeal port (VPP) closed; during the production of nasal sounds, the velum lowers, opening the VPP and allowing for sounds to resonate in the nasal and sinus cavities.

Motor control of the velum is not well understood. While closure is primarily due to activation of the levator veli palatini, it is not known if velar opening is due to active or passive control [1,2]. Examining the speed of the velum is one way to gain insight into the control of the velum. Previous literature has examined velum speed in a variety of contexts, such as velum velocity when raising versus lowering [3,4], and velum velocity in speech versus non-speech segments [5].

While previous studies have looked at velum velocity, few have compared the velocity between segment types, such as consonants and vowels. Previous studies report that there is a positive correlation between velopharyngeal openings (VPO) and velum velocity [5,6] and that French nasal consonants and nasal vowels have similar sized VPOs [7]. Based on this, we predict that there will be no significant difference in velum velocity between the production of nasal consonants and nasal vowels in French. This would suggest that the velar movement for these segments are controlled in a similar manner.

2 Method

2.1 Database and annotation

The data was taken from the Université Laval X-ray videofluorography database which included 17 X-ray video files of sentence-level speech from nine native speakers (5M/4F) of Québécois French [8]. The speakers' age ranged from 19 to 30 years.

The audio from the films was extracted and force-aligned, with any misaligned boundary manually corrected. The start and end timestamps for each segment were extracted using a Praat [9] script.

2.2 Measurement

Using the imaging software ImageJ [10], a diagonal line was drawn along the velum's path of movement (i.e., between the pharyngeal wall and the upper surface of the velum; see Figure 1). The height and angle of these lines were determined by visually inspecting a full stack of images within a video.

Figure 1: an example of the location of VPO measurement on the sagittal X-ray image.

To measure the degree of VPO, the number of black and white pixels along the diagonal line was counted. The proportion of black pixels was then normalized between 0 and 1 within each video, with 1 representing the widest opening for the film, and 0 representing no opening (see Figure 2).
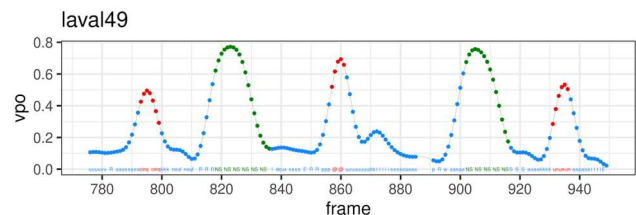

Figure 2: VPO as a function of time (frame is used as a proxy for time) blue=oral, red=nasal, green=speech pause.

To measure the velocity of velum movement, R [11] was used to fit simple linear regression models with the VPO values from each opening and closing phase separately. Slopes from the regression models were used as a proxy for velocity.

Thus, for each nasal segment, we obtained two slope values: one for the opening phase and one for the closing phase. Adjacent nasal consonants and phonemically nasal vowels were excluded due to difficulties separating the segments.

2.3 Statistical analysis

The effect of segment type (nasal consonant versus nasal vowel) on velocity was analysed using linear mixed-effects models. The fixed effects included segment type, phase (opening versus closing), duration in frames, distance (size of VPO) and sex, with random intercepts for each speaker. Using a significance level of $p= 0.05$, p values for individual predictors were obtained via model summary.

* apurnomo@student.ubc.ca

3 Results

Figure 3 shows boxplots of velum velocity by segment type for closing and opening phases of the velum. The x-axis indicates closing or opening phase, and the y-axis shows the velocity (in arbitrary units) as obtained from the slopes of simple linear regression. Figure 3 indicates that vowels have slightly higher median velocities than the consonants in both closing and opening phases.
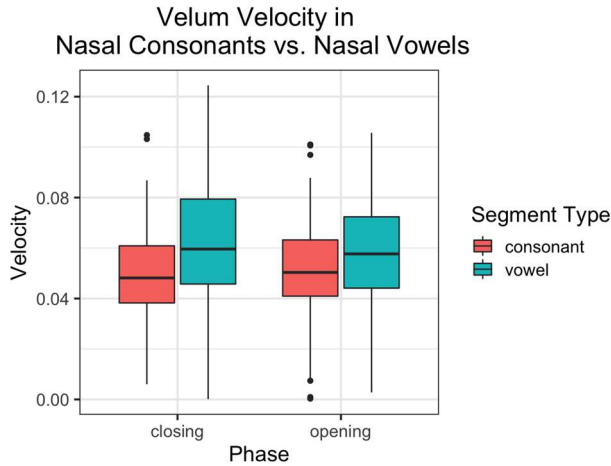

Figure 3: Boxplot comparing the velum velocity of nasal consonants and nasal vowels in opening and closing phases.

The model found significant effects for distance ($\beta=0.14$, DF=553, t=22.53, p<0.001) and duration in frames ($\beta=-0.007$, DF=567, t=-17.52, p<0.001) but there was no significant difference in velocity between nasal consonants and nasal vowels ($\beta=0.002$, DF=567, t=1.53, p=0.126). The fixed effects of sex and phase were not significant either.

4 Discussion

The results suggest that in both opening and closing phases of the velum, its velocity during nasal consonant and nasal vowel production in Québécois French remains similar. This matches our hypothesis that nasal consonants and nasal vowels would have similar velum velocities and suggests that velum movement in consonants and vowels are controlled in a similar manner. As well, the significant effects found for distance and duration in frames suggest that the larger the VPO size, the faster the velum moves, as found in [5,6].

The analysis was limited to a database from 1974, thus our results may not apply to present day Québécois French. It is likely that the non-significant effect would become significant given a larger dataset. Future work should run analyses with a larger dataset.

Acknowledgments

References

[1] Bell-Berti F. Velopharyngeal function: A spatial-temporal model. Haskins Laboratories Status Report on Speech Research 1980 Jul;63-64(-):41-65.

[2] Halle M. On distinctive features and their articulatory implementation. Natural Language and Linguistic Theory 1983;1(1):91.

[3] Kuehn DP. A cineradiographic investigation of velar movement variables in two normals. The Cleft Palate Journal. 1976 Apr 1;13(2):88-103.

[4] Birkholz P, Kleiner C. Velocity Differences Between Velum Raising and Lowering Movements. In: Karpov A, Potapova R, editors. Speech and Computer. Cham: Springer International Publishing; 2021. p. 70–80. (Lecture Notes in Computer Science).

[5] slam J, de Boer G, & Gick B. Speed of velum movement during nasal segments and rest intervals: A cineradiographic study of French and English speech. J Acoust Soc of Am. 151 (4), A64-A64

[6] Kollia HB, Gracco VL, Harris KS. Articulatory organization of mandibular, labial, and velar movements during speech. J Acoust Soc Am. 1995 Sep;98(3):1313–24.

[7] de Boer G, Islam J, Purnomo C, Wu L, & Gick B. Revisiting the nasal continuum hypothesis: A study of French nasals in continuous speech. University of British Columbia. [under review]

[8] Munhall KG, Vatikiotis-Bateson E, Tohkura Y. X-ray film database for speech research. J Acoust Soc Am. 1995 Aug;98(2):1222–4.

[9] Boersma P, Weenink D. Praat: doing phonetics by computer [Computer program]. 2022. Version 6.2.12, Available from: http://www.praat.org/

[10] Schneider CA, Rasband WS, Eliceiri KW. NIH Image to ImageJ: 25 years of image analysis. Nature Methods. 2021 [cited 2022 Jul 26]. 9, 671-675. Available from: https://www.nature.com/articles/nmeth.2089

[11] R Core Team. R: The R Project for Statistical Computing [Internet]. R: A language and environment for statistical computing. 2020 [cited 2022 Jul 26]. Available from: https://www.r-project.org/

Abstracts for Presentations without Proceedings Paper
Résumés des communications sans article

The Estimation Of Tongue Stiffness During Phonation: An Investigation Using Ultrasound Shear Wave Elastography

Chenhao Chiu, Wei-Cheng Hsiao, Bao-Yu Hsieh, Yining Weng

While biomechanical modeling studies have proposed that sound variants or alternations may be associated with physiological preferences, such as muscle-induced stress and strain of the tongue surface (Stavness et al., 2012, Chiu and Lu, 2021), empirical evidence remains sparse. Miura et al. (2021) employed ultrasound elastography with ultrafast imaging to estimate the stiffness (hardness, in their term) and pressure of the tongue. However, the measurement of the stiffness was performed with no phonation involved. It is yet to be determined whether the stiffness of the tongue may vary during speech production.The current study uses ultrafast imaging (3,000 fps) to capture the states of the tongue during phonation. Through the examination of the wave amplitude and velocity, associated with the stiffness of the tongue can then be estimated. The results show that the wave amplitude and frequency measured at the tongue (Figure 1) match with those measured from the vocal folds (Figure 2 top), suggesting that the vibrations of the vocal folds propagate waves and these waves can be transmitted through the tongue. More generally, this result also suggests that the vocal folds may serve as the intrinsic source of vibration, suitable for shear wave estimation with ultrafast imaging and quantification of tongue stiffness. The shear wave velocity results, on the other hand, show vowel differences (Figure 2 bottom), predicting differentiated stiffness of the tongue for different vowels. Taken together, the findings of the current study demonstrate the application of ultrasound shear wave elastography to speech production, which crucially provide insight into the quantification of the tongue stiffness, which can consequently account for sound combinations or changes.

UNDERWATER ACOUSTICS - GENERAL - ACOUSTIQUE SOUS-MARINE - GÉNÉRALE

Modelling Split-Beam Sonar

Axel Belgarde

The split-beam echosounder has been developed to enable the direct measurement of target strength by locating the angular location of a target within the echosounder's beam pattern. That angular location is determined by measuring the phase difference in signals received by independent quadrants of the transducer. The complex geometry of split-beam sonars can present difficulties to predict the exact performance in the design process. We report on a model of the split-beam system that can be used to evaluate and optimize sonar performance before committing to a particular hardware design. To evaluate the implications of transducer geometry choices, transmitter and receiver beam patterns have been generated and tested from multiple transducer shapes. The model simulates acoustic backscatter based on scattering of sound from particles in a three-dimensional domain. The sum of the contribution of the scatterers is sampled at the transducer locations to create representative received signals. Traditional data processing algorithms are compared to potential new method to improve accuracy on angular position and target strength measurement. Processing of the simulated received signals allows us to assess performance against the known model input.

Bayesian Inversion Of Ocean Acoustic Data For Seabed Geoacoustic Profiles

Stan Dosso

This paper describes and illustrates a general approach to the inversion of ocean acoustic data to estimate depth-dependent profiles and uncertainties for seabed geoacoustic properties (e.g., sound speed, density, attenuation coefficient). To quantify the information content of acoustic data to resolve seabed structure, a Bayesian approach is formulated that includes rigorous approaches to nonlinear inversion, model selection, and data error modeling. Model parameterizations are determined probabilistically from the data as part of the inversion based on trans-dimensional (trans-D) inversion, which considers the number of seabed layers as an unknown hyper-parameter, marginalized over in considering results. Trans-D inversion is carried out with the reversible-jump Markov-chain Monte Carlo method, which constructs a Markov chain that samples from the posterior probability density (PPD) of the geoacoustic model parameters. Wide but efficient sampling of the trans-D parameter space is achieved by combining principal-component reparameterization and parallel tempering. The data error model is based on the assumption of multivariate Gaussian errors with unknown variance and covariance. Error correlations are represented by an autoregressive process, with trans-D sampling of zeroth- and first-order processes applied to avoid under- or over-parameterizing the error model. The applicability of these statistical assumptions can be investigated for a specific problem with residual analyses. Inversion results are considered as marginal probability profiles for geoacoustic properties, which quantify the resolution of seabed structure versus depth below the seafloor. The Bayesian geoacoustic inversion approach is illustrated for a number of ocean acoustic data sets collected at a test site where the seabed sediments consist of a mud layer overlying sand and deeper layers, and where sediment coring information is available for comparison.

Investigating Seasonal And Spatial Changes In Acoustic Backscatter Characteristics On The South Coast Of Newfoundland

Nurul B. Ibrahim, Sebastien Donnet, Andry Ratsimandresy, Len Zedel, Olivia Gibb, Dounia Hamoutene

We are interested in understanding differences in ecosystems along the south coast of Newfoundland. One way to explore these differences over time and between locations is to use Acoustic Backscatter data that can be collected from self-contained instruments called ADCPs (Acoustic Doppler Current Profilers). ADCPs use the signal scattered back from small suspended drifting particles to measure water current velocity. They can also detect signals scattered from fish and other pelagic organisms. The acoustic backscatter from the ADCP data can provide a record of fish activity at the instrument location. Similarly, the overall volume backscatter levels can be used as an indication of zooplankton concentration. Data on acoustic backscatter from 300 kHz ADCP sonar systems were collected from 7 separate locations along Newfoundland's south coast from August 2019 until June 2022. The instruments were calibrated in a lab setting to allow for comparison between separate instruments in different locations. We report on the calibration method, and the preliminary analysis of the resulting data.

Remote Detection Of Ocean Sound Speed Profile Using Acoustic Profiling Techniques

Seyed Mohammad Reza Mousavi

Knowing the ocean sound speed profile is of particular interest in many applications such as underwater acoustic imaging and sound propagation modeling. A significant additional capability is that the sound speed profile could be used in the remote detection of the vertical temperature profile in the same way that acoustic tomography can infer the spatial structure of a temperature field. Geophysical seismic exploration techniques provide sound speed measurements, and some studies have successfully probed ocean temperature structures, but such systems require very large hydrophone arrays and have only limited spatial resolution of tens of meters. More direct methods of measuring sound speed profile have been described notably by the Ph.D. thesis of R. D. Huston at the University of Victoria and descriptions in patents written by B. H. Brumley with patent number US8,385,152 B2, but none of these present a working system. Another area where the sound speed profile is of interest is in ultrasound imaging for medical applications, and there are several reports of such systems providing profiles on the order of 10 cm. The basic approach for acoustic sound speed profiling is to transmit sound pulses and then receive signals reflected from scatterers at different depths. The sound speed profile is then estimated by considering propagation geometries and estimated travel times. We consider various possible approaches by using a model of acoustic backscatter to generate synthetic received signals that can then be inverted to evaluate system performance. Our goal is to determine which methods would have the most promise in oceanographic or limnological applications. For these methods, characteristics of transmitted signals and types of arrays are analyzed using synthetic received signals.

Measurements And Modelling Of A One-Year Under-Ice Acoustic Propagation Data Set

Sean Pecknold, Bruce Martin, David Barclay

During the fall of 2019, Defence Research and Development Canada (DRDC) deployed a drifting vertical line array (VLA) of hydrophones in the Beaufort Sea. Eight hydrophones, evenly spaced between 32 and 300 m beneath the water and ice surface, recorded underwater ambient noise and acoustic transmissions over the span of one year. Ambient noise data were on the topmost and bottommost hydrophones for 4 minutes every 30 minutes, and acoustic transmissions were recorded during two 80-minute periods each day. The transmissions included 35 Hz signals from projectors that were deployed as part of the Coordinated Arctic Acoustic Thermometry Experiment (CAATEX), located at ranges of approximately 500 km and approximately 2200 km. Transmissions of 925 Hz signals were also received from a set of projectors that were deployed as part of the Arctic Mobile Observing System (AMOS) experiment. Here, we describe the measured received sound pressure levels from these projectors, and compare measured and modelled receive levels using an under-ice acoustic propagation model.

UNDERWATER ACOUSTICS - SHIP NOISE - ACOUSTIQUE SOUS-MARINE - BRUIT DES NAVIRES

INTERFACE FORCES IDENTIFICATION USING COMPONENT TPA IN-SITU METHOD FOR TRANSFER PATH ANALYSIS (TPA)

Hamdi Ben Amar[*1]**, Raef Cherif**[†1]**, and Yacine Yaddaden** [‡1]

[1]Université du Québec a Rimouski.

1 Introduction

The marine transport industry uses a lot of subsystems such as engines, that produce tonal vibrations which propagate through different paths into the receiving structure. TPA methods are mainly used to solve NVH problems using substructuring applications. The most challenging part of a TPA analysis is estimating the equivalent forces at the contact points between the active and the passive side which require numerical inversion of some matrices. Matrix inversion could pose problems due to the ill-conditioning leading to inaccurate results. In this paper, a TPA model is established for an academic system consisting of two plates linked by four springs. Several parameters are studied and discussed to improve the equivalent forces identification, such as the singular value rejection, and the number and position of indicator points.

2 Theoretical background

2.1 Component TPA In-situ Method

Component TPA In-situ Method allows performing operational tests on the assembled product AB to obtain equivalent forces between the active (A) and the passive (B) side, avoiding dismounting of any part [1].
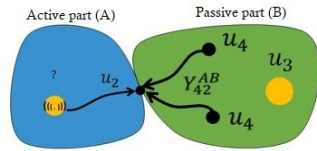

Figure 1: In-situ method.

The Component TPA In-situ Method defines the response of the target points u_3 (node 3) by multiplying the equivalent forces f_2^{eq} on the surface (node 2) to the transfer mobility matrix Y_{32}^{AB}, as given by the following expression [1]:

$$u_3 = Y_{32}^{AB} f_2^{eq} \qquad (1)$$

The calculation of f_2^{eq} involves operational data of indicator points (node 4) measured at a series of locations close to the contact points between the active and the passive side. The equivalent forces are given by the following expression [1]:

$$f_2^{eq} = [Y_{42}^{AB}]^+ u_4 \qquad (2)$$

where $[Y_{42}^{AB}]^+$ and u_4 are respectively the pseudo-inverse of the transfer mobility function.

---
[*]benh0063@uqar.ca

[†]Raef_Cherif@uqar.ca

[‡]Yacine_Yaddaden@uqar.ca

2.2 Matrix conditioning

Component TPA In-situ Method requires inverting the transfer mobility matrices Y_{42}^{AB} which could lead to erroneous results if they were ill-conditioned. The condition number reflects how well-conditioned a matrix is. It is a property of the matrix and its expression is given by [2]:

$$Cond_2(A) = \frac{max(Singularvalue(A))}{min(Singularvalue(A))} \qquad (3)$$

where the subscript 2 indicates the 2-norm. A lower condition number indicates a better conditioned matrix. In case of ill-conditioned matrices, singular value rejection is applied.

2.3 Singular value decomposition

SVD of a matrix A with dimensions m*n is the factorisation in the following form [3]:

$$A = USV^T \qquad (4)$$

With U an m*m unitary matrix, S an m*n diagonal matrix with non negative real numbers and V^T the transpose of an n*n unitary matrix [3] . The diagonal elements of $S(S_{ii}, 1 \leq i \leq min(m,n))$ are the singular values of A. The inverse of the matrix A is given by [2]:

$$A^* = VS^*U^T \qquad (5)$$

With S* is an n*m diagonal matrix and its diagonal elements are given by:

$$S_{ii}^* = \left\{ \begin{array}{ll} \frac{1}{S_{ii}} & \text{if } S_{ii} > 0 \\ 0 & \text{else.} \end{array} \right.$$

3 Numerical study

In this section, the Component TPA In-situ method was applied to an academic system (figure 2). It consists of two alu-
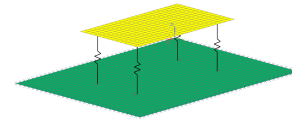

Figure 2: The academic system

minum plates linked by four springs. The upper plate (free boundary conditions) represents the active part and the lower plate with clamped edges represents the passive part. The upper plate was chosen to be stiffer than its lower counterpart to imitate the dynamic behavior of a Ship's engine.Their properties are given in Table 1. A point load was applied to the upper panel along the Z axis.The numerical model was developed with Simcenter 3D-Siemens software, and the simulations have been performed using Modal Frequency Response solution, with a frequency step of 2 Hz over a frequency range

from 0 to 3000 Hz.

Table 1: Physical Proprieties.

	Young Modulus (GPa)	Model Density (kg/m3)	Poisson's Ratio	DLF(%)	Length (m)	Width(m)	Thickness (m)	Mass (Kg)
Upper plate	73.1	2730	0.33	2	0.25	0.1	0.04	2.73
Lower plate	73.1	2700	0.33	2	0.5	0.3	0.01	4.05
Isolators	3D Spring ; Stiffness : Kx = Ky = Kz = 5E7 N/m STIFFNESS IS APPLIED ONLY ON X, Y , Z AXIS							0

The singular value rejection approach was applied to the ill-conditioned matrices that have high condition numbers' values. It is advised to neglect the lower singular values during the process of inversion by defining a threshold for the condition number and reject the lower singular values accordingly [3]. It is suggested that regularization is necessary for condition numbers value higher than 1000, regularization is recommended for condition numbers between 100 and 1000, and no regularization is needed for condition numbers lower than 100 [4]. With consideration of these criteria, S^* is therefore defined as:

$$S_{ii}^* = \begin{cases} \frac{1}{S_{ii}} & \text{if } S_{ii} > \frac{S_{11}}{100} \\ 0 & \text{else.} \end{cases}$$

4 Results and discussion

In this section, numerical results concerning the application of the Component TPA In-situ Method to the academic systems are presented. First, a comparison between two matrix inversion approaches: direct inversion and singular value rejection were applied. These two approaches are compared with the reference test which is a direct result of the finite element analysis.The figure 3 represents the velocities of a target point along the X, Y, and Z axes.
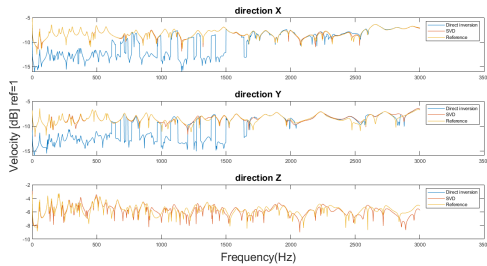

Figure 3: Comparison between SVD method and direct inversion.

The results show that the SVD method and direct inversion method are almost identical, especially along the Z direction which is dominant since the excitation is along the Z axis. This is due to the fact that the error in numerical simulations is limited. However, along the X and Y axes, the error is much higher since these directions are non-dominant. SVD is more accurate, especially for frequencies lower than 1500 Hz. Figure 4 presents the condition number of each matrix. Matrices of frequencies higher than 1500 have a condition number lower than 350. A Singular value rejection process is necessary for these matrices. The influence of the number and position of the used indicator points in the inversion matrix is discussed in what follows. For each path, 8 indicator points were selected, 4 in the neighborhood of
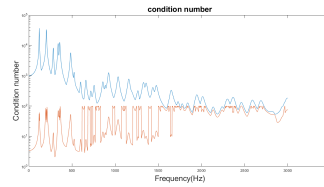

Figure 4: Condition number.

each path (orange color) and 4 farther away (yellow color), as shown in figure 5.

Figure 5: Indicator points

The average error with the reference test was established.

Table 2: Average error.

	neighborhood points	far points
1 per path	2.31e-3	2.40e-3
2 per path	1.80e-3	1.26e-3
3 per path	1.34e-3	9.47e-4
4 per path	1.26e-3	9.37e-4

As table 2 mentions, the more indicator points defined the less the average error gets. For practical cases, it is advised to use more than two indicator points per path. Two is sufficient in case of tight budgets and difficulties in mounting the measurement devices. In the case of using one indicator point per path, it is advised to define the points in the neighborhood of each path, and for the other cases, it is advised to define the points on the entirety of the contact surface.

5 Conclusions

This article investigated the accuracy of the Component TPA In-situ Method to predict the behaviour of an academic system. Various parameters were discussed to enhance the process of equivalent forces identification. The results show that it is advised to apply the singular value rejection process and to apply at least two indicators per path on the entirety of the contact surface.

References

[1] Maarten V van der Seijs, Dennis de Klerk, and Daniel J Rixen. General framework for transfer path analysis: History, theory and classification of techniques. *Mechanical Systems and Signal Processing*, 68:217–244, 2016.

[2] Wei Cheng, Yapeng Chu, Xuefeng Chen, Guanghui Zhou, Diane Blamaud, and Jingbai Lu. Operational transfer path analysis with crosstalk cancellation using independent component analysis. *Journal of Sound and Vibration*, 473:115224, 2020.

[3] Wei Cheng, Diane Blamaud, Yapeng Chu, Lei Meng, Jingbai Lu, and Wajid Ali Basit. Transfer path analysis and contribution evaluation using svd-and pca-based operational transfer path analysis. *Shock and Vibration*, 2020, 2020.

[4] Nicolas Bert Roozen, Quentin Leclere, and Céline Sandier. Operational transfer path analysis applied to a small gearbox test set-up. In *Acoustics 2012*, 2012.

Identification of Sources and Their Directivity in the Global Underwater Radiated Noise from a Merchant Ship

Hugo Catineau *[1], Pierre Cauchy [1], Olivier Robin [2], Cédric Gervaise[1, 3], Pierre Mercure-Boissonnault [1], Sylvain Lafrance [4] et Guillaume St-Onge [1]

[1] Institut des sciences de la mer de Rimouski (ISMER), Université du Québec à Rimouski, Rimouski, Canada.
[2] Université de Sherbrooke – Centre de Recherche Acoustique-Signal-Humain, Sherbrooke, Canada.
[3] Institut de recherche CHORUS, Grenoble, France.
[4] Innovation maritime, 53 Rue Saint Germain Ouest, Rimouski, Canada.

1   Introduction

Global marine traffic is intensifying and generates noise with potential adverse effects on marine species. Traffic noise indeed contributes to continuous anthropogenic noise, known to affect communication, echolocation and stress levels, impacting marine animal behaviour, social life and nutrition. To limit the effects of marine traffic on the environment, traffic noise must be reduced in the entire ocean. The current standard (ANSI/ASA S12/64-2009, [1]) models a ship's acoustic signature as a single, punctual and omnidirectional source. However, the noise sources under consideration, like engines and propellers, are actually spatially distributed over the ship's dimensions. This work aims to identify individual noise sources and establish their directivity pattern in order to better understand and model underwater noise radiated by ships.

The MARS (Marine Acoustic Research Station, https://www.projet-mars.ca/) is specifically designed to measure individual ships' acoustic signatures according to the current standard [1], including in its optimal configuration four vertical three-hydrophone arrays at 80 m, 173 m and 300 m. It is deployed in the St. Lawrence Estuary (Eastern Canada), in 350 m deep water, along the commercial shipping lane in order to have minimal impact on ships' route when their acoustic signature is measured.

2   Method

In this study, the same cargo/passenger ship was measured in the station with three passages with different speeds: 4.9 m.s^{-1} (9.5 knots), 7.1 m.s^{-1} (13.8 knots) and 7.4 m.s^{-1} (14.3 knots). The slowest ship speed was sampled on starboard, and the two other ship speeds were sampled on port side. The underwater radiated noise was sampled from different listening angles (Figure 2). From these three passages, azimuthal maps are built for specific frequency peaks to represent the underwater radiated noise and the variation of the source level on the listening angles. The directivity of the specific frequency peaks is shown by the azimuthal maps.

The acoustic signature (Figure 1) of a ship passing through the station is measured from the recorded noise of the ship, averaged on angles ranging from 60° to 120° (Figure 2) following the method presented in [2] . The ship is

considered as a punctual acoustic source. A propagation model is used to account for propagation loss and establish the emitted noise level at 1 m from the source (SL in dB *re* 1μPa^2 .Hz^{-1} .m^{-1}).
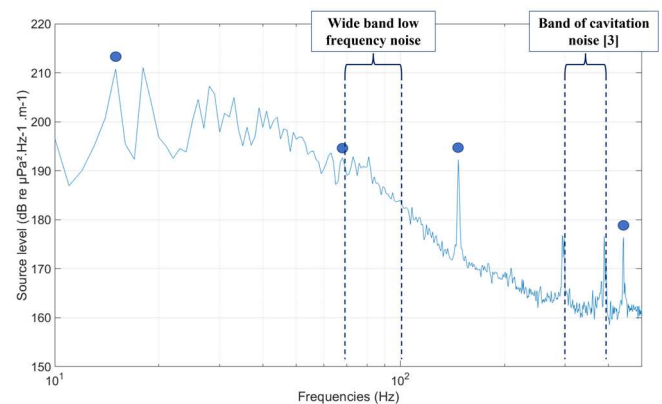

Figure 1 : 1 Hz resolution spectrum of the ship passage 14.3 knots). Blue points illustrate the chosen wide bands low frequency of cavitation noise.
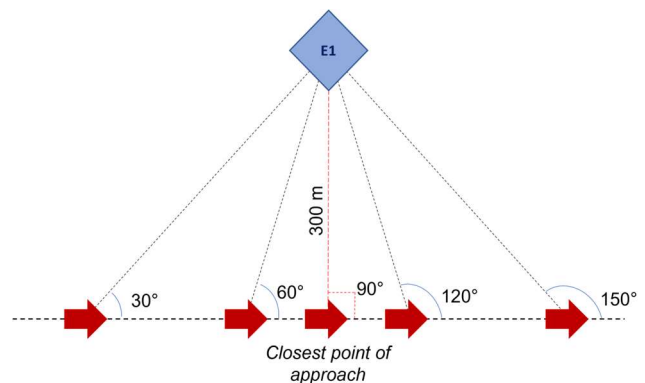

Figure 2 : Listening angle method of the passing ship in the MARS station. Red arrows illustrate the ship direction.

The source level narrow-band spectra (1 Hz resolution), created to establish the acoustic signature, is used here to analyse the frequency content of the underwater radiated noise (URN) and identify features such as frequency peaks corresponding to machinery and wide band low frequency noise typical of cavitation (Figure 1) [3]. For the frequency peaks of the machinery, noise level is averaged on a 10 Hz frequency band centered on peak frequency. For the wide band

*hugo.catineau@uqar.ca

low frequency noise, characterising cavitation noise, noise level is averaged on the 70 – 105 Hz and 340 – 360 Hz bands [3]. URN is measured from a wide range of angles, from 30° (bow) to 150 ° (stern) on port side (respectively 330° to 210° on starboard), as the ship passes through the station (Figure 2). Each identified frequency band of interest is then analysed individually. A directivity map is built, representing the emitted noise level for a varying emission angle (Figure 4).

3 Results

We analysed the noise emitted by the ship during the passage at 7.4 m.s^{-1} and recorded from the hydrophone located at 173 m depth. Analysis of two spectra of the emitted noise level at 30° and 150° makes it possible to identify frequency bands where differences between noise level radiated towards the bow and stern of the ship are slightly directive (Figure 3).
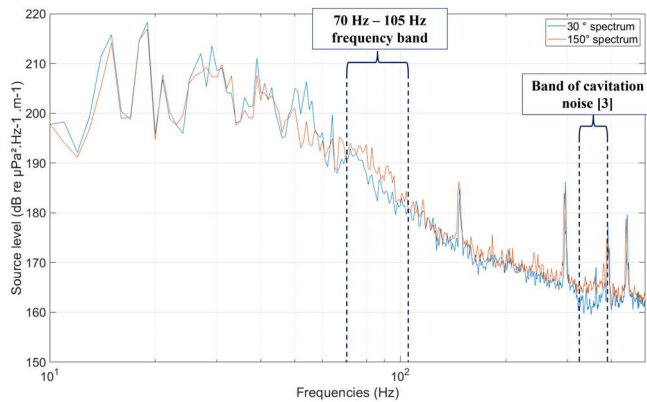

Figure 3 : 1 Hz resolution spectra of the source level (dB re 1μPa .Hz^{-1}.m^{-1}) emitted towards 30° and 150° for the passage at 7.4 m.s^{-1} (14.3 knots).

The 70 Hz – 105 Hz and the 340 Hz – 360 Hz bands in particular present a slightly offset. The corresponding wide bands noise has been identified in the literature as generated by cavitation of the propeller [3]. The directivity pattern (Figure 4) shows higher noise level emitted towards angles ranging from 90° to 140°. Such directivity pattern is consistent with the literature, noise radiated from the propeller area towards the front of the ship being masked by the hull.

Further analysis of this frequency band, using the remaining hydrophones of the antenna will be done, making it possible to complete the directivity pattern in the vertical dimension. Analysis of the noise emitted by the same ship during other passages at different speed and from both starboard and port side will allow to complete the directivity map. A catalogue of directivity patterns will be built for each identified frequency of interest, providing meaningful information to identify clusters of sounds based on their directivity and clues about their location and mechanical properties.

This method will be applied to the fleet being currently measured in the framework of the MARS project (34 vessels in 2021, ~150 per year expected in 2022 and 2023), representative of the merchant fleet. Knowledge of sources directi
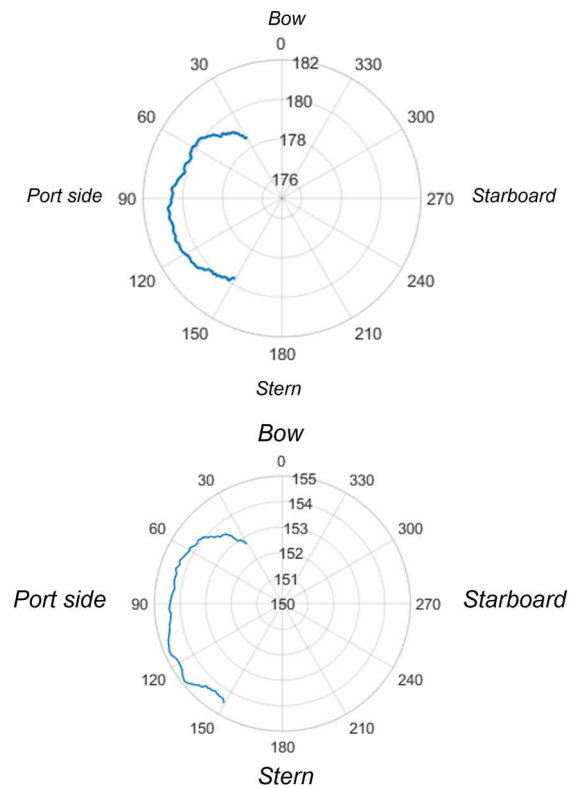

Figure 4 : Directivity patterns of the 70 Hz – 105 Hz and the 340 Hz – 360 Hz [3] frequency bands (dB re 1μPa² .Hz^{-1} m^{-1}) at 7.4 m.s^{-1} (14.3 knots).

-vity at various frequencies will allow the improvement of ships URN models and better assessment of the impact of shipping on the marine environment. Also, source directivity will improve the understanding of ship detection by cetaceans and therefore the prevention of collision risk.

Acknowledgments

References

[1] ANSI/ASA S12.64-2009/Part 1 (R2019). Quantities and procedures for description and measurement of underwater sound from ships - part 1: General requirements. 2019.

[2] Simard, Y., Roy, N., Gervaise, C., et Giard, S. Analysis and modeling of 255 source levels of merchant ships from an acoustic observatory along St. Lawrence Seaway. *J Acoust Soc Am*, 140:143, 2002-2018.

[3] P. T. Arveson et D. J. Vendittis. Radiated noise characteristics of a modern cargo ship. *J Acoust Soc Am*, 118:129, 2000.

Assessment of The Underwater Noise Levels from a Fishing Vessel Using Passive Acoustic Monitoring and Structure Hull Vibration

Khaled Mohsen Helal[*1] and **Lorenzo Moro**[†2]

[1]Dpt. of Mechanical Engineering, Memorial University of Newfoundland, St. John's, Newfoundland and Labrador, Canada
[2]Dpt. of Ocean and Naval Architectural Engineering, Memorial University of Newfoundland, St. John's, Newfoundland and Labrador, Canada

1 Introduction

Sound is crucial to the survival of several species of the marine ecosystem [1], and vessels' underwater radiated noise (URN) has been reported to have a broad range of detrimental impacts on aquatic life [2]. In fact, the ocean ambient noise is increasing at a rate of 0.5 dB/year at low-frequency ranges (100 Hz), according to a 2005 study conducted by Ross [3]. So far, researchers have mainly focused their studies on the source characterization of large commercial vessels, considered as the main sources of URN.

This paper presents the results of a study carried out to investigate the URN from a small fishing vessel operating in the Province of Newfoundland and Labrador, Canada. The objectives of the study were i) quantify the URN from the small fishing vessel at different operating conditions, ii) understand the contribution of the vessel's main acoustic sources—i.e. prime mover and propeller—to the overall URN, and iii) evaluate the monopole source levels (MSL) of the vessel.

2 Method

The experimental measurements were performed in August and December 2021 of the coast of Petty Harbour-Maddox, Newfoundland.

2.1 Fishing vessel specifications

The fishing vessel is 34 ft in length overall. It is powered by a fast six-cylinder four-stroke diesel engine coupled to a four-blade propeller through a gearbox (gear ratio 2.4).

2.2 Measurement procedure

We followed the relevant ISO 17208 series to perform the MSL measurements and assess the results uncertainties [4], and simultaneously performed onboard structure-borne noise tests to evaluate the engine's contribution to the overall URN. The trials were performed where the vessel and hydrophone array was 225 m apart, titled the closest point of approach (CPA).

The ship was tested at two operating conditions: i) straight-line route and constant advance speed at engine's maximum continuous rating (2200 rpm), ii) Propeller disengaged, and only engine was on where vessel located at the CPA. The background noise level was measured when the vessel was located 2 Km from the array, and the engine was turned off [4].

*kmhelal@mun.ca
†lmoro@mun.ca

2.3 Passive acoustic measurement

We used an array of three icListen HF omnidirectional hydrophones attached to a surface buoy associated with GPS and a ballast drop-weight made by Ocean Sonics. The recordings were sampled at a rate of 32 KS/s. The system was deployed at 47°27'14.28" N and 52°36' 7.5" W at depths of 32 m, 63 m, and 94 m from the sea surface and the ocean floor was 160 m deep.

The source sound levels were analyzed in one-third octave and narrow bands in the frequency range of 10 to 10 kHz. Firstly, the background noise levels (BNL) were used to adjust the received sound levels (RSL). Secondly, the vessel's monopole source levels were obtained per the simplified approach proposed by ISO 17208-2 and by developing a numerical propagation loss model for a more accurate assessment [5].

2.4 Structure-borne noise

Four uniaxial accelerometers made by PCB Piezotronics were mounted in the engine room. Data was collected via National instrument card and analyzed using Matlab in a frequency range 1 to 8 kHz. The structure-borne noise was correlated with the RSL by estimating magnitude-squared coherence function using Welch's method. The data was normalized to create a reasonable comparison between the two different parameters.

3 Results

Table 1 shows the broadband RSL before starting the trails.

Table 1: Broadband levels (dB re 1 uPa @ 1 m) of background noise levels before every sea trial in August and December.

Date	63 Hz	125 Hz	250 Hz	2/8 kHz	0.01/10 kHz
Aug	99.61	97.36	95.17	87.97	99.34
Dec	102.33	100.68	95.24	86.68	102.36

Figure 1 shows the MSL of the vessel at maximum engine speed for both trials. The overall MSLs estimated by the PL model and ISO 17208-2 were similar at frequencies below 125 Hz, in contrast to high levels at higher frequencies for the PL model.

The engine radiated noise levels higher than the BNL by 35 to 45 dB over the broadband at no propeller trail. The narrowband analysis of the structure-borne and underwater radiated noise illustrated a high coherence between the signals. The engine's frequencies were detected in the underwa-
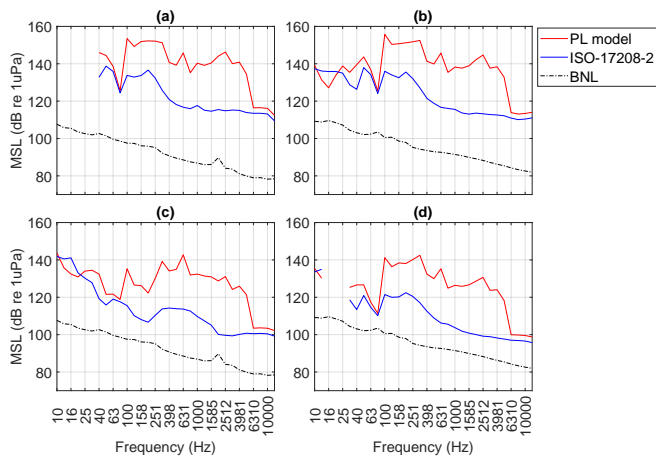
Figure 1: Monopole source levels estimated using ISO 17028-2 and propagation loss model. For August trial, (a) Vessel ran at 2200 rpm between two points and (c) No-propeller and engine on at 1400 rpm. For December trial, (b) Vessel ran at 2200 rpm and (d) No propeller trial at 1600 rpm

ter radiated noise measurements, as shown in Figure 2. The cylinder firing frequency divided by the 2.4 gear ratio demonstrates the single blade frequency equal 13.9 Hz, which dominates the underwater radiated noise. In comparison, the main contributor of the engine was the tonal frequency at 101.3 Hz, which corresponds to the engine firing frequency.
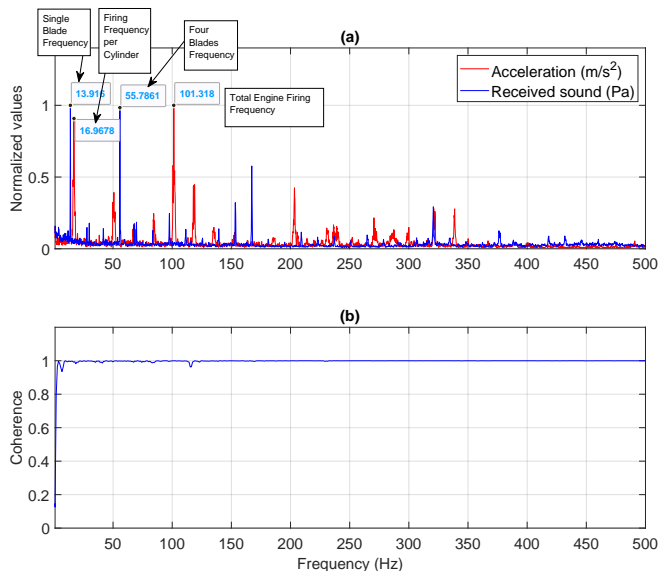

Figure 2: (a) Normalized PSD narrowband of received sound pressure and acceleration. (b) The coherence between both values

4   Discussion

BNL were high at frequencies below 80 Hz for both August and December trials. We can notice that there was no significant difference in the BNL measured at the two dates over the frequency range of interest.

The MSL is higher when using the propagation loss model, compared to the MSL calculated in accordance with the recommendation by the ISO 17208-2. The discrepancy

is evident at frequencies above 125 Hz, where the MSL is higher of more than 20 dB, when calculated using the propagation loss model. The ISO 17208-2 corrected equation added weight to the low frequencies to adjust the sea surface interference. On the other hand, the propagation loss model provided useful information about sound propagation at higher frequencies, showing that the ISO 17208-2 method underestimate the MSL in this range.

The no-propeller trials on both days showed the significant contribution of the internal engine to the overall radiated noise generated by the vessel. The engine radiated noise is 40 dB higher than the BNL. This contribution is confirmed by the outcomes of the narrow band analysis.

5   Conclusions

The results from these measurements show that the studied fishing vessel, which is a typical fishing vessel in the NL fleet, generates URN levels that are potentially dangerous for the ecosystem. In addition, our results show that onboard engines contribute to the overall URN at high frequencies. With regard to the MSL assessment, the current standard seems to estimate well the low frequencies, but underestimate higher frequencies. Further tests should be conducted to confirm this.

References

[1] Samara M. Haver, Holger Klinck, Sharon L. Nieukirk, Haru Matsumoto, Robert P. Dziak, and Jennifer L. Miksis-Olds. The not-so-silent world: Measuring arctic, equatorial, and antarctic soundscapes in the atlantic ocean. *Deep Sea Research Part I: Oceanographic Research Papers*, 122:95–104, 2017.

[2] Christine Erbe, Sarah A. Marley, Renée P. Schoeman, Joshua N. Smith, Leah E. Trigg, and Clare Beth Embling. The Effects of Ship Noise on Marine Mammals—A Review. *Frontiers in Marine Science*, 6(October), 2019.

[3] Donald Ross. Ship sources of ambient noise. *IEEE Journal of Oceanic Engineering*, 30(2):257–261, 2005.

[4] International Standard Organization - ISO 17208-1. Underwater acoustics — Quantities and procedures for description and measurement of underwater sound from ships — Part 1: Requirements for precision measurements in deep water used for comparison purposes, 2016.

[5] Michael A. Ainslie, S. Bruce Martin, Krista B. Trounce, David E. Hannay, Justin M. Eickmeier, Terry J. Deveau, Klaus Lucke, Alexander O. MacGillivray, Veronique Nolet, and Pablo Borys. International harmonization of procedures for measuring and analyzing of vessel underwater radiated noise. *Marine Pollution Bulletin*, 2022.

The MARS Project: Identifying and Reducing Underwater Noise from Ships in the St. Lawrence Estuary

Olivier Robin[*1]**, Pierre Cauchy**[2]**, Pierre Mercure-Boissonault**[2]**, Hugo Catineau**[2]**, Jeanne Mérindol**[2]**, Guillaume St Onge**[2]**, Cédric Gervaise**[3]**, Jean-Christophe Gauthier-Marquis**[4]**, Kamal Kesour**[4]**, Marie-Laurence Bazinet**[4]**, and Sylvain Lafrance**[4]

[1]Centre de Recherche Acoustique-Signal-Humain, Université de Sherbrooke, Sherbrooke (QC) J1K 2R1, Canada.
[2]Institut des sciences de la mer de Rimouski, Université du Québec à Rimouski, Rimouski (QC) G5L 3A1, Canada
[3]Institut de recherche CHORUS, 5 Rue Gallice, 38100 Grenoble, France
[4]Innovation Maritime, 53 Rue St Germain O, Rimouski (QC) G5L 4B4, Canada

1 Introduction

The Marine Acoustics Research Station (MARS) is an applied research project dedicated to understanding the underwater noise radiated by ships and proposing efficient methods or actions for its reduction. This project relies on the design and operation of world-class instrumentation deployed in the St. Lawrence Estuary, offshore of Rimouski (Québec, Canada). Two measurements systems are here developed and combined: the URNS station (Underwater Radiated Noise Signatures) and the OBAVSI system (On-Board Acoustic and Vibratory Sources Identification).

2 The URNS station

The URNS platform consists of four vertical arrays of three hydrophones. A picture and a schematic view are provided in upper and lower parts of Figure 1, respectively. The geometry of the arrays makes it possible to implement measurements in accordance with the ANSI/ASA S12/64-2009 standard [1] for precise and efficient measurement of radiated underwater noise. The four arrays are used to form two port / starboard measurement points, both separated by 8 km and moored closely to the two shipping lanes of the St. Lawrence off Rimouski. Each port / starboard measurement point includes two arrays separated by less than 1 km. Such configuration for acoustic signature measurements allows that (1) candidate ships are not required to significantly deviate from their routes, and (2) a ship's signature on both port and starboard is evaluated from a single passage.

The antennas are energy self-sufficient and can communicate their data in nearly real time. They are launched and recovered from ISMER-UQAR Coriolis II vessel, and typically operated from May to November. In addition to recording the candidate ship's signatures, they continuously acquire ambient noise created by all traffic, as well as geophony and biophony to provide a complete picture of the soundscape of the St. Lawrence Estuary. All the results obtained are compared to existing databases of St. Lawrence seaway [2].

3 The OBAVSI equipment

The OBAVSI equipment (On-Board Acoustics and Vibratory Source identification) consists of a set of tachometers, microphones and accelerometers deployed in parallel at strategic locations on ships to identify and rank vibroacoustic sources
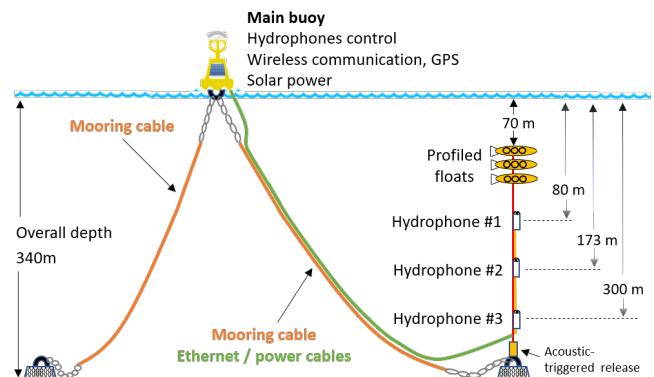

Figure 1: Upper part - A picture of one of the buoys before its deployment from ISMER Coriolis II vessel. Lower part - Description of the common configuration of each of the four individual buoys.

that contribute to underwater noise (that is mainly sources related to machinery and propulsion, including cavitation). A first part of the work is mostly dedicated to machinery noise (engines, gears), with the aim of identifying internal sources and paths of transmission from the sources to outside the ship. A second part of the network is focused on the detection of cavitation from an array of accelerometers positioned near the propeller but inside the ship. Indeed, the modulation at the blade passing is due to the variation of cavitation noise generated by each passing blade, and can be identified using techniques like Detection of Envelope Modulation On Noise (DEMON) [3]. To allow flexible and convenient measurements and data storage, a specific equipment has been designed and

*Presenter, on behalf of the whole team - olivier.robin@usherbrooke.ca

built (Figure 2). This system was designed to be operated very easily (a simple start/stop button), and can handle up to six Integrated Electronics Piezo-Electric (IEPE) sensors like accelerometers and microphones. It is based on a Raspberry Pi small single-board computer on which 3 two-channel data acquisition cards (Measurement Computing MCC 172) are stacked. This card features analog-to-digital 24-bit converters with a maximum sample rate of 51.2 kS/s/Ch. The calibration, acquisition and storage of signal is based on a Python[TM] code. Measurements are automatically stored for monitoring, which can last up to one month.
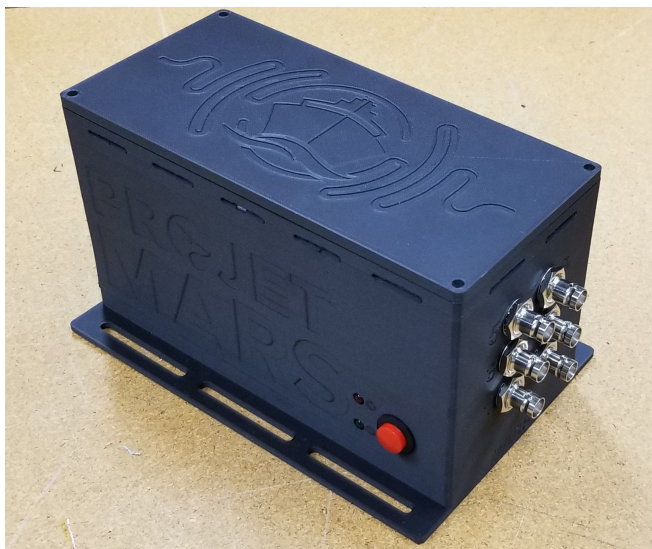

Figure 2: Picture of the current OBAVSI equipment, an autonomous 6-channel recorder.

4 An example of what brings URNS + OBAVSI

Figure 3 provides a typical example of how results can be gathered and compared. It is meant to be a general example, and therefore the investigated ship is kept anonymous. Using height and color codes, the level and contribution of vibration components to radiated noise are depicted in the upper part of Figure 3. The peak-normalized height of the peak is between 0 (minimum) and 1 (maximum) as compared with other measurement points. The color indicates if the contribution to radiated noise is limited, average or important. The upper part of Figure 3 has to be put into perspective with the mid part of Figure 3 (corresponding vibration power spectral density) and the lower part of Figure 3 (corresponding underwater noise power spectral density). The vibration and acoustic spectra are calculated for synchronized time frames.

It is apparent from Figure 3 that combining information taken onboard on ships and by the station makes it possible to link the most problematic underwater noises to their actual sources in ships (identification and ranking). The combination of URNS and OBAVSI ensures a quality diagnosis over a wide range of operating conditions, that can be varied when passing through the URNS station. Making informed decisions is eased, and so the most efficient noise mitigation actions can be proposed to each ship. This makes it possible

to adopt a pragmatic approach for the solutions proposed for noise reduction, and to maximize their environmental impact.
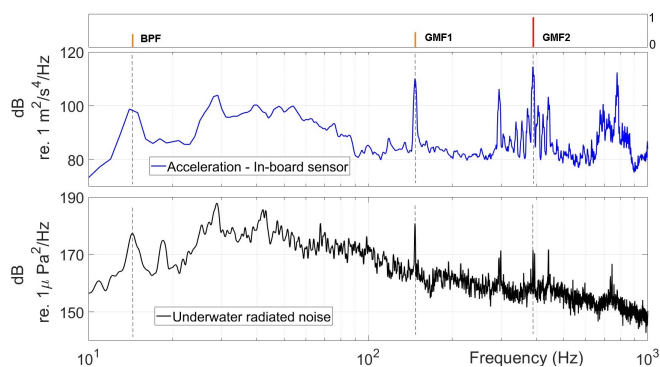

Figure 3: Example for an accelerometer located close to a ship's stern. Upper part - Importance and contribution of notable and identified frequencies (BPF: Blade passing frequency; GMF: Gear mesh frequency). Mid part - Onboard measurement result using OBAVSI, given in terms of acceleration power spectral density - Lower part - Measurement results for radiated underwater noise at URNS (spectra are calculated for the same time frame - the dotted black vertical lines identify the notable vibrational frequencies of the main sources on board).

5 Perspectives

This short paper presented the main components of the MARS project, a unique instrumentation system, that started in early 2021. While the project implementation has been slowed by the COVID pandemic, 38 signatures were measured for 34 participating ships during year 2021. The three main goals for the following years are to (1) enlarge the number of measured signatures (up to 150 per year), (2) improve post-processing of inboard and underwater measurements, and (3) propose optimal noise mitigation actions that could be taken on voluntary ships and to test before-and-after configurations.

References

[1] ANSI/ASA S12.64-2009/Part 1 (R2019). Quantities and procedures for description and measurement of underwater sound from ships - part 1: General requirements. 2019.

[2] Y. Simard et al. Analysis and modeling of 255 source levels of merchant ships from an acoustic observatory along st. lawrence seaway. *J Acoust Soc Am*, 140:2002–2018, 2016.

[3] Y. Gao et al. Automatic detection of underwater propeller signals using cyclostationarity analysis. *Mech Syst Signal Process*, 146:107032, 2021.

Identification Of The Dynamic Stiffnes Of Vibration Isolation Interfaces By Tpa Engineering Methods

Houssine Bakkali, Raef Cherif, Yacine Yaddaden

The transport manufacturing industry integrates a large number of systems that are responsible for tonal vibrations which propagate through the isolators and radiate structure-borne noise (SNB) into the cabin. These unwanted vibrations could be mitigated by improving the interfaces that connect the vibrating systems and the receiving structures. TPA methods are mainly used as troubleshooting tools to identify the origins of noise, vibration, and harshness (NVH) in vehicles. This paper presents a hybrid TPA method that allows for the in-situ characterisation of a mechanical vibration isolator whilst incorporated into an assembly, and therefore under representative mounting conditions. The studied academic system is representative of a ship's propulsion engines coupled through four isolators to an aluminum plate. The proposed method combines two TPA methods to determine the translational transfer stiffness components over a large frequency range without the need for any test rigs. The numerical results show a good agreement between the predicted translational transfer stiffness components and the reference one.Keywords Dynamic stiffness, Insitu, TPA, mechanical isolator, tonal vibration, structure-borne noise

Experimental Model To Predict Underwater Noise Produced By Structural Radiation

Jacopo Fragasso

Underwater noise radiated from marine vessel has become a primary cause of concern in the preservation of the ocean wildlife. Its impact on the marine fauna —primarily marine mammals— is well documented. Chronic exposure to anthropogenic underwater noise interferes with the animals' ability to perceive biologically important noises, used for communication and orientation, and causes temporary or permanent shifts in hearing threshold, psychological stress, and concerning behavioral responses. Commercial ships are one of the main sources of anthropogenic noise in the ocean, and there is a need for accurate models to control the sound radiation from marine vessels. To do this, it is crucial to estimate the contribution of each noise source on the overall noise levels that the ship produces. Generally, structural radiation from the ship hull has, along with noise originating from the propulsion system, a primary role in the vessel noise signature. Its contribution is especially notable in the case of low-power vessels, and ships moving at low speed. In this paper we present the experimental procedure we developed to represent sound transmission from the ship's prime mover to the surrounding underwater environment. We built a mock-up model of the engine foundation, and we tested its dynamic response to harmonic excitation using vibrational modal analysis. Then, we measured the noise levels produced by the mock-up structure suspended over a water tank. The experimental results were compared with the numerical solution produced by a Finite Element model, in order to estimate the dynamic properties of the mock-up structure and the water tank. We estimated a coefficient of sound radiation efficiency, that allows us to calculate the energy transmitted from the engine to the receiver in a broadband representation. Vibration transfer path analysis is used to estimate the dynamic behaviour of each component separately, and then combine their contributions together.

Influence Of Background Noise In Propeller Induced Noise Measurement In Atmospheric Towing Tank

Md Saiful Islam, Lorenzo Moro, Mohammed Islam

The growing threat that anthropogenic underwater noise poses to the ocean ecosystem worldwide has driven the development of new standards and guidelines to assess underwater radiated noise (URN) from marine vessels. These mainly focus on full-scale measurements to characterize ships as monopole or dipole sources or experimental model tests to understand the contribution of propeller cavitation to URN. Non-cavitating propellers are generally more silent than cavitating propellers, but given their increasing use in the maritime industry, it is important to develop procedures to characterize them acoustically. Tests on URN from non-cavitating propellers are performed in atmospheric towing tanks and the measurements of their URN require remarkably silent configurations. However, background noise in these complex facilities may affect the accuracy of the acoustic measurements. In this study, a set of model testing experiments were conducted in the atmospheric towing tank at the National Research Council Coastal and River Engineering Research Centre in St. John's, Canada. These tests aimed to assess and characterize the towing tank's background noise and its influence on URN measurements from

non-cavitating propellers. We performed resistance, self-propulsion, and bollard tests to estimate the contribution of hydrodynamic and propeller noise and compared the results against background noise measurements. Results show that the background noise generated by the towing carriage and drive system affects the URN measurements. The spectral analysis highlights its tonal components at different advanced speeds, while cross-spectral density (CSD) showed that there was no correlation among the sources. The structure used to support the hydrophones during hydrodynamics tests contribute to transmit the background noise, particularly at higher advanced speeds. This study highlights that special attention should be paid to the acoustic design of the towing carriage and hydrophones' supporting structure, while other sources in the facility should be kept quiet during tests.

Hybrid Model For Acoustic And Vibration Predictions Based On Vessel Induced Acoustic Vibration: A Review

SOLOMON OCHUKO OCHUKO OLOGE

Acoustic and vibration are basically induced in Vessels and ships due to complex installation of machineries and marine plant with adverse effect on crew members and aquatic lives. The demand to protect the aquatic lives has become necessary based on the fact that, if urgent step is not taken, it could lead to complete extinction of some marine species. In the past, there are a lot of studies done and some are currently going on in the development of models for estimation and prediction of acoustic and vibrations level in vessels and its environment. These model shows various applicability and limitations. This work review the most relevant prediction methods with regards to their level of engineering sustainability and applicability. This work also reveals that not all models are sustainable due to their limitation and applicability based on their level of accuracy, however, a hybrid of these various techniques is encouraged for greater efficiency.

Realistic Corrections For Ship Source Levels Measured At Canadian Acoustic Ranges

Cristina Tollefsen

The Royal Canadian Navy (RCN) operates two ranges for ship acoustic signature measurement: Ferguson's Cove in Halifax Harbour, Nova Scotia, and Patricia (Pat) Bay in Saanich Inlet, British Columbia. In recent years, there has been increased interest in using measurements from Canadian and allied acoustic ranges to estimate ship source levels. Current practice in ship source level measurement applies a correction for spherical spreading between the ship and the receiver, and the source level is calculated using the measured level in each 1-Hz frequency bin when the ship is at its closest point of approach (CPA). No correction is made for dependence on frequency, sound speed profile, or bottom depth and composition. An acoustic modelling study was carried out for the two Canadian ranges in order to understand the limitations of the spherical spreading correction. Spherical spreading was compared with modelled transmission loss from three acoustic models, for frequencies between 10 Hz – 1000 Hz: a normal mode model, a wavenumber integration model, and a parabolic equation model. The effects of realistic environmental parameters as well as averaging technique were evaluated. At Ferguson's Cove, the spherical spreading correction was 5-17 dB too low (f < 100 Hz), approximately correct at 100 Hz, and within 1-5 dB of the model (f > 100 Hz). At Pat Bay the spherical spreading correction was 2-15 dB too high for all frequencies modelled. Seasonal effects were frequency-dependent and added another 1-5 dB variation. Combining a simple model of ship movement with typical averaging assumptions resulted in source levels that were 0.5-11.5 dB too high, depending on frequency and location. It is therefore recommended that a simple, easy-to-use interface to an acoustic model be built in order to calculate corrections specific to local conditions each time a ship is ranged. This work was supported by Cooperative Research Ships.

ACOUSTICS WEEK IN CANADA

MONTRÉAL, QUÉBEC, OCTOBER 3-6, 2023

The **Acoustics Week in Canada will be held from October 3-6, 2023** in downtown Montreal, Quebec. You are invited to be part of this three days conference featuring the latest developments in Canadian acoustics and vibration. The keynote talks and technical sessions will be framed by a welcome reception, conference banquet, ASTM Building Acoustics Standards Committee meeting, technical tour and an exhibition of products and services relating to the field of acoustics and vibration.

Take a few days before or after the conference to enjoy the area! Quebec is famous for its fall colours, when trees all over the place turn bright shades of red, orange, and yellow before losing their leaves. It's an annual spectacle that draws tourists from around the world and remains impressive even to those of us who see it every year! Montreal still has important events to offer at this time of year such as the OFF Jazz Festival and the Festival du nouveau cinema.

Montréal's congress center

Venue and Accommodation

The conference will be held at Westin Hotels and Resorts in Montreal. A block of rooms in the hotel is available at a special conference rate of $279 per night for reservations made under "AWC2023 conference" codename. Extend your stay and enjoy the local area at the same special rate. Guests have free access to the large WestinWORKOUT® Fitness Studio and the indoor pool. Please refer to the conference website for further registration details: https://awc.caa-aca.ca

Jacques Cartier's Bridge

Plenary, technical sessions.

Plenary, technical, and workshop sessions are planned throughout the conference. Each day will begin with a keynote talk of broader interest and relevance to the acoustics community. Technical sessions are planned to cover all areas of acoustics including:

Montréal Downtown

AEROACOUSTICS / ARCHITECTURAL AND BUILDING ACOUSTICS / BIO-ACOUSTICS AND BIOMEDICAL ACOUSTICS / MUSICAL ACOUSTICS / NOISE AND NOISE CONTROL / PHYSICAL ACOUSTICS / PSYCHO- AND PHYSIO-ACOUSTICS / SHOCK AND VIBRATION / SIGNAL PROCESSING / SPEECH SCIENCES AND HEARING SCIENCES / STANDARDS AND GUIDELINES IN ACOUSTICS / ULTRASONICS / UNDERWATER ACOUSTICS

Abstracts

Abstract for technical papers are due before June 15, 2023 through the conference web site. Two-page summaries for publication in the proceedings are due August 1st, 2023. If you would like to organize a session on a specific topic please contact the Technical Chair as soon as possible.

Exhibition and sponsorship.

The conference offers opportunities for suppliers of products and services to engage the acoustic community through exhibition and sponsorship.

The tabletop exhibition facilitates in-person and hands-on interaction between suppliers and interested individuals. Companies and organizations that are interested in participating in the exhibition should contact the Exhibition and Sponsorship coordinator for an information package. Exhibitors are encouraged to book early for best selection.

The conference will be offering sponsorship opportunities of various conference features. In addition to the platinum, gold and silver levels, selected technical sessions, social events and coffee breaks will be available for sponsorship. Sponsors can have their logo placed on the conference web site within 10 days of their sponsorship. Additional features and benefits of sponsorship can be obtained from the Exhibition and Sponsorship coordinator or the conference web site.

Students.

Students are strongly encouraged to participate. Students presenting papers will be eligible for one of three $500 prizes to be awarded. Conference bursaries will also be available to those students whose papers are accepted for presentation.

Registration details.

Please refer to the conference web site: https://awc.caa-aca.ca

Contacts.

Conference Chair:

Pr. Olivier Doutres (ÉTS)
(conference@caa-aca.ca)

Technical Chair:

Pr. Thomas Padois (ÉTS)
(technical-chair@caa-aca.ca)

Exhibits and Sponsorship coordinator:

Mr. Julien Biboud (MÉCANUM)
(awc2023exhibitors@caa-aca.ca)

Semaine Canadienne de l'Acoustique

Montréal, Québec, 3-6 Octobre 2023

La Semaine Canadienne de l'acoustique aura lieu du 3 au 6 octobre 2023 au centre-ville de Montréal, au Québec. Vous êtes invités à assister à cette conférence de trois jours durant laquelle les derniers développements en matière d'acoustique et de vibration au Canada seront présentés. Chaque journée débutera par une conférence plénière qui sera suivie de sessions thématiques. Vous pourrez échanger lors de la réception de bienvenue et du banquet. Une réunion du comité des normes d'acoustique du bâtiment de l'ASTM sera également organisée ainsi qu'une visite technique et une exposition de produits et services liés à l'acoustique et à la vibration.

Prenez quelques jours avant ou après la conférence pour profiter de la région! Le Québec est célèbre pour ses couleurs d'automne, lorsque les arbres prennent des teintes vives de rouge, d'orange et de jaune avant de perdre leurs feuilles. C'est un spectacle annuel qui attire des touristes du monde entier et qui reste impressionnant même pour ceux d'entre nous qui le voient chaque année ! Montréal garde aussi quelques évènements de marque à cette période de l'année comme l'OFF Festival de Jazz et le Festival du nouveau cinéma.

Palais des congrès de Montréal

Lieu et hébergement

La conférence se déroulera à l'hôtel Westin Hotels and Resorts dans le centre-ville de Montréal. Des chambres sont disponibles au tarif spécial de $279 par nuit, pour les réservations faites sous le nom "AWC2023 conference". Prolonger votre séjour à l'hôtel au même tarif afin de profiter du centre-ville et de la région. Vous pourrez accéder gratuitement au centre de fitness WestinWORKOUT® Fitness Studio et à la piscine intérieure. Veuillez consulter le site web de la conférence pour plus d'informations sur l'inscription : https://awc.caa-aca.ca

Pont Jacques Cartier

Centre ville de Montréal

Sessions plénières et techniques

Des sessions plénières, techniques et des ateliers sont prévues tout au long de la conférence. Chaque journée débutera par une conférence plénière d'intérêt pour la communauté de l'acoustique. Des sessions techniques sont également prévues pour couvrir tous les domaines de l'acoustique, à savoir

AÉROACOUSTIQUE / ACOUSTIQUE DU BÂTIMENT ET ARCHITECTURALE / BIOACOUSTIQUE / ACOUSTIQUE BIOMÉDICALE / ACOUSTIQUE MUSICALE / BRUIT ET CONTRÔLE DU BRUIT / ACOUSTIQUE PHYSIQUE / PSYCHOACOUSTIQUE / CHOCS ET VIBRATIONS / LINGUISTIQUE / AUDIOLOGIE / ULTRASONS / ACOUSTIQUE SOUS-MARINE / NORMES EN ACOUSTIQUE

Résumés

Les **résumés des articles doivent être soumis au plus tard le 15 juin 2023** sur le site Web de la conférence. Les articles de deux pages, à soumettre le 1er août 2023, seront publiés dans les actes de la conférence. Si vous désirez organiser une session sur un sujet précis, veuillez communiquer avec le président technique le plus tôt possible.

Exposition et parainage

La conférence offre aux entreprises fournissant des produits et des services la possibilité de s'engager auprès de la communauté acoustique par le biais d'expositions et de parrainages.

L'exposition des produits et services facilite l'interaction entre les vendeurs et les personnes intéressées. Les entreprises et les organisations souhaitant participer à l'exposition doivent contacter le coordinateur de l'exposition et du parrainage pour obtenir de plus amples informations. Les exposants sont encouragés à réserver le plus tôt possible pour bénéficier des meilleures places.

La conférence offrira des possibilités de parrainage. En plus des niveaux platine, or et argent, certaines sessions techniques, événements sociaux et pauses café pourront être sponsorisées. Les sponsors peuvent ajouter leur logo sur le site web de la conférence dans les 10 jours suivant leur parrainage. D'autres informations et avantages du parrainage peuvent être obtenus auprès du coordinateur des expositions et du parrainage ou sur le site web de la conférence.

Étudiant·e·s

Les étudiant·e·s sont vivement encouragé·e·s à participer à la conférence. Les étudiant·e·s présentant un article seront éligibles pour obtenir un des trois prix de $500 à décerner. Des bourses de participation seront également offertes aux étudiant·e·s dont les communications sont acceptées pour présentation.

Inscription

Pour plus d'informations sur l'inscription, veuillez consulter le site Web de la conférence. https://awc.caa-aca.ca

Contacts.

Président de la conférence:

Pr. Olivier Doutres (ÉTS)
(conference@caa-aca.ca)

Président technique:

Pr. Thomas Padois (ÉTS)
(technical-chair@caa-aca.ca)

Coordonateur des expositions et du parrainage:

Mr. Julien Biboud (MÉCANUM)
(awc2023exhibitors@caa-aca.ca)

CANADIAN ACOUSTICS ANNOUNCEMENTS - ANNONCES TÉLÉGRAPHIQUES DE L'ACOUSTIQUE CANADIENNE

Looking for a job in Acoustics?

There are many job offers listed on the website of the Canadian Acoustical Association!

You can see them online, under http://www.caa-aca.ca/jobs/

August 5th 2015

Acoustic Training in Canada Database: Help us to help the younger generation and seasoned professionals

CAA is building a comprehensive list of all training programs offered in acoustics in Canada and we need your help! Below is a survey to help us populate that database that will eventually be available on CAA website. Please return all valuable input at your earliest convenience to Mr. DeGagne (wdegagne@caa-aca.ca)!

Dear CAA members, past members and friends, The purpose of this survey is to develop an online database of all the professional, undergraduate, and graduate acoustical courses and training programs offered through universities, colleges, associations, etc. This database would benefit the entire Canadian acoustic community in the following manner: 1. Track the different acoustical courses and training programs offered nationally 2. Allow CAA members to plan their acoustical training and easily select their perfect training program to meet their career aspirations 3. Allow CAA members to compare and contrast courses and training programs from different institutions 4. Allow institutions and the CAA to determine where the training gaps are and to plan for future programs demands To help us populate this database, simply return the following information at your earliest convenience to Mr. William DeGagne (wdegagne@caa-aca.ca), volunteer for CAA: 1. Place of the Course or Training program (university, colleges, etc.): 2. Name of Course or Training program: 3. Approx. date the Course or Training was followed: 4. Level (graduate, undergraduate, college course or professional training program, etc.): 5. Brief description of the Course or Training program: 6. Webpage of Course or Training program: 7. Location of Course or Training program (City, Province): 8. Course or Training program language: Thanks for you help towards the younger generation and seasoned professionals! :-)

May 31st 2021

Acoustics Week in Canada 2022 (AWC22): Call for abstracts

Acoustics Week in Canada is happening in-person in St. John's, Newfoundland and Labrador from September 27-30 2022. The conference will take place at the Sheraton Hotel Newfoundland, and is being hosted by Dr. Len Zedel and Dr. Ben Zendel from Memorial University of Newfoundland. Submissions related to any aspect of acoustics are welcome until June 30th 2022 at https://awc.caa-aca.ca

Acoustics researchers, professionals, educators, and students are welcomed to St. John's for three days of plenary lectures and technical sessions from September 27-30 2022. The Canadian Acoustical Association Annual General Meeting will be held in conjunction with the conference, along the conference reception, the conference banquet (held at the provincial museum: The Rooms), and an exhibition of acoustical equipment and services. Participants will be able to take an acoustics tour of a ship in St. John's harbour, and a tour of the acoustics facilities at Memorial University. The conference will include a Harbour Symphony, where the music is made by the horns on ships in St. John's Harbour. And of course, participants will get to experience the hospitality and old world charm of downtown St. John's. We hope you will join us for Acoustics Week in Canada 2022 in St. John's Newfoundland and Labrador! Abstract submissions are open until June 30th 2022, and registrations will open soon. Submissions related to any aspect of acoustics are welcome. For more information, visit https://awc.caa-aca.ca or contact the organizers at conference@caa-aca.ca

June 4th 2022

Acoustics Week in Canada 2022 (AWC22): Call for abstracts

Acoustics Week in Canada is happening in-person in St. John's, Newfoundland and Labrador from September 27-30

2022. The conference will take place at the Sheraton Hotel Newfoundland, and is being hosted by Dr. Len Zedel and Dr. Ben Zendel from Memorial University of Newfoundland. Submissions related to any aspect of acoustics are welcome until June 30th 2022 at https://awc.caa-aca.ca

Acoustics researchers, professionals, educators, and students are welcomed to St. John's for three days of plenary lectures and technical sessions from September 27-30 2022. The Canadian Acoustical Association Annual General Meeting will be held in conjunction with the conference, along the conference reception, the conference banquet (held at the provincial museum: The Rooms), and an exhibition of acoustical equipment and services. Participants will be able to take an acoustics tour of a ship in St. John's harbour, and a tour of the acoustics facilities at Memorial University. The conference will include a Harbour Symphony, where the music is made by the horns on ships in St. John's Harbour. And of course, participants will get to experience the hospitality and old world charm of downtown St. John's. We hope you will join us for Acoustics Week in Canada 2022 in St. John's Newfoundland and Labrador! Abstract submissions are open until June 30th 2022, and registrations will open soon. Submissions related to any aspect of acoustics are welcome. For more information, visit https://awc.caa-aca.ca or contact the organizers at conference@caa-aca.ca

June 4th 2022

Acoustics Week in Canada 2022 (AWC22): Call for abstracts extended to July 15th!

Acoustics Week in Canada is happening in-person in St. John's, Newfoundland and Labrador from September 27-30 2022. The conference will take place at the Sheraton Hotel Newfoundland, and is being hosted by Dr. Len Zedel and Dr. Ben Zendel from Memorial University of Newfoundland. Submissions related to any aspect of acoustics are welcome now until July 15th 2022 at https://awc.caa-aca.ca

Please note that all authors will have to submit their 2-page article and pay their registration fees by August 1st (hard deadline) in order to have their proceedings paper published in the September issue of Canadian Acoustics (https://jcaa.caa-aca.ca). The authors are encouraged to use the available Microsoft™ Word or Latex templates. For more information, visit https://awc.caa-aca.ca or contact the organizers at conference@caa-aca.ca

July 6th 2022

INTER-NOISE 2023 to be held August 20-23, 2023, in Makuhari Messe (Japan)

We are very pleased to inform you that the website of INTER-NOISE 2023 has been launched. Its link is https://internoise2023.org/.

The INTER-NOISE 2023 is held at Makuhari Messe (https://www.m-messe.co.jp/en/) from August 20-23, 2023, which is sponsored by International Institute of Noise Control Engineering (I-INCE) and is co-organized by Institute of Noise Control Engineering of Japan (INCE/J), Acoustical Society of Japan (ASJ).

August 12th 2022

À la recherche d'un emploi en acoustique ?

De nombreuses offre d'emploi sont affichées sur le site de l'Association canadienne d'acoustique !

Vous pouvez les consulter en ligne à l'adresse http://www.caa-aca.ca/jobs/

August 5th 2015

Répertoire des formations en acoustique au Canada : aidez-nous à aider la jeune génération et nos professionels d'expérience

L'ACA est en train de dresser une liste complète de tous les programmes de formation offerts en acoustique au Canada et nous avons besoin de votre aide ! Vous trouverez ci-dessous un sondage qui nous aidera à alimenter cette base de données qui sera éventuellement disponible sur le site Web de la CAA. Veuillez retourner vos précieux commentaires à M. DeGagne (wdegagne@caa-aca.ca) dans les plus brefs délais !

Chers membres, anciens membres et amis de l'ACA, Le but de cette enquête est de développer une base de données en ligne de tous les cours et programmes de formation en acoustique professionnels, de premier et de deuxième cycle, offerts par les universités, les collèges, les associations, etc. Cette base de données profiterait à l'ensemble de la communauté acoustique canadienne de la manière suivante : 1. Suivre les différents cours et programmes

de formation en acoustique offerts à l'échelle nationale. 2. Permettre aux membres de l'ACA de planifier leur formation en acoustique et de choisir facilement le programme de formation idéal pour répondre à leurs aspirations professionnelles. 3. Permettre aux membres de l'ACA de comparer et d'opposer les cours et les programmes de formation de différentes institutions. 4. Permettre aux institutions et à l'ACA de déterminer où se trouvent les lacunes en matière de formation et de planifier les demandes de programmes futurs. Pour nous aider à alimenter cette base de données, il vous suffit de retourner les informations suivantes dans les meilleurs délais à M. William DeGagne (wdegagne@caa-aca.ca), bénévole pour l'ACA : 1. Lieu du cours ou du programme de formation (université, collèges, etc.) : 2. Nom du cours ou du programme de formation : 3. Date approximative à laquelle le cours ou la formation a été suivi. 4 : 4. Niveau (études supérieures, premier cycle, cours collégial ou programme de formation professionnelle, etc :) 5. Brève description du cours ou du programme de formation : 6. Page web du cours ou du programme de formation : 7. Lieu du cours ou du programme de formation (ville, province) : 8. Langue du cours ou du programme de formation : Merci pour votre aide à l'intention de la jeune génération et de nos professionels d'expérience ! :-)

May 31st 2021

Semaine canadienne de l'acoustique (AWC22): Appel à résumés

La Semaine canadienne de l'acoustique se déroulera en personne à St. John's, Terre-Neuve-et-Labrador, du 27 au 30 septembre 2022. La conférence aura lieu au Sheraton Hotel Newfoundland et sera organisée par le Dr Len Zedel et le Dr Ben Zendel de l'Université Memorial de Terre-Neuve. Les soumissions relatives à tout aspect de l'acoustique sont les bienvenues jusqu'au 30 juin 2022 à l'adresse https://awc.caa-aca.ca

Les chercheurs, professionnels, éducateurs et étudiants en acoustique sont les bienvenus à St. John's pour trois jours de conférences plénières et de sessions techniques du 27 au 30 septembre 2022. L'assemblée générale annuelle de l'Association canadienne d'acoustique aura lieu en même temps que la conférence, ainsi que la réception de la conférence, le banquet de la conférence (qui se tiendra au musée provincial : The Rooms) et une exposition d'équipements et de services acoustiques. Les participants pourront faire une visite acoustique d'un navire dans le port de St. John's, et une visite des installations acoustiques de l'Université Memorial. La conférence comprendra une symphonie portuaire, au cours de laquelle la musique sera jouée par les sirènes des navires dans le port de St. John's. Et bien sûr, les participants auront l'occasion de découvrir l'hospitalité et le charme du vieux monde du centre-ville de St. John's. Nous espérons que vous vous joindrez à nous pour la Semaine canadienne de l'acoustique 2022 à St. John's, Terre-Neuve et Labrador ! Les soumissions de résumés sont ouvertes jusqu'au 30 juin 2022, et les inscriptions seront bientôt ouvertes. Les soumissions liées à tous les domaines de l'acoustique sont les bienvenues. Pour plus d'informations, visitez https://awc.caa-aca.ca ou contactez les organisateurs à conference@caa-aca.ca .

June 4th 2022

Semaine canadienne de l'acoustique (AWC22): Appel à résumés

La Semaine canadienne de l'acoustique se déroulera en personne à St. John's, Terre-Neuve-et-Labrador, du 27 au 30 septembre 2022. La conférence aura lieu au Sheraton Hotel Newfoundland et sera organisée par le Dr Len Zedel et le Dr Ben Zendel de l'Université Memorial de Terre-Neuve. Les soumissions relatives à tout aspect de l'acoustique sont les bienvenues jusqu'au 30 juin 2022 à l'adresse https://awc.caa-aca.ca

Les chercheurs, professionnels, éducateurs et étudiants en acoustique sont les bienvenus à St. John's pour trois jours de conférences plénières et de sessions techniques du 27 au 30 septembre 2022. L'assemblée générale annuelle de l'Association canadienne d'acoustique aura lieu en même temps que la conférence, ainsi que la réception de la conférence, le banquet de la conférence (qui se tiendra au musée provincial : The Rooms) et une exposition d'équipements et de services acoustiques. Les participants pourront faire une visite acoustique d'un navire dans le port de St. John's, et une visite des installations acoustiques de l'Université Memorial. La conférence comprendra une symphonie portuaire, au cours de laquelle la musique sera jouée par les sirènes des navires dans le port de St. John's. Et bien sûr, les participants auront l'occasion de découvrir l'hospitalité et le charme du vieux monde du centre-ville de St. John's. Nous espérons que vous vous joindrez à nous pour la Semaine canadienne de l'acoustique 2022 à St. John's, Terre-Neuve et Labrador ! Les soumissions de résumés sont ouvertes jusqu'au 30 juin 2022, et les inscriptions seront bientôt ouvertes. Les soumissions liées à tous les domaines de l'acoustique sont les bienvenues. Pour plus d'informations, visitez https://awc.caa-aca.ca ou contactez les organisateurs à conference@caa-aca.ca .
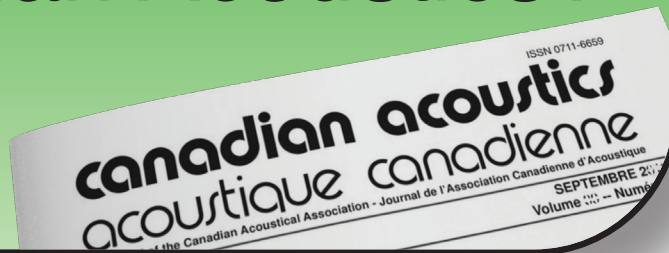
June 4th 2022

Semaine canadienne de l'acoustique (AWC22): Appel à résumés reporté au 15 juillet!

La Semaine canadienne de l'acoustique se déroulera en personne à St. John's, Terre-Neuve-et-Labrador, du 27 au 30 septembre 2022. La conférence aura lieu au Sheraton Hotel Newfoundland et sera organisée par le Dr Len Zedel et le Dr Ben Zendel de l'Université Memorial de Terre-Neuve. Les soumissions de résumés sont ouvertes jusqu'au 15 juillet 2022 sur le site https://awc.caa-aca.ca.

Veuillez noter que tous les auteurs devront soumettre leur article de 2 pages et payer leurs frais d'inscription avant le 1er août (date limite immuable) afin que leur article soit publié dans le numéro de septembre de Canadian Acoustics (https://jcaa.caa-aca.ca). Les auteurs sont encouragés à utiliser les gabarits Microsoft™ Word ou LaTex disponibles. Pour plus d'informations, visitez https://awc.caa-aca.ca ou contactez les organisateurs à conference@caa-aca.ca .

July 6th 2022

Canadian Acoustical Association
Association canadienne d'acoustique

CAA
ACA

Application for Membership

CAA membership is open to all individuals who have an interest in acoustics. Annual dues total $120.00 for individual members and $50.00 for student members. This includes a subscription to *Canadian Acoustics*, the journal of the Association, which is published 4 times/year, and voting privileges at the Annual General Meeting.

Subscriptions to *Canadian Acoustics* *or* Sustaining Subscriptions

Subscriptions to *Canadian Acoustics* are available to companies and institutions at a cost of $120.00 per year. Many organizations choose to become benefactors of the CAA by contributing as Sustaining Subscribers, paying $475.00 per year (no voting privileges at AGM). The list of Sustaining Subscribers is published in each issue of *Canadian Acoustics* and on the CAA website.

Please note that online payments will be accepted at http://jcaa.caa-aca.ca

Address for subscription / membership correspondence:

Name / Organization _____

Address _____

City/Province _____ Postal Code _____ Country _____

Phone _____ Fax _____ E-mail _____

Address for mailing Canadian Acoustics, if different from above:

Name / Organization _____

Address _____

City/Province _____ Postal Code _____ Country _____

Areas of Interest: (Please mark 3 maximum)

1. Architectural Acoustics
2. Engineering Acoustics / Noise Control
3. Physical Acoustics / Ultrasound
4. Musical Acoustics / Electro-acoustics

5. Psychological / Physiological Acoustic
6. Shock and Vibration
7. Hearing Sciences
8. Speech Sciences

9. Underwater Acoustics
10. Signal Processing / Numerical Methods
11. Other

For student membership, please also provide:

_____ _____ _____

(University) (Faculty Member) (Signature of Faculty Member) (Date)

I have enclosed the indicated payment for:
[ ] CAA Membership $ 120.00
[ ] CAA Student Membership $ 50.00

Corporate Subscriptions (4 issues/yr)
[ ] $120 including mailing in Canada
[ ] $128 including mailing to USA,
[ ] $135 including International mailing

[ ] Sustaining Subscription $475.00
  (4 issues/yr)

Please note that the preferred method of payment is by credit card, online at http://jcaa.caa-aca.ca

For individuals or organizations wishing to pay by check, please register online at *http://jcaa.caa-aca.ca* and then mail your check to:

Executive Secretary, Canadian Acoustical:
Dr. Roberto Racca
c/o JASCO Applied Sciences
2305–4464 Markham Street
Victoria, BC V8Z 7X8 Canada

Association Canadienne d'Acoustique
Canadian Acoustical Association

CAA
ACA

Formulaire d'adhésion

L'adhésion à l'ACA est ouverte à tous ceux qui s'intéressent à l'acoustique. La cotisation annuelle est de 120.00$ pour les membres individuels, et de 50.00$ pour les étudiants. Tous les membres reçoivent *l'Acoustique Canadienne*, la revue de l'association.

Abonnement pour la revue *Acoustique Canadienne* et abonnement de soutien

Les abonnements pour la revue *Acoustique Canadienne* sont disponibles pour les compagnies et autres établissements au coût annuel de 120.00$. Des compagnies et établissements préfèrent souvent la cotisation de membre bienfaiteur, de 475.00$ par année, pour assister financièrement l'ACA. La liste des membres bienfaiteurs est publiée dans chaque issue de la revue *Acoustique Canadienne*..

Notez que tous les paiements électroniques sont acceptés en ligne http://jcaa.caa-aca.ca

Pour correspondance administrative et financière:

Nom / Organisation _____

Adresse _____

Ville/Province _____ Code postal_____Pays _____

Téléphone _____ Téléc. _____Courriel _____

Adresse postale pour la revue Acoustique Canadienne

Nom / Organisation _____

Adresse _____

Ville/Province _____ Code postal_____Pays _____

Cocher vos champs d'intérêt: (maximum 3)

1. Acoustique architecturale
2. Génie acoustique / Contrôle du bruit
3. Acoustique physique / Ultrasons
4. Acoustique musicale / Électro-acoustique

5. Physio / Psycho-acoustique
6. Chocs et vibrations
7. Audition
8. Parole

9. Acoustique sous-marine
10. Traitement des signaux /Méthodes numériques
11. Autre

Prière de remplir pour les étudiants et étudiantes:

_____ _____ _____ _____ _____

(Université) (Nom d'un membre du corps professoral) (Signature du membre du corps professoral) (Date)

Cocher la case appropriée:
[ ] Membre individuel 120.00 $
[ ] Membre étudiant(e) 50.00 $
Abonnement institutionnel
[ ] 120 $ à l'intérieur du Canada
[ ] 128 $ vers les États-Unis
[ ] 135 $ tout autre envoi international
[ ] Abonnement de soutien 475.00 $
  (comprend l'abonnement à *L'acoustique Canadienne*)

Merci de noter que le moyen de paiement privilégie est le paiement par carte crédit en ligne à *http://jcaa.caa-aca.ca*

Pour les individus ou les organisations qui préféreraient payer par chèque, l'inscription se fait en ligne à *http://jcaa.caa-aca.ca* puis le chèque peut être envoyé à :

Secrétaire exécutif, Association canadienne d'acoustique :
Dr. Roberto Racca
c/o JASCO Applied Sciences
2305–4464 Markham Street
Victoria, BC V8Z 7X8 Canada

Canadian Acoustical Association
Association canadienne d'acoustique

Board of Directors - Conseil d'administration

OFFICERS - OFFICIERS

President
Président

Jérémie Voix
ÉTS, Université du Québec
president@caa-aca.ca

Executive Secretary
Secrétaire

Roberto Racca
JASCO Applied Sciences
secretary@caa-aca.ca

Treasurer
Trésorier

Dalila Giusti
Jade Acoustics Inc.
treasurer@caa-aca.ca

Editor-in-Chief
Rédacteur en chef

Umberto Berardi
Ryerson University
editor@caa-aca.ca

DIRECTORS - ADMINISTRATEURS

Alberto Behar
Ryerson University
albehar31@gmail.com

Bill Gastmeier
HGC Engineering
bill@gastmeier.ca

Bryan Gick
University of British Columbia
gick@mail.ubc.ca

Michael Kiefte
Dalhousie University
mkiefte@dal.ca

Andy Metelka
SVS Canada Inc.
ametelka@cogeco.ca

Hugues Nelisse
Institut de Recherche Robert-Sauvé
en Santé et Sécurité du Travail
(IRSST)
nelisse.hugues@irsst.qc.ca

Joana Rocha
Carleton University
Joana.Rocha@carleton.ca

Mehrzad Salkhordeh
dB Noise Reduction Inc.
mehrzad@dbnoisereduction.com

Upcoming Conference Chair
Directeur de conférence (future)

Len Zedel
Memorial University of Newfoundland
conference@caa-aca.ca

Benjamin Zendel
conference@caa-aca.ca

Past Conference Chair
Directeur de conférence (passée)

Olivier Robin
Université de Sherbrooke
olivier.robin@usherbrooke.ca

Past President
Président sortant

Frank A. Russo
Ryerson University
past-president@caa-aca.ca

Awards Coordinator
Coordinateur des prix

Victoria Duda
Université de Montréal
awards-coordinator@caa-aca.ca

System Administrator
Administrateur système

Cécile Le Cocq
ÉTS, Université du Québec
sysadmin@caa-aca.ca

Webmaster
Webmestre

Philip Tsui
RWDI
web@caa-aca.ca

Social Media Editor
Rédacteur média sociaux

Romain Dumoulin
Soft dB
r.dumoulin@softdb.com

SUSTAINING SUBSCRIBERS - ABONNÉS DE SOUTIEN

The Canadian Acoustical Association gratefully acknowledges the financial assistance of the Sustaining Subscribers listed below. Their annual donations (of \$475 or more) enable the journal to be distributed to all at a reasonable cost.

L'Association Canadienne d'Acoustique tient à témoigner sa reconnaissance à l'égard de ses Abonnés de Soutien en publiant ci-dessous leur nom et leur adresse. En amortissants les coûts de publication et de distribution, les dons annuels (de 475\$ et plus) rendent le journal accessible à tous les membres.

Acoustec Inc.
Jean-Philippe Migneron - 418-496-6600
info@acoustec.qc.ca
acoustec.qc.ca

Acoustex Specialty Products
Mr. Brian Obratoski - 2893895564
Brian@acoustex.ca
www.acoustex.net

AcoustiGuard-Wilrep Ltd.
Mr. William T. Wilkinson - 888-625-8944
wtw@wilrep.com
acoustiguard.com

AECOM
Alan Oldfield - 9057127058
alan.oldfield@aecom.com
aecom.com

Aercoustics Engineering Ltd.
Nicholas Sylvestre-Williams - (416) 249-3361
NicholasS@aercoustics.com
aercoustics.com

Audio Precision (c/o GerrAudio Distribution in Canada)
Peter Snelgrove -
peter@gerr.com
www.gerr.com

Dalimar Instruments Inc
Monsieur Daniel Larose - 450-424-0033
daniel@dalimar.ca
www.dalimar.ca

dB Noise Reduction
Mehrzad Salkhordeh - 519-651-3330 x 220
mehrzad@dbnoisereduction.com
dbnoisereduction.com

GRAS Sound & Vibration (c/o GerrAudio Distribution in Canada)
Peter Snelgrove -
peter@gerr.com
www.gerr.com

HGC Engineering Ltd.
Mr. Bill Gastmeier -
bill@gastmeier.ca
hgcengineering.com

Hottinger Bruel & Kjaer inc.
Andrew Khoury - 514-695-8225
andrew.khoury@hbkworld.com
bksv.com

Jade Acoustics Inc.
Ms. Dalila Giusti - 905-660-2444
dalila@jadeacoustics.com
jadeacoustics.com

JASCO Applied Sciences (Canada) Ltd.
Roberto Racca - +1.250.483.3300 ext.2001
roberto.racca@jasco.com
www.jasco.com

Pyrok Inc.
Howard Podolsky - 914-777-7770
mrpyrok@aol.com
pyrok.com

RWDI
Mr. Peter VanDelden - 519-823-1311
peter.vandelden@rwdi.com
rwdi.com

Scantek Inc.
Edward Okorn -
E.Okorn@ScantekInc.com
scantekinc.com

Soft dB Inc.
Dr. Roderick Mackenzie - 5148056734
r.mackenzie@softdb.com
softdb.com

Xprt Integration
Mr. Rob W Sunderland - 604-985-9778
rob@xprt.ca